



University of
Massachusetts
Amherst

Molecular Changes Following Skeletal Muscle Disuse in Humans

Item Type	Dissertation (Open Access)
Authors	Reich, Kimberly A.
DOI	10.7275/1079181
Download date	2026-05-20 16:58:19
Link to Item	https://hdl.handle.net/20.500.14394/38580

**MOLECULAR CHANGES FOLLOWING SKELETAL MUSCLE
DISUSE IN HUMANS**

A Dissertation Presented

By

KIMBERLY A. REICH

Submitted to the Graduate School of the
University of Massachusetts Amherst in partial fulfillment
of the requirements for the degree of

DOCTOR OF PHILOSOPHY

September 2009

Kinesiology

© Copyright by Kimberly A. Reich 2009
All Rights Reserved

**MOLECULAR CHANGES FOLLOWING SKELETAL MUSCLE
DISUSE IN HUMANS**

A Dissertation Presented

By

KIMBERLY A. REICH

Approved as to style and content by:

Priscilla M. Clarkson, Chair

Patty S. Freedson, Member

Lawrence M. Schwartz, Member

Patty S. Freedson, Department Chair
Department of Kinesiology

DEDICATION

To my parents, Chuck and Bonnie Sewright, who instilled in me the idea that I could attempt anything and who love and support me even when I trip in the process. To Matthew, my husband, who makes it all worth it.

ACKNOWLEDGMENTS

The first person I wish to thank is my advisor, Dr. Priscilla Clarkson for giving me an opportunity to join her lab group and for all of her tireless effort in turning me into a scientist, which was no easy task. Her patience and dedication to all of her students is unparalleled, and I will be forever grateful that she was willing to take a chance on an unknown like me. The doors she has helped opened for me, both within the field and within my own brain have been invaluable. Her mentorship has been a tremendous gift.

I also wish to thank the members of my dissertation committee. To Dr. Schwartz, for helping me to see the simple ways to answer complex queries and for always taking time to answer my countless questions. To Dr. Freedson, for her big picture approach and helping me to not miss the forest for the trees.

I could not have done this without the help and support of my past and present labmates. Karen Riska, the benchtop goddess with McGuyver skills to solve any technical problem. Rob Hyldahl for his willingness to help me with all of my questions in the cell culture room and beyond. Kevin O'Fallon who made sure I saw the humor in what seemed like the most dire of circumstances. Nina Moore, whose sunny disposition (and musical ability) made even tedious tasks in the hood a pleasurable experience. Ling Xin and Stephanie Cole, who jumped right in without missing a beat. I would also like to thank the members of the Schwartz lab who took me on as an honorary labmate, and to Christine Brown who met my millionth question with patience and a smile. To past labmates from whom I learned so much, especially Maria Urso and Monica Hubal whose brains I still pick today and am honored to consider friends and colleagues.

My time at the University of Massachusetts was a huge growth experience for me and a pleasure. I would like to thank each member of the Kinesiology faculty who helped me learn what it is to be an exercise scientist, and who served as models for collegiality and professionalism. And of course, to Florrie Blackbird, who helped me keep my head on straight and even find my keys when I left them behind (which happened too many times to count).

This dissertation would not have been possible without the generous help of individuals outside of the University including Dr. Paul Thomson and Cherie Bilbie at Hartford Hospital, and Drs. Yi-Wen Chen and Eric Hoffman at Children's National Medical Center. This work could also not have been possible without funding from The American College of Sports Medicine Foundation, NASA, Sigma-Xi Grants-in-aid of Research, and the NCMRR Integrated Molecular Core for Rehabilitation Medicine.

I wish to thank my family (Mom, Dad, Traci, Megan and Stephen) who have supported my crazy idea of switching careers to become an exercise scientist—and to all the Reiches, my new family who take an interest in my work and celebrate all the little successes. Finally, I wish to thank my husband, Matthew, who didn't sign up to share the life of a crazy grad student, but decided to date and marry me nonetheless.

ABSTRACT

MOLECULAR CHANGES FOLLOWING SKELETAL MUSCLE

DISUSE IN HUMANS

SEPTEMBER 2009

KIMBERLY A. REICH, B.S., INDIANA UNIVERSITY

M.A.M., CARNEGIE MELLON UNIVERSITY

M.S., SOUTHERN CONNECTICUT STATE UNIVERSITY

Ph.D., UNIVERSITY OF MASSACHUSETTS AMHERST

Directed by: Priscilla M. Clarkson

The purpose of this dissertation was to investigate the molecular events associated with the onset of skeletal muscle disuse in humans. Study I examined global gene expression changes in vastus lateralis muscle following 48h unloading (UL) and 24h reloading (RL) in humans. Results showed that functions related to protein degradation and oxidative stress were enriched following UL and that these global gene expression patterns were not readily reversed following RL, thus indicating that molecular events associated with short-term disuse may persist beyond the duration of the stimulus. In contrast to previous work in IM, collagen gene expression increased in this study, demonstrating that differences in molecular signaling may exist among disuse models in humans.

Study II of this dissertation expanded on the findings of Study I to investigate global gene expression patterns related to the early stage of multiple disuse models. Microarray data collected 48h post-UL in Study I were analyzed within the context of data previously collected in our laboratory following 48h immobilization (IM) and spinal

cord injury (SCI). Results showed that the disuse models shared a small subset of commonly differentiated genes. Furthermore, the similarities between IM, SCI, and UL extended beyond specific genes to include commonly enriched functions and pathways such as protein degradation and oxidative stress, suggesting that these molecular mechanisms are involved in the early stages of disuse, regardless of specific stimulus.

In Study III, an *in vitro* model of skeletal muscle was used to test the exploratory hypothesis that induction of oxidative stress response gene heme oxygenase-1 (HMOX1) would lead to decreases in gene expression associated with proteolysis, namely ubiquitin E3 ligases atrogin1 and MuRF1, as well as increased XXT cleavage (a marker of metabolic enzyme activity). In this study, C₂C₁₂ myotubes were pre-treated with hemin (an inducer of HMOX1) and then treated with H₂O₂ to elicit oxidative stress. Results showed that hemin treatment resulted in increased HMOX1 expression and decreased E3 ligase expression. Furthermore, hemin-treated cells exhibited increased XTT cleavage compared to controls. HMOX1 may be a promising gene target to protect against oxidative stress that accompanies early stages of disuse.

TABLE OF CONTENTS

	Page
ACKNOWLEDGMENTS	v
ABSTRACT.....	vii
LIST OF TABLES.....	xi
LIST OF FIGURES	xii
CHAPTER	
I. DEVELOPMENT OF THE PROBLEM.....	1
Introduction.....	1
Research Plan Development	5
Summary	9
References.....	11
II. REVIEW OF THE LITERATURE.....	17
Introduction.....	17
Functional and Structural Changes in Skeletal Muscle Associated with Disuse.....	18
Molecular Changes with Skeletal Muscle Disuse.....	27
Summary	46
References.....	48
III. GLOBAL GENE EXPRESSION CHANGES WITH MUSCLE UNLOADING AND RELOADING IN HUMANS.....	61
Abstract.....	61
Introduction.....	62
Methods.....	64
Results.....	70
Discussion	75
Conclusions.....	86
References.....	88
IV. GLOBAL GENE EXPRESSION ANALYSIS OF HUMAN SKELETAL MUSCLE TWO DAYS POST-IMMOBILIZATION, -UNLOADING, AND -SPINAL CORD INJURY	106
Abstract.....	106
Introduction.....	107
Methods.....	109
Results.....	113
Discussion.....	118
Conclusions.....	125
References.....	126

V. THE EFFECT OF HEMIN TREATMENT ON E3 LIGASE GENE EXPRESSION AND MITOCHONDRIAL DEHYDROGENASE ACTIVITY FOLLOWING AN OXIDATIVE STRESS STIMULUS IN C2C12 MYOTUBES	141
Abstract	141
Introduction.....	142
Methods.....	144
Results.....	148
Discussion.....	150
Conclusions.....	155
References.....	156
VI. SUMMARY.....	170
Introduction.....	170
Study I.....	170
Study II.....	173
Study III	175
References.....	177
APPENDICES	
A. Informed Consent Form.....	179
B. Medical Screening Form	187
C. Raw Data Study I	188
D. Raw Data Study III	192
BIBLIOGRAPHY.....	206

LIST OF TABLES

Table	Page
3.1. Subject demographics	96
3.2. qRT-PCR primers	97
3.3. Over-represented functional annotations for clusters 1 and 7.....	98
3.4a. Cluster 1 Up-regulated genes associated with ubiquitin conjugation	99
3.4b. Cluster 7 Down-regulated genes associated with mitochondrial function.....	100
3.5. Ingenuity canonical pathways associated with clusters 1 (upregulated) and cluster 7 (downregulated) genes	101
3.6. qRT PCR results.	102
4.1. Shared changes in gene expression among all three conditions	132
4.2. Over-represented functional groups associated with each disuse condition	134
4.3. Gene expression in NRF2-mediated oxidative stress response pathway	135
4.4. Chaperone genes differentially expressed among three models of disuse	136
5.1. qRT-PCR primers	162
C1. qRT-PCR Atrogin1	188
C2. qRT-PCR COL4A3	189
C3. qRT-PCR HMOX1	190
C4. qRT-PCR MuRF1	191
D1. C ₂ C ₁₂ XTT raw data	192
D2. C ₂ C ₁₂ gene expression raw data	204

LIST OF FIGURES

Figure	Page
2.1. Ubiquitin proteasome pathway.	28
2.2. AKT signaling pathway with decreased growth factor conditions.....	34
3.1. Gene clustering.	103
3.2a. HMOX protein levels via Western blot	104
3.2b. HMOX protein by individual subject.	105
4.1. Distribution of differentially expressed genes among disuse models.....	137
4.2a. Chaperone-related network associated with immobilization	138
4.2b. Chaperone-related network associated with spinal cord injury	139
4.2c. Chaperone-related network associated with unloading.....	140
5.1. HMOX1 gene expression (Mean±SEM) increased following 100uM H2O2 treatment	163
5.2. HMOX1 gene expression (Mean±SEM) increases with hemin treatment in a dose dependent manner.	164
5.3. Atrogin1 and MuRF1 gene expression decreased with 100uM hemin treatment.....	165
5.4. XTT Cleavage decreased with H2O2 treatment	166
5.5 Hemin treatment increased cell XTT cleavage.....	167
5.6. 100uM Hemin prevented/reversed effects of 1mM H2O2 treatment.	168

CHAPTER I

DEVELOPMENT OF THE PROBLEM

Introduction

Disuse muscle atrophy occurs in response to immobilization (IM) (25, 36, 65), unloading (UL) (1, 5-6), bed rest (7-8, 50), spaceflight (1, 61, 63), and spinal cord injury (SCI) (13, 26, 56, 64). Although studies in humans have documented the effects of disuse on skeletal muscle structure and function (5-6, 9, 16-18, 23, 26-27, 35, 37, 48, 56), the underlying mechanisms regulating these changes are not well understood. Investigations of limb immobilization (3, 40), hindlimb suspension (10, 30-32, 57), and denervation (30, 58) in animals have shown that there is a coordinated alteration in expression of genes encoding for proteins that function in the initiation of the muscle atrophy process. Furthermore, it has also been proposed that genes with transcription most sensitive to UL and reloading (RL) may be key regulators in this atrophy process (10).

The molecular mechanisms leading to atrophy are likely complex and involve alterations in molecular signaling of multiple pathways. The most elucidated molecular pathway associated with atrophy in animals is the ubiquitin proteasome pathway (UPP), which is the intracellular signaling pathway responsible for the majority of protein degradation in the cell (10, 12, 28, 33, 44, 54, 59) and is dependent, in part, on AKT/FOXO pathway activity (12, 28). Recent findings by Urso *et al.* (64-65) confirmed decreases in phosphorylation of AKT 48h following SCI as well as after short-term (48h) limb IM in humans, although accompanying elevations in UPP protein products (*i.e.*, E3 ligases Atrogin1, MuRF1) were not found. In addition, alterations have been observed in

mRNA levels for FBXO32 (aka Atrogin1) following 2wk IM (36) and 20d of bed rest (50), as well as MuRF1 (36) with 2wk IM.

Other intriguing (potentially interrelated) mechanisms associated with the early stages of disuse identified in the animal literature include oxidative stress (43, 53-54, 60), decreased abundance of protein chaperones (30, 41, 60), alterations in signaling related to growth factors (42, 55, 60), and inflammation (32, 34, 36, 60). Following 48h of immobilization, Urso *et al.* showed that metallothionein gene transcription was upregulated (65), and unpublished microarray data from biopsies taken 48h post-SCI in humans showed that metallothionein gene transcription was upregulated following that disuse stimulus as well. Thus, oxidative stress may be a common component to various disuse stimuli in humans. Furthermore, unpublished data from both of these studies showed that protein chaperones may also be decreased in agreement with the animal literature. Finally, alterations in gene transcription and related protein products for extracellular matrix (ECM) components may accompany the early stages of disuse (2-3, 39, 65). The most abundant ECM component is collagen (4). Following 48h IM, gene expression and protein levels for two collagen isoforms (COL3 and COL4) were found to be to be decreased (65) in agreement with the animal literature (2-3, 39), yet unpublished microarray data from biopsies collected 48h post-SCI showed that transcripts for these isoforms may have been increased. These contrary findings suggest that while the responses to IM and SCI may share common components as noted above, they may also display distinct and unique signaling mechanisms contributing to subsequent muscle atrophy.

Many conditions of disuse (such as bed rest, and spaceflight) restrict load. When a muscle is immobilized, there is no change in muscle length; with UL, the muscle can lengthen and shorten but experiences little mechanotransduction (24, 29, 66). Therefore, although data from animal studies suggest similar expression of atrophy-related genes with UL and IM (11, 43), it is unknown whether limb UL in humans leads to alterations in gene expression and protein products similar to that demonstrated with IM. Furthermore, while gene expression and related protein products of individual molecules have been investigated following IM and SCI disuse in humans (64-65), the potential relationship between these genes was not studied.

The purpose of this dissertation was to investigate the molecular events associated with the onset of skeletal muscle unloading in humans and to explore common signaling pathways found in multiple forms of disuse. Previous work in our laboratory by Urso *et al.* (64-65) revealed increases in gene expression related to protein degradation and decreases in expression related to ECM remodeling following 48h IM. However, molecular signaling following limb UL (without joint movement restriction such as that seen with IM) had not yet been investigated at this early timepoint. Furthermore, little was known about the effects of resumption of activity following these short-term periods of inactivity in humans. While it may be assumed that the effects of short-term disuse were quickly reversed, evidence in rats (10) showed that, with low-intensity RL following short-term UL, genes upregulated following disuse were more resistant to the effects of RL than those that were downregulated. It was unknown if human muscle responded in a similar fashion. Therefore, the first specific aim of this dissertation was to

study global gene expression changes following short-term UL and RL in human skeletal muscle.

Previous studies in animals (12, 43) indicated that key molecular pathways relating to protein degradation may play a central role in multiple forms of disuse, and that global gene expression following different forms of disuse shared common patterns (43). It was unknown however if gene expression responses following multiple disuse stimuli in humans shared common pathways and functions. Because our laboratory had previously collected global gene expression data following both 48h IM and 48h SCI, (64-65), I was presented with the unique opportunity to investigate the early molecular signaling patterns of UL within the context of gene expression following these two common forms of disuse in humans. Therefore, the second specific aim of this dissertation was to investigate global gene expression patterns related to disuse in biopsies collected following 48h post-IM, SCI, and UL.

Molecular signaling leading to disuse atrophy is likely a complex sequence of events involving numerous interrelated pathways and may begin as early as 48h following the introduction of a disuse stimulus. Systems biology is an emerging discipline that focuses on the relationships between multiple cellular components (22). To this end, bioinformatic tools have been developed capable of analyzing complex gene expression data. Microarray technology allows us to measure expression levels of thousands of genes at once, and software tools such as Database for Annotation, Visualization and Integrated Discovery (DAVID) (20) and Ingenuity Pathway Analysis (IPA) (51) use microarray results to identify functional groups and build potential signaling networks encompassing many differentially expressed genes (51). Employing

high-throughput technology to interpret gene expression results may lead to a better understanding of functions and pathways associated with disuse.

Studying global gene expression patterns at the early time point of 48h of disuse (before any measurable atrophy has occurred) led to the identification of molecules and pathways that may provide therapeutic targets to prevent or attenuate disuse-associated atrophy. Before findings of such investigations can be translated to intervention studies however further experimentation is required. The C₂C₁₂ mouse muscle immortal cell line is often used as an *in vitro* model for skeletal muscle because these cells differentiate into multinucleated myotubes that exhibit similar phenotypes and gene expression patterns as mammalian skeletal muscle cells *in vivo*. Therefore, an exploratory aim of this dissertation was to develop hypotheses based on the findings of the two previous dissertation studies and to devise a proof of concept experiment to test these hypotheses *in vitro*.

Research Plan Development

Although studies in humans have documented the effects of disuse on skeletal muscle structure and function (5-6, 9, 16-18, 23, 26-27, 35, 37, 48, 56), the underlying mechanisms regulating these changes are not well understood. Investigations of multiple forms of disuse in animals have shown that there is a coordinated alteration in expression of genes encoding for proteins that function in the initiation of the muscle atrophy process (11, 21, 31, 38, 43, 45, 49, 60). Mechanisms identified in these studies have included increases in gene expression related to protein degradation and stress response as well as decreases in gene expression related to transcription and translation, energy metabolism, and ECM proteins (43).

Of the few studies that have been undertaken in humans (14, 19, 36, 46, 64-65), lower limb studies have primarily involved immobilization of the ankle (19, 36) or knee joint (64-65). As with the animal models, these studies have shown alterations in expression of components of the ubiquitin proteasome pathway (UPP) such as Atrogin1 and MuRF1, ECM components such as collagen, and metabolic enzymes such as NADH dehydrogenase and pyruvate dehydrogenase. With the exception of one study in our laboratory (65) that measured gene expression following 48h of knee IM, these investigations have measured time points from 5d – 3wk of IM (15, 19, 36). However, measurable proteolysis has been detected as early as 72h post-UL in humans (62), and therefore, molecular atrophy triggers (such as alterations in the transcription of key genes) likely occur prior to that time point. Furthermore, it has been proposed that key regulators of muscle atrophy are likely those most sensitive to the disuse stimulus (10).

Study I of this dissertation examined the global gene expression patterns following short-term unloading (48h UL) and reloading (24h RL) in human skeletal muscle using a human suspension model most analogous to hindlimb unloading in rodents, unilateral lower limb suspension (ULLS). Microarray technology was employed to identify gene expression changes in up to 60,000 genes represented on the U133 plus 2.0 gene chip. Cluster analysis was then performed for significantly altered gene expression, and each cluster was analyzed using DAVID and IPA to identify functional groups and signaling pathways associated with the UL/RL protocol. Target genes were further measured via qRT-PCR and protein products were measured via Western blot analysis.

The results of Study I indicated that upregulation in molecular signaling related to UPP activity and to oxidative stress response were the most abundantly altered functional groups and/or canonical pathways following UL, and in general, these gene expression patterns persisted following RL. Conversely, downregulated functional groups and pathways were involved primarily in mitochondrial metabolism. Key genes related to the UPP and oxidative stress response were confirmed via qRT-PCR, and measurement of selected protein products (using available tissue) identified which of these differentially expressed genes were also altered at the protein level. Finally, contrary to findings from previous work in our laboratory (65), results also indicated that genes encoding for components of the ECM may be upregulated following 48h UL in humans, rather than down-regulated as observed following 48h IM. Study I identified global gene expression patterns associated with short-term UL and RL in humans, fulfilling the purpose of the first specific aim of this dissertation.

Study II of this dissertation expanded upon the findings of Study I by using the microarray results collected in that study to explore similarities between global gene expression patterns following UL and two other common forms of skeletal muscle disuse in humans: IM and SCI. Gene expression changes following 48h UL were analyzed along with previously collected microarray data following 48h IM and 48h SCI in our laboratory, the results of which are published elsewhere. As with Study I, high-throughput software was used to identify functional groups and canonical pathways via DAVID and IPA, respectively. In addition, IPA was used to identify potential gene networks (interrelated groups of genes) common to all three forms of disuse.

The results of Study II revealed that, although only a small group of genes were shared by the three datasets, there were key common functional groups and pathways associated with all three related to chelation, protein chaperone, protein degradation, and stress response. This led me to believe that there is potential to develop therapies in the future which may help protect against multiple forms of disuse atrophy by targeting early molecular events following disuse. Study II identified global gene expression patterns common to 48h IM, UL, and SCI, fulfilling the purpose of the second specific aim of this dissertation.

Global gene expression findings from both Study I and Study II suggested oxidative stress as a probable effect (although to varying degrees) of the first 48h following disuse, regardless of the disuse stimulus. This supported the findings of previous literature (reviewed in (53)) which showed that oxidative stress may, indeed, be an upstream contributor to the cascade of events leading to protein degradation associated with longer periods of disuse. Evidence of oxidative stress in both Studies I and II of this dissertation came in the form of the upregulation of stress response genes including those believed to have antioxidant properties. In fact, the gene with the greatest degree of upregulation in Study I codes for one such molecule: heme oxygenase-1 (HMOX1). Furthermore in Study II, HMOX1 was found to be upregulated in two out of the three forms of disuse (SCI and UL). HMOX1 was consistently shown in the animal literature to be increased following various disuse stimuli (21, 31, 47, 52) and it was proposed in these studies that, although increases in HMOX1 gene expression were not adequate to prevent disuse atrophy, superphysiological expression levels of the gene may help attenuate protein degradation, though expression of genes associated with proteolysis

were not measured (47). Therefore, a relationship between HMOX1 expression and proteolytic gene expression had not been established.

Study III of this dissertation utilized an *in vitro* cell model of skeletal muscle to investigate the effects of hemin-induced superphysiological HMOX1 gene expression on E3 ligase expression and XTT cleavage (a marker for cellular metabolic enzyme activity) following an oxidative stress stimulus. Hemin is a substrate of HMOX1 (and an inducer of the HMOX1 gene) which is already available as a drug (Panhematin) used to treat the blood disorder, porphyria, under a physician's care in a hospital setting. The results of this study demonstrated that, in C₂C₁₂ myotubes, there was a relationship between magnitude of HMOX1 induction, XTT cleavage, and E3 ligase gene expression such that increased HMOX1 expression was associated with greater XTT cleavage and decreased E3 ligase gene expression. The findings of Study III supported the hypothesis generated by Studies I and II, that HMOX1 may serve a protective effect against protein degradation during oxidative stress, thus fulfilling the exploratory aim of this dissertation.

Summary

The overall purpose of this dissertation was to investigate the molecular events associated with the onset of skeletal muscle unloading in humans and to explore common signaling pathways found in multiple forms of disuse. In Study I, I examined the global gene expression patterns in human skeletal muscle associated with short-term UL and RL and performed selective conformational analysis. In Study II, I expanded upon these findings to compare the global gene expression patterns associated with short-term UL to those found at the same time point following IM and SCI. The findings of Study I and Study II led me to test the hypothesis that induction of the stress response gene HMOX1

in an *in vitro* model of skeletal muscle would lead to a decreases in expression of proteolytic genes and increases in XTT cleavage. Results from these three studies serve to further elucidate the complex molecular response to periods of disuse in human skeletal muscle and help to lay the foundation for potential treatments aimed at attenuating atrophy by targeting molecular mechanisms at play in the early stages of disuse, before measurable atrophy has occurred.

References

1. **Adams GR, Caiozzo VJ, and Baldwin KM.** Skeletal muscle unweighting: Spaceflight and ground-based models. *J Appl Physiol* 95: 2185-2201, 2003.
2. **Ahtikoski AM, Koskinen SO, Virtanen P, Kovanen V, Risteli J, and Takala TE.** Synthesis and degradation of type iv collagen in rat skeletal muscle during immobilization in shortened and lengthened positions. *Acta Physiol Scand* 177: 473-481, 2003.
3. **Ahtikoski AM, Koskinen SO, Virtanen P, Kovanen V, and Takala TE.** Regulation of synthesis of fibrillar collagens in rat skeletal muscle during immobilization in shortened and lengthened positions. *Acta Physiol Scand* 172: 131-140, 2001.
4. **Aszodi A, Legate KR, Nakchbandi I, and Fassler R.** What mouse mutants teach us about extracellular matrix function. *Annu Rev Cell Dev Biol* 22: 591-621, 2006.
5. **Berg HE, Dudley GA, Haggmark T, Ohlsen H, and Tesch PA.** Effects of lower limb unloading on skeletal muscle mass and function in humans. *J Appl Physiol* 70: 1882-1885, 1991.
6. **Berg HE, Dudley GA, Hather B, and Tesch PA.** Work capacity and metabolic and morphologic characteristics of the human quadriceps muscle in response to unloading. *Clin Physiol* 13: 337-347, 1993.
7. **Berg HE, Eiken O, Miklavcic L, and Mekjavic IB.** Hip, thigh and calf muscle atrophy and bone loss after 5-week bed rest inactivity. *Eur J Appl Physiol* 99: 283-289, 2007.
8. **Berg HE, Larsson L, and Tesch PA.** Lower limb skeletal muscle function after 6 wk of bed rest. *J Appl Physiol* 82: 182-188, 1997.
9. **Berg HE, and Tesch PA.** Changes in muscle function in response to 10 days of lower limb unloading in humans. *Acta Physiol Scand* 157: 63-70, 1996.
10. **Bey L, Akunuri N, Zhao P, Hoffman EP, Hamilton DG, and Hamilton MT.** Patterns of global gene expression in rat skeletal muscle during unloading and low-intensity ambulatory activity. *Physiol Genomics* 13: 157-167, 2003.
11. **Bodine SC, Latres E, Baumhueter S, Lai VK, Nunez L, Clarke BA, Poueymirou WT, Panaro FJ, Na E, Dharmarajan K, Pan ZQ, Valenzuela DM, DeChiara TM, Stitt TN, Yancopoulos GD, and Glass DJ.** Identification of ubiquitin ligases required for skeletal muscle atrophy. *Science* 294: 1704-1708, 2001.

12. **Bodine SC, Stitt TN, Gonzalez M, Kline WO, Stover GL, Bauerlein R, Zlotchenko E, Scrimgeour A, Lawrence JC, Glass DJ, and Yancopoulos GD.** Akt/mTOR pathway is a crucial regulator of skeletal muscle hypertrophy and can prevent muscle atrophy in vivo. *Nat Cell Biol* 3: 1014-1019, 2001.
13. **Castro MJ, Apple DF, Jr., Staron RS, Campos GE, and Dudley GA.** Influence of complete spinal cord injury on skeletal muscle within 6 mo of injury. *J Appl Physiol* 86: 350-358, 1999.
14. **Chen S, Khan ZA, Barbin Y, and Chakrabarti S.** Pro-oxidant role of heme oxygenase in mediating glucose-induced endothelial cell damage. *Free Radic Res* 38: 1301-1310, 2004.
15. **Chen Y-W, Gregory CM, Scarborough MT, Shi R, Walter GA, and Vandeborn K.** Transcriptional pathways associated with skeletal muscle disuse atrophy in humans. *Physiol Genomics* 31: 510-520, 2007.
16. **Cramer RM, Cooper P, Sinclair PJ, Bryant G, and Weston A.** Effect of load during electrical stimulation training in spinal cord injury. *Muscle Nerve* 29: 104-111, 2004.
17. **Cramer RM, Weston A, Climstein M, Davis GM, and Sutton JR.** Effects of electrical stimulation-induced leg training on skeletal muscle adaptability in spinal cord injury. *Scand J Med Sci Sports* 12: 316-322, 2002.
18. **Cramer RM, Weston AR, Rutkowski S, Middleton JW, Davis GM, and Sutton JR.** Effects of electrical stimulation leg training during the acute phase of spinal cord injury: A pilot study. *Eur J Appl Physiol* 83: 409-415, 2000.
19. **de Palma L, Marinelli M, Pavan M, and Orazi A.** Ubiquitin ligases murf1 and mafbx in human skeletal muscle atrophy. *Joint Bone Spine* 75: 53-57, 2008.
20. **Dennis G, Jr., Sherman BT, Hosack DA, Yang J, Gao W, Lane HC, and Lempicki RA.** David: Database for annotation, visualization, and integrated discovery. *Genome Biol* 4: P3, 2003.
21. **DeRuisseau KC, Shanely RA, Akunuri N, Hamilton MT, Van Gammeren D, Zengeroglu AM, McKenzie M, and Powers SK.** Diaphragm unloading via controlled mechanical ventilation alters the gene expression profile. *Am J Respir Crit Care Med* 172: 1267-1275, 2005.
22. **Drubin DA, Way JC, and Silver PA.** Designing biological systems. *Genes Dev* 21: 242-254, 2007.

23. **Dudley GA, Castro MJ, Rogers S, and Apple DF, Jr.** A simple means of increasing muscle size after spinal cord injury: A pilot study. *Eur J Appl Physiol Occup Physiol* 80: 394-396, 1999.
24. **Fitts RH, Riley DR, and Widrick JJ.** Physiology of a microgravity environment invited review: Microgravity and skeletal muscle. *J Appl Physiol* 89: 823-839, 2000.
25. **Fluck M, Chiquet M, Schmutz S, Mayet-Sornay MH, and Desplanches D.** Reloading of atrophied rat soleus muscle induces tenascin-c expression around damaged muscle fibers. *Am J Physiol Regul Integr Comp Physiol* 284: R792-801, 2003.
26. **Gregory CM, Vandenborne K, Castro MJ, and Dudley GA.** Human and rat skeletal muscle adaptations to spinal cord injury. *Can J Appl Physiol* 28: 491-500, 2003.
27. **Hather BM, Adams GR, Tesch PA, and Dudley GA.** Skeletal muscle responses to lower limb suspension in humans. *J Appl Physiol* 72: 1493-1498, 1992.
28. **Hoffman EP, and Nader GA.** Balancing muscle hypertrophy and atrophy. *Nat Med* 10: 584-585, 2004.
29. **Hornberger TA, and Esser KA.** Mechanotransduction and the regulation of protein synthesis in skeletal muscle. *Proc Nutr Soc* 63: 331-335, 2004.
30. **Hornberger TA, Hunter RB, Kandarian SC, and Esser KA.** Regulation of translation factors during hindlimb unloading and denervation of skeletal muscle in rats. *Am J Physiol Cell Physiol* 281: C179-187, 2001.
31. **Hunter RB, Mitchell-Felton H, Essig DA, and Kandarian SC.** Expression of endoplasmic reticulum stress proteins during skeletal muscle disuse atrophy. *Am J Physiol Cell Physiol* 281: C1285-1290, 2001.
32. **Hunter RB, Stevenson E, Koncarevic A, Mitchell-Felton H, Essig DA, and Kandarian SC.** Activation of an alternative nf-kappab pathway in skeletal muscle during disuse atrophy. *Faseb J* 16: 529-538, 2002.
33. **Ikemoto M, Nikawa T, Takeda S, Watanabe C, Kitano T, Baldwin KM, Izumi R, Nonaka I, Towatari T, Teshima S, Rokutan K, and Kishi K.** Space shuttle flight (sts-90) enhances degradation of rat myosin heavy chain in association with activation of ubiquitin-proteasome pathway. *Faseb J* 15: 1279-1281, 2001.
34. **Jackman RW, and Kandarian SC.** The molecular basis of skeletal muscle atrophy. *Am J Physiol Cell Physiol* 287: C834-843, 2004.
35. **Jayaraman A, Gregory CM, Bowden M, Stevens JE, Shah P, Behrman AL, and Vandenborne K.** Lower extremity skeletal muscle function in persons with incomplete spinal cord injury. *Spinal Cord* 44: 680-687, 2006.

36. **Jones SW, Hill RJ, Krasney PA, O'Conner B, Peirce N, and Greenhaff PL.** Disuse atrophy and exercise rehabilitation in humans profoundly affects the expression of genes associated with the regulation of skeletal muscle mass. *Faseb J* 18: 1025-1027, 2004.
37. **Kauhanen S, Leivo I, and Michelson JE.** Early muscle changes after immobilization. An experimental study on muscle damage. *Clin Orthop Relat Res* 44-50, 1993.
38. **Kim JW, Kwon OY, and Kim MH.** Differentially expressed genes and morphological changes during lengthened immobilization in rat soleus muscle. *Differentiation* 75: 147-157, 2007.
39. **Kjaer M.** Role of extracellular matrix in adaptation of tendon and skeletal muscle to mechanical loading. *Physiol Rev* 84: 649-698, 2004.
40. **Krawiec BJ, Frost RA, Vary TC, Jefferson LS, and Lang CH.** Hindlimb casting decreases muscle mass in part by proteasome-dependent proteolysis but independent of protein synthesis. *Am J Physiol Endocrinol Metab* 289: E969-980, 2005.
41. **Ku Z, Yang J, Menon V, and Thomason DB.** Decreased polysomal hsp-70 may slow polypeptide elongation during skeletal muscle atrophy. *Am J Physiol* 268: C1369-1374, 1995.
42. **Latres E, Amini AR, Amini AA, Griffiths J, Martin FJ, Wei Y, Lin HC, Yancopoulos GD, and Glass DJ.** Insulin-like growth factor-1 (igf-1) inversely regulates atrophy-induced genes via the phosphatidylinositol 3-kinase/akt/mammalian target of rapamycin (pi3k/akt/mtor) pathway. *J Biol Chem* 280: 2737-2744, 2005.
43. **Lecker SH, Jagoe RT, Gilbert A, Gomes M, Baracos V, Bailey J, Price SR, Mitch WE, and Goldberg AL.** Multiple types of skeletal muscle atrophy involve a common program of changes in gene expression. *Faseb J* 18: 39-51, 2004.
44. **Lecker SH, Solomon V, Mitch WE, and Goldberg AL.** Muscle protein breakdown and the critical role of the ubiquitin-proteasome pathway in normal and disease states. *J Nutr* 129: 227S-237S, 1999.
45. **Leger B, Cartoni R, Praz M, Lamon S, Deriaz O, Crettenand A, Gobelet C, Rohmer P, Konzelmann M, Luthi F, and Russell AP.** Akt signalling through gsk-3beta, mtor and foxo1 is involved in human skeletal muscle hypertrophy and atrophy. *J Physiol* 576: 923-933, 2006.
46. **Levine S, Nguyen T, Taylor N, Friscia ME, Budak MT, Rothenberg P, Zhu J, Sachdeva R, Sonnad S, Kaiser LR, Rubinstein NA, Powers SK, and Shrager JB.**

Rapid disuse atrophy of diaphragm fibers in mechanically ventilated humans. *N Engl J Med* 358: 1327-1335, 2008.

47. **McClung JM, Whidden MA, Kavazis AN, Falk DJ, Deruisseau KC, and Powers SK.** Redox regulation of diaphragm proteolysis during mechanical ventilation. *Am J Physiol Regul Integr Comp Physiol* 294: R1608-1617, 2008.

48. **Miles MP, Clarkson PM, Bean M, Ambach K, Mulroy J, and Vincent K.** Muscle function at the wrist following 9 d of immobilization and suspension. *Med Sci Sports Exerc* 26: 615-623, 1994.

49. **Nikawa T, Ishidoh K, Hirasaka K, Ishihara I, Ikemoto M, Kano M, Kominami E, Nonaka I, Ogawa T, Adams GR, Baldwin KM, Yasui N, Kishi K, and Takeda S.** Skeletal muscle gene expression in space-flown rats. *Faseb J* 18: 522-524, 2004.

50. **Ogawa T, Furochi H, Mameoka M, Hirasaka K, Onishi Y, Suzue N, Oarada M, Akamatsu M, Akima H, Fukunaga T, Kishi K, Yasui N, Ishidoh K, Fukuoka H, and Nikawa T.** Ubiquitin ligase gene expression in healthy volunteers with 20-day bed rest. *Muscle Nerve* 34: 463-469, 2006.

51. **Park J-J, Berggren JR, Hulver MW, Houmard JA, and Hoffman EP.** Grb14, gpd1, and gdf8 as potential network collaborators in weight loss-induced improvements in insulin action in human skeletal muscle. *Physiol Genomics* 27: 114-121, 2006.

52. **Powers SK, Decramer M, Gayan-Ramirez G, and Levine S.** Pressure support ventilation attenuates ventilator-induced protein modifications in the diaphragm. *Crit Care* 12: 191, 2008.

53. **Powers SK, Kavazis AN, and McClung JM.** Oxidative stress and disuse muscle atrophy. *J Appl Physiol* 2007.

54. **Reid MB.** Response of the ubiquitin-proteasome pathway to changes in muscle activity. *Am J Physiol Regul Integr Comp Physiol* 288: R1423-1431, 2005.

55. **Rommel C, Bodine SC, Clarke BA, Rossman R, Nunez L, Stitt TN, Yancopoulos GD, and Glass DJ.** Mediation of igf-1-induced skeletal myotube hypertrophy by pi(3)k/akt/mtor and pi(3)k/akt/gsk3 pathways. *Nat Cell Biol* 3: 1009-1013, 2001.

56. **Shah PK, Stevens JE, Gregory CM, Pathare NC, Jayaraman A, Bickel SC, Bowden M, Behrman AL, Walter GA, Dudley GA, and Vandenborne K.** Lower-extremity muscle cross-sectional area after incomplete spinal cord injury. *Arch Phys Med Rehabil* 87: 772-778, 2006.

57. **Siu PM, and Alway SE.** Id2 and p53 participate in apoptosis during unloading-induced muscle atrophy. *Am J Physiol Cell Physiol* 288: C1058-1073, 2005.
58. **Siu PM, and Alway SE.** Mitochondria-associated apoptotic signalling in denervated rat skeletal muscle. *J Physiol* 565: 309-323, 2005.
59. **St-Amand J, Okamura K, Matsumoto K, Shimizu S, and Sogawa Y.** Characterization of control and immobilized skeletal muscle: An overview from genetic engineering. *Faseb J* 15: 684-692, 2001.
60. **Stevenson EJ, Giresi PG, Koncarevic A, and Kandarian SC.** Global analysis of gene expression patterns during disuse atrophy in rat skeletal muscle. *J Physiol* 551: 33-48, 2003.
61. **Tesch PA, and Berg HE.** Effects of spaceflight on muscle. *J Gravit Physiol* 5: P19-22, 1998.
62. **Tesch PA, von Walden F, Gustafsson T, Linnehan RM, and Trappe TA.** Skeletal muscle proteolysis in response to short-term unloading in humans. *J Appl Physiol* 105: 902-906, 2008.
63. **Trappe SW, Trappe TA, Lee GA, Widrick JJ, Costill DL, and Fitts RH.** Comparison of a space shuttle flight (sts-78) and bed rest on human muscle function. *J Appl Physiol* 91: 57-64, 2001.
64. **Urso ML, Chen YW, Scrimgeour AG, Lee PC, Lee KF, and Clarkson PM.** Alterations in mrna expression and protein products following spinal cord injury in humans. *J Physiol* 579: 877-892, 2007.
65. **Urso ML, Scrimgeour AG, Chen YW, Thompson PD, and Clarkson PM.** Analysis of human skeletal muscle after 48 h immobilization reveals alterations in mrna and protein for extracellular matrix components. *J Appl Physiol* 101: 1136-1148, 2006.
66. **Vandenburgh H, Chromiak J, Shansky J, Del Tatto M, and Lemaire J.** Space travel directly induces skeletal muscle atrophy. *Faseb J* 13: 1031-1038, 1999.

CHAPTER II

REVIEW OF THE LITERATURE

Introduction

Skeletal muscle inactivity (disuse) due to bed rest, limb immobilization, exposure to micro-gravity or spinal cord injury result in profound functional and structural adaptations such as decreases in muscle size (1, 11, 13, 16, 22, 34, 38-39, 53, 61, 66-67, 70, 75, 89, 93, 96, 106, 116, 123, 133, 139, 146) and force generating capacity (20, 27-29, 32, 35, 38, 42, 48, 63, 69, 75, 88-89, 93, 96, 120, 139, 146). These adaptations have mainly been attributed to the muscle unloading that occurs because of the reduction in weight-bearing activity (1, 12, 17), although the molecular mechanisms underlying these changes are not well understood. Recent technological and theoretical advances in the area of gene expression (e.g. microarray analysis, qRT-PCR, and other advances in field of systems biology) have allowed researchers to begin to describe the complex transcriptional events associated with skeletal muscle disuse atrophy, including those molecular changes that may precede morphological and functional alterations in muscle tissue.

The purpose of this review will be to describe the current understanding of alterations in skeletal muscle related to decreases in muscle size associated with disuse. Unlike cachexia-associated atrophy or sarcopenia, disuse atrophy is directly related to changes in load or contractile activity without the concomitant contribution of disease or age. First, I will address the functional and morphological changes associated with skeletal muscle disuse at the whole muscle and microscopic level in various human and animal models. I will then present the molecular mechanisms currently proposed as

factors that may contribute to the initiation and persistence of protein degradation leading to disuse muscle atrophy.

Functional and Structural Changes in Skeletal Muscle Associated with Disuse

Experimental models of disuse in humans and animals have been used to examine the associated alterations in muscle size and strength. In humans, the most popular disuse models are voluntary bed rest (10, 20, 35, 38-39, 42, 48, 88-89, 102), limb immobilization (IM) via casting/bracing (32, 63, 120, 139), and unloading via unilateral lower limb suspension (ULLS) (24, 36, 59, 107, 109). Data has also been collected from individuals who have sustained accidental spinal cord injury (SCI) (22, 29, 136). In animals, unloading via hind-limb suspension (HS) is the most popular, though immobilization via casting/joint fixation has been used as well (15, 41, 66-67, 106, 116); and denervation and spinal cord transaction have been used as models for SCI .

Bed Rest

Bed rest has long been used to model profound disuse in humans (10-11, 13, 20, 35, 38-39, 42, 48, 88-89). In fact, it has served as the primary micro-gravity model to simulate musculoskeletal changes during spaceflight (1, 20, 40, 132, 135). In the knee extensors (KE), force decrements of 15% were detectable after 14d (20), ~20% after 20 – 35d (35, 38, 42), and ~29% after 42d (11). After 120d of bed rest, force decrements reached 30% (89). These results suggest the rate of performance deficit development may be higher in the earlier stages of bed rest compared to later time-points. Gastrocnemius and soleus muscles demonstrated a strength deficit of ~25% by 35d (48, 88), showing that the rate of decrement development may be greater for these antigravity muscles than the KE muscles.

Muscle size measurements following bed rest have generally been of the lower extremity, and the rate of decreases in muscle size was greatest in the first few weeks (2 – 3wk). After 7d of bed rest, a 3% decrease in thigh muscle volume was already apparent (39), and by 14d, the decrement in KE CSA was 10% (10). After 20d, decrements of 6 – 11% were reported, and after 30d, the greatest decrements reported were 11% (13). By 42d, decrements in KE muscle size were 14 – 17% (13, 39), and after ~120d of bedrest, 15% decreases in muscle size were reported compared to baseline (89). In the case of the calf muscles, the time-course of decrements in muscle size corresponded with the thigh, except at 120d when the decreases in calf muscle were approximately twice those of the thigh (89), suggesting that various muscle groups may follow a different atrophy pattern in chronic (>3mo) unloading.

Changes at the microscopic level with bed rest have shown decreases (22) in fiber cross-sectional area (CSA). Fiber-size decrements were similar for type I and type II fibers at earlier time-points, but diverged at later time-points such that the degree of decrease in CSA was different across time, and the pattern of change across fiber-type was not the same in all muscle groups. In the soleus, the CSA of type I fibers decreased from 7 – 29% after 60d and 35 – 48% after 120 days (103-104, 125). Furthermore, the type I fibers showed a continuous decrease in CSA whereas the type II fibers exhibited a different pattern such that there was a 34% decrease at 60d, but no further decreases at 120d (125). The reverse was true of the KEs: type II fiber CSA was decreased by 13% at 60d and 32% at 120d (125), whereas Type I fiber CSA was decreased by 16% at 60d with no further decrease at 120d (125).

Immobilization (IM)

Referred to as “limb immobilization,” this disuse model is, practically speaking, actually joint immobilization. By immobilizing bones together that contribute proximally and distally to a joint, movement about the joint is constricted, and therefore contraction of the muscles that act upon that joint are also largely diminished. Although the joint is immobilized, the neuromuscular infrastructure is left largely intact, and there is a small degree of neuromuscular activity, as evidenced via electromyography; though it is greatly decreased compared to pre-immobilization or control conditions (63).

Humans

In humans, the knee or elbow joints are typically immobilized. In the case of the lower extremity, a leg cast is used and the knee is fixed in a slightly flexed position, and subjects are usually provided with crutches to assist in ambulation. IM can result in substantial decreases in strength. For example, KE torque measured via maximum voluntary contraction resulted in a 17% decrease in peak torque following 14d of IM (32), a 45% decrease following 21d (63), and a 53% decrease after 28d (139). Interestingly, after merely 9d of IM, Maximum voluntary contraction was decreased by 13% (120), suggesting that the molecular events leading to performance decrements may exhibit a relatively rapid onset.

Few studies in healthy subjects have been conducted that measure muscle size, but the limited data available suggests that whole muscle size measured via MRI is decreased with immobilization and that protein degradation in the muscle exhibits a relatively rapid onset (1). 10 – 14d of IM resulted in an ~11% decrease in KE group CSA (61, 133). Interestingly, a recent study of 14d of leg immobilization reported only a 4.7%

reduction in lean muscle mass via dual energy x-ray absorptiometry (70); the difference between these results and those of the previously cited studies may have been due to the method of measurement. In the 28d study cited above, subjects demonstrated a 21% decrease in KE group cross-sectional area (CSA) (139). On the microscopic level, muscle fiber CSA decrements in the biopsies from vastus lateralis (VL) were 8% for type I, 11% for type IIa, and 9% for IIb (61). With increased periods of immobilization these decrements increased such that at 28d of IM, decrements of 26% for type I, 13% for type IIa, and 36% type IIb were demonstrated (139) showing preferential atrophy of type 2A fibers.

The body of literature examining functional losses in upper extremity muscles with IM is small, and the documented decrements with regard to muscle size and function were less dramatic than in lower limb IM (75, 93, 96, 146). Twenty-eight days of elbow joint IM showed an 11% loss in elbow flexor muscle group CSA measured via MRI, and force decrements of 35% were reported (146). Shorter durations of IM have produced conflicting results, however. Following 21d of wrist joint IM, no significant size decrements were reported in the forearm though grip strength was decreased by 19% (75). Conversely, 9d of wrist joint IM resulted in 29% reduction in isometric wrist flexion strength, but only 4% decrement in forearm CSA (96). On the microscopic level, 6wk of elbow joint immobilization resulted in decrements of 25% for type I and 26% for type II (93). This suggests that in the upper limb, there may be no difference between rate of type I and type II size decrement.

Immobilization in humans results in decreases in whole muscle size with lower extremity IM, showing that protein degradation outpaces protein synthesis. The muscle

size changes with upper extremity IM are less definitive, especially in the periods of disuse <28d. It is clear that, at the least, the muscle atrophy is less dramatic in the upper extremity than that found in the lower extremity. Furthermore, strength losses are demonstrated even in the absence of size decrement in the upper extremity, suggesting that functional losses can be experienced in the absence of contractile protein loss, suggesting that perhaps neuromuscular and/or muscle quality adaptations are responsible for the strength deficits. The more dramatic size and strength losses in the lower extremity compared to upper extremity with immobilization may be a reflection of the relative disuse stimulus. In other words, the weight-bearing sustained by the lower extremity during normal ambulation far exceeds that of the upper extremity, and when IM is introduced, the relative decrease in load for the lower extremity is far greater for the lower extremity compared to upper extremity. Lower limb immobilization in humans shows the greatest degree of atrophy in type II fibers compared to type I, while the results with regard to fiber type preference in upper extremity immobilization is not conclusive.

Animals

Limb IM in rats and mice results in rapid yet selective decreases in muscle mass. Post-IM, muscle mass measurements show much greater decrements than in humans depending on the muscle and its relative position during IM. For example, muscle loss in the lower leg can reach between 35 – 45% in less than 2wk of IM (15, 66-67, 106, 116) and can reach as much as 45% following 4wk of IM in young mice (116). Furthermore, the relative position of the muscle (short vs. lengthened) can have a large impact on the degree of muscle mass loss. In the shortened position, rat soleus muscle showed 44% decrease in muscle mass following 21d of IM compared to control, while the tibialis

anterior (which was in the lengthened position during the same experiment) showed no significant atrophy compared to control (26). Limb IM in animals results in a fiber-type shift from type I to type II. However, unlike with lower limb IM in humans where type II fibers show greater relative decreases in CSA, there is preferential atrophy of type I fibers in animals (18).

Limb Suspension

Limb suspension protocols in animals and humans were originally designed as ground-based models for studying unweighting experienced in the microgravity environment during spaceflight (1, 132). As with the immobilization models discussed earlier, the neuromuscular system remains intact. However, while immobilization involves constant fixation of the joint, suspension models allow for movement at the joint, yet no weight-bearing activity.

Humans (Unilateral Lower Limb Suspension)

Unilateral lower limb suspension (ULLS) is a model in which one leg does not bear weight because the foot is not allowed to touch the ground. To facilitate this suspension (without requiring the subject to actively keep the foot off the ground by contracting hip and knee flexors) one of two methods is used: an older protocol involving a strap that suspends one lower limb (8), and a newer protocol involving the use of a platform shoe on the contralateral limb to prevent weightbearing (24, 35, 59, 107-108). The difference between the three methods is that the strap keeps the knee in a flexed position during ambulation while the use of the platform shoe allows the unloaded leg to remain in anatomical position during ambulation.

ULLS results in less dramatic decrements in both muscle strength and size compared to immobilization, but similar results compared to those seen with bed rest (1). ULLS studies of short duration (10 – 12d) showed KE MVS decreases of ~12 - 17% (8-9). Data regarding accompanying size decreases at these earlier time points were not reported. The earliest time-point for which whole muscle CSA was measured was 16d which showed an 8% decrease in KE CSA (2). Longer duration studies (28 – 42d) showed strength decrements of ~20% regardless of time-point (8, 24, 36, 107-108), while muscle size measurements across studies showed greater size decrements the longer the period of ULLS. For example, by 42d of ULLS, the KE exhibited a 16% relative decrease in CSA and the gastrocnemius and soleus muscles showed a 17% and 25% decline in CSA, respectively (59). Few studies are available that reported changes in fiber size with ULLS, but the studies that are available suggest that they may be comparable with that seen in bed rest studies (1).

Animals

Hindlimb suspension (HS) is the most popular rodent disuse model. In this model, the animal is suspended by ~30° (angle of torso to floor of the cage) so that the weight of their body is borne by their forelimbs and tail traction, leaving their hindlimbs unweighted, yet free to move at all limb joints (97). As with human ULLS, the greatest losses in strength and size were shown in the anti-gravity muscles such as the soleus (144). Measurable atrophy is apparent at very early time points in rodents. For example, bodyweight of HS rats were less than control at 3d post-HS and reached significance at 6d (30). By 30d of HS, their bodyweight was 70% of control (114). For this reason,

researchers have often preferred this model to study the molecular changes associated with disuse.

To summarize, prolonged periods of disuse in humans result in measurable and sometimes dramatic decreases in muscle strength and size (at both the whole muscle and single fiber levels). The most striking decrements appear to occur at early time-points (within first 2 – 3 weeks), after which muscle loss continues, but the rate of loss diminishes. Evidence from animal models shows an even sooner and more rapid decline in strength and size than in humans, and findings show that morphological changes begin in the first days following the unloading stimulus, suggesting that changes at the molecular level may occur almost immediately. Limited evidence in human biopsy studies suggests that this may be true for humans, as well. The next section of this literature review will outline the molecular changes shown to occur with skeletal muscle disuse in animal models as well as findings from the limited number of human studies.

Spinal Cord Injury

Spinal cord injury (SCI) directly affects the function of skeletal muscle function in that affected neurons no longer effectively carry information to the muscles they innervate. Chronic changes in skeletal muscle following both complete and incomplete spinal cord injury have long been established including profound muscle atrophy, increases in connective tissue abundance, and fiber type shifts from type I to type II (22). These changes result from decreased muscle contraction and load stemming from the decrease or cessation of activation by affected neurons.

Humans

The time-course for these changes have been difficult to ascertain because testing is rarely conducted prior to 4 – 6 wk post-injury, generally considered to be the point at which SCI patients are clinically stable (29). However, it has been suggested that muscle remodeling post-SCI is rapid. For example, in a study measuring atrophy in quadriceps femoris muscles 6 – 46 wk post-SCI, it was found that while muscle size decreased by 40% post-SCI in ~10 months, the most dramatic losses were within the first few months post-SCI: At 6wk, the muscle was 25% smaller than that of able-bodied controls; by 10wk, this decrement reached ~30%; and by 24wk, it was ~38%. (34). On the microscopic level, it was found that in muscle biopsies collected 4wk post-complete SCI, distribution of type I to type II fibers was 50%, whereas by 16wk, type I fibers represented less than 10% of total fibers. In addition, CSA of fibers decreased by 40 – 50% (29, 53). Following incomplete SCI, decreases in CSA compared to able-bodied controls showed a decrease of over 30% in thigh CSA (123).

Animals

Spinal cord transection (SI) and denervation are animal models for SCI. In SI, a lesion is created in the alpha motor neuron impairing communication between the neuron and the affected muscle; in denervation communication between the neuron is impaired by either crushing a nerve or administering a chemical such tetrodotoxin which prevents acetylcholine release. In both models, the fiber-type shift is greater than that seen in humans (53). Furthermore, the loss in muscle mass, as evidenced by relative wet-weight of affected muscles is more rapid than that seen in humans. For example, 72h post-denervation decreases of 20% were observed compared to control in mice, and by 14d

post-denervation, this decrement increased to 35% (113). Rodents and humans have both shown decreases in size and fiber-type shift post-SCI, though the changes are more rapid in animals than in humans making the translation of animal research to humans relevant, but difficult.

Molecular Changes with Skeletal Muscle Disuse

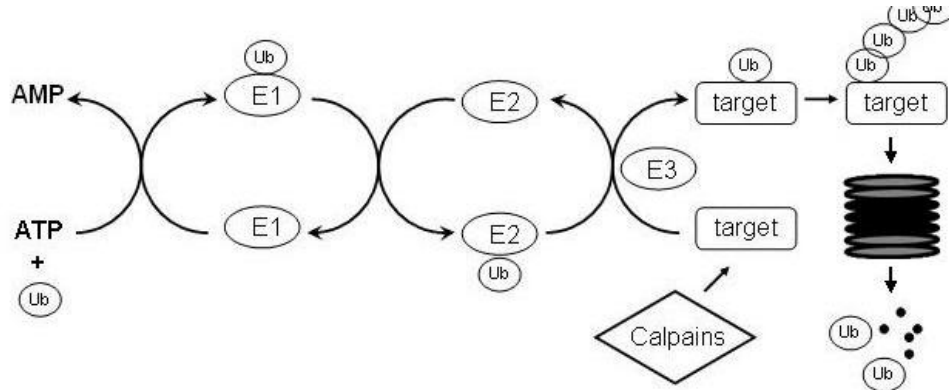
Little research has been performed in humans to study the effects of skeletal muscle disuse on gene expression and related protein products (70, 102, 136-137). In fact, to my knowledge, only two study has investigated the early (≤ 48 h) effects of disuse signaling pathways in skeletal muscle (136-137). Urso et al. (137) found that 48h of leg immobilization resulted in increases in mRNA for components of the ubiquitin proteasome pathway (UPP) and increases in metallothionein (MT) expression. Urso et al. (136) also found that 48h after SCI, MTs were upregulated. These findings were generally in line with animal literature, which suggests that skeletal muscle disuse may set off a cascade of events involving increases in the rate of proteolysis (46, 62, 68, 73) and that this increase may be triggered, in part, by increases in oxidative stress (68, 111-112, 128).

Ubiquitin Proteasome Pathway (UPP)

There are several proteolytic mechanisms in skeletal muscle including lysosomal proteolysis (44, 79, 131, 141, 143), calpain-mediated proteolysis (51, 84, 111, 126, 128), and the proteasome system (7, 14, 16, 47, 65-66, 70, 101, 122, 127-128). While lysosomal proteases are activated during disuse (44), evidence suggests that calpain and proteasome activity, coordinated within a multi-faceted ubiquitin proteasome pathway, are the primary means of protein breakdown in the cell (44, 112). I will, therefore, focus

on these two important mechanisms and the pathway within which they function. For an illustration of the UPP, see figure 2.1.

Figure 2.1: Ubiquitin proteasome pathway. Target = protein destined for degradation.



Proteasome Machinery

The 20S core and the 26S proteasome are proteolytic machinery responsible for the disassembly of proteins into their peptide components (47), and is the primary system by which muscle cells decrease protein content leading to atrophy (115). The 26S proteasome is comprised of the 20S complex flanked by 2 19S complexes on either side. The 19S complex facilitates ATP-dependent protein unfolding into the barrel-shaped 20S complex, while the 20S complex consists of 2 outer α -rings which serve as the “gatekeepers” of the proteolytic core comprised of 2 β -rings. These 2 β -rings contain trypsin-like activities which serve to cleave and degrade the core’s contents, respectively (47).

Proteasome units are abundant in skeletal muscle and, therefore, it has been a subject of debate as to whether increases in mRNA for genes encoding proteins contributing to the structure of the proteolytic machinery are necessary precursors for increases in proteolysis. Studies have shown that, at least in some cases, genes related to the 20S complex are indeed upregulated with disuse (128, 137). A greater body of

evidence exists, however, to support the theory that proteolytic activity is regulated in greater part by the upregulation of the “escort system” that delivers proteins targeted for degradation to the proteasome (16, 46-47, 128).

Ubiquitination Cascade

Although the proteasome is the primary means by which proteins are degraded in the cell, it will generally only degrade those proteins that have been tagged for proteolysis via ubiquitination. Ubiquitination is achieved through a cascade of events involving the small molecule ubiquitin (Ub) and 3 classes of enzymes (E1, E2, and E3). This is a multi-step cascade in which ubiquitin is activated by E1 (ubiquitin activating enzyme), transferred to E2 (ubiquitin conjugating enzyme) and eventually attached by E3 (ubiquitin ligase) to a target protein destined for degradation. This ubiquitination cascade involves increasing levels of specificity such that there is only one ubiquitin molecule, one isoform of E1 per cell type (e.g. muscle), 20 – 40 E2s, yet over 1000 E3s (124). As a result, transcription of their encoding mRNAs and translation of specific E3s are believed to be important means by which proteolysis of skeletal muscle contractile proteins is regulated leading to atrophy (15, 52, 62, 70).

The first step of this multi-step process is activation of ubiquitin by E1 through ATP-dependent adenylation. E1 adenylates the ubiquitin molecule at its C-terminus, forms a high-energy thioester bond between the two molecules, and releases AMP. In the next step, E1 adenylates a second molecule of ubiquitin leading to the transfer of a ubiquitin molecule to E2’s catalytic site. In the third step, E3 transfers ubiquitin from E2 to the protein molecule destined for degradation (115). Free E3s have much higher affinity for E2’s bond to ubiquitin than to free E2s, and this difference in affinity helps

drive the enzymatic cascade (74). Several ubiquitin molecules must be attached to a substrate before it is recognized for degradation by the proteasome (145)

E3 Specificity

Two muscle specific ligases have been implicated in disuse atrophy: Atrogin-1 (FBXO32/MAFbx) and muscle ring finger-1 (MuRF-1) (15). Like the majority of E3s, both of these proteins contain RING (Really Interesting New Gene)-finger domains which allow the E3 molecule to serve as a scaffold bringing the targeted substrate and the E2 molecule together for conjugation (73). Upregulation of the genes that encode Atrogin-1 and MuRF-1 (FBX32 and MuRF, respectively), as well as increases in related protein levels, are associated with skeletal muscle atrophy (15, 60).

MuRF-1 is a monomeric RING-finger protein shown to be selectively recruited to the M-line of the sarcomere by the A168-A170 region of titin where it binds via a C-terminal helical domain (98). Evidence has shown MuRF-1 may play a role in maintenance of the M-line and thick filament structure, yet overexpression of MuRF-1 leads to titin protein degradation (95). Furthermore, MuRF-1 has a nuclear component, binds with nuclear import proteins as well as a transcriptional regulator (GMEB-1), and has been localized not only to the sarcomere *in vivo*, but to the nuclei in myocytes (95), suggesting that it also may play a role in gene transcription.

Atrogin-1 is also a RING finger E3. However, rather than being a monomeric protein, it has multiple subunits and is a member of the Skp1-Cull-F-box group of cullin-RING ligases known as SCF complexes (52). The core of Atrogin-1 is the cullin subunit, one end of which binds the RING component and the E2 enzyme. The other end of the cullin subunit binds the F-box protein subunit containing the substrate binding motif. The

F-box protein subunit, in turn, binds to the target substrate via an adaptor protein, Skp1 (52). Atrogin-1 has been shown to be located at the Z-line of the sarcomere (90).

Therefore, like MuRF-1, it likely targets sarcomeric proteins, although specific protein targets have not been identified. Furthermore, it has been suggested that atrophy is not only associated with increases in transcription of FBXO32 and subsequent translation/aggregation of Atrogin-1 (16), but also with phosphorylation of the complex since it has been shown to lead to F-box/substrate binding and Ub conjugation (111).

Both Atrogin-1 and MuRF-1 have been found to be differentially expressed with disuse atrophy. For example, the genes that encode for both of these proteins have been shown to be upregulated as early as 24h following the initiation of immobilization and unloading in rat muscle (15). Furthermore, Atrogin-1 and MuRF-1 knockout mice showed attenuated atrophy following unloading (15), and C₂C₁₂ myotubes transfected with Atrogin-1 were measurably thinner than controls (15). Taken together, these findings suggest that Atrogin-1 and MuRF-1 proteins may be important early regulators of skeletal muscle atrophy and that they (or their protein targets) may be excellent candidates for early intervention following disuse via drug-mediated modification to attenuate atrophy in humans. However, findings from human studies have not yet fully supported this hypothesis. While both 20d of bed rest (102) and 2wk of leg immobilization (70) led to a significant 1.6-fold increase in Atrogin-1 gene expression and a trend for an upregulation in MuRF-1 expression (70), no differential expression was found for these two genes following 48h of leg immobilization (137) or 48h after SCI (136). Though they may play an important role in disuse atrophy in humans, the time-courses for their effects are not clear.

Calpains

The majority of skeletal muscle proteins exist in actomyosin complexes (134). Therefore, because the 20S proteolytic core can only degrade monomeric proteins, contractile proteins destined for degradation (e.g. actin myosin, and titin) must not only be ubiquitinated in order to undergo proteolysis by the proteasome, but must first be released from the sarcomere. Recent research suggests that the calpains may be responsible for actomyosin disassociation prior to proteolytic degradation by the 20S proteolytic core or the 26 proteasome (51, 134), and as such, could play an important role in skeletal muscle remodeling following a disuse stimulus.

Calpains are non-lysosomal, calcium ion (Ca^{2+})-dependent, cysteine proteases (51). There are three members of the family abundant in skeletal muscle, (ubiquitous calpains 1 and 2, and the muscle-specific isoform, calpain-3). They are found primarily at the Z-disk of the sarcomere where they are transformed from their inactive to active state through Ca^{2+} -dependent autolysis. (37). Active calpains cleave proteins into polypeptide components, and in this way, may render them vulnerable to ubiquitination and subsequent proteolysis.

Calpain-3 has been of particular interest lately in regards to its potential role in sarcomere remodeling since a loss-of-function mutation in CAPN3 results in limb-girdle muscular dystrophy type 2A (LGMD2A), which is characterized by progressive atrophy and weakness of the proximal limb muscles (117). In addition to a potential role for calpain-3 during muscle anabolism, it has been proposed that calpain-3 plays a role in muscle catabolism during disuse atrophy (84). Indeed, in a study using CAPN3 knock-out (C3KO) mice, it was shown that following hind-limb unloading, the rate of muscle mass

loss was lower in C3KO mice compared to wild-type (WT) (84). Furthermore, this study provided evidence to support the theory that proteolytic activity of the 26S proteasome may be predicated on caplain-3 cleavage of sarcomeric proteins because C3KO mice did not show increases in ubiquitination following hindlimb suspension, while WT mice did (84).

Molecular Changes Influencing UPP Activity

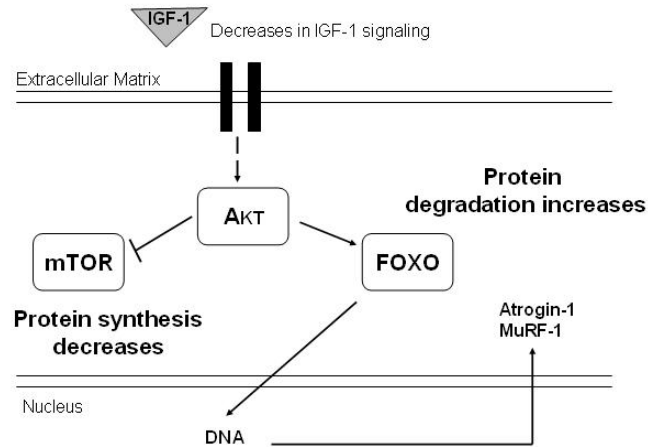
The increase in UPP activity is likely influenced by multiple molecular mechanisms including (but not limited to) activity of the AKT/FOXO and NFkB pathways, oxidative stress, and decreases in protective protein chaperones. Furthermore, recent work has shown that extracellular matrix (ECM) remodeling (specifically decreases in collagen proteins) is found with skeletal muscle disuse not only in animals (3-4, 6, 76) , but in humans (137), although the relationship with the UPP is unclear.

AKT/FOXO Pathway

UPP activity is influenced by an upstream regulating signaling cascade involving AKT and forkhead box O (FOXO) transcription factors. AKT1 has been identified as the “master switch” modulating the balance between protein synthesis and protein degradation (16, 46, 62). When phosphorylate (activated), AKT in turn phosphorylates downstream targets including FOXO transcription factors and mammalian target of rapamycin (mTOR). Phosphorylation of mTOR results in its activation and a signaling cascade favoring protein synthesis. At the same time, phosphorylation of FOXO transcription factor sequesters the molecules in the cytosol, rendering them inactive. Conversely, when AKT phosphorylation decreases, FOXO transcription factors become dephosphorylated, allowing them to translocate to the nucleus where they serve to

upregulate transcription of E3 ligases Atrogin-1 and MuRF-1 (99). Figure 2.2 illustrates the effects of a decrease in growth factors on the pathway when AKT phosphorylation is decreased.

Figure 2.2: AKT signaling pathway with decreased growth factor conditions.



As discussed earlier, increased cellular levels of these important enzymes in the ubiquitination cascade lead to increased proteolytic activity. Evidence shows that in both animals (23, 31, 85) and humans (137), levels of phosphorylated AKT decrease with immobilization. While this also been demonstrated with unloading in animals (56, 130), it has yet to be investigated in humans.

IGF-1 Signaling

An important factor contributing to decreases in AKT phosphorylation status with disuse are likely decreases in Insulin-like Growth Factor-1 (IGF-1) (87, 119, 128). IGF-1 is a polypeptide that is secreted by the liver as well as generated in paracrine/autocrine fashion in the muscle tissue and preferentially binds to the insulin-like growth factor receptor (IGFR) (138). Physical activity has been shown to increase IGF binding at the muscle cell membrane leading to increases in protein synthesis (49-50). IGF exerts its effects via a signaling cascade whereby IGF-1 binding leads to phosphorylation of the

IGF-1 receptor, AKT, mTOR, and downstream signaling molecules that promote hypertrophy (62). Decreases in IGF-1 signaling secondary to muscle disuse result in the opposite effect whereby dephosphorylation of the IGF-1 receptor leads to dephosphorylation of AKT and an increase in AKT/FOXO pathway activity (Figure 2.2) (62). IGF-1 treatment has been used in an *in vitro* model of hypertrophy where post-fusion IGF-1 treatment resulted in measurable hypertrophy in C₂C₁₂ myotubes compared to control (87, 119, 142). It is unknown whether removal of this growth stimulus would result in measurable atrophy, through it is an intriguing question worthy of further investigation, as it may provide a model system within which to study atrophy-related molecular signaling.

IGF binding proteins 1 – 6 (IGFBP 1 – 6) are carrier proteins that can interact with IGF to modify its signaling capability (118). Differential expression of IGFBPs has been found with disuse atrophy; IGFBP-5 gene expression has been shown to be upregulated in both hind-limb unloading and diaphragm unloading via mechanical ventilation (111, 128). It can sequester IGF in the ECM (111), and the results from these disuse studies suggest that IGFBP-5 may contribute to disuse atrophy by decreasing IGF signaling and subsequently promoting the activity of the AKT/FOXO and UPP pathways. In addition to interacting with IGF-1, IGFBPs can regulate cell growth and survival via IGF-independent mechanisms. For example, IGFBP-3, 5 and 6 have been identified as pro-apoptotic mediators, though the related signaling pathways are poorly understood (118), and the potential activity of these pathways during disuse are unknown.

Oxidative Stress

Oxidants are molecules with unpaired electrons in their outer electron shells. Common oxidants, known as reactive oxygen species (ROS) are superoxide (O_2^-), and hydroxyl radicals (OH). Molecules in this state are highly reactive and are important in a number of normal cellular processes (111). However, when their levels increase dramatically in the cell, oxidative stress can result. Oxidative stress is the cellular damage to proteins, lipids, and DNA that occurs when the production of reactive oxygen outweighs the cells ability to buffer oxidants via reduction/oxidation (redox) reactions and/or repair oxidant-induced alterations in cellular components (33). A related reactive species called reactive nitrogen species (RNS) can be produced secondary to ROS production. These are highly reactive molecules contain nitrogen instead of oxygen. Because their production follows that of ROS, their negative cellular effects can still be considered the result of oxidative stress.

It has been documented that oxidative stress increases with disuse atrophy (73, 111-112, 128), and increased levels of ROS in the cytosol have received growing attention in the literature. Theories for how ROS may potentially contribute to increased activity of the proteasome pathway include: 1) increases in Ca^{2+} levels in the cell resulting in activation of calpains (83); 2) promotion of Atrogin-1 and MuRF-1 transcription (112); 3) oxidation of proteins that then undergo degradation in the 20S proteolytic core without first requiring ubiquitination (54); and 4) signaling cascades leading to increased NFkB pathway activity (112).

Oxidative Stress and Calpain Activity

As previously discussed, calpains likely promote UPP activity by cleaving titin and/or nebulin, thereby releasing actin and myosin from the sarcomere, freeing them for ubiquitination and then degradation by the proteasome (134). Because calpain activity is triggered by Ca^{2+} -mediated autolysis, it follows that increases in calcium levels in the cell may lead to increased calpain activity. Evidence from *in vitro* studies suggests that oxidative stress may lead to Ca^{2+} overload and subsequent calpain activation (83). Plasma membrane Ca^{2+} ATPase facilitates Ca^{2+} removal from the cell, yet levels of this enzyme are reduced by oxidant-generated reactive aldehydes. Therefore, increases in cellular levels of ROS may retard Ca^{2+} removal from the cell, thereby contributing to cellular Ca^{2+} accumulation. The increased calpain activation may, in turn, lead to increased proteolysis via the proteasome.

Oxidative Stress and E3 Ligase Pool

Oxidative stress has been shown to upregulate Atrogin-1 and MuRF-1 in myotubes (91). Therefore, increases in ROS may promote proteolytic activity by increasing E3 ligases available to deliver ubiquitinated proteins to the proteasome. Indeed, ROS (as evidenced by H_2O_2) has been shown to activate FOXO transcription factor signaling in muscle cells (43), while increased FOXO signaling has been linked to increased Atrogin-1 expression and decreased fiber size (122). These findings provide evidence for the theory that ROS initiates FOXO-mediated transcription of E3 ligases leading to increased protein degradation via the UPP. Furthermore, increased ROS may also lead to degradation of non-ubiquitinated proteins. Studies indicate that the proteolytic core of the proteasome can degrade oxidated proteins without ubiquitination

(54). Therefore, it is possible that oxidative stress promotes protein degradation via the proteasome either by increasing the size of the pool of E3 ligases, by oxidizing proteins, or by both of these mechanisms.

Oxidative Stress and the NFkB Pathway

Nuclear Factor kappa B (NFkB) is a family of “stress response” transcription factors that are activated by over 150 molecules, and in turn, transcribe over 100 genes depending on the cell type and stimulus. Among the many stimuli that may induce NFkB activation, is disease-associated oxidative stress (68, 112). A likely molecular trigger for NFkB, in this case, is the intercellular signaling molecule tumor necrosis factor alpha (TNF- α). TNF- α is a cytokine that exerts its effects on muscle cells via tumor necrosis factor receptors one and two (TNFR1 and TNFR2). It has been established that when TNF- α binds to the skeletal muscle membrane via one of these receptors, the NFkB pathway is activated (64), and studies have shown that elevations in TNF- α stimulate the degradation of NFkB inhibitor proteins and NFkB-DNA binding in the nucleus (91). In addition, increased TNF- α levels have been associated with increased ubiquitin proteasome activity (55), suggesting a strong relationship between the NFkB and ubiquitin proteasome pathways.

TNF- α has been found to be a potent atrophy stimulus both *in vitro* (91-92, 129) and *in vivo* (5, 114). Elevated TNF- α levels have been linked to increased NFkB pathway activity associated with disease-related muscle wasting (5) and aging-related sarcopenia (114). It is not known whether a similar relationship between TNF- α levels and NFkB pathway activity may exist with disease atrophy. In fact, research has shown that increases in NFkB pathway activity may be stimulated by another molecular mechanism (64). It

was shown that, following 7 days of hind-limb unloading, TNF α levels were not elevated even though there was evidence of increases in NF κ B transcriptional activity. These findings suggest that an alternative activation pathway may exist for NF κ B associated molecular signaling during disuse atrophy.

In the inactive state, NF κ B is in complex with its inhibitor I κ B. In this state, the transcription factor is sequestered in the cytosol. When NF κ B is cleaved from I κ B by the enzyme I κ B kinase (IKK), it becomes activated and translocates to the nucleus where it may transcribe a variety of genes including Atrogin-1 and MuRF-1 (68). Increased oxidative stress in the cell may lead to enhanced NF κ B activation because ROS have been shown to promote activation of kinases that participate in the NF κ B/I κ B cleaving process (64). As such, this is an additional way in which oxidative stress may increase ubiquitin proteasome activity.

Recently there has been debate regarding the effects of oxidative stress on the NF κ B pathway (71, 105). Oxidative stress may lead to oxidation of direct and indirect activators of NF κ B, thereby enhancing NF κ B pathway activity, and in turn, UPP activity. Conversely, recent evidence has also shown that oxidation of the NF κ B molecules, themselves, diminishes their DNA-binding activity, suggesting that oxidative stress could also inhibit NF κ B transcriptional activity (71). Because NF κ B activity and interaction with subsequent transcriptional targets is a complex mechanism regulated by diverse stimuli and may differ between cell types, more research will be necessary to elucidate the role of the NF κ B pathway during disuse muscle atrophy.

Reactive Oxygen and Nitrogen Species Production

For oxidative stress to occur, oxidant levels must first be increased in the cell. Multiple mechanisms exist by which oxidants may be produced during disuse. Examples of these mechanisms include NO \cdot production via nitric oxide synthase (NOS) activity and O $_2^-$ production via the xanthine oxidase (XO) pathway (57). Furthermore, increased levels of reactive iron can participate in reactions that produce ROS

Oxidant Production via NOS and XO

NOS produces NO by catalysing a five-electron oxidation of a guanidino nitrogen of L-arginine (L-Arg). Evidence has shown that NOS activity is likely increased during limb immobilization, leading to increased NO production (80). There are two NOS isoforms in muscle: neuronal NOS (nNOS) and endothelial NOS (eNOS) (77), the latter of which is calcium-activated. Therefore, increased cellular Ca $^{2+}$ levels may promote eNOS activity, which would lead to increased production of NO. Also, the production of NO via NOS can result in the formation of RNS which can lead to increased lipid peroxidation and nitrosylation of proteins causing further cellular damage (72).

The role of NOS and NO in disuse atrophy is a subject of debate as it has also been shown that NO can function as an anti-inflammatory mediator during disuse (100), and that it can inhibit calpain activity, thus potentially attenuating atrophy during unloading (78). Whether NO works as a pro-inflammatory mediator (promoting atrophy), or an anti-inflammatory mediator (preventing atrophy), is yet to be determined. The experiments in which NO was found to attenuate atrophy were studies in which mice were genetically altered to over-express NOS (100). Since NOS appears to be tightly regulated (21), a hyper-physiological state may not represent a relevant cellular

environment. Furthermore, the study in which NO prevented catalytic activity of calpains was performed *in vitro* with ionophore-induced proteolysis which may or may not translate to muscle disuse *in vivo* (78). This is an area where more research is need.

Calpains can degrade xanthine dehydrogenase to produce XO which in turn can catalyze the formation of O_2^- . O_2^- is quite benign when compared to other radicals. However, it can be used to form more damaging reactive species. For example, O_2^- and NO can react to form peroxynitrite (ONOO-), one of the RNS (57).

Reactive Iron

Transition metals, such as reactive iron (Fe^{2+}), can participate in reactions that produce hydroxyl radicals ($\cdot OH$) (57). The production of ROS from reactive iron may be a feed-forward process since bound iron, which is not reactive, can be released from the iron-binding protein by O_2^- , thereby becoming reactive. In this way, increases of O_2^- , a free radical, can lead to increases in reactive iron, which in turn, would lead to further increases in ROS. Heme-oxygenase-1 (HMOX1) protein activity may also lead to increases in cellular levels of reactive iron by releasing iron bound to heme proteins (57). Research has shown that HMOX1, the gene encoding for the HMOX1 protein, was upregulated with diaphragm unloading via mechanical ventilation (111) and hindlimb unloading (128). However, the role of hmox-1 is unclear, in that it may have antioxidant properties, as well. Evidence suggests that hmox1-mediated iron release may lead to increased ferritin synthesis (140). Ferritin is an abundant iron-binding protein in the cell (57), and increases in hmox-1 protein could provide protection against iron-mediated oxidative damage associated with disuse because increased ferritin may lead to a decrease in reactive iron in the cytosol by binding free iron. Nonetheless, increases in total muscle

iron levels have been shown with immobilization (81), and these increases in muscle iron were found to be associated with increases in lipid peroxidation. Furthermore, when a systemically delivered iron chelator (a chemical sequesteror of iron) was administered, atrophy was attenuated (81). Taken together, these findings suggest that immobilization leads to increases in muscle iron, and that oxidative stress caused by ROS (produced in an iron-dependent reaction) may contribute to the immobilization-associated muscle atrophy.

Oxidative Stress Markers and Disuse

The theory that muscle disuse increases intracellular oxidative stress is supported by findings showing upregulation of oxidative stress markers associated with disuse atrophy (111, 128, 137). In addition to the upregulation of HMOX1 (the antioxidant properties of which are a source of debate as discussed above), other oxidative markers have also been shown to be upregulated with disuse atrophy. These include iron and heavy metal response genes such as ferroxidase (128), the transferrin receptor (128), and metallothioneins (MT) (111, 128, 137), as well as the chemoprotective enzyme glutathione-s-transferase (111, 128, 137).

Ferroxidase catalyzes the oxidation of Fe^{2+} to Fe^{3+} , while transferrin is a carrier of Fe^{3+} . The transferrin receptor mediates the endocytosis of Fe^{3+} into the cell (82).

Ferroxidase and transferrin are known to work together in the blood plasma to respond to oxidative stress. Transferrin can only bind Fe^{3+} , and therefore ferroxidase activity promotes transferrin-iron binding (109). Elevated levels for transferrin and ferroxidase in the blood are considered biomarkers for inflammation (19). However, the roles of these proteins in the muscle cell are not clear. Furthermore, an increase in transferrin receptor

activity may lead to an increase in intracellular iron, though its association with disease-related molecular changes is not known.

Metallothioneins (MTs)

Members of the MT family of antioxidant molecules have been shown to be upregulated with hindlimb unloading (128) and mechanical ventilation-mediated diaphragm unloading (111). Furthermore, following 48h of immobilization in humans (137) and 48h after SCI (136) a number of (MTs) were found to be upregulated. MTs are small cysteine-rich molecules with antioxidant properties. MTs have the capacity to bind heavy metals through the thiol group of their cysteine residues, especially zinc ions (Zn^{+}). Zn^{+} is an important component in the activation and binding of some zinc-finger proteins that interact with DNA. The zinc-finger is a DNA-binding protein domain comprised of two anti-parallel β -strands and an α -helix. The zinc ion is crucial to the functionality of the zinc-finger domain because it unfolds if it does not bind a zinc ion (25). MTs regulate cellular levels of Zn^{+} by binding and releasing it, and as such, are important for zinc signaling.

MTs are purported to serve as antioxidants by capturing ROS (25). From this $^{+}$ reaction, the MT's cysteine residue is oxidized to cystine, and the metal ions which were previously bound to cysteine (usually Zn) are liberated. Zinc is widely considered to be an antioxidant (110). However, while Zn can directly protect the cell from oxidative damage to a small degree, the primary way in which it exerts its antioxidant effect is through its role in the production of MTs. Once the Zn, previously bound to cysteine is liberated, it can translocate to the nucleus where it interacts with the metal response

element (MTE) in the MT gene promoter to activate the transcription of MT, so that more MT protein can be transcribed and ultimately translated (121).

Decreases in Protective Chaperone Proteins

Chaperone proteins are very important for maintenance of healthy muscle fibers. They play a role in protein stabilization during synthesis, refolding of proteins damaged by stress, and protecting proteins from degradation. Many protein chaperones are categorized as heat shock proteins (HSP) and a number of members of this protein superfamily have been shown to be downregulated with disuse atrophy. For example, HSP70 was shown to be decreased in rat soleus muscle following 12 – 18h and 24h – 14d of hindlimb unloading (128). Furthermore, this decrease in HSP70 protein was associated with decreases in protein synthesis rates (86). HSP70 is known for facilitating protein translation by associating with nascent polypeptides as they exit the ribosome. It has been suggested that decreases in HSP70 during disuse may slow protein synthesis rate, contributing to atrophy (128). The role of other heat shock protein chaperones is unknown, but the downregulation of the genes that code for a number of them have been found with hindlimb unloading (128), suggesting that a decrease in heat shock proteins may contribute to disuse atrophy.

Extracellular Matrix Integrity

The extracellular matrix (ECM) is found in the connective tissue and basement membrane (BM) around muscle fibers and is a mixture of water, sugars, and proteins (collagens, proteoglycans (PG), noncollagenous glycoproteins, and elastins). Not only does the ECM provide the three-dimensional framework for skeletal muscle organization and fiber anchorage, but it is also involved in the regulation of intracellular signaling and

provides storage for signaling molecules such as growth factors, cytokines, chemokines, and enzymes (6). The ECM is a highly dynamic structure that is subject to constant remodeling (6, 76), and evidence suggests that muscle disuse leads to decreases in ECM integrity and that these molecular changes, in turn, lead to alterations in cellular signaling (137).

Collagen

Collagen is, perhaps, the most abundant protein in the ECM. The predominant collagen isoforms in the connective tissue surrounding muscle fibers are fibrillar collagens I and III. They consist of 3 polypeptide alpha chains containing triple-helical collagenous (COL) domains as well as noncollagenous (NC) domains. Upon deposition, they assemble into polymer scaffolds (enclosing PGs and glycoproteins) designed to withstand tensile forces and provide stability to the connective tissue. The predominant collagen isoform in the BM is fibrillar collagen IV. It is a heterotrimeric combination of 6 individual α -polypeptide chains (6), and while not essential to the formation of the BM, is likely required for maintaining ECM integrity under mechanical stress (6, 94).

The animal literature has shown that disuse atrophy is associated with decreases in mRNA expression for genes encoding collagen proteins and decreases in collagen protein levels (3-4, 45, 76). These findings were recently corroborated in humans following 48h leg immobilization where mRNA levels for the genes encoding for collagen III and collagen IV mRNA were decreased post-immobilization, as were related protein products (137). Furthermore, evidence suggests that decreases in collagen are associated with increases in cellular signaling leading to proteolysis and disuse atrophy (45, 58, 106). Since it has already been established that the majority of protein

degradation occurs via proteasome activity, these findings provide evidence to support the theory that decreases in ECM integrity may lead to increases in signaling cascades associated with the UPP.

Matrix Metalloproteinases (MMPs)

Collagen degradation is initiated by matrix metalloproteinases (MMPs) which cleave ECM components (45). MMPs are zinc-dependent endopeptidases that are first secreted in an inactive state that includes a propeptide domain, a catalytic domain, and a C-terminal domain. A cysteine residue in the propeptide domain binds to a Zn^{2+} ion, which is bound to the catalytic domain. In this way, the catalytic domain is prevented from binding any other molecules. When the propeptide domain is cleaved, MMPs are activated. In an animal model, it was shown that MMP-2 and -9 gene expression is upregulated with 14d of rat hindlimb suspension (16). This finding was not confirmed following 48h of leg immobilization in humans (137). In fact, MMP28 was significantly decrease by 1.9-fold. One possible explanation for these contrasting findings is that the time-course for MMPs is such that it is not an early responder to disuse, but takes days or weeks to manifest a change in gene expression. Another possibility is that human and rat MMP responses differ. The limited *in vivo* literature on the topic makes it difficult to explain those results, but they are of interest because, to date, the study from which they were derived is the only human atrophy study to document alterations in MMPs with disuse, and is contrary to the previous animal study (45).

Summary

Animal models have shown that a decrease in protein synthesis and an increase in proteolysis lead to atrophy in skeletal muscle with disuse and that the majority of the

protein degradation occurs as a result of increased activity of the UPP. Limited research in humans suggests that the degradation mechanism may be similar since gene expression for components of the UPP are increased with immobilization. The time-course for these changes in humans, however, is unclear. Furthermore, the animal literature suggests that factors regulating the rate of proteolysis via the UPP may include IGF-1 signaling, oxidative stress, decreases in protective chaperone protein availability, and changes in extracellular matrix integrity. The molecular signaling networks associated with these interrelated factors are likely dynamic and complex.

References

1. **Adams GR, Caiozzo VJ, and Baldwin KM.** Skeletal muscle unweighting: spaceflight and ground-based models. *J Appl Physiol* 95: 2185-2201, 2003.
2. **Adams GR, Hather BM, and Dudley GA.** Effect of short-term unweighting on human skeletal muscle strength and size. *Aviat Space Environ Med* 65: 1116-1121, 1994.
3. **Ahtikoski AM, Koskinen SO, Virtanen P, Kovanen V, Risteli J, and Takala TE.** Synthesis and degradation of type IV collagen in rat skeletal muscle during immobilization in shortened and lengthened positions. *Acta Physiol Scand* 177: 473-481, 2003.
4. **Ahtikoski AM, Koskinen SO, Virtanen P, Kovanen V, and Takala TE.** Regulation of synthesis of fibrillar collagens in rat skeletal muscle during immobilization in shortened and lengthened positions. *Acta Physiol Scand* 172: 131-140, 2001.
5. **Argiles JM, Alvarez B, Carbo N, Busquets S, Van Royen M, and Lopez-Soriano FJ.** The divergent effects of tumour necrosis factor-alpha on skeletal muscle: implications in wasting. *Eur Cytokine Netw* 11: 552-559, 2000.
6. **Aszodi A, Legate KR, Nakchbandi I, and Fassler R.** What mouse mutants teach us about extracellular matrix function. *Annu Rev Cell Dev Biol* 22: 591-621, 2006.
7. **Attaix D, Arousseau E, Combaret L, Kee A, Larbaud D, Ralliere C, Souweine B, Taillandier D, and Tilignac T.** Ubiquitin-proteasome-dependent proteolysis in skeletal muscle. *Reprod Nutr Dev* 38: 153-165, 1998.
8. **Berg HE, Dudley GA, Haggmark T, Ohlsen H, and Tesch PA.** Effects of lower limb unloading on skeletal muscle mass and function in humans. *J Appl Physiol* 70: 1882-1885, 1991.
9. **Berg HE, Dudley GA, Hather B, and Tesch PA.** Work capacity and metabolic and morphologic characteristics of the human quadriceps muscle in response to unloading. *Clin Physiol* 13: 337-347, 1993.
10. **Berg HE, Eiken O, Miklavcic L, and Mekjavic IB.** Hip, thigh and calf muscle atrophy and bone loss after 5-week bedrest inactivity. *Eur J Appl Physiol* 99: 283-289, 2007.
11. **Berg HE, Larsson L, and Tesch PA.** Lower limb skeletal muscle function after 6 wk of bed rest. *J Appl Physiol* 82: 182-188, 1997.
12. **Berg HE, and Tesch PA.** Changes in muscle function in response to 10 days of lower limb unloading in humans. *Acta Physiol Scand* 157: 63-70, 1996.

13. **Berry P, Berry I, and Manelfe C.** Magnetic resonance imaging evaluation of lower limb muscles during bed rest--a microgravity simulation model. *Aviat Space Environ Med* 64: 212-218, 1993.
14. **Bey L, Akunuri N, Zhao P, Hoffman EP, Hamilton DG, and Hamilton MT.** Patterns of global gene expression in rat skeletal muscle during unloading and low-intensity ambulatory activity. *Physiol Genomics* 13: 157-167, 2003.
15. **Bodine SC, Latres E, Baumhueter S, Lai VK, Nunez L, Clarke BA, Poueymirou WT, Panaro FJ, Na E, Dharmarajan K, Pan ZQ, Valenzuela DM, DeChiara TM, Stitt TN, Yancopoulos GD, and Glass DJ.** Identification of ubiquitin ligases required for skeletal muscle atrophy. *Science* 294: 1704-1708, 2001.
16. **Bodine SC, Stitt TN, Gonzalez M, Kline WO, Stover GL, Bauerlein R, Zlotchenko E, Scrimgeour A, Lawrence JC, Glass DJ, and Yancopoulos GD.** Akt/mTOR pathway is a crucial regulator of skeletal muscle hypertrophy and can prevent muscle atrophy in vivo. *Nat Cell Biol* 3: 1014-1019, 2001.
17. **Booth FW, and Gollnick PD.** Effects of disuse on the structure and function of skeletal muscle. *Med Sci Sports Exerc* 15: 415-420, 1983.
18. **Booth FW, and Kelso JR.** Effect of hind-limb immobilization on contractile and histochemical properties of skeletal muscle. *Pflugers Arch* 342: 231-238, 1973.
19. **Brailsford S, Lunec J, Winyard P, and Blake DR.** A possible role for ferritin during inflammation. *Free Radic Res Commun* 1: 101-109, 1985.
20. **Caiozzo VJ, Baker MJ, Herrick RE, Tao M, and Baldwin KM.** Effect of spaceflight on skeletal muscle: mechanical properties and myosin isoform content of a slow muscle. *J Appl Physiol* 76: 1764-1773, 1994.
21. **Cary SPL, and Marletta MA.** The case of CO signaling: why the jury is still out. *J Clin Invest* 107: 1071-1073, 2001.
22. **Castro MJ, Apple DF, Jr., Staron RS, Campos GE, and Dudley GA.** Influence of complete spinal cord injury on skeletal muscle within 6 mo of injury. *J Appl Physiol* 86: 350-358, 1999.
23. **Childs TE, Spangenburg EE, Vyas DR, and Booth FW.** Temporal alterations in protein signaling cascades during recovery from muscle atrophy. *Am J Physiol Cell Physiol* 285: C391-398, 2003.
24. **Clark BC, Manini TM, Bolanowski SJ, and Ploutz-Snyder LL.** Adaptations in human neuromuscular function following prolonged unweighting: II. Neurological properties and motor imagery efficacy. *J Appl Physiol* 101: 264-272, 2006.

25. **Colangelo D, Mahboobi H, Viarengo A, and Osella D.** Protective effect of metallothioneins against oxidative stress evaluated on wild type and MT-null cell lines by means of flow cytometry. *Biometals* 17: 365-370, 2004.
26. **Coutinho EL, Gomes AR, Franca CN, and Salvini TF.** A new model for the immobilization of the rat hind limb. *Braz J Med Biol Res* 35: 1329-1332, 2002.
27. **Cramer RM, Cooper P, Sinclair PJ, Bryant G, and Weston A.** Effect of load during electrical stimulation training in spinal cord injury. *Muscle Nerve* 29: 104-111, 2004.
28. **Cramer RM, Weston A, Climstein M, Davis GM, and Sutton JR.** Effects of electrical stimulation-induced leg training on skeletal muscle adaptability in spinal cord injury. *Scand J Med Sci Sports* 12: 316-322, 2002.
29. **Cramer RM, Weston AR, Rutkowski S, Middleton JW, Davis GM, and Sutton JR.** Effects of electrical stimulation leg training during the acute phase of spinal cord injury: a pilot study. *Eur J Appl Physiol* 83: 409-415, 2000.
30. **Darr KC, and Schultz E.** Hindlimb suspension suppresses muscle growth and satellite cell proliferation. *J Appl Physiol* 67: 1827-1834, 1989.
31. **Dehoux M, Gobier C, Lause P, Bertrand L, Ketelslegers J-M, and Thissen J-P.** IGF-I does not prevent myotube atrophy caused by proinflammatory cytokines despite activation of Akt/Foxo and GSK-3beta pathways and inhibition of atrogen-1 mRNA. *Am J Physiol Endocrinol Metab* 292: E145-150, 2007.
32. **Deschenes MR, Giles JA, McCoy RW, Volek JS, Gomez AL, and Kraemer WJ.** Neural factors account for strength decrements observed after short-term muscle unloading. *Am J Physiol Regul Integr Comp Physiol* 282: R578-583, 2002.
33. **Droge W.** Free radicals in the physiological control of cell function. *Physiol Rev* 82: 47-95, 2002.
34. **Dudley GA, Castro MJ, Rogers S, and Apple DF, Jr.** A simple means of increasing muscle size after spinal cord injury: a pilot study. *Eur J Appl Physiol Occup Physiol* 80: 394-396, 1999.
35. **Dudley GA, Duvoisin MR, Convertino VA, and Buchanan P.** Alterations of the in vivo torque-velocity relationship of human skeletal muscle following 30 days exposure to simulated microgravity. *Aviat Space Environ Med* 60: 659-663, 1989.
36. **Dudley GA, Hather BM, and Buchanan P.** Skeletal muscle responses to unloading with special reference to man. *J Fla Med Assoc* 79: 525-529, 1992.

37. **Duguez S, Bartoli M, and Richard I.** Calpain 3: a key regulator of the sarcomere? *Febs J* 273: 3427-3436, 2006.
38. **Duvoisin MR, Convertino VA, Buchanan P, Gollnick PD, and Dudley GA.** Characteristics and preliminary observations of the influence of electromyostimulation on the size and function of human skeletal muscle during 30 days of simulated microgravity. *Aviat Space Environ Med* 60: 671-678, 1989.
39. **Ferrando AA, Stuart CA, Brunder DG, and Hillman GR.** Magnetic resonance imaging quantitation of changes in muscle volume during 7 days of strict bed rest. *Aviat Space Environ Med* 66: 976-981, 1995.
40. **Fitts RH, Riley DR, and Widrick JJ.** Physiology of a microgravity environment invited review: microgravity and skeletal muscle. *J Appl Physiol* 89: 823-839, 2000.
41. **Frimel TN, Kapadia F, Gaidosh GS, Li Y, Walter GA, and Vandenberg K.** A model of muscle atrophy using cast immobilization in mice. *Muscle Nerve* 32: 672-674, 2005.
42. **Funato K, Matsuo A, Yata H, Akima H, Suzuki Y, Gunji A, and Fukunaga T.** Changes in force-velocity and power output of upper and lower extremity musculature in young subjects following 20 days bed rest. *J Gravit Physiol* 4: S22-30, 1997.
43. **Furukawa-Hibi Y, Kobayashi Y, Chen C, and Motoyama N.** FOXO transcription factors in cell-cycle regulation and the response to oxidative stress. *Antioxid Redox Signal* 7: 752-760, 2005.
44. **Furuno K, and Goldberg AL.** The activation of protein degradation in muscle by Ca²⁺ or muscle injury does not involve a lysosomal mechanism. *Biochem J* 237: 859-864, 1986.
45. **Giannelli G, De Marzo A, Marinosci F, and Antonaci S.** Matrix metalloproteinase imbalance in muscle disuse atrophy. *Histol Histopathol* 20: 99-106, 2005.
46. **Glass DJ.** Signalling pathways that mediate skeletal muscle hypertrophy and atrophy. *Nat Cell Biol* 5: 87-90, 2003.
47. **Glickman MH, and Ciechanover A.** The ubiquitin-proteasome proteolytic pathway: destruction for the sake of construction. *Physiol Rev* 82: 373-428, 2002.
48. **Gogia P, Schneider VS, LeBlanc AD, Krebs J, Kasson C, and Pientok C.** Bed rest effect on extremity muscle torque in healthy men. *Arch Phys Med Rehabil* 69: 1030-1032, 1988.

49. **Goldspink G.** Gene expression in muscle in response to exercise. *J Muscle Res Cell Motil* 24: 121-126, 2003.
50. **Goldspink G, and Yang SY.** Effects of activity on growth factor expression. *Int J Sport Nutr Exerc Metab* 11 Suppl: S21-27, 2001.
51. **Goll DE, Thompson VF, Li H, Wei W, and Cong J.** The calpain system. *Physiol Rev* 83: 731-801, 2003.
52. **Gomes MD, Lecker SH, Jagoe RT, Navon A, and Goldberg AL.** Atrogin-1, a muscle-specific F-box protein highly expressed during muscle atrophy. *Proc Natl Acad Sci U S A* 98: 14440-14445, 2001.
53. **Gregory CM, Vandenborne K, Castro MJ, and Dudley GA.** Human and rat skeletal muscle adaptations to spinal cord injury. *Can J Appl Physiol* 28: 491-500, 2003.
54. **Grune T, Merker K, Sandig G, and Davies KJ.** Selective degradation of oxidatively modified protein substrates by the proteasome. *Biochem Biophys Res Commun* 305: 709-718, 2003.
55. **Guttridge DC, Mayo MW, Madrid LV, Wang CY, and Baldwin AS, Jr.** NF-kappaB-induced loss of MyoD messenger RNA: possible role in muscle decay and cachexia. *Science* 289: 2363-2366, 2000.
56. **Haddad F, Adams GR, Bodell PW, and Baldwin KM.** Isometric resistance exercise fails to counteract skeletal muscle atrophy processes during the initial stages of unloading. *J Appl Physiol* 100: 433-441, 2006.
57. **Halliwell B.** Antioxidant defence mechanisms: from the beginning to the end (of the beginning). *Free Radic Res* 31: 261-272, 1999.
58. **Han XY, Wang W, Myllyla R, Virtanen P, Karpakka J, and Takala TE.** mRNA levels for alpha-subunit of prolyl 4-hydroxylase and fibrillar collagens in immobilized rat skeletal muscle. *J Appl Physiol* 87: 90-96, 1999.
59. **Hather BM, Adams GR, Tesch PA, and Dudley GA.** Skeletal muscle responses to lower limb suspension in humans. *J Appl Physiol* 72: 1493-1498, 1992.
60. **Herrmann J, Lerman LO, and Lerman A.** Ubiquitin and ubiquitin-like proteins in protein regulation. *Circ Res* 100: 1276-1291, 2007.
61. **Hespel P, Op't Eijnde B, Van Leemputte M, Urso B, Greenhaff PL, Labarque V, Dymarkowski S, Van Hecke P, and Richter EA.** Oral creatine supplementation facilitates the rehabilitation of disuse atrophy and alters the expression of muscle myogenic factors in humans. *J Physiol* 536: 625-633, 2001.

62. **Hoffman EP, and Nader GA.** Balancing muscle hypertrophy and atrophy. *Nat Med* 10: 584-585, 2004.
63. **Hortobagyi T, Dempsey L, Fraser D, Zheng D, Hamilton G, Lambert J, and Dohm L.** Changes in muscle strength, muscle fibre size and myofibrillar gene expression after immobilization and retraining in humans. *J Physiol* 524: 293-304, 2000.
64. **Hunter RB, Stevenson E, Koncarevic A, Mitchell-Felton H, Essig DA, and Kandarian SC.** Activation of an alternative NF-kappaB pathway in skeletal muscle during disuse atrophy. *Faseb J* 16: 529-538, 2002.
65. **Ikemoto M, Nikawa T, Takeda S, Watanabe C, Kitano T, Baldwin KM, Izumi R, Nonaka I, Towatari T, Teshima S, Rokutan K, and Kishi K.** Space shuttle flight (STS-90) enhances degradation of rat myosin heavy chain in association with activation of ubiquitin-proteasome pathway. *Faseb J* 15: 1279-1281, 2001.
66. **Isfort RJ, Wang F, Greis KD, Sun Y, Keough TW, Bodine SC, and Anderson NL.** Proteomic analysis of rat soleus and tibialis anterior muscle following immobilization. *J Chromatogr B Analyt Technol Biomed Life Sci* 769: 323-332, 2002.
67. **Isfort RJ, Wang F, Greis KD, Sun Y, Keough TW, Farrar RP, Bodine SC, and Anderson NL.** Proteomic analysis of rat soleus muscle undergoing hindlimb suspension-induced atrophy and reweighting hypertrophy. *Proteomics* 2: 543-550, 2002.
68. **Jackman RW, and Kandarian SC.** The molecular basis of skeletal muscle atrophy. *Am J Physiol Cell Physiol* 287: C834-843, 2004.
69. **Jayaraman A, Gregory CM, Bowden M, Stevens JE, Shah P, Behrman AL, and Vandenborne K.** Lower extremity skeletal muscle function in persons with incomplete spinal cord injury. *Spinal Cord* 44: 680-687, 2006.
70. **Jones SW, Hill RJ, Krasney PA, O'Conner B, Peirce N, and Greenhaff PL.** Disuse atrophy and exercise rehabilitation in humans profoundly affects the expression of genes associated with the regulation of skeletal muscle mass. *Faseb J* 18: 1025-1027, 2004.
71. **Kabe Y, Ando K, Hirao S, Yoshida M, and Handa H.** Redox regulation of NF-kappaB activation: distinct redox regulation between the cytoplasm and the nucleus. *Antioxid Redox Signal* 7: 395-403, 2005.
72. **Kaminski HJ, and Andrade FH.** Nitric oxide: biologic effects on muscle and role in muscle diseases. *Neuromuscul Disord* 11: 517-524, 2001.
73. **Kandarian SC, and Stevenson EJ.** Molecular events in skeletal muscle during disuse atrophy. *Exerc Sport Sci Rev* 30: 111-116, 2002.

74. **Kerscher O, Felberbaum R, and Hochstrasser M.** Modification of proteins by ubiquitin and ubiquitin-like proteins. *Annu Rev Cell Dev Biol* 22: 159-180, 2006.
75. **Kitahara A, Hamaoka T, Murase N, Homma T, Kurosawa Y, Ueda C, Nagasawa T, Ichimura S, Motobe M, Yashiro K, Nakano S, and Katsumura T.** Deterioration of muscle function after 21-day forearm immobilization. *Med Sci Sports Exerc* 35: 1697-1702, 2003.
76. **Kjaer M.** Role of extracellular matrix in adaptation of tendon and skeletal muscle to mechanical loading. *Physiol Rev* 84: 649-698, 2004.
77. **Kobzik L, Reid MB, Bredt DS, and Stamler JS.** Nitric oxide in skeletal muscle. *Nature* 372: 546-548, 1994.
78. **Koh TJ, and Tidball JG.** Nitric oxide inhibits calpain-mediated proteolysis of talin in skeletal muscle cells. *Am J Physiol Cell Physiol* 279: C806-812, 2000.
79. **Koncarevic A, Jackman RW, and Kandarian SC.** The ubiquitin-protein ligase Nedd4 targets Notch1 in skeletal muscle and distinguishes the subset of atrophies caused by reduced muscle tension. *Faseb J* 21: 427-437, 2007.
80. **Kondo H, Nakagaki I, Sasaki S, Hori S, and Itokawa Y.** Mechanism of oxidative stress in skeletal muscle atrophied by immobilization. *Am J Physiol* 265: E839-844, 1993.
81. **Kondo H, Nishino K, and Itokawa Y.** Hydroxyl radical generation in skeletal muscle atrophied by immobilization. *FEBS Lett* 349: 169-172, 1994.
82. **Kotamraju S, Chitambar CR, Kalivendi SV, Joseph J, and Kalyanaraman B.** Transferrin receptor-dependent iron uptake is responsible for doxorubicin-mediated apoptosis in endothelial cells: role of oxidant-induced iron signaling in apoptosis. *J Biol Chem* 277: 17179-17187, 2002.
83. **Kourie JI.** Interaction of reactive oxygen species with ion transport mechanisms. *Am J Physiol* 275: C1-24, 1998.
84. **Kramerova I, Kudryashova E, Venkatraman G, and Spencer MJ.** Calpain 3 participates in sarcomere remodeling by acting upstream of the ubiquitin-proteasome pathway. *Hum Mol Genet* 14: 2125-2134, 2005.
85. **Krawiec BJ, Frost RA, Vary TC, Jefferson LS, and Lang CH.** Hindlimb casting decreases muscle mass in part by proteasome-dependent proteolysis but independent of protein synthesis. *Am J Physiol Endocrinol Metab* 289: E969-980, 2005.

86. **Ku Z, Yang J, Menon V, and Thomason DB.** Decreased polysomal HSP-70 may slow polypeptide elongation during skeletal muscle atrophy. *Am J Physiol* 268: C1369-1374, 1995.
87. **Latres E, Amini AR, Amini AA, Griffiths J, Martin FJ, Wei Y, Lin HC, Yancopoulos GD, and Glass DJ.** Insulin-like growth factor-1 (IGF-1) inversely regulates atrophy-induced genes via the phosphatidylinositol 3-kinase/Akt/mammalian target of rapamycin (PI3K/Akt/mTOR) pathway. *J Biol Chem* 280: 2737-2744, 2005.
88. **LeBlanc A, Gogia P, Schneider V, Krebs J, Schonfeld E, and Evans H.** Calf muscle area and strength changes after five weeks of horizontal bed rest. *Am J Sports Med* 16: 624-629, 1988.
89. **LeBlanc AD, Schneider VS, Evans HJ, Pientok C, Rowe R, and Spector E.** Regional changes in muscle mass following 17 weeks of bed rest. *J Appl Physiol* 73: 2172-2178, 1992.
90. **Li HH, Kedar V, Zhang C, McDonough H, Arya R, Wang DZ, and Patterson C.** Atrogin-1/muscle atrophy F-box inhibits calcineurin-dependent cardiac hypertrophy by participating in an SCF ubiquitin ligase complex. *J Clin Invest* 114: 1058-1071, 2004.
91. **Li YP, Chen Y, Li AS, and Reid MB.** Hydrogen peroxide stimulates ubiquitin-conjugating activity and expression of genes for specific E2 and E3 proteins in skeletal muscle myotubes. *Am J Physiol Cell Physiol* 285: C806-812, 2003.
92. **Li YP, and Reid MB.** NF-kappaB mediates the protein loss induced by TNF-alpha in differentiated skeletal muscle myotubes. *Am J Physiol Regul Integr Comp Physiol* 279: R1165-1170, 2000.
93. **MacDougall JD, Elder GC, Sale DG, Moroz JR, and Sutton JR.** Effects of strength training and immobilization on human muscle fibres. *Eur J Appl Physiol Occup Physiol* 43: 25-34, 1980.
94. **Mackey AL, Donnelly AE, Turpeenniemi-Hujanen T, and Roper HP.** Skeletal muscle collagen content in humans after high-force eccentric contractions. *J Appl Physiol* 97: 197-203, 2004.
95. **McElhinny AS, Kakinuma K, Sorimachi H, Labeit S, and Gregorio CC.** Muscle-specific RING finger-1 interacts with titin to regulate sarcomeric M-line and thick filament structure and may have nuclear functions via its interaction with glucocorticoid modulatory element binding protein-1. *J Cell Biol* 157: 125-136, 2002.
96. **Miles MP, Clarkson PM, Bean M, Ambach K, Mulroy J, and Vincent K.** Muscle function at the wrist following 9 d of immobilization and suspension. *Med Sci Sports Exerc* 26: 615-623, 1994.

97. **Morey-Holton ER, and Globus RK.** Hindlimb unloading rodent model: technical aspects. *J Appl Physiol* 92: 1367-1377, 2002.
98. **Mrosek M, Labeit D, Witt S, Heerklotz H, von Castelmur E, Labeit S, and Mayans O.** Molecular determinants for the recruitment of the ubiquitin-ligase MuRF-1 onto M-line titin. *Faseb J* 21: 1383-1392, 2007.
99. **Nader GA.** Molecular determinants of skeletal muscle mass: getting the "AKT" together. *Int J Biochem Cell Biol* 37: 1985-1996, 2005.
100. **Nguyen HX, and Tidball JG.** Expression of a muscle-specific, nitric oxide synthase transgene prevents muscle membrane injury and reduces muscle inflammation during modified muscle use in mice. *J Physiol* 550: 347-356, 2003.
101. **Nikawa T, Ishidoh K, Hirasaka K, Ishihara I, Ikemoto M, Kano M, Kominami E, Nonaka I, Ogawa T, Adams GR, Baldwin KM, Yasui N, Kishi K, and Takeda S.** Skeletal muscle gene expression in space-flown rats. *Faseb J* 18: 522-524, 2004.
102. **Ogawa T, Furochi H, Mameoka M, Hirasaka K, Onishi Y, Suzue N, Oarada M, Akamatsu M, Akima H, Fukunaga T, Kishi K, Yasui N, Ishidoh K, Fukuoka H, and Nikawa T.** Ubiquitin ligase gene expression in healthy volunteers with 20-day bedrest. *Muscle Nerve* 34: 463-469, 2006.
103. **Ohira Y, Yoshinaga T, Nonaka I, Ohara M, Yoshioka T, Yamashita-Goto K, Izumi R, Yasukawa K, Sekiguchi C, Shenkman BS, and Kozzlovskaya IB.** Histochemical responses of human soleus muscle fibers to long-term bedrest with or without countermeasures. *Jpn J Physiol* 50: 41-47, 2000.
104. **Ohira Y, Yoshinaga T, Ohara M, Nonaka I, Yoshioka T, Yamashita-Goto K, Shenkman BS, Kozlovskaya IB, Roy RR, and Edgerton VR.** Myonuclear domain and myosin phenotype in human soleus after bed rest with or without loading. *J Appl Physiol* 87: 1776-1785, 1999.
105. **Pantano C, Reynaert NL, van der Vliet A, and Janssen-Heininger YM.** Redox-sensitive kinases of the nuclear factor-kappaB signaling pathway. *Antioxid Redox Signal* 8: 1791-1806, 2006.
106. **Pattison JS, Folk LC, Madsen RW, and Booth FW.** Selected Contribution: Identification of differentially expressed genes between young and old rat soleus muscle during recovery from immobilization-induced atrophy. *J Appl Physiol* 95: 2171-2179, 2003.
107. **Ploutz-Snyder LL, Tesch PA, Crittenden DJ, and Dudley GA.** Effect of unweighting on skeletal muscle use during exercise. *J Appl Physiol* 79: 168-175, 1995.

108. **Ploutz-Snyder LL, Tesch PA, Hather BM, and Dudley GA.** Vulnerability to dysfunction and muscle injury after unloading. *Arch Phys Med Rehabil* 77: 773-777, 1996.
109. **Ponka P, Beaumont C, and Richardson DR.** Function and regulation of transferrin and ferritin. *Semin Hematol* 35: 35-54, 1998.
110. **Powell SR.** The antioxidant properties of zinc. *J Nutr* 130: 1447S-1454, 2000.
111. **Powers SK, Kavazis AN, and DeRuisseau KC.** Mechanisms of disuse muscle atrophy: role of oxidative stress. *Am J Physiol Regul Integr Comp Physiol* 288: R337-344, 2005.
112. **Powers SK, Kavazis AN, and McClung JM.** Oxidative stress and disuse muscle atrophy. *J Appl Physiol* 2007.
113. **Raffaello A, Laveder P, Romualdi C, Bean C, Toniolo L, Germinario E, Megighian A, Danieli-Betto D, Reggiani C, and Lanfranchi G.** Denervation in murine fast-twitch muscle: short-term physiological changes and temporal expression profiling. *Physiol Genomics* 25: 60-74, 2006.
114. **Rall LC, Rosen CJ, Dolnikowski G, Hartman WJ, Lundgren N, Abad LW, Dinarello CA, and Roubenoff R.** Protein metabolism in rheumatoid arthritis and aging. Effects of muscle strength training and tumor necrosis factor alpha. *Arthritis Rheum* 39: 1115-1124, 1996.
115. **Reid MB.** Response of the ubiquitin-proteasome pathway to changes in muscle activity. *Am J Physiol Regul Integr Comp Physiol* 288: R1423-1431, 2005.
116. **Reznick AZ, Menashe O, Bar-Shai M, Coleman R, and Carmeli E.** Expression of matrix metalloproteinases, inhibitor, and acid phosphatase in muscles of immobilized hindlimbs of rats. *Muscle Nerve* 27: 51-59, 2003.
117. **Richard I, Broux O, Allamand V, Fougousse F, Chiannikulchai N, Bourg N, Brenguier L, Devaud C, Pasturaud P, Roudaut C, and et al.** Mutations in the proteolytic enzyme calpain 3 cause limb-girdle muscular dystrophy type 2A. *Cell* 81: 27-40, 1995.
118. **Ricort JM.** Insulin-like growth factor binding protein (IGFBP) signalling. *Growth Horm IGF Res* 14: 277-286, 2004.
119. **Rommel C, Bodine SC, Clarke BA, Rossman R, Nunez L, Stitt TN, Yancopoulos GD, and Glass DJ.** Mediation of IGF-1-induced skeletal myotube hypertrophy by PI(3)K/Akt/mTOR and PI(3)K/Akt/GSK3 pathways. *Nat Cell Biol* 3: 1009-1013, 2001.

120. **Rozier CK, Elder JD, and Brown M.** Prevention of atrophy by isometric exercise of a casted leg. *J Sports Med Phys Fitness* 19: 191-194, 1979.
121. **Sadhu C, and Gedamu L.** Regulation of human metallothionein (MT) genes. Differential expression of MTI-F, MTI-G, and MTII-A genes in the hepatoblastoma cell line (HepG2). *J Biol Chem* 263: 2679-2684, 1988.
122. **Sandri M, Sandri C, Gilbert A, Skurk C, Calabria E, Picard A, Walsh K, Schiaffino S, Lecker SH, and Goldberg AL.** Foxo transcription factors induce the atrophy-related ubiquitin ligase atrogin-1 and cause skeletal muscle atrophy. *Cell* 117: 399-412, 2004.
123. **Shah PK, Stevens JE, Gregory CM, Pathare NC, Jayaraman A, Bickel SC, Bowden M, Behrman AL, Walter GA, Dudley GA, and Vandenborne K.** Lower-extremity muscle cross-sectional area after incomplete spinal cord injury. *Arch Phys Med Rehabil* 87: 772-778, 2006.
124. **Shen C, Ye Y, Robertson SE, Lau AW, Mak DO, and Chou MM.** Calcium/calmodulin regulates ubiquitination of the ubiquitin-specific protease TRE17/USP6. *J Biol Chem* 280: 35967-35973, 2005.
125. **Shenkman B, Belozeroва I, Nemirovskaya T, Cheglova I, Yudaitcheva A, Kiseleva E, and Mazin M.** Time-course of human muscle fibre size reduction during head-down tilt bedrest. *J Gravit Physiol* 5: P71-72, 1998.
126. **Smith IJ, and Dodd SL.** Calpain activation causes a proteasome-dependent increase in protein degradation and inhibits the Akt signalling pathway in rat diaphragm muscle. *Exp Physiol* 92: 561-573, 2007.
127. **St-Amand J, Okamura K, Matsumoto K, Shimizu S, and Sogawa Y.** Characterization of control and immobilized skeletal muscle: an overview from genetic engineering. *Faseb J* 15: 684-692, 2001.
128. **Stevenson EJ, Giresi PG, Koncarevic A, and Kandarian SC.** Global analysis of gene expression patterns during disuse atrophy in rat skeletal muscle. *J Physiol* 551: 33-48, 2003.
129. **Stevenson EJ, Koncarevic A, Giresi PG, Jackman RW, and Kandarian SC.** Transcriptional profile of a myotube starvation model of atrophy. *J Appl Physiol* 98: 1396-1406, 2005.
130. **Sugiura T, Abe N, Nagano M, Goto K, Sakuma K, Naito H, Yoshioka T, and Powers SK.** Changes in PKB/Akt and calcineurin signaling during recovery in atrophied soleus muscle induced by unloading. *Am J Physiol Regul Integr Comp Physiol* 288: R1273-1278, 2005.

131. **Taillandier D, Aurousseau E, Meynial-Denis D, Bechet D, Ferrara M, Cottin P, Ducastaing A, Bigard X, Guezennec CY, Schmid HP, and et al.** Coordinate activation of lysosomal, Ca²⁺-activated and ATP-ubiquitin-dependent proteinases in the unweighted rat soleus muscle. *Biochem J* 316 (Pt 1): 65-72, 1996.
132. **Tesch PA, and Berg HE.** Effects of spaceflight on muscle. *J Gravit Physiol* 5: P19-22, 1998.
133. **Thom JM, Thompson MW, Ruell PA, Bryant GJ, Fonda JS, Harmer AR, De Jonge XA, and Hunter SK.** Effect of 10-day cast immobilization on sarcoplasmic reticulum calcium regulation in humans. *Acta Physiol Scand* 172: 141-147, 2001.
134. **Tidball JG, and Spencer MJ.** Expression of a calpastatin transgene slows muscle wasting and obviates changes in myosin isoform expression during murine muscle disuse. *J Physiol* 545: 819-828, 2002.
135. **Trappe SW, Trappe TA, Lee GA, Widrick JJ, Costill DL, and Fitts RH.** Comparison of a space shuttle flight (STS-78) and bed rest on human muscle function. *J Appl Physiol* 91: 57-64, 2001.
136. **Urso ML, Chen YW, Scrimgeour AG, Lee PC, Lee KF, and Clarkson PM.** Alterations in mRNA expression and protein products following spinal cord injury in humans. *J Physiol* 579: 877-892, 2007.
137. **Urso ML, Scrimgeour AG, Chen YW, Thompson PD, and Clarkson PM.** Analysis of human skeletal muscle after 48 h immobilization reveals alterations in mRNA and protein for extracellular matrix components. *J Appl Physiol* 101: 1136-1148, 2006.
138. **Vandenburgh HH, Karlisch P, Shansky J, and Feldstein R.** Insulin and IGF-I induce pronounced hypertrophy of skeletal myofibers in tissue culture. *Am J Physiol* 260: C475-484, 1991.
139. **Veldhuizen JW, Verstappen FT, Vroemen JP, Kuipers H, and Greep JM.** Functional and morphological adaptations following four weeks of knee immobilization. *Int J Sports Med* 14: 283-287, 1993.
140. **Vile GF, Basu-Modak S, Waltner C, and Tyrrell RM.** Heme oxygenase 1 mediates an adaptive response to oxidative stress in human skin fibroblasts. *Proc Natl Acad Sci U S A* 91: 2607-2610, 1994.
141. **Voisin L, Breuille D, Combaret L, Pouyet C, Taillandier D, Aurousseau E, Obled C, and Attaix D.** Muscle wasting in a rat model of long-lasting sepsis results from the activation of lysosomal, Ca²⁺-activated, and ubiquitin-proteasome proteolytic pathways. *J Clin Invest* 97: 1610-1617, 1996.

142. **Vyas DR, Spangenburg EE, Abraha TW, Childs TE, and Booth FW.** GSK-3beta negatively regulates skeletal myotube hypertrophy. *Am J Physiol Cell Physiol* 283: C545-551, 2002.
143. **Weinstein RB, Slentz MJ, Webster K, Takeuchi JA, and Tischler ME.** Lysosomal proteolysis in distally or proximally denervated rat soleus muscle. *Am J Physiol* 273: R1562-1565, 1997.
144. **Yajid F, Mercier JG, Mercier BM, Dubouchaud H, and Prefaut C.** Effects of 4 wk of hindlimb suspension on skeletal muscle mitochondrial respiration in rats. *J Appl Physiol* 84: 479-485, 1998.
145. **Young P, Deveraux Q, Beal RE, Pickart CM, and Rechsteiner M.** Characterization of two polyubiquitin binding sites in the 26 S protease subunit 5a. *J Biol Chem* 273: 5461-5467, 1998.
146. **Yue GH, Bilodeau M, Hardy PA, and Enoka RM.** Task-dependent effect of limb immobilization on the fatigability of the elbow flexor muscles in humans. *Exp Physiol* 82: 567-592, 1997.

CHAPTER III

GLOBAL GENE EXPRESSION CHANGES WITH SKELETAL MUSCLE

UNLOADING AND RELOADING IN HUMANS

Abstract

PURPOSE: Although short-term disuse does not result in measurable muscle atrophy, recent studies suggest that molecular changes associated with protein degradation may be initiated within days of the onset of a disuse stimulus such as immobilization. However, little is known, about molecular changes accompanying disuse stimuli that allow free joint movement such as unloading (UL). This study sought to examine the global gene expression patterns following 48h UL and 24h reloading (RL) in human skeletal muscle. **METHODS:** Seven sedentary young men underwent 48h UL via unilateral lower limb suspension, followed by 24h RL. Biopsy samples of the left vastus lateralis were collected at baseline as well as after the UL and RL periods. Global gene expression changes were identified using Affymetrix microarrays (U133 Plus 2.0), gene clustering was performed using Genespring software, enriched functions within the dataset were identified using the Database for Annotations, Visualization and Integrated Discovery (DAVID), and significant canonical pathways were identified using Ingenuity Pathway Analysis (IPA). Candidate genes were confirmed via qRT-PCR, and relative protein levels were measured via Western blot. **RESULTS:** Of the upregulated genes, the most enriched functional group in the dataset was related to protein ubiquitination, as was the highest ranked canonical pathway (the protein ubiquitination pathway). Furthermore, the oxidative stress response pathway was the second highest ranked canonical pathway. Of the downregulated genes, functions related to the mitochondrion and aerobic

metabolism were the mostly highly enriched. In general, gene expression patterns following UL persisted following RL. qRT-PCR analysis confirmed increases in mRNA for UPP-related E3 ligase atrogin1 (but not accompanying increases in protein products) and stress response gene HMOX1 (which showed a trend towards increases in protein products at 48h UL) as well as extracellular matrix (ECM) component COL4.

CONCLUSIONS: Short-term skeletal muscle unloading in humans led to increases in transcription of protein degradation and stress response genes as well as decreases in genes associated with mitochondrial metabolism; the gene expression patterns were not readily reversed upon reloading suggesting that molecular responses to short-term periods of skeletal muscle inactivity may persist even after activity resumes.

Introduction

Disuse muscle atrophy occurs in response to immobilization (IM) (40, 80), unloading (UL) (2, 7-8), bed rest (9-10, 61), spaceflight (2, 75, 78), and spinal cord injury (SCI) (79). Studies in humans have documented the effects of disuse on skeletal muscle structure and function (7-8, 11, 27, 34, 43, 58) such as decreases in muscle size and strength as well as increases in rate of muscle fatigue. The underlying mechanisms regulating these changes are not well understood, though investigations in IM, UL, and denervation (13-14, 31) in animals have shown that there are coordinated alterations in expression of genes encoding for proteins that may function in the initiation of the muscle atrophy process. Differential gene expression has been detected for molecules related to protein degradation and synthesis (13-14, 31), extracellular matrix (ECM) remodeling (4-5, 30), oxidative stress response (reviewed in (66)), and metabolism (50). Also, it has

been proposed that key regulators of muscle atrophy are likely those most sensitive to the disuse stimulus (12).

Recently, studies have been undertaken in humans to investigate the gene expression changes in skeletal muscle associated with disuse (17, 25, 40, 80). As with the animal models, these studies have shown alterations in expression of components of the ubiquitin proteasome pathway (UPP) such as fbox-only protein 32 (FBXO32, aka atrogin1) and muscle specific ring finger 1 (MuRF1), ECM components such as collagen, and metabolic enzymes such as NADH dehydrogenase and pyruvate dehydrogenase. With the exception of one study from our laboratory (80) that measured gene expression following 48h of knee IM, these investigations have measured time points from 5d – 3wk of IM (17, 25, 40). However, measurable proteolysis has been detected as early as 72h post-unloading in humans (76), and therefore, molecular atrophy triggers (such as alterations in the transcription of key genes) likely occur prior to that time point in humans.

This study examined the global gene expression patterns following short-term unloading (48h UL) and reloading (24h RL) in human skeletal muscle using a human suspension model most analogous to hindlimb unloading in rodents, unilateral lower limb suspension (ULLS). By learning more about the molecular events accompanying the earliest stages of disuse, we sought to uncover information that may aid in future efforts to prevent or attenuate disuse atrophy. Furthermore, by also investigating transcription immediately following RL, we aimed to discover key genes that were most sensitive to disuse stimuli. Microarray technology and high-throughput array analysis provided us with the tools to analyze the global expression patterns of thousands of genes within each

tissue sample, and these technologies allowed us to gain valuable insight by investigating the multifaceted regulation of biological processes associated with disuse.

Methods

Subjects

Seven ($n = 7$) sedentary young men were recruited from the University of Massachusetts community (for demographic data see Table 3.1). Those with bleeding problems, known allergies to Lidocaine, orthopedic problems, or use of medications that could increase bleeding (such as aspirin) were excluded from the study, as were individuals who are taking muscle building supplements or restricting caloric intake. All subjects signed an informed consent form approved by the University of Massachusetts and Hartford Hospital institutional review boards and completed a medical history questionnaire and physical activity questionnaire before being enrolled in the study to insure they met the inclusion/exclusion criteria. In addition, each potential subject was carefully screened to ensure that he was aware of the inconvenience inherent in the UL protocol, understood the potential discomfort from the biopsy procedure, and felt confident that he could comply with all study requirements.

Unloading and Reloading Protocol

Lower limb UL was achieved using the ULLS model which required that subjects wear a shoe with a 10-cm sole (Kintec Footlabs, Surrey, BC) on the right foot. The left foot did not have contact with the ground. Therefore, the left lower limb was unloaded for the duration of the 48h UL protocol. All ambulatory activity was performed on crutches with only the right foot having contact with the ground. Although the UL leg was free to move, no load was placed on it, and any physical activity requiring use of the

left quadriceps muscles was restricted. Berg *et al.* (7) and others (3, 20, 33) have used this ULLS model up to 6 wk. Compliance during the UL phase of the current study was confirmed through the use of activity monitors (Model #7164 Computer Science and Applications, Inc., Shalimar FL) worn on both ankles, which showed a 29% - 35% reduction in acceleration in the UL leg compared to the loaded leg. Following 48h UL, subjects were instructed to ambulate normally for 24h, which constituted the RL condition.

Biopsies

Three biopsies were taken from the left vastus lateralis of each subject over the course of the study. A baseline biopsy was taken 2wk prior to UL. Biopsies were also taken immediately following 48h UL and 24h RL. All biopsy procedures were conducted at Hartford Hospital and were taken at the same time of day to reduce circadian influences. Subjects were fed a standardized meal 3h prior to each biopsy because meal patterns alter the activity of certain genes related to muscle atrophy and hypertrophy (22).

Percutaneous needle muscle biopsies were obtained using a Bergstrom 5-mm biopsy needle (Depuy, Warsaw, IN) in a sterile field. First, skin was lightly anesthetized with 2% Lidocaine hydrochloride solution. Next, a small (5-6mm) incision was made through the skin and muscle fascia, and the biopsy needle was inserted. Up to 150mg of tissue was removed and divided into 3 aliquots (up to 50mg each). Biopsy samples were immediately snap-frozen in liquid nitrogen upon excision. All samples were stored at -80° C until analysis. After each biopsy, subjects were escorted home and contacted every 12hr for the next 3d to ensure the biopsy site was healing properly.

Expression Profiling

Affymetrix Human Genome U133 Plus 2.0 microarrays for analysis of over 47,000 transcripts were used for this study. The procedures including total RNA isolation, cDNA synthesis, cRNA labeling, microarray hybridization and image acquiring was done as described in our previous publications (18). Briefly, total RNA isolated with TRIzol reagent and purified with RNeasy MinElute Cleanup Kit (Qiagen, Valencia, CA). Three microgram of total RNA from each sample were converted into double-stranded cDNA then cRNA using one-cycle target labeling and control reagents and protocol (Affymetrix, Santa Clara, CA). After purification using GeneChip® Sample Cleanup Module (Affymetrix, Santa Clara, CA), biotin-labeled cRNA was then fragmented randomly prior to hybridizing to the microarrays. Each array was washed and stained on the Affymetrix Fluidics Station 450, and then probe arrays were scanned via the GeneChip® Scanner 3000. The quality control criteria developed at Children's National Medical Center Microarray Center for each array were followed (1, 18).

Absolute analysis of Affymetrix "raw" data was conducted using Affymetrix MAS5.0 and DNA-Chip Analyzer software (dCHIP) (52, 54). The data were then imported into the GeneSpring 7.0 (Silicon Genetics, Redwood City, CA) for data filtering and statistical analysis. First, genes with 2 "present calls" (~10% of the total arrays) were selected for statistical analysis. Probe sets showing significant ($p < 0.05$) expression changes (using Welch's *t*-test) in both MAS5.0 and dCHIP were retained for hierarchical clustering, functional and pathway analysis.

Functional and Pathway Analysis of Expression Profiles

First, a two-dimensional cluster map was constructed using Genespring. Cluster gene lists were then uploaded into the Database for Annotation, Visualization and Integrated Discovery (DAVID) (26), a web-accessible gene database provided by the National Institutes of Health (<http://david.abcc.ncifcrf.gov>). The functional classification tool in DAVID provides enrichment analysis and correction for multiple testing. For this study, the Benjamini and Hochberg false discovery rates (5% false positive discovery rate) was used. In DAVID, the magnitude of enrichment is represented as a fold-change such that the percentage of genes in the uploaded dataset belonging to a particular functional group is expressed as a ratio of the percentage of genes belonging to that functional group in the entire human genome. In the present study, functional groups passed filtering if they that not only reached statistical significance after multiple testing correction ($p < 0.05$), but that also reached an enrichment level ≥ 1.5 -fold as directed by Huange *et al.* (36).

Clusters which contained functional groups passing the filtering criteria were then uploaded into Ingenuity Pathway Analysis (IPA) (Ingenuity Systems, Redwood City, CA) in order to identify canonical pathways that were altered by the 48h UL and 24h RL conditions. The significance of the association between the genes in each dataset and the canonical pathway was determined by using Fischer's exact test to calculate a p-value determining the probability that the association between the genes in the dataset and the canonical pathway was explained by chance alone. Pathways were then ranked according to p-value.

RNA isolation and cDNA synthesis

Total mRNA was isolated using TRIZOL reagent (following manufacturer's instructions) and quantified via spectrophotometry (Nanodrop, Wilmington, DE). Equal amounts of total RNA was synthesized into cDNA using a First-Strand cDNA Synthesis kit (Fermentas, Hanover, MD). ABgene Absolute qPCR SYBR Green Master Mix (ABgene, Surrey, UK) with ROX dye was used for all PCR protocols. Forward and reverse primers (Integrated DNA Technologies, Coralville, IA) were designed using NCBI gene sequences with IDT DNA SciTools for all genes of interest (Table 3.2).

Gene Expression Analysis via qRT-PCR

Reactions were run in 96-well plates with all cDNA samples from each treatment condition run in triplicate for each gene of interest. Thus, each plate allowed me to analyze two genes of interest and one reference standard for all subjects at all time points as well as no-template controls in triplicate for both the gene of interest and the reference standard (Glyceraldehyde-3-phosphate dehydrogenase (GAPDH)). The average Ct (comparative threshold) value for triplicate samples was be used for data analysis. Ct values were directly related to fluorescence of the respective SYBR-green probe after 40 cycles of amplification on a MX3000p Real-Time PCR System (Stratagene, La Jolla, CA) available in the central Bioinformatics and Genomics Facility at the University of Massachusetts. At the end of each reaction, a melting curve analysis was run to identify possible primer dimmers. The results of the melting curve analysis were confirmed, and appropriate product size determined via 2% agarose gel electrophoresis with ethidium bromide staining.

Protein Quantification

Protein was isolated using TRIZOL reagent (Invitrogen, Carlsbad, CA) and quantitated through measurement on a FLUostar plate reader (BMG Lab Technologies, Chapel Hill, NC) using NANO Orange reagent (. Target proteins were then quantified via Western blot analysis. Densitometry calculations of protein bands was used to compare changes in the relative amount of protein product between the 48h UL condition and baseline. 15ug of protein from each sample was loaded into 4-15% gradient sodium dodecyl sulfate (SDS) poly-acrylamide gels (Bio-Rad Laboratories, Hercules, CA) and separated by electrophoresis (60-90min@100v). Precision Plus Kaleidoscope Protein Standards (Bio-Rad Laboratories) was used as molecular weight markers for each gel.

Following electrophoresis, proteins were transferred onto a polyvinylidene difluoride membrane (Millipore, Inc, Billerica, MA) at 100v for 3h. Membranes were then cut horizontally (based on the placement of the molecular weight markers) so that the membrane could be probed for both the protein of interest at one position in the lane and GAPDH. (In the case of HMOX1, which is of similar molecular weight to GAPDH, the membrane was stripped and reprobbed).

Each membrane was then blocked for 2h at room temperature with rocking motion in a solution of PBST containing 5% non-fat dry milk (Carnation, Nestle, Wilkes-Barre, PA) and 0.1% Tween-20. The membrane was then washed (3X5 minutes each in 1XPBST) and incubated in primary antibody (HMOX1, atrogin1, or GAPDH), at the appropriate dilution (HMOX 1:1000, atrogin1 1:500, GAPDH 1:3500) with rocking motion overnight at 4 degrees. The membrane was then washed (5X10 min each with 1XPBST) and incubated in the appropriate HRP-labeled secondary antibody for 1.5

hr, after which 4X10 washes in 1XPBST followed. Membranes were then treated for 2m with enhanced chemiluminescence (ECL) solution (GE Healthcare, Piscataway, NJ) in clear plastic sheet holders, and exposed to Kodak film for the appropriate duration. Antibodies for GAPDH (rabbit polyclonal) and HMOX1 (rabbit monoclonal) were obtained from Abcam (Abcam, Cambridge, MA), as were anti-rabbit, anti-mouse, and anti-goat secondary antibodies. The antibody against atrogen1 (goat polyclonal) was acquired from Santa Cruz Biotechnology (Santa Cruz Biotechnology, Santa Cruz, CA)

Bands from each blot were scanned from the respective film using a Fotodyne Transilluminator (Hartland, WI) and quantified via densitometry using ImageJ software (NIH). To quantify protein products for each time point, densitometer values for protein bands in each condition were normalized to the densitometer value of the GAPDH protein band from the same sample. Although this is an arbitrary value (au), the calculated ratio identifies differences in protein product.

Results

Global Gene Expression

There were 1130 transcripts that were differentially expressed in this experiment ($p < 0.05$) with 48h UL and 24h RL conditions normalized to baseline. To manage the large number of transcripts differentially expressed on the genechip, hierarchical clustering was performed, and 8 expression clusters were identified (Figure 3.1). In Figure 1, conditions (Baseline, 48h UL, 24h RL) are represented in the horizontal dimension, and gene trees (clusters) are represented in the vertical dimension. Red color intensity represents upregulation (higher mRNA levels), blue color intensity represents downregulation (lower mRNA levels), and yellow color intensity represents no change in

gene expression. 48h UL and 24h RL conditions were normalized to baseline, and therefore, the color intensity for the baseline condition in Figure 1 is yellow. As the figure illustrates, a large number of transcripts showed expression changes such that gene upregulation following 48h UL persisted following 24h RL, while conversely, a considerable number of genes showing downregulation following 48 UL continued to be downregulated following 24h RL.

Functional Groups via DAVID

Genes within each cluster were grouped by function using DAVID. Of the 8 clusters identified through hierarchical clustering (Figure 1), only cluster 1 (n=579) and cluster 7 (n=241) contained functional groups that reach significance ($p < 0.05$) after correcting multiple testing. The changes in gene expression resulting from the short-term 48h UL and 24h RL conditions were small compared to those found with pathophysiological muscular conditions (18, 67) or longer disuse perturbations (61) to muscle; the majority of the gene expression changes in this study ranged from 1.2 – 1.5-fold up- or downregulated relative to baseline. Although the expression changes were modest with the subclinical intervention used in the current study, the majority of the p-values for these transcripts were $p < 0.005$. Table 3.3 summarizes the noteworthy functional groups for these two clusters.

Genes in cluster 1 (Table 3.3) were upregulated. Over-represented groups were related to ubiquitin conjugation, post-translational modification, and mRNA metabolism and were enriched 180-330% in this dataset compared to the number of genes related to these functions in the human genome. Enrichment values $\geq 150\%$ are generally considered biologically relevant (36). Because ubiquitin conjugation has consistently

been identified as an important component of disuse atrophy (13), members of the ubiquitin conjugation functional group from cluster 1 that met more stringent filtering criteria (± 1.2 -fold, $p \leq 0.01$) are listed in Table 3.4a. This functional group contained E2 conjugating enzymes, E3 ligases (including atrogin1), ubiquitin-specific proteases, and other proteolytic mediators, suggesting an increase in the activity of the UPP.

Interestingly, a number of the ubiquitin conjugation genes that were significantly upregulated following 48h UL were also upregulated following 24h RL; furthermore, the number of significantly upregulated transcripts almost doubled following 24h RL compared to the previous 48h UL (Table 3.4a).

Genes in cluster 7 (Table 3.3) were downregulated, and functional groups identified via DAVID were largely related to mitochondrial function, energy metabolism, and catalytic activity. These groups were over-represented in the dataset 150-530% (for full list of cluster 7 genes in these functional groups, see Appendix B, Tables B4 – B6). Because disuse has been shown to lead to decreases in mitochondrial activity (17), genes in cluster 7 associated with the mitochondrion (± 1.2 -fold, $p \leq 0.01$) are listed in Table 3.4b. These genes include those that encode proteins involved in mitochondrial metabolism—especially those related to aerobic metabolism. While the majority of upregulated ubiquitin conjugation genes in cluster 1 were upregulated both at 48h UL and 24h RL, only 5 of the 29 downregulated mitochondrial genes were significantly altered at 48h UL. The remaining genes in the functional group were not significantly altered until the subsequent 24h RL.

Canonical Pathways via IPA

Clusters 1 and 7 were analyzed using IPA, and canonical pathways were identified. For cluster 1, 10 canonical pathways reached significance ($p < 0.05$, Table 3.5). As expected, the top ranking pathway was the Protein ubiquitination pathway ($p = 0.0007$) with 11 participating genes, followed by the NRF2-mediated Oxidative Stress Response Pathway ($p = 0.005$) with 9 participating genes. Oxidative stress has been highlighted in the literature as a likely contributor to the initiation of muscle atrophy (reviewed in (66)), and genes from the dataset found in this canonical pathway included heme oxygenase-1 (HMOX1), the gene with the most dramatic differential expression in the entire dataset (48h UL=15.4-fold, $p = 0.002$; 24h RL=6.5-fold, $p = 0.007$). Other upregulated pathways identified by IPA were related to inflammation (IL-8 and IL-10 pathways), vitamin D receptor activity (VDR/RXR activation), and glucocorticoid signaling.

For cluster 7, 12 canonical pathways reached significance ($p < 0.05$, Table 3.5). The top three canonical pathways identified in IPA for cluster 7 included the oxidative phosphorylation, ubiquinone biosynthesis, and the citrate cycle pathways (Table 5). These results were in agreement with the DAVID analysis which identified mRNA downregulation related to mitochondrial function and especially to electron transport and energy production (Table 3.4b). Consistent with the DAVID functional categories, IPA revealed a greater number of transcripts in these pathways reaching significance following 24h RL than following the previous 48h UL.

Protein Synthesis

Recent literature (76) has proposed that decreased protein synthesis plays an important role in the regulation of disuse muscle atrophy. Functional groups associated

with protein synthesis did not reach significance via DAVID or IPA. However, global screening, using search tools in NetAffx (<http://www.affymetrix.com>), did reveal that a previously identified key protein synthesis mediator, S6 kinase, 70kDa, polypeptide 1 (S6K1) (28) was, indeed, differentially expressed in the current dataset. S6K1, a participant in mTOR-mediated cell growth, was significantly upregulated following 24h RL (1.3-fold; $p=0.029$). However, other genes in this muscle growth pathway, such as TORC1 and 4EBP1, were not differentially expressed.

Gene Expression Confirmation

Four genes were chosen for expression confirmation via qRT-PCR (Table 3.6). Among the transcripts in the dataset, HMOX1 was chosen for analysis because it showed the greatest expression changes via microarray following both 48h UL and 24h RL conditions (15.4 and 6.51 respectively). E3 ligase atrogen1 was chosen for confirmation because it has previously been found to be a key regulator of disuse atrophy in humans and in animals; a member of the ubiquitin conjugation functional group in the DAVID analysis in this study, atrogen1 was upregulated via microarray across conditions (UL=1.4, RL=1.3). Collagen type IV, alpha-3 (COL4A3), a subunit of collagen-IV (COL4), was also upregulated via microarray (UL=1.7, RL=1.3), which was surprising because the down-regulation of COL4 has been previously proposed as an early trigger of disuse atrophy (80). Therefore, COL4A3 was chosen for expression confirmation (Table 7). Finally, because no probe-sets for E3 ligase MuRF1 existed on the U133 plus 2 Gene Chip, qRT-PCR was also performed for this gene, as it has been identified, along with atrogen1, as an important atrophy regulator. The qRT-PCR experiments verified that mRNA levels for HMOX1, atrogen1, and COL4 were significantly upregulated following

UL (Table 3.7) and that HMOX1 expression remained elevated following 24h RL. Consistent with previous findings in our laboratory, which showed no differential expression for MuRF1 following immobilization (80), there were no significant difference in MURF1 mRNA levels following either 48h UL or 24h RL compared to baseline (Table 7).

Protein Quantification

With limited protein available, protein products for only two of the genes confirmed via qRT-PCR were chosen for protein quantification: HMOX1 (Figure 3.2a) and atrogin1 (Figure 3.2b). Protein was not available for all subjects at all time points, but samples for 4 subjects were available at both baseline and 48h UL. There was a trend towards increased protein products for HMOX1 following 48h UL (Figure 3.2a, $p=0.09$) in agreement with the microarray and qRT-PCR data. Relative intensity of protein bands for HMOX1 increased for all 4 subjects (Figure 3.2b). There were no significant differences in protein products for atrogin1 48h UL relative to baseline (mean \pm S.E.=1.40 \pm 0.70, $p=0.74$).

Discussion

The major findings in this study were that: 1) of the upregulated genes, the most enriched functional group and highest ranked canonical pathway both were related to the UPP; 2) the oxidative stress response pathway was ranked second only to the protein ubiquitination pathway; 3) of the downregulated genes, the most enriched functional group and the three highest ranked canonical pathways were related to mitochondrial function—specifically to aerobic metabolism; and 4) general patterns showed differential gene expression in the same direction for both the 48h UL and 24h RL conditions with

greater numbers of significant changes following reloading. qRT-PCR confirmed upregulation of the UPP-related gene atrogin1 and oxidative stress-related gene HMOX1, while Western blotting showed a trend towards an increase in protein products for HMOX1. Furthermore, COL4 showed an increase in mRNA levels following 48h UL via microarray (which was confirmed through qRT-PCR).

The Ubiquitin Proteasome Pathway (UPP)

For cluster 1, which showed increased gene expression following both 48h UL and 24h RL (Figure 3.1), the most enriched functional group via DAVID, ubiquitin conjugation (Table 3.3) and highest ranked canonical pathway, protein ubiquitination (Table 3.5), were both related to the UPP. The UPP is the pathway by which proteins are tagged for destruction and then degraded by the proteasome. Increases in gene expression related to this pathway have been shown in both animal and human models of skeletal muscle atrophy. Differential expression at the very early time point of unloading (48h) in the current study is consistent with previous work in our laboratory showing changes in expression of UPP-related genes following 48h of immobilization (80) in which range of motion at the knee joint, but not load, was restricted. Furthermore, measurable increases in proteolysis have been shown as early as 72h post-ULLS (76); therefore, UPP gene expression with unloading, as found in the current study, may portend muscle catabolism and decreases in muscle size that have been found at later time points.

The highest ranked pathway identified via IPA was the protein ubiquitination pathway with Ubiquitin specific peptidases (USPs) and Proteasome 26S subunit non-ATPase 11 (PSMD11) mRNA increased following 48h UL (Table 3.5). USPs deubiquitinate (and therefore replenish) the ubiquitin pool in the cell and may play a role

in increasing ubiquitin availability during catabolic states such as immobilization in humans, as evidenced by previous work of Urso *et al.* (21, 80). PSMD11 is a gene that encodes for a subunit of the 26S proteasome, the catalytic complex that performs ubiquitin-dependent protein degradation; in previous work in our laboratory, it was found to be increased at both the mRNA and protein levels following spinal cord injury in humans (79). In the current study, USP-3, 32, and 34 were upregulated (Table 3.4a), as was PSMD11 (Table 3.5; FC=1.4, p=0.02), following 48h UL. These findings in the current study showed that increases in components necessary for protein degradation were in evidence in the first 48h of disuse.

The high throughput analysis afforded by DAVID allowed us to identify 24 differentially expressed genes associated with the UPP, 14 of which met the more stringent p<0.01 cut-off; these genes included E2 conjugating enzymes that attach ubiquitin to proteins, E3 ligases that deliver these proteins to the proteasome, and ubiquitin specific peptidases that recycle ubiquitin, among others.

E3 Ligases

There were five different E3 ligases that displayed increased mRNA levels via microarray in this study (Table 4a). atrogin1 was upregulated following 48h UL and subsequent 24h RL via microarray (Table 3.4a), with the 48h UL increase confirmed through qRT-PCR (Table 3.7). Atrogin1 has been shown to be located at the Z-line of the sarcomere (53), and therefore, likely targets sarcomeric proteins such as contractile filaments actin and myosin. It was also recently found to target important growth regulators myoD (77) and calcineurin (53). Furthermore, data of Urso *et al.* (79) suggested that atrogin1 may target sarcolemmal proteins such as dystrophin, which

anchors and secures myofibular proteins to the cell membrane. atrogin1 has been found to be upregulated with disuse atrophy in animals (13) and in humans 5d (17) and 12d (40) post-immobilization and as early as 48h post-spinal cord injury (79), so it was not surprising to see similar results following 48h UL in the current study.

However, these findings were in disagreement with previous work in our laboratory, which found significant increases in atrogin1 via microarray analysis (1.79-fold, $p = 0.02$; unpublished) following 48h immobilization, but no significant differences when measured with the more sensitive qRT-PCR (80). Furthermore, in the current study, protein quantification via Western blot revealed no significant differences in protein products for atrogin1 following 48h UL. It has been suggested that atrogin1 expression is controlled at the translational level, and that the level of expression is dependent on the magnitude and duration of the disuse stimulus (51). It is also possible that the Western blot was not sensitive enough to detect small changes in protein levels. In a study by Urso *et al.* (79), which measured mRNA and protein levels 2d and 5d post-spinal cord injury, atrogin1 mRNA levels were increased, but protein levels were not. It was proposed that because atrogin1 is a key player in the atrophy process, this E3 ligase is tightly controlled on the translational level so as to prevent active atrophy following transient periods of disuse. The findings from the current study support this assertion.

MuRF1 not measured via microarray in this study. Because this E3 ligase has been identified in animals as an important regulator of the atrophy process, we measured mRNA levels via qRT-PCR, but found no significant differences for expression of this gene (Table 3.7). This was in agreement with findings of Urso *et al.* (80) who reported no significant differences in MuRF1 gene expression following 48h immobilization in

humans. Previous work in mice found MuRF1, along with atrogin1, to be an important regulator of atrophy following immobilization and unloading in rat muscle (13, 45), and MuRF1 knock-out mice exhibited attenuated rates of atrophy (13). Although MuRF1 gene expression was recently shown to be upregulated in humans following immobilization (24), significant increases in MuRF1 mRNA were not detected until 10d post-immobilization. The lack of increased gene expression of MuRF1 following 48h UL in the current study suggests that if MuRF1 is a key regulator of atrophy in humans, its increase in gene expression follows a later time-course than atrogin1.

Additional E3 ligases were identified as members of cluster 1 (Table 3.4a). Several of them are of particular interest because of their apparent functions. Activity of SMAD-specific E3 Ubiquitin Protein Ligase 2 (SMURF2) has been found to decrease bone (42) and also to decrease AKT signaling (62), which could potentially promote muscle wasting. Ring Finger Protein 19 (RNF19, aka Dorfin) is an E3 ligase that has been shown to be increased in neurodegenerative diseases such as ALS and localized to inclusions containing misfolded proteins (6, 35, 60); its activity is facilitated by Vatinin Containing Protein (VCP), which was also upregulated in this dataset (Table 3.4a) (38). It has been proposed that remodeling of the neuromuscular junction may be an important component of disuse muscle atrophy (68). The fact that increases in RNF19 and VCP mRNA in the current study reached significance following reloading suggests that increased transcription of the E3 ligase and its facilitator may have been induced after the disuse stimulus was removed, potentially to aid in the removal of damaged protein. In fact, although the roles of E3 ligases following short term unloading and reloading are unclear, what was interesting in the current study was that E3 ligases upregulated

following 48h UL largely remained upregulated following subsequent 24h RL (Table 3.4a).

E2 Conjugating Enzymes

Ubiquitin conjugating enzymes (UBEs) in cluster 1 included UBE2D2, UBE2E2, and UBE2G1 (Table 3.4a). Two of these enzymes (UBE2D2 and UBE2E2) were only significantly upregulated following 24h RL, while the latter (UBE2G1) was significantly upregulated across both time points. UBE2G1 is a UBC7 homologue (82) that has been found to be associated with dexamethasone-induced skeletal muscle wasting (19) and cardiac cachexia (72) in rats. The two UBEs showing significant upregulation at only the 24h reloading time point have both been associated with the degradation of apoptosis- and catabolism-inducing proteins. UBE2D2 interacts with E3 ligase Mouse Double Minute-2 Human Homolog (69) to selectively target p53 for degradation. In healthy muscle, p53 is largely inactive; however, following the introduction of stressful stimuli including oxidative stress, p53 becomes activated and can induce apoptosis. In fact, increases in p53 activity have been found to be associated with apoptosis following atrophic stimuli (70-71). UBE2E2 is a UBE about which little is known, although yeast-two-hybrid experiments have shown that it interacts with RNF8, a ring-finger E3 ligase (39). Increases in UBE2D2 and following reloading may act to reverse proapoptotic and procatabolic molecular events occurring during the previous 48h unloading.

Oxidative Stress Response

The canonical pathway, NRF2-mediate Oxidative Stress Response, was ranked second only to the Protein ubiquitination pathway for cluster 1 in IPA (Table 3.5). Increases in molecules with purported antioxidant capabilities in this pathway

accompanied both the 48h UL and 24h RL conditions, suggesting that oxidative stress accompanied these conditions and that compensatory transcription may have occurred in an attempt to offset the effects of this cellular assault. The gene with the greatest increase in expression via microarray (confirmed through qRT-PCR (Table 3.7) and also via Western blot (Figures 2A, 2B) was HMOX1, a component of this pathway.

Oxidative stress has been implicated as a potential contributor in the initiation of disuse atrophy. Accumulation of reactive oxygen species (ROS) has been proposed to initiate a cascade of events leading to the release of actomyosin complexes from sarcomeres of skeletal muscle fibers with disuse (66). Cellular increases in ROS are accompanied by increases in stress response molecules which have the role of neutralizing ROS and other reactive molecules, such as reactive iron, and maintaining REDOX balance. Therefore, it is not surprising that increases in stress response proteins following atrophy stimuli have often been observed in animals (37, 41, 50, 73). HMOX1 is one such molecule (29, 37). HMOX1 mRNA has been consistently shown to be increased following skeletal disuse in animals (37, 41, 50, 73), and work in our laboratory has shown that HMOX1 mRNA increases following spinal cord injury in humans (Urso *et al.*, unpublished), HMOX1 may provide a protective mechanism in addition to its catalytic activity in heme breakdown. It has been shown HMOX1 to activate AKT (56), and therefore may decrease FOXO transcription factor activity. In addition, increases in HMOX1 transcription has been shown to lead to increases in ferritin, which functions to binding reactive iron (74), and therefore may serve an antioxidant function.

To provide evidence to support the hypothesis that HMOX1 expression increases antioxidant activity, McClung *et al.* (57) recently restored redox balance during disuse

(mechanical ventilation) in mice via treatment with hemin, a potent HMOX1 inducer. In the current study, the increase in HMOX1 transcripts across both time points (48h UL and 24h RL) was likely a protective strategy in response to oxidative stress associated with these conditions. The relationship between HMOX1 expression and proteolysis has not been established, however.

Additional member genes of the NRF2-mediate oxidative stress response pathway that were upregulated in this dataset were heat shock proteins (HSPs) such as HSPB8 and DNAJ subfamily B and C (Table 3.7). DNAJ proteins are chaperones that interact with HSPs, such as HSP70 (46), and the genes which encode them have been shown (32, 49, 63-64) to both increase and decrease following disease stimuli, as well as following reloading. In fact, in addition to these DNAJ proteins that were upregulated in the current study, cluster 7 (which contained downregulated genes) also included DNAJ encoding genes reaching significance during reloading (Table 3.4b). Their role during these conditions is not clear.

HSPB8 is a member of the superfamily of small HSPs (sHSP) and has been shown to exert cytoprotective and anti-apoptotic effects following insults to muscle tissue such as ischemic/reperfusion injury (48). Although little is known about this newly discovered sHSP, a loss of function mutation in the gene has been associated with the neurodegenerative disorder, Charcot-Marie-Tooth disease type 2Lc (48). Conversely, over-expression of HSPB8 has been associated with hypertrophy in cardiac muscle cells (44). Although the mechanism by which HSPB8 exerts its effects is unknown, it is possible that in the current study, sub-clinical levels of oxidative stress resulting from

unloading and reloading conditions led to compensatory increases in HSPB8 mRNA levels.

Mitochondrial Metabolism

Cluster 7 contained genes showing downregulation at both time points. The most significantly altered functional group in this cluster was related to mitochondrial function (Table 3.3), and the majority of genes in this group did not reach significance until the 24h RL condition (Table 3.4b), though decreases in transcription of genes associated with aerobic metabolism and cell growth were in evidence following 48h UL.

Genes that encode enzymes participating in oxidative phosphorylation have been shown to be decreased following multiple models of disuse in animals (50) and humans (17). The current study found that aerobic enzymes were downregulated at both 48h UL and 24h RL. Although genes encoding NADH dehydrogenase and coenzymeQ, have been previously shown to be downregulated with disuse in animals and in humans, this is the first study to show these alterations (Table 3.4b) as early as 48h following the initiation of the disuse stimulus in humans. Following prolonged disuse, muscle fatigue is increased and a shift from slow to fast twitch fibers has been reported preceded by decreases in oxidative phosphorylation (75). In the current study, the oxidative phosphorylation pathway was the top ranked downregulated pathway via IPA (Table 3.5). Furthermore, not only did these genes continue to show downregulation following 24h RL, but the number of oxidative phosphorylation genes showing significant downregulation increased at this time point (Table 3.4b, Table 3.5). The alterations in expression of mitochondrial metabolism genes following 48h UL not only failed to reverse upon reloading (24h RL), but the downregulation extended to additional genes in

the category. Although the cause for this is unknown, it is important to note because it illustrates that effects of inactivity may continue even after short-term disuse ceases.

Furthermore, the current study found decreases in transcription of enzymes participating in the citric acid cycle. For example, dihydrolipoamide s-acetyltransferase (DLAT), which codes for a subunit of the pyruvate dehydrogenase complex (PDC) in the inner mitochondrial membrane was downregulated following 24h RL (Table 3.4b). This enzyme converts pyruvate into acetyl co-A, the rate limiting step in carbohydrate oxidation. Following 4wk of immobilization in humans (81), the activity of this complex was significantly decreased compared to control. Furthermore, genes encoding components of this complex were downregulated in atrophy models associated with four disease states (cancer cachexia, diabetes, fasting, and uremia (50)). It has been proposed that decreases in carbohydrate oxidation are regulated by the same pathway regulating protein degradation (AKT-FOXO pathway) (23) as FOXO transcribes PDC inhibitors (15), though these inhibitors were not upregulated in the current study. In fact, protein phosphatase 2C magnesium-dependent catalytic subunit (PPM2C), which codes for a protein that believed to activate the PDC, was downregulated (Table 3.4b). It is unclear how this pattern of PPM2C expression contributes to regulation of carbohydrate oxidation following disuse and reloading.

While the majority of downregulated genes related to mitochondrial metabolism did not reach statistical significance until 24h RL, there were genes related to oxidative phosphorylation downregulated immediately following 48h UL. Two genes that encode for key components of the electron transport chain (*i.e.*, COQ3 and NDUFS4) were downregulated, as was Monoamine Oxidase B (MAOB), a deanimating enzyme.

Decreases in mRNA transcription or deficiency of protein products of these genes have been associated with muscle abnormalities such as mitochondrial myopathy (47), Duchene muscular dystrophy (65), and Leigh-like syndrome (16). This suggests that UL disuse may involve changes in metabolic transcription associated with (if not compromised) decreased muscle function. These changes could be set in motion as early as 48h post-UL; following 24RL, these transcripts remained decreased (compared to baseline) showing that the downregulation of these genes were not immediately reversed.

Extracellular Matrix Remodeling

An interesting finding in this study was that a component of COL4 (encoding for collagen protein) was upregulated via microarray and qRT-PCR (Table 3.6), in contrast to previous studies that consistently found downregulation of collagen proteins with disuse, including previous work in our laboratory (80). COL4 genes encode for multiple subunits of the most abundant ECM collagen protein, and it has been suggested that a decrease in this collagen and others following disuse lead to both a decrease in the integrity of the ECM (80) as well as an increase in the intracellular signaling that regulates protein degradation (4-5). In the current study, the increase in transcripts of COL4A3, which encodes for a subunit of COL4, may, ironically, be related to proteolysis of the ECM, apoptosis, and decreases in protein synthesis. Tumstatin is a protein derived from COL4A3 that has been shown to function as an inhibitor of endothelial cell proliferation and a promoter of apoptosis (59). The mechanism by which tumstatin exerts its effects is mediated by the AKT/mTOR pathway and leads to protein synthesis inhibition (55). COL4A3 has been consistently detected in skeletal muscle tissue, although the effects of increased tumstatin in this tissue have not been studied. However,

function of this $\alpha 4$ fragment is dependent on cleavage of the subunit from COL4 protein and then proteolysis of COL4, thus potentially leading to its increased COL4A3 transcription in the current study. Finally, while previous work in our laboratory has shown that COL4A3 is increased with 48h immobilization in humans (80), investigation of muscle biopsies following 48h spinal cord injury has shown 2-fold downregulation of this transcript (Urso, et al.) in agreement with the UL results. Therefore, it is possible that transcription of this gene is not only regulated by disuse, but may differ among disuse models.

Conclusions

Microarray technology and high through-put software tools have allowed us to examine not only the global patterns of gene expression associated with short-term UL and RL, but also the biological significance of these changes. The results of this study suggest that alterations in gene expression associated with atrophy-related functions such as protein degradation and oxidative stress following UL as previously found in the literature (17, 40, 61), may occur as early as 48h following the introduction of the UL stimulus, though increased magnitude or duration of that stimulus may be necessary in order for translation of protein products to occur. Furthermore, while increases in proteolytic gene expression found in this study suggest that there are similarities between expression patterns following 48h UL and IM, differences likely exist between the two disuse models as evidenced by decreases in collagen found with UL. Prior to this study, HMOX1 had emerged as a potential regulator following UL in animals (37, 41, 50, 73), and the current study extends this important finding to humans. Finally, the gene expression patterns with UL were not readily reversed upon RE, suggesting that

molecular responses to short-term periods of skeletal muscle inactivity in humans may persist even after activity resumes. Future studies could employ these high through-put technologies to examine the effects of targeted interventions on expression of genes in pathways and functional groups identified in the current study and shed light on how atrophy could be prevented or attenuated in the earliest stages of disuse.

References

1. Expression profiling--best practices for data generation and interpretation in clinical trials. *Nat Rev Genet* 5: 229-237, 2004.
2. **Adams GR, Caiozzo VJ, and Baldwin KM.** Skeletal muscle unweighting: spaceflight and ground-based models. *J Appl Physiol* 95: 2185-2201, 2003.
3. **Adams GR, Hather BM, and Dudley GA.** Effect of short-term unweighting on human skeletal muscle strength and size. *Aviat Space Environ Med* 65: 1116-1121, 1994.
4. **Ahtikoski AM, Koskinen SO, Virtanen P, Kovanen V, Risteli J, and Takala TE.** Synthesis and degradation of type IV collagen in rat skeletal muscle during immobilization in shortened and lengthened positions. *Acta Physiol Scand* 177: 473-481, 2003.
5. **Ahtikoski AM, Koskinen SO, Virtanen P, Kovanen V, and Takala TE.** Regulation of synthesis of fibrillar collagens in rat skeletal muscle during immobilization in shortened and lengthened positions. *Acta Physiol Scand* 172: 131-140, 2001.
6. **Bendotti C, Atzori C, Piva R, Tortarolo M, Strong MJ, DeBiasi S, and Migheli A.** Activated p38MAPK is a novel component of the intracellular inclusions found in human amyotrophic lateral sclerosis and mutant SOD1 transgenic mice. *J Neuropathol Exp Neurol* 63: 113-119, 2004.
7. **Berg HE, Dudley GA, Haggmark T, Ohlsen H, and Tesch PA.** Effects of lower limb unloading on skeletal muscle mass and function in humans. *J Appl Physiol* 70: 1882-1885, 1991.
8. **Berg HE, Dudley GA, Hather B, and Tesch PA.** Work capacity and metabolic and morphologic characteristics of the human quadriceps muscle in response to unloading. *Clin Physiol* 13: 337-347, 1993.
9. **Berg HE, Eiken O, Miklavcic L, and Mekjavic IB.** Hip, thigh and calf muscle atrophy and bone loss after 5-week bed rest inactivity. *Eur J Appl Physiol* 99: 283-289, 2007.
10. **Berg HE, Larsson L, and Tesch PA.** Lower limb skeletal muscle function after 6 wk of bed rest. *J Appl Physiol* 82: 182-188, 1997.
11. **Berg HE, and Tesch PA.** Changes in muscle function in response to 10 days of lower limb unloading in humans. *Acta Physiol Scand* 157: 63-70, 1996.
12. **Bey L, Akunuri N, Zhao P, Hoffman EP, Hamilton DG, and Hamilton MT.** Patterns of global gene expression in rat skeletal muscle during unloading and low-intensity ambulatory activity. *Physiol Genomics* 13: 157-167, 2003.

13. **Bodine SC, Latres E, Baumhueter S, Lai VK, Nunez L, Clarke BA, Poueymirou WT, Panaro FJ, Na E, Dharmarajan K, Pan ZQ, Valenzuela DM, DeChiara TM, Stitt TN, Yancopoulos GD, and Glass DJ.** Identification of ubiquitin ligases required for skeletal muscle atrophy. *Science* 294: 1704-1708, 2001.
14. **Bodine SC, Stitt TN, Gonzalez M, Kline WO, Stover GL, Bauerlein R, Zlotchenko E, Scrimgeour A, Lawrence JC, Glass DJ, and Yancopoulos GD.** Akt/mTOR pathway is a crucial regulator of skeletal muscle hypertrophy and can prevent muscle atrophy in vivo. *Nat Cell Biol* 3: 1014-1019, 2001.
15. **Bowker-Kinley MM, Davis WI, Wu P, Harris RA, and Popov KM.** Evidence for existence of tissue-specific regulation of the mammalian pyruvate dehydrogenase complex. *Biochem J* 329 (Pt 1): 191-196, 1998.
16. **Budde SM, van den Heuvel LP, Janssen AJ, Smeets RJ, Buskens CA, DeMeirleir L, Van Coster R, Baethmann M, Voit T, Trijbels JM, and Smeitink JA.** Combined enzymatic complex I and III deficiency associated with mutations in the nuclear encoded NDUFS4 gene. *Biochem Biophys Res Commun* 275: 63-68, 2000.
17. **Chen Y-W, Gregory CM, Scarborough MT, Shi R, Walter GA, and Vandeborn K.** Transcriptional pathways associated with skeletal muscle disuse atrophy in humans. *Physiol Genomics* 31: 510-520, 2007.
18. **Chen YW, Zhao P, Borup R, and Hoffman EP.** Expression profiling in the muscular dystrophies: identification of novel aspects of molecular pathophysiology. *J Cell Biol* 151: 1321-1336, 2000.
19. **Chrysis D, and Underwood LE.** Regulation of components of the ubiquitin system by insulin-like growth factor I and growth hormone in skeletal muscle of rats made catabolic with dexamethasone. *Endocrinology* 140: 5635-5641, 1999.
20. **Clark BC, Manini TM, Bolanowski SJ, and Ploutz-Snyder LL.** Adaptations in human neuromuscular function following prolonged unweighting: II. Neurological properties and motor imagery efficacy. *J Appl Physiol* 101: 264-272, 2006.
21. **Combaret L, Adegoke OAJ, Bedard N, Baracos V, Attaix D, and Wing SS.** USP19 is a ubiquitin-specific protease regulated in rat skeletal muscle during catabolic states. *Am J Physiol Endocrinol Metab* 288: E693-700, 2005.
22. **Cross DA, Watt PW, Shaw M, van der Kaay J, Downes CP, Holder JC, and Cohen P.** Insulin activates protein kinase B, inhibits glycogen synthase kinase-3 and activates glycogen synthase by rapamycin-insensitive pathways in skeletal muscle and adipose tissue. *FEBS Lett* 406: 211-215, 1997.
23. **Crossland H, Constantin-Teodosiu D, Gardiner SM, Constantin D, and Greenhaff PL.** A potential role for Akt/FOXO signalling in both protein loss and the

- impairment of muscle carbohydrate oxidation during sepsis in rodent skeletal muscle. *J Physiol* 586: 5589-5600, 2008.
24. **de Boer MD, Maganaris CN, Seynnes OR, Rennie MJ, and Narici MV.** Time course of muscular, neural and tendinous adaptations to 23 day unilateral lower-limb suspension in young men. *J Physiol* 583: 1079-1091, 2007.
 25. **de Palma L, Marinelli M, Pavan M, and Orazi A.** Ubiquitin ligases MuRF1 and MAFbx in human skeletal muscle atrophy. *Joint Bone Spine* 75: 53-57, 2008.
 26. **Dennis G, Jr., Sherman BT, Hosack DA, Yang J, Gao W, Lane HC, and Lempicki RA.** DAVID: database for annotation, visualization, and integrated discovery. *Genome Biol* 4: P3, 2003.
 27. **Deschenes MR, Giles JA, McCoy RW, Volek JS, Gomez AL, and Kraemer WJ.** Neural factors account for strength decrements observed after short-term muscle unloading. *Am J Physiol Regul Integr Comp Physiol* 282: R578-583, 2002.
 28. **Drummond MJ, Glynn EL, Lujan HL, Dicarlo SE, and Rasmussen BB.** Gene and protein expression associated with protein synthesis and breakdown in paraplegic skeletal muscle. *Muscle Nerve* 37: 505-513, 2008.
 29. **Falk DJ, Deruisseau KC, Van Gammeren DL, Deering MA, Kavazis AN, and Powers SK.** Mechanical ventilation promotes redox status alterations in the diaphragm. *J Appl Physiol* 101: 1017-1024, 2006.
 30. **Giannelli G, De Marzo A, Marinosci F, and Antonaci S.** Matrix metalloproteinase imbalance in muscle disuse atrophy. *Histol Histopathol* 20: 99-106, 2005.
 31. **Glass DJ.** Signalling pathways that mediate skeletal muscle hypertrophy and atrophy. *Nat Cell Biol* 5: 87-90, 2003.
 32. **Goto K, Honda M, Kobayashi T, Uehara K, Kojima A, Akema T, Sugiura T, Yamada S, Ohira Y, and Yoshioka T.** Heat stress facilitates the recovery of atrophied soleus muscle in rat. *Jpn J Physiol* 54: 285-293, 2004.
 33. **Haddad F, Adams GR, Bodell PW, and Baldwin KM.** Isometric resistance exercise fails to counteract skeletal muscle atrophy processes during the initial stages of unloading. *J Appl Physiol* 100: 433-441, 2006.
 34. **Hather BM, Adams GR, Tesch PA, and Dudley GA.** Skeletal muscle responses to lower limb suspension in humans. *J Appl Physiol* 72: 1493-1498, 1992.
 35. **Hishikawa N, Niwa J, Doyu M, Ito T, Ishigaki S, Hashizume Y, and Sobue G.** Dofin localizes to the ubiquitylated inclusions in Parkinson's disease, dementia with

Lewy bodies, multiple system atrophy, and amyotrophic lateral sclerosis. *Am J Pathol* 163: 609-619, 2003.

36. **Huang W, Kutner N, and Bliwise DL.** A systematic review of the effects of acupuncture in treating insomnia. *Sleep Med Rev* 13: 73-104, 2009.
37. **Hunter RB, Mitchell-Felton H, Essig DA, and Kandarian SC.** Expression of endoplasmic reticulum stress proteins during skeletal muscle disuse atrophy. *Am J Physiol Cell Physiol* 281: C1285-1290, 2001.
38. **Ishigaki S, Hishikawa N, Niwa J-i, Iemura S-i, Natsume T, Hori S, Kakizuka A, Tanaka K, and Sobue G.** Physical and Functional Interaction between Dorsfin and Valosin-containing Protein That Are Colocalized in Ubiquitylated Inclusions in Neurodegenerative Disorders. *J Biol Chem* 279: 51376-51385, 2004.
39. **Ito K, Adachi S, Iwakami R, Yasuda H, Muto Y, Seki N, and Okano Y.** N-Terminally extended human ubiquitin-conjugating enzymes (E2s) mediate the ubiquitination of RING-finger proteins, ARA54 and RNF8. *Eur J Biochem* 268: 2725-2732, 2001.
40. **Jones SW, Hill RJ, Krasney PA, O'Conner B, Peirce N, and Greenhaff PL.** Disuse atrophy and exercise rehabilitation in humans profoundly affects the expression of genes associated with the regulation of skeletal muscle mass. *Faseb J* 18: 1025-1027, 2004.
41. **Kandarian SC, and Jackman RW.** Intracellular signaling during skeletal muscle atrophy. *Muscle Nerve* 33: 155-165, 2006.
42. **Kaneki H, Guo R, Chen D, Yao Z, Schwarz EM, Zhang YE, Boyce BF, and Xing L.** Tumor necrosis factor promotes Runx2 degradation through up-regulation of Smurf1 and Smurf2 in osteoblasts. *J Biol Chem* 281: 4326-4333, 2006.
43. **Kauhanen S, Leivo I, and Michelsson JE.** Early muscle changes after immobilization. An experimental study on muscle damage. *Clin Orthop Relat Res* 44-50, 1993.
44. **Kim MV, Seit-Nebi AS, and Gusev NB.** The problem of protein kinase activity of small heat shock protein Hsp22 (H11 or HspB8). *Biochem Biophys Res Commun* 325: 649-652, 2004.
45. **Krawiec BJ, Frost RA, Vary TC, Jefferson LS, and Lang CH.** Hindlimb casting decreases muscle mass in part by proteasome-dependent proteolysis but independent of protein synthesis. *Am J Physiol Endocrinol Metab* 289: E969-980, 2005.

46. **Ku Z, Yang J, Menon V, and Thomason DB.** Decreased polysomal HSP-70 may slow polypeptide elongation during skeletal muscle atrophy. *Am J Physiol* 268: C1369-1374, 1995.
47. **Lalani SR, Vladutiu GD, Plunkett K, Lotze TE, Adesina AM, and Scaglia F.** Isolated mitochondrial myopathy associated with muscle coenzyme Q10 deficiency. *Arch Neurol* 62: 317-320, 2005.
48. **Laskowska E.** [Small heat shock proteins--role in apoptosis, cancerogenesis and diseases associated with protein aggregation]. *Postepy Biochem* 53: 19-26, 2007.
49. **Lawler JM, Song W, and Kwak HB.** Differential response of heat shock proteins to hindlimb unloading and reloading in the soleus. *Muscle Nerve* 33: 200-207, 2006.
50. **Lecker SH, Jagoe RT, Gilbert A, Gomes M, Baracos V, Bailey J, Price SR, Mitch WE, and Goldberg AL.** Multiple types of skeletal muscle atrophy involve a common program of changes in gene expression. *Faseb J* 18: 39-51, 2004.
51. **Leger B, Vergani L, Soraru G, Hespel P, Derave W, Gobelet C, D'Ascenzio C, Angelini C, and Russell AP.** Human skeletal muscle atrophy in amyotrophic lateral sclerosis reveals a reduction in Akt and an increase in atrogin-1. *Faseb J* 20: 583-585, 2006.
52. **Li C, and Hung Wong W.** Model-based analysis of oligonucleotide arrays: model validation, design issues and standard error application. *Genome Biol* 2: RESEARCH0032, 2001.
53. **Li HH, Kedar V, Zhang C, McDonough H, Arya R, Wang DZ, and Patterson C.** Atrogin-1/muscle atrophy F-box inhibits calcineurin-dependent cardiac hypertrophy by participating in an SCF ubiquitin ligase complex. *J Clin Invest* 114: 1058-1071, 2004.
54. **Liu WM, Mei R, Di X, Ryder TB, Hubbell E, Dee S, Webster TA, Harrington CA, Ho MH, Baid J, and Smeekens SP.** Analysis of high density expression microarrays with signed-rank call algorithms. *Bioinformatics* 18: 1593-1599, 2002.
55. **Maeshima Y, Sudhakar A, Lively JC, Ueki K, Kharbanda S, Kahn CR, Sonenberg N, Hynes RO, and Kalluri R.** Tumstatin, an endothelial cell-specific inhibitor of protein synthesis. *Science* 295: 140-143, 2002.
56. **Martin D, Rojo AI, Salinas M, Diaz R, Gallardo G, Alam J, De Galarreta CM, and Cuadrado A.** Regulation of heme oxygenase-1 expression through the phosphatidylinositol 3-kinase/Akt pathway and the Nrf2 transcription factor in response to the antioxidant phytochemical carnosol. *J Biol Chem* 279: 8919-8929, 2004.

57. **McClung JM, Whidden MA, Kavazis AN, Falk DJ, Deruisseau KC, and Powers SK.** Redox regulation of diaphragm proteolysis during mechanical ventilation. *Am J Physiol Regul Integr Comp Physiol* 294: R1608-1617, 2008.
58. **Miles MP, Clarkson PM, Bean M, Ambach K, Mulroy J, and Vincent K.** Muscle function at the wrist following 9 d of immobilization and suspension. *Med Sci Sports Exerc* 26: 615-623, 1994.
59. **Ninichuk V, Gross O, Segerer S, Hoffmann R, Radomska E, Buchstaller A, Huss R, Akis N, Schlondorff D, and Anders HJ.** Multipotent mesenchymal stem cells reduce interstitial fibrosis but do not delay progression of chronic kidney disease in collagen4A3-deficient mice. *Kidney Int* 70: 121-129, 2006.
60. **Niwa J, Ishigaki S, Hishikawa N, Yamamoto M, Doyu M, Murata S, Tanaka K, Taniguchi N, and Sobue G.** Dornin ubiquitylates mutant SOD1 and prevents mutant SOD1-mediated neurotoxicity. *J Biol Chem* 277: 36793-36798, 2002.
61. **Ogawa T, Furochi H, Mameoka M, Hirasaka K, Onishi Y, Suzue N, Oarada M, Akamatsu M, Akima H, Fukunaga T, Kishi K, Yasui N, Ishidoh K, Fukuoka H, and Nikawa T.** Ubiquitin ligase gene expression in healthy volunteers with 20-day bed rest. *Muscle Nerve* 34: 463-469, 2006.
62. **Ohashi N, Yamamoto T, Uchida C, Togawa A, Fukasawa H, Fujigaki Y, Suzuki S, Kitagawa K, Hattori T, Oda T, Hayashi H, Hishida A, and Kitagawa M.** Transcriptional induction of Smurf2 ubiquitin ligase by TGF-beta. *FEBS Lett* 579: 2557-2563, 2005.
63. **Oishi Y, Ishihara A, Talmadge RJ, Ohira Y, Taniguchi K, Matsumoto H, Roy RR, and Edgerton VR.** Expression of heat shock protein 72 in atrophied rat skeletal muscles. *Acta Physiol Scand* 172: 123-130, 2001.
64. **Oishi Y, Taniguchi K, Matsumoto H, Kawano F, Ishihara A, and Ohira Y.** Upregulation of HSP72 in reloading rat soleus muscle after prolonged hindlimb unloading. *Jpn J Physiol* 53: 281-286, 2003.
65. **Pescatori M, Broccolini A, Minetti C, Bertini E, Bruno C, D'Amico A, Bernardini C, Mirabella M, Silvestri G, Giglio V, Modoni A, Pedemonte M, Tasca G, Galluzzi G, Mercuri E, Tonali PA, and Ricci E.** Gene expression profiling in the early phases of DMD: a constant molecular signature characterizes DMD muscle from early postnatal life throughout disease progression. *Faseb J* 21: 1210-1226, 2007.
66. **Powers SK, Kavazis AN, and McClung JM.** Oxidative stress and disuse muscle atrophy. *J Appl Physiol* 2007.
67. **Richard I, Broux O, Allamand V, Fougousse F, Chiannikulchai N, Bourg N, Brenguier L, Devaud C, Pasturaud P, Roudaut C, and et al.** Mutations in the

proteolytic enzyme calpain 3 cause limb-girdle muscular dystrophy type 2A. *Cell* 81: 27-40, 1995.

68. **Sacheck JM, Hyatt JP, Raffaello A, Jagoe RT, Roy RR, Edgerton VR, Lecker SH, and Goldberg AL.** Rapid disuse and denervation atrophy involve transcriptional changes similar to those of muscle wasting during systemic diseases. *Faseb J* 21: 140-155, 2007.

69. **Saville MK, Sparks A, Xirodimas DP, Wardrop J, Stevenson LF, Bourdon JC, Woods YL, and Lane DP.** Regulation of p53 by the ubiquitin-conjugating enzymes UbcH5B/C in vivo. *J Biol Chem* 279: 42169-42181, 2004.

70. **Siu PM, and Alway SE.** Id2 and p53 participate in apoptosis during unloading-induced muscle atrophy. *Am J Physiol Cell Physiol* 288: C1058-1073, 2005.

71. **Siu PM, and Alway SE.** Mitochondria-associated apoptotic signalling in denervated rat skeletal muscle. *J Physiol* 565: 309-323, 2005.

72. **Steffen BT, Lees SJ, and Booth FW.** Anti-TNF treatment reduces rat skeletal muscle wasting in monocrotaline-induced cardiac cachexia. *J Appl Physiol* 105: 1950-1958, 2008.

73. **Stevenson EJ, Giresi PG, Koncarevic A, and Kandarian SC.** Global analysis of gene expression patterns during disuse atrophy in rat skeletal muscle. *J Physiol* 551: 33-48, 2003.

74. **Suttner DM, Sridhar K, Lee CS, Tomura T, Hansen TN, and Dennery PA.** Protective effects of transient HO-1 overexpression on susceptibility to oxygen toxicity in lung cells. *Am J Physiol* 276: L443-451, 1999.

75. **Tesch PA, and Berg HE.** Effects of spaceflight on muscle. *J Gravit Physiol* 5: P19-22, 1998.

76. **Tesch PA, von Walden F, Gustafsson T, Linnehan RM, and Trappe TA.** Skeletal muscle proteolysis in response to short-term unloading in humans. *J Appl Physiol* 105: 902-906, 2008.

77. **Tisdale MJ.** Is there a common mechanism linking muscle wasting in various disease types? *Curr Opin Support Palliat Care* 1: 287-292, 2007.

78. **Trappe SW, Trappe TA, Lee GA, Widrick JJ, Costill DL, and Fitts RH.** Comparison of a space shuttle flight (STS-78) and bed rest on human muscle function. *J Appl Physiol* 91: 57-64, 2001.

79. **Urso ML, Chen YW, Scrimgeour AG, Lee PC, Lee KF, and Clarkson PM.** Alterations in mRNA expression and protein products following spinal cord injury in humans. *J Physiol* 579: 877-892, 2007.
80. **Urso ML, Scrimgeour AG, Chen YW, Thompson PD, and Clarkson PM.** Analysis of human skeletal muscle after 48 h immobilization reveals alterations in mRNA and protein for extracellular matrix components. *J Appl Physiol* 101: 1136-1148, 2006.
81. **Ward GR, MacDougall JD, Sutton JR, Toews CJ, and Jones NL.** Activation of human muscle pyruvate dehydrogenase with activity and immobilization. *Clin Sci (Lond)* 70: 207-210, 1986.
82. **Watanabe TK, Kawai A, Fujiwara T, Maekawa H, Hirai Y, Nakamura Y, and Takahashi E.** Molecular cloning of UBE2G, encoding a human skeletal muscle-specific ubiquitin-conjugating enzyme homologous to UBC7 of *C. elegans*. *Cytogenet Cell Genet* 74: 146-148, 1996.

Table 3.1: Subject demographics (n=7).

	Mean±S.D.
Age (y)	22.1±3.7
Height (m)	1.4±0.1
Weight (kg)	78.2±3.1

Table 3.2 qRT-PCR primers.

Gene Symbol	Forward Primer	Reverse Primer
Atrogin1	5'-TCA CAG CTC ACA TCC CTG AG-3'	5'-TCA CAG CTC ACA TCC CTG AG-3'
COL4A3	5'-GTT CTC TGT GGC AAA GCA GCA ACT-3'	5'-ACA ATC ACC GTA GTG ACA GTG CCT-3'
HMOX1	5'-ATT GCC AGT GCC ACC AAG TTC AAG-3'	5'-ACG CAG TCT TGG CCT CTT CTA TCA-3'
MuRF1	5'-TGA GCC AGA AGT TTG ACA CG-3'	5'-TGA TGA GTT GCT TGG CAG TC-3'
GAPDH	5'-CAT TGC CCT CAA CGA CCA CTT TGT-3'	5'-TCT CTC TCT TCC TCT TGT GCT CTT GC-3'

Table 3.3. Over-represented functional annotations for clusters 1 and 7.
 Count=# of genes in category; fold enrichment=magnitude of over-representation in data set; adjusted p-value= Benjamini and Hochberg multiple testing correction.
 Functional annotations are listed in order of p-value.

Functional Annotation Category	Count	Fold Enrichment	Adjusted p-value
<u>Cluster 1</u>			
Ubiquitin Conjugation	23	3.3	2.00E-05
Post-translational Modification	64	1.8	3.00E-04
mRNA Metabolism	21	3.1	6.70E-03
<u>Cluster 7</u>			
Mitochondrion	56	5.3	9.80E-23
Catalytic Activity	87	1.5	1.20E-02
Generation of precursor metabolites and energy	21	3.1	3.90E-02

Table 3.4a. Cluster 1 Up-regulated genes associated with ubiquitin conjugation
 UL=unloading; RL=reloading; ^aE2 ligase, ^bE3 ligase, ^cubiquitin protease; all fold-
 changes significantly different from baseline, p<0.05; NS = Not significant.

Affymetrix	Gene		48h	24h
Accession	Symbol	Gene Title	UL	RL
213295_at	CYLD	cylindromatosis (turban tumor syndrome)	1.3	1.3
209943_at	FBXL4 ^b	F-box and leucine-rich repeat protein 4	1.4	1.3
225345_s_at	FBXO32 ^b	F-box protein 32 (Atrogin1)	1.7	1.6
203068_at	KLHL21	kelch-like 21 (Drosophila)	1.3	1.5
242712_x_at	RANBP2	RAN binding protein 2	1.2	1.4
228980_at	RFFL ^b	Rififylin (ring finger)	NS	1.5
230599_at	RNF19 ^b	Ring finger protein 19 (dorfin)	1.1	1.3
205596_s_at	SMURF2 ^b	SMAD specific E3 ubiquitin protein ligase 2	NS	1.3
209142_s_at	UBE2D2 ^a	ubiquitin-conjugating enzyme E2D 1	NS	1.6
224747_at	UBE2E2 ^a	ubiquitin-conjugating enzyme E2E 1	NS	1.3
236107_at	UBE2G1 ^a	ubiquitin-conjugating enzyme E2G 1	1.2	1.2
221654_s_at	USP3 ^c	ubiquitin specific peptidase 3	1.2	1.3
226505_x_at	USP32 ^c	ubiquitin specific peptidase 32	1.2	1.3
233595_at	USP34 ^c	ubiquitin specific peptidase 34	NS	1.3
208648_at	VCP	valosin-containing protein	NS	1.3

Table 3.4b. Cluster 7 Down-regulated genes associated with mitochondrial function. Expression (fold-change) relative to baseline. All reported fold-changes significant at $p < 0.05$. UL=unloading; RL=reloading; NS=Not significant.

Affymetrix Accession	Gene Symbol	Gene Title	48h UL	24h RL
204824_at	ENDOG	endonuclease G	NS	-1.2
224509_s_at	RTN4IP1	reticulon 4 interacting protein 1 (aka NIMP)	-1.3	-1.4
211662_s_at	VDAC2	voltage-dependent anion channel 2	NS	-1.2
213379_at	COQ2	coenzyme Q2 homolog, prenyltransferase (yeast)	NS	-1.2
223515_s_at	COQ3	coenzyme Q3 homolog, methyltransferase (<i>S. cerevisiae</i>)	-1.3	-1.4
225747_at	COQ10A	coenzyme Q10 homolog A (<i>S. cerevisiae</i>)	NS	-1.4
203858_s_at	COX10	COX10 homolog, cytochrome c oxidase assembly protein	NS	-1.2
202447_at	DECR1	2,4-dienoyl CoA reductase 1, mitochondrial	NS	-1.2
239161_at	FDX1	ferredoxin 1	NS	-1.4
204041_at	MAOB	monoamine oxidase B	-1.2	-1.4
203745_at	HCCS	holocytochrome c synthase (cytochrome c heme-lyase)	-1.2	-1.3
209303_at	NDUFS4	NADH dehydrogenase (ubiquinone) Fe-S protein 4	-1.2	-1.2
218160_at	NDUFA8	NADH dehydrogenase (ubiquinone) 1 alpha subcomplex, 8	NS	-1.3
208969_at	NDUFA9	NADH dehydrogenase (ubiquinone) 1 alpha subcomplex, 9	NS	-1.2
219195_at	PPARGC1A	peroxisome proliferative activated receptor, gamma, coactivator 1 alpha	NS	-1.4
226154_at	DNM1L	dynamamin 1-like	NS	-1.2
218246_at	MUL1	mitochondrial ubiquitin ligase activator of NFKB 1	NS	-1.2
215792_s_at	DNAJC11	DnaJ (Hsp40) homolog, subfamily C, member 11	NS	-1.2
225358_at	DNAJC19	DnaJ (Hsp40) homolog, subfamily C, member 19	NS	-1.2
211538_s_at	HSPA2	heat shock 70kDa protein 2	NS	-1.2
<i>TCA Cycle</i>				
222572_at	PPM2C	protein phosphatase 2C, magnesium-dependent, catalytic subunit	NS	-1.5
213149_at	DLAT	dihydrolipoamide S-acetyltransferase	NS	-1.3
<i>Transporter Activity</i>				
203339_at	SLC25A12	solute carrier family 25 (mitochondrial carrier, Aralar), member 12	NS	-1.2
227012_at	SLC25A40	solute carrier family 25, member 40	NS	-1.3
226059_at	TOMM40L	translocase of outer mitochondrial membrane 40 homolog (yeast)-like	NS	-1.6
<i>Miscellaneous and Unknown</i>				
221069_s_at	CCDC44	coiled-coil domain containing 44	NS	-1.2
224415_s_at	HINT2	histidine triad nucleotide binding protein 2	NS	-1.3
223154_at	MRPL1	mitochondrial ribosomal protein L1	NS	-1.2
56197_at	PLSCR3	phospholipid scramblase 3	NS	-1.2

Table 3.5. Ingenuity canonical pathways associated with clusters 1 (upregulated) and cluster 7 (downregulated) genes. Pathways listed in order of p-value. UL=unloading; RL=reloading.

Canonical Pathways	p-value	48h UL Genes	24h RL Genes
CLUSTER 1 (Upregulated)			
Protein Ubiquitination	7.28E-04	PSMD11, UBE2G1, USP3, USP32, USP53	B2M, SMURF2, UBE2G1, UBE4A, USP3, USP6, USP32, USP34, USP38, USP53
NRF2-mediate Oxidative Stress Response	5.37E-03	ACTG1, HMOX1, HSPB8	CREBBP, DNAJB14, DNAJC16, FTL, HMOX1, HSPB8, PRKCI, VCP
VDR/RXR Activation	1.60E-02	CEBPB, YY1	NCOA3, PRKCI, SP1
TGF- β Signaling	1.77E-02	SMAD4, TGIF1	CREBBP, SMAD4, SMURF2, SOS1
Estrogen Receptor Signaling	1.94E-02	TAF12	CDK7, CREBBP, HNRNPD, NCOA3, SOS1, TAF12
Mechanism of Viral Exit from Host Cell	2.77E-02	ACTG1	PRKCI, SH3GLB1
IL-10 Signaling	3.05E-02	ARG2, HMOX1,	ARG2, HMOX1, MAP4K4, SP1
Wnt/ β -Catenin Signaling	3.07E-02	GJA1, SOX4, SOX13,	CREBBP, CSNK1A1, FZD5, GJA1, TGFB3
Il-8 Signaling	4.09E-02	ANGPT2, HMOX1, IRAK3, RHOQ	BCL2, HMOX1, MAP4K4, PRKCI, RHOQ
Glucocorticoid Signaling	4.49E-02	CEBPB, SMAD4, TAF12,	BCL2, CDK7, CREBBP, NCOA3, NFATC3, SMAD4, SOS1, TAF12
Oxidative Phosphorylation	5.17E-04	ATP5G3, NDUFS4	COX10, COX7A2, NDUFA8, NDUFA9, NDUFC1, UCRC
CLUSTER 7 (Downregulated)			
Ubiquinone Biosynthesis	1.88E-04	COQ3, NDUFS4	NDUFA8, NDUFA9, NDUFC1
Citrate Cycle	3.48E-04	ATP5G3	DLST, IDH1, MDH1
Mitochondrial Dysfunction	2.07E-03	MAOB, NDUFS4	COX10, COX7A2, NDUFA8, NDUFA9
Arginine and Proline Metabolism	7.29E-03	MAOB	CKB, GOT1
TR/RXR Activation	1.52E-02	NCOR2, PPARGC1A, SLC16A3	NCOA4
Tyrosine Metabolism	2.30E-02	MAOB	GOT1, TYRP1
Pyruvate Metabolism	3.53E-02		ACSL3, DLAT, MDH1
Xenobiotic Metabolism Signaling	3.60E-02	MAOB, NCOR2, PPARGC1A	CUL3, NDST1, PP2R3A
PXR/RXR Activation	3.68E-02	ALAS1, PPARGC1A	ALAS1, PPARA

Table 3.6. qRT PCR results. All fold-changes relative to baseline significant at $p < 0.05$.
 UL=unloading; RL = reloading; NS=not significant.

	Microarray		qRT-PCR	
	48h UL	24h RL	48h UL	24h RL
Atrogin1	1.7	1.6	1.4 ($p=0.01$)	NS
COL4A3	1.7	1.4	1.8 ($p < 0.01$)	NS
HMOX1	15.4	6.5	12.7 ($p=0.01$)	NS
MURF1	NS	1.5	NS	NS

Figure 3.1. Gene clustering. Unloading and reloading normalized to baseline. Yellow=no change, Red=upregulated, Blue=downregulated. Clusters are numbered 1 – 8.

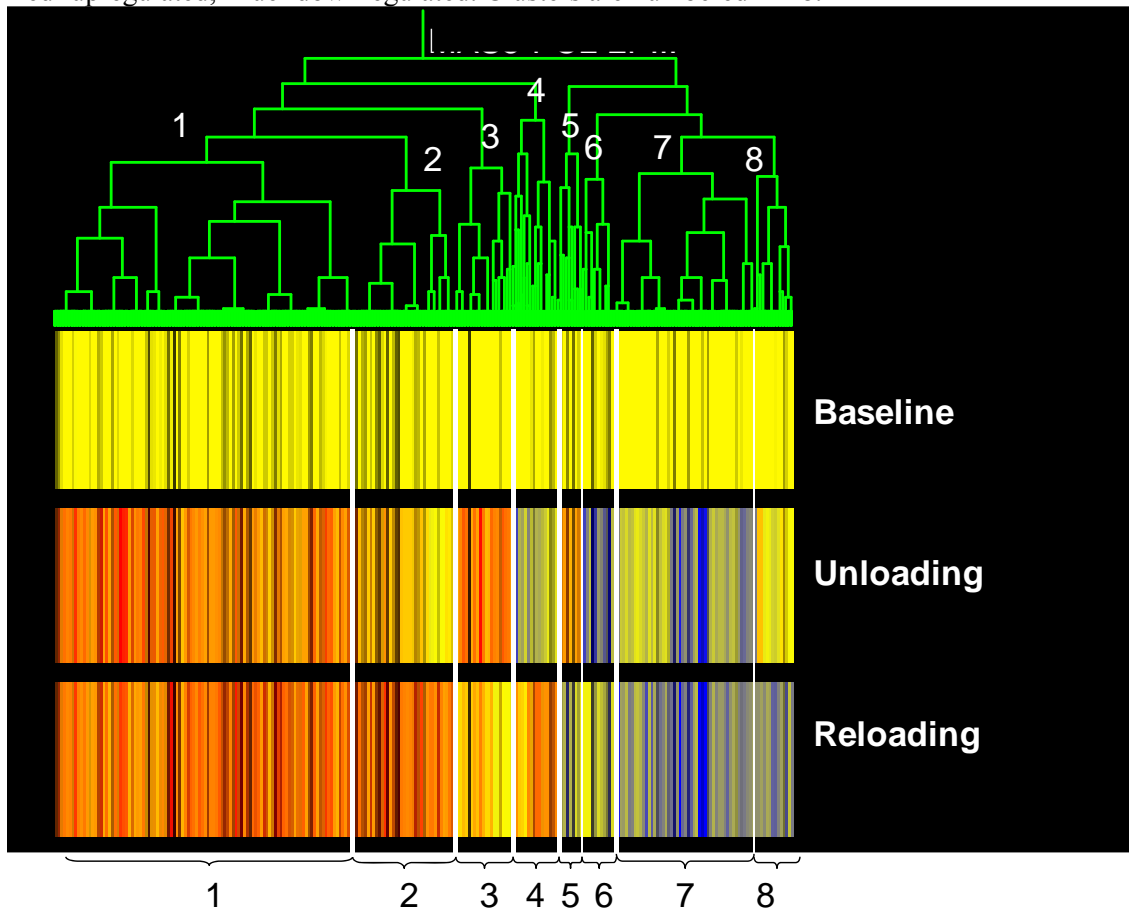


Figure 3.2a. HMOX protein levels via Western blot.

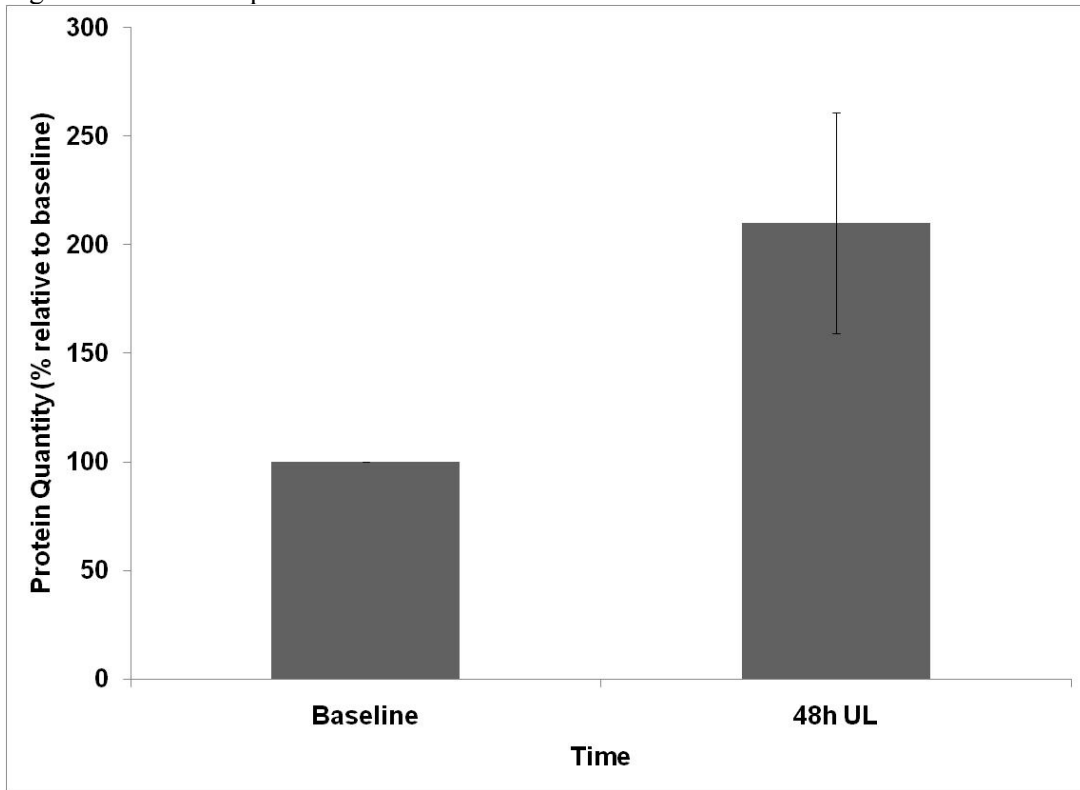
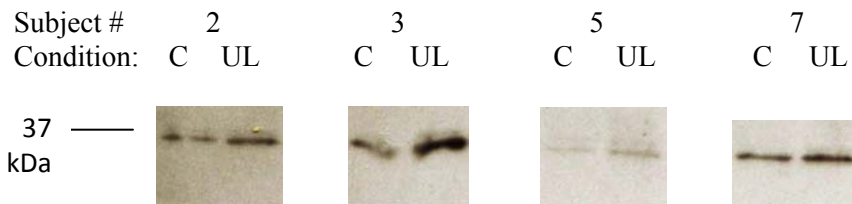
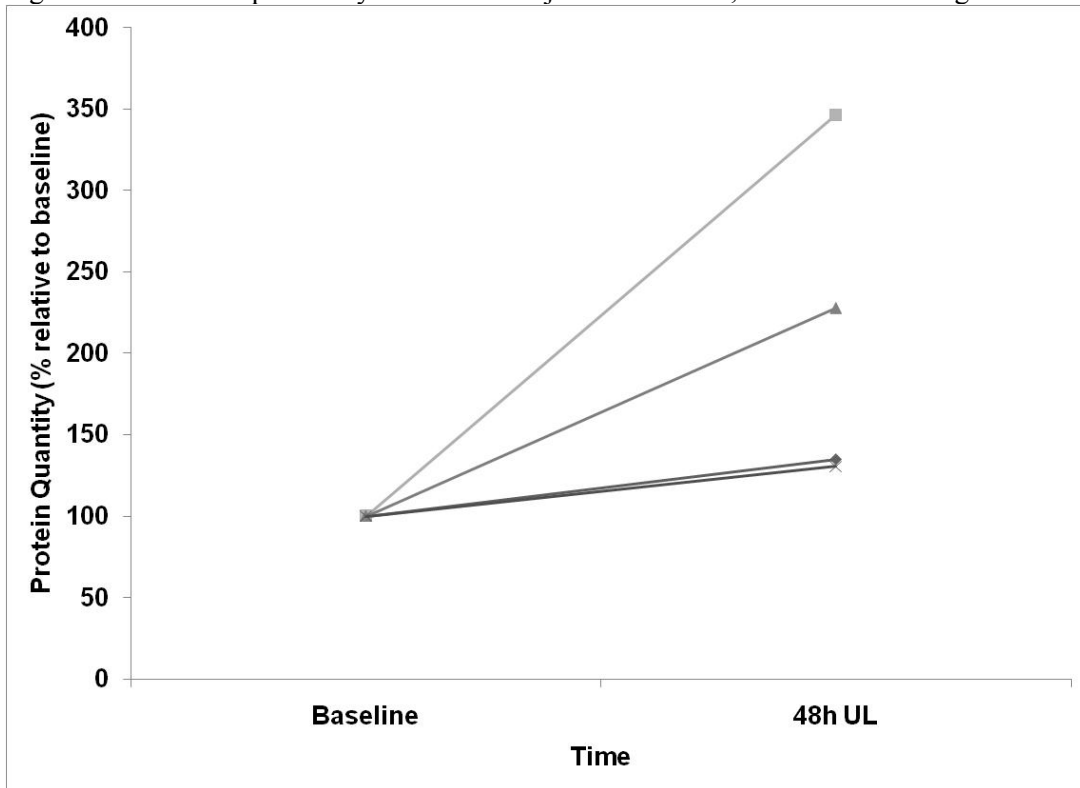


Figure 3.2b. HMOX protein by individual subject. C= control; UL=48h unloading.



CHAPTER IV

GLOBAL GENE EXPRESSION ANALYSIS OF HUMAN SKELETAL MUSCLE TWO DAYS POST-IMMOBILIZATION, -UNLOADING, AND -SPINAL CORD INJURY

Abstract

PURPOSE: Prolonged skeletal muscle disuse with immobilization (IM), spinal cord injury (SCI) and unloading (UL), results in decreased muscle size and function.

Identifying universal mechanisms associated with early stages of disuse may lead to the development of interventions to attenuate these deleterious effects. The purpose of this study was to identify molecular markers following 48h of disuse (IM, SCI, and UL) common to these three conditions.

METHODS: Microarray technology was used to measure global gene expression in biopsy samples collected 48h following IM, SCI, and UL from the vastus lateralis of male volunteers. Enriched functions were identified within the datasets using the Database for Annotations, Visualization and Integrated Discovery (DAVID), and significant canonical pathways and gene networks were

identified using Ingenuity Pathway Analysis (IPA). **RESULTS:** Between 636 and 1602 transcripts were differentially expressed within each dataset, with all three models of disuse sharing 32 commonly expressed genes. Functions of these shared genes included transcription, protein degradation, chaperone/protein-folding, and metallotheionins, among others.

When the functional and pathway analysis was expanded to include all differentially expressed genes in each dataset, further expression pattern similarities among the disuse models were discovered including the enrichment of the protein degradation functional group and the oxidative stress response pathway.

CONCLUSIONS: Although only a small subset of differentially expressed genes were common to skeletal muscle response to 48h IM, SCI, and UL, functions of protein degradation and oxidative stress were statistically over-represented in all the models, suggesting that these molecular mechanisms are likely key regulators in the early stages of disuse, regardless of the specific stimulus.

Introduction

Disuse muscle atrophy occurs in response to immobilization (IM) (37, 63), unloading (UL) (2, 5-6), bed rest (7-8, 53), spaceflight (2, 60-61), and spinal cord injury (SCI) (13, 31, 57, 62). Although studies in humans have documented the effects of disuse on skeletal muscle structure and function (5-6, 9, 18-20, 26, 31, 33, 36, 38, 51, 57), the underlying mechanisms regulating these changes are not well understood. Investigations of multiple forms of disuse in animals have shown that there is a coordinated alteration in expression of genes encoding for proteins that function in the initiation of the muscle atrophy process. Mechanisms identified in these studies have included increases in gene expression related to protein degradation and stress response as well as decreases in gene expression related to transcription and translation, energy metabolism, and extracellular matrix proteins (44).

Of the few studies that have been undertaken in humans (14, 37, 63), our laboratory (62-63) reported that differential gene expression is evident as early as 48h following disuse via IM and SCI; these results suggested that the molecular changes ultimately leading to atrophy associated with later time points (*e.g.*, weeks and months), may be initiated in the first few days—before measurable decreases in size or strength have manifested. However, while gene expression and related protein products of

individual molecules have been investigated following 48h IM and SCI (62-63), the global gene expression patterns in these disuse models have not been studied or compared to one another. Recent data collected in our laboratory following 48h UL afforded me the unique opportunity to compare gene expression profiles of these three common models of disuse by analyzing microarray datasets from the UL experiment to those of 48h IM and SCI (data from the latter two studies have been published elsewhere (62-63)).

Molecular signaling leading to disuse atrophy is likely a complex sequence of events that involve numerous interrelated pathways. Systems biology is an emerging discipline that focuses on the relationships between multiple cellular components (25). Microarray technology provides the means to measure expression levels of thousands of genes at once, and analysis tools have been developed to analyze the expression patterns of these high through-put experiments. The Database for Annotation, Visualization and Integrated Discovery (DAVID) and Ingenuity Pathway Analysis (IPA) use results from microarray experiments to identify functions and pathways as well as to construct potential gene networks associated with the gene expression patterns revealed via microarray.

Employing this technology to interpret gene expression results may lead to a better understanding of functions and pathways universal to IM, SCI, and UL in humans. Furthermore, studying global gene expression patterns at the early time-point of 48h of disuse (before any measurable atrophy has occurred) may lead to the identification of molecules and pathways for therapeutic targets to prevent or attenuate disuse-associated atrophy.

Methods

Subjects

Seven (n=7) sedentary men completed the UL study. Mean (\pm S.D.) age, height, and weight were 22.1 (3.7) yr, 1.4 (0.1) m, and 78.2 (3.1) kg, respectively. Those with bleeding problems, known allergies to Lidocaine, orthopedic problems, or use of medications that could increase bleeding (such as aspirin) were excluded from the study, as were individuals who are taking muscle building supplements or restricting caloric intake. All subjects signed an informed consent form approved by the University of Massachusetts and Hartford Hospital Review Boards and completed a medical history questionnaire and physical activity questionnaire before being enrolled in the study to insure they met the inclusion/exclusion criteria. In addition, each potential subject was carefully screened to ensure that he was aware of the inconvenience inherent in the unloading protocol, understood the potential discomfort from the biopsy procedure, and the felt confident that he could comply with all study requirements. Subjects (n=5) for the IM study were recruited using similar inclusion/exclusion criteria (63) while subjects (n=10) for the SCI study were recruited within 48h of their injury and were over the age of 18 (62).

Disuse Protocols

Lower limb unloading (UL) was achieved using the ULLS model which required that subjects wear a shoe with a 10-cm sole (Kintec Footlabs, Surrey, BC) on the right foot. The left foot did not have contact with the ground; therefore, the left lower limb was unloaded for the duration of the 48h UL protocol. All ambulatory activity was performed on crutches with only the right foot having contact with the ground. Although the UL leg

was free to move, no load was placed on it, and any physical activity requiring use of the left quadriceps muscles was restricted. Berg *et al.* (5) and others (3, 16, 32) have used this ULLS model up to 6 wk. Compliance during the UL phase of the current study was confirmed through the use of activity monitors (Model #7164 Computer Science and Applications, Inc., Shalimar FL) worn on both ankles, which showed a 29% - 35% reduction in acceleration in the unloaded leg compared to the loaded leg. IM and SCI protocols are published elsewhere (62-63). In brief, the IM protocol was similar to the UL protocol with the exception that immobilization was achieved through the use of a long-leg cast which was secured with fiberglass casting tape to ensure compliance.

Data Collection

Biopsies were collected at baseline and 48h post-disuse (in the case of the UL and IM conditions). All biopsy procedures for these two conditions were conducted at Hartford Hospital and were taken at the same time of day to reduce circadian influences. Subjects were fed a standardized meal 3h prior to each biopsy because meal patterns alter the activity of certain genes related to muscle atrophy and hypertrophy (21). In the case of the SCI condition, biopsies were collected 48h post-SCI. Percutaneous needle muscle biopsies were obtained using a Bergstrom 5-mm biopsy needle (Depuy, Warsaw, IN) in a sterile field. First, skin was lightly anesthetized with 2% lidocaine hydrochloride solution. Next, a small (5-6mm) incision was made through the skin and muscle fascia, and the biopsy needle was inserted. Up to 150mg of tissue was removed and divided into 3 aliquots (up to 50mg each). Biopsy samples were immediately snap-frozen in liquid nitrogen upon excision. All samples were stored at -80° C until analysis.

Gene Expression Profiling

The microarray data for this study were acquired from previous studies in our laboratory, the results of which have been published elsewhere (62-63), and from Study I of this dissertation. Affymetrix Human Genome U133 Plus 2.0 microarrays for analysis of over 47,000 transcripts were used for this study. The procedures including total RNA isolation, cDNA synthesis, cRNA labeling, microarray hybridization and image acquiring was done as described previously (15). Briefly, total RNA isolated with TRIzol reagent and purified with RNeasy MinElute Cleanup Kit (Qiagen, Valencia, CA). Three microgram of total RNA from each sample were converted into double-stranded cDNA then cRNA using one-cycle target labeling and control reagents and protocol (Affymetrix, Santa Clara, CA). After purification using GeneChip® Sample Cleanup Module (Affymetrix, Santa Clara, CA), biotin-labeled cRNA was then fragmented randomly prior to hybridizing to the microarrays. Each array was washed and stained on the Affymetrix Fluidics Station 450, and then probe arrays were scanned via the GeneChip® Scanner 3000. The quality control criteria developed at Children's National Medical Center Microarray Center for each array were followed (1, 15).

Absolute analysis of Affymetrix "raw" data was conducted using Affymetrix MAS5.0 and DNA-Chip Analyzer software (dCHIP) (46, 49). The data were then imported into the GeneSpring 7.0 (Silicon Genetics, Redwood City, CA) for data filtering and statistical analysis. First, genes with 2 "present calls" (~10% of the total arrays) were selected for statistical analysis. Probe sets showing significant ($p < 0.05$) expression changes (using Welch's *t*-test) in both MAS5.0 and dCHIP were retained for hierarchical clustering, functional and pathway analysis.

Each subject served as his own control (in the case of IM and UL conditions). In the case of SCI, baseline biopsies from the IM and UL conditions were pooled and served as the control for the 48h SCI condition.

Identification of Functional Classifications and Groups

The datasets (IM, SCI, and UL) were compared to identify those genes that were differentially expressed in all three. The resulting list of gene identifiers were input into the DAVID online interface (<http://david.abcc.ncifcrf.gov/>), and the functional annotation tool was employed to classify genes on the list by function.

DAVID analysis was also expanded to identify enriched functional groups for each individual dataset using DAVID as described in Huang *et al* (35). In brief, complete lists of Affymetrix probe set IDs for each dataset were uploaded into the DAVID online interface, and the functional annotation tool was employed to filter functional groups associated with the each list. Filtering criteria included: 1) adjusted p-value (Benjamini & Hochberg) of $p < 0.05$ and 2) enrichment score of ≥ 1.5 .

Identification of Canonical Pathways

Ingenuity software (Ingenuity Systems, Inc., Redwood City, CA) identified the pathways from the IPA library of canonical pathways that were significant within each dataset (IM, SCI, UL). The significance of the association between the dataset and the canonical pathway was measured in two ways: 1) A ratio of the number of genes from the dataset that map to the pathway divided by the total number of genes that map to the canonical pathway is displayed; and 2) Fischer's exact test was used to calculate a p-value determining the probability that the association between the genes in the dataset

and the canonical pathway is explained by chance alone. Canonical pathways with a p-value < 0.05 were reported.

Gene Network Generation

Custom gene networks were generated within IPA for each dataset. To build gene networks, the Ingenuity software mapped each Affymetrix probeset to its corresponding gene object in the Ingenuity Pathways Knowledge Base. These genes were overlaid onto a global molecular network developed from information contained in the Ingenuity Pathways Knowledge Base. Networks of these genes were then algorithmically generated based on their connectivity and ranked by network score. The network score was based on the hypergeometric distribution and was calculated with the right-tailed Fisher's Exact Test that returned a p-value determining the probability that the interconnectivity of the genes in the network are due to chance alone. The score is the negative log of the p-value.

Results

Microarray Analysis

Microarray findings for the three models of disuse (IM, SCI, UL) included in this analysis showed that there were 3303 differentially expressed transcripts representing 2393 genes. Figure 4.1 illustrates the distribution of these genes among the datasets. Among the three, 48h SCI resulted in the greatest number of altered transcripts compared to control, followed by 48h IM, and then 48h UL. Whereas 60 – 74% of differentially expressed genes in each dataset were stimulus-specific, the remaining 26 – 40% of the genes in each list were shared by multiple models of disuse.

Expression Shared by IM, SCI, and UL Models of Disuse

Thirty-two genes were differentially expressed in all three disuse models (Figure 4.1). Of these shared genes, 26 had known biological functions (Table 4.1). Twenty genes were upregulated following all three models of disuse and were classified under functions such as transcription, protein degradation, stress response, and ECM, among others. Six genes were downregulated following all three models of disuse. Of these, 3 were related to chaperone/protein folding, whereas the remaining 3 were related to transcription.

Biological Functions and Pathways within Individual Models of Disuse

Table 4.2 lists functional groups associated with the individual disuse conditions. Protein degradation-related functional groups (*e.g.*, ubiquitin conjugation, ubiquitin-protein ligase activity, and proteasome) were enriched in all three individual models of disuse. In addition to shared functions, unique functional themes were found. Gene expression changes related to oxidative phosphorylation and mitochondrion were observed following 48h SCI; stress response reached significance following 48h UL; and heatshock proteins and chaperone reached significance following 48h IM. Functional analysis via DAVID showed that, while common global expression patterns related to protein degradation were evident, changes in oxidative phosphorylation and stress response, may have varied depending on the disuse stimulus.

The only significantly altered ($p < 0.05$) canonical pathway shared by all three models of disuse was the NRF2-mediated oxidative stress response pathway. This is of particular interest because oxidative stress has been proposed as an early trigger of the atrophy program in skeletal muscle following disuse (54). In brief, cellular stress results in translocation of transcription factor NRF2 to the nucleus where it activates genes that

encode antioxidant proteins (to neutralize reactive molecules), chaperones and co-chaperones (to repair damaged proteins), and detoxifying enzymes (to metabolize harmful chemicals). In this way, the muscle cell works to combat the oxidative damage that can lead to deleterious effects such as contractile protein degradation, and thus, decreased muscle size.

The altered gene expression (compared to control) in the NRF2-mediated Oxidative Stress Pathway for all three conditions is represented in Table 4.3. While all three models of disuse resulted in downregulation of co-chaperone genes in the pathway (*i.e.*, DNAJ), expression profiles for the three datasets still showed differing patterns of expression. Aside from the downregulated expression of three DNAJ transcripts, the remaining altered components of the pathway in the UL dataset were upregulated; the majority of those genes are purported to serve a protective role in the cell. Of particular interest is heme oxygenase-1 (HMOX1) because of the 15.4-fold increase observed in the, otherwise, subtly altered UL expression profile. HMOX1 encodes for an enzyme that is proposed to have direct and/or indirect antioxidant effects in skeletal muscle (4); increases in transcripts for this protein have been shown in multiple models of disuse (44, 59). Although HMOX1 was not found to be differentially expressed following 48h IM (4.1-fold increase, $p=0.12$), there was a trend towards a significance increase following 48h SCI (3.4-fold, $p=0.07$). Evidence from the UL expression profile suggests that while there were decreases in pathway products related to chaperone activity, the majority of expression in this canonical pathway following 48h UL was upregulated and consistent with increased antioxidant activity.

The expression profile for the SCI disuse model showed the greatest number of differentially expressed genes of the three datasets for this pathway; in addition to 6 downregulated DNAJs, decreases in mRNA levels for 8 genes encoding for antioxidant glutathione S-transferase (GST) proteins were observed. Even so, there were increases in expression of cytoprotective genes following 48h SCI in this pathway including FTL, glutathione reductase (GSR), and superoxidase dismutase-2 (SOD). GSR codes for glutathione reductase, an enzyme that helps maintain the antioxidant capacity of the cell (40); and SOD is a potent oxidant scavenger (52). Regardless of the downregulation of certain components of the NRF2 pathway following 48h SCI, there is evidence of increased antioxidant gene transcription in this model of disuse.

Conversely, the expression profile for the IM disuse model showed expression for the majority of differentially expressed genes in the NRF2 pathway were downregulated. In addition to the shared expression pattern of downregulated DNAJ chaperone genes, other protein-folding genes were down-regulated (*e.g.*, STIP1 and GST member gene, GSTM4). Furthermore, as was the case with the SCI expression profile, both NRF2-activity enhancer, ATF4 (an NRF2 nuclear enhancer), and NRF2 encoding gene NFE2L2 were downregulated. Decreased activity of NRF2 could lead to decreases in antioxidant transcription. While there were genes upregulated in this pathway for the IM model of disuse, they were primarily related to protein degradation at the proteasome (USP14) and the transport of lysosomal enzymes to the lysosome (PIK3C3). Therefore, unlike the UL and SCI models of disuse, the IM model does not appear to result in a substantial increase in antioxidant gene expression via the NRF2-mediated Oxidative Stress Response Pathway.

Finally, two additional findings related to this pathway are worthy of note: the SCI and IM expression profiles both showed a decrease in MAP2K expression. MAP2K expression is associated with activation of the p38 MAPK pathway which leads to increases in apoptosis (47). Decreases in MAP2K serve a protective mechanism by downregulating MAPK activation.

Ingenuity network generation revealed that the top networks for all three conditions contained downregulated chaperone genes (*e.g.*, those encoding heat shock proteins and DNAJ co-chaperones) (Figures 4.2a – c).

DAVID analysis was employed to discover genes within each dataset that were categorized under the functional term “chaperone” (Table 4.4). As found in the smaller subset of shared genes, mRNA levels of transcripts in the chaperone functional category within each of the datasets were largely decreased, thus showing that down-regulation of chaperone and protein-folding activity was likely associated with cellular response to all three disuse stimuli.

Of particular interest were HSPA1A and HSPA8, which are genes that encode a member of Hsp70 and Hsp70 cognate protein (Hsc70), respectively. Hsp70 responds to oxidative stress but has been shown to decrease with disuse muscle atrophy (43). This is relevant because Hsp70 downregulation may make skeletal muscle more vulnerable to the oxidative stress associated with disuse. Hsc70 interacts with the stress-inducible Hsp70-member proteins as a co-chaperone; furthermore, under resting conditions, this constitutively expressed chaperone participates in the maintenance of cellular homeostasis and in the folding of nascent proteins including myosin (58). Also of importance in these findings, was the preponderance of downregulated DNAJ and BAG

genes in all three datasets because these genes function as co-chaperones, regulating Hsp70 and Hsc70 activity (39). These results suggest that a complex network of downregulated chaperone and protein-folding genes associated with the IM, SCI, and UL models of disuse contributed to protein degradation signaling activity.

Discussion

The global analyses in the current study revealed that, following 48h of disuse, there were 636 – 1602 differentially expressed transcripts in IM, SCI, and UL datasets, but only 32 genes were shared by all three. Hosack *et al.* (23) have shown that, when comparing the microarray datasets of multiple studies, it is common for there to be very little overlap in differential expression of individual transcripts. In fact, a recent meta-analysis of expression profiles drawn primarily from studies in rats and mice (12) found no shared expression patterns of individual transcripts, yet common biological functions. Given these previous findings, we discovered a relatively robust percentage of shared altered expression among the three disuse models in this study (32 genes). This was likely due to the following factors: 1) muscle samples from all three studies were processed for storage and shipping by members of our laboratory; 2) mRNA isolation, cRNA synthesis, and microarray analysis were all conducted in the same genomics facility (Center for Genetic Medicine, Children's National Medical, Washington, D.C.) using the same genechip technology and the same parameters for statistical analysis; and 3) the inclusion criteria for the IM and UL studies were the same, as were the procedures in place for subject preparation and biopsy (including biopsy excision by the same physician).

The global gene expression analysis revealed that all three models of disuse shared common functions and pathways within the individual datasets. The chelation group (comprised of upregulated metallothioneine isoforms) was enriched in all three conditions. Chaperone-coding genes were found in the highest ranked IPA networks for both UL and IM as well as the seventh highest ranked network in the SCI condition. Furthermore, the NRF2-mediated Oxidative Stress Response Pathway was the only canonical pathway identified as statistically significant in all three models.

Metallothioneines

Metallothioneins (MTs; MT1F, MT1E, MT1X, MT1 pseudogene 2, and MT2A) were consistently upregulated following 48h IM, UL, and SCI. This is in agreement with findings in animal models (44) of skeletal muscle atrophy including denervation, spinal cord dissection, fasting, 2004), and uremia (44), as well as in a cell culture model of atrophy (55). Metallothioneins are small molecular weight metal-binding proteins that have been found to increase following oxidative stress and to scavenge reactive oxygen species (ROS) (17). Because oxidative stress has been implicated as a contributor in the initiation of disuse atrophy, it has been proposed that the increase in MT expression consistently observed across multiple models of disuse may confer a protective effect following atrophy stimuli (63). The current study confirmed that increases in MT mRNA may also be a consistent early response to multiple disuse stimuli in humans. However, although increases in MT protein products were observed following 5d SCI (62) increases in protein products were not found following 48h SCI or 48h IM in humans (63). This suggests that while MT mRNA levels may rise regardless of disuse stimulus,

perhaps MT translation is regulated by duration and/or intensity of the stimulus and controlled at the post-transcriptional level.

Protein Chaperones

Protein chaperones were largely decreased following 48h IM, SCI, and UL (Table 4.4). Downregulated genes encoding for heat shock protein chaperones has been observed in rats following short-term (12h and 25h) hindlimb unloading (10, 29, 59) however this is the first time that downregulation of these genes has been observed with disuse in humans. Chaperones are molecules that function to protect proteins from degradation by stabilizing nascent proteins during folding and damaged proteins during refolding (43). HSP70 (a subunit of which is encoded by HSPA1A) and its co-chaperone HSC70 (encoded by HSPA8) have been identified as key proteins in oxidative stress response in muscle and may aid in the folding of the contractile protein myosin (24, 58). While it has been argued that skeletal muscle atrophy is driven by the upregulation of protein degradation (24), attention has also been paid to the contribution of decreased protein synthesis (22). Downregulation of protein folding genes, as observed in the current study, may serve to attenuate the rate of protein synthesis.

The protein complex HSP70/HSC70 associates with nascent polypeptides and newly translated proteins. While HSC70 aids with protein folding (29), HSP70 regulates the rate of elongation, and thus protein synthesis (42). Ku *et al.* observed that following hind-limb unloading in rats, elongation-dependent protein synthesis rate was slowed, and in a subsequent study (42) established that HSP70 and HSC70 association with nascent polypeptides were decreased following 12h and 24h unloading. Perhaps, in the current study, decreases in HSPA1A and HSPA8 gene expression not only rendered the skeletal

muscle more vulnerable to oxidative stress, but also led to decreases in elongation, and thus protein synthesis. Oxidative damage and decreased protein synthesis 48h post-disuse stimulus may both be early precursors to the atrophy associated with longer durations of IM, SCI, and UL in humans.

These shared chaperone coding genes, took part in the highest rated IPA network (Figure 4.2a) for the 124-member subset of shared genes among the three models of disuse. This network featured HSP-coding genes and genes that code for chaperones which regulate these HSPs such as HSPE1 and DNAJA4. HSPE1 codes for HSP10, a heat-shock protein that prevents the ubiquitination of IGF-1 and the IGF-1 receptor in cardiac myocytes, and may perform the same function in skeletal muscle. As IGF-1 is a key signaling molecule in the AKT-mTOR pathway leading to protein synthesis, decreases in HSP10 protein may lead to decreased IGF-1 signaling and, therefore, a cellular environment that favors AKT-FOXO signaling and protein degradation. DNAJ genes code for HSP40 proteins that interact with and mediate HSP70 activity. Importantly, the network also included key components of degradation-related pathways such as NFK β , ERK, and p38 MAPK, the activity of which have been shown to lead to skeletal muscle atrophy.

Increases in chaperone proteins have been associated with decreases in the activity of these pathways. For example, Senf *et al.* (56) found that by overexpressing HSP70 in rat soleus muscle, NFK β expression was decreased and atrophy was attenuated. Furthermore, chaperone proteins have been shown to inhibit ERK, and ERK inhibition has been shown to blunt hypertrophy (reviewed in (27)). Finally, p38 MAPK has been shown to be an important signaling molecule in the molecular events leading to atrogen1

transcription, with activation of p38 via phosphorylation leading to atrogin1 upregulation. HSP70 has been shown to decrease p38 activation (48).

Although only 32 genes were shared by IM, SCI, and UL. DAVID and IPA analysis revealed that a larger group of genes within each dataset were related to functions common, if not to all three, at least to two of the models of disuse. This is consistent with previous meta-analyses that found few, if any, commonly expressed genes, yet still found significantly shared biological functions among datasets (34).

Protein Degradation

Within each of the models of disuse, functional groups related to protein degradation were enriched with the vast majority of genes within each dataset upregulated. Although measurable atrophy has not been detected following durations as short as 48h disuse, the upregulation of protein degradation genes support the hypotheses that the atrophy program may be put in motion as early as 48h after the onset of the disuse stimulus (63).

Notably, transcription of FBXO32 (which codes for the atrogin1 protein) was increased following 48h of disuse in each of the three models. atrogin1 is an E3 ligase that is a key component of the ubiquitin proteasome pathway, and it has been previously shown to be differentially expressed with disuse atrophy. For example, 24h following the initiation of immobilization and unloading in rat muscle, atrogin1 and the related E3 ligase MuRF1 were upregulated (11). Furthermore, atrogin1 knockout mice displayed attenuated atrophy following unloading (11), and C₂C₁₂ myotubes transfected with atrogin1 were measurably thinner than controls (11). Taken together, these findings suggest that atrogin1 is likely an important early regulator of skeletal muscle atrophy and

that it (or its protein targets) may represent candidates for early intervention following disuse via drug-mediated modification to attenuate atrophy in humans.

Findings from human studies have not been in agreement regarding atrogin1. While both 20d of bed rest (53) and 2wk of leg immobilization (37) led to a significant 1.6-fold increase in atrogin1 gene expression (37), findings in our laboratory have been equivocal. While analysis of biopsies from the UL (Reich *et al.*, unpublished) and SCI (62) protocol measured with the more sensitive quantitative real-time polymerase chain reaction (qRT-PCR) confirmed increases in atrogin1, analysis of biopsies from the IM samples (63) found no significant differences (63). Furthermore, protein quantification via Western blot found no significant differences in protein products for atrogin1 following 48h UL (unpublished), IM (63), or SCI (64). However, it has been suggested that atrogin1 expression is controlled at the translational level, and that the level of expression is dependent on the magnitude and duration of the disuse stimulus (45). Therefore, it is possible that 48h of disuse, regardless of stimulus (IM, SCI, or UL) is not adequate duration in humans to lead to decreases in protein content.

Stress Response

IPA analysis revealed that the NRF2-mediated Stress Response Pathway was the only pathway found to be significant in all three models of atrophy (Table 4.6). Oxidative stress has been identified as a likely contributor to the cellular response to disuse, ultimately leading to atrophy if the disuse stimulus persists (54). Oxidative may lead to increases in calpain cleavage of acto-myosin complexes (30), NFK β activity (65), and E3 ligases such as atrogin1 (54). Upregulated stress response genes in this pathway following 48h SCI and UL such as HMOX1 in UL, GSR, and SOD in SCI, is evidence

that oxidative stress is likely a component of the molecular changes following disuse (41, 44). However, the downregulation of many member genes in the NRF2-mediated Stress Response Pathway such as DNAJ co-chaperone genes suggests that this stress response may be impaired following disuse. The hypothesis is supported by previous work of McClug *et al.* (50) who found redox imbalance associated with disuse in mouse diaphragm following unloading.

It is unclear as to why the IM model of disuse did not exhibit increases in cytoprotective stress response genes as seen with SCI and UL, but rather only increases in genes related to protein degradation (Table 4.6). One difference between the IM model and the latter two was that with IM, subjects were prevented from moving the knee joint, but were not restricted from standing on the leg; conversely, no weight-bearing activity was permitted in the experimental leg in the UL or SCI models of disuse. Little is known about this stress response pathway and mechanotransduction. However, Fluck *et al.* (28) showed that there are differences in structure and function at the cellular level when comparing high-contractile/low-loading conditions to low-contractile/high-loading conditions such that mitochondrial metabolism is uncompromised in the former condition, but not the latter. Since many of the stress response components of this pathway localize to the mitochondria, it is possible that differences in how stress response contributes to molecular changes following IM (compared to SCI and UL) are related to differences at the mitochondrial level. In fact, differences in mitochondrial function are further evidenced in the current study with regard to mitochondrial metabolism; the mitochondrion functional group was significantly enriched following both SCI (2.4-fold,

p<0.05) and UL (2.1-fold, p<0.05), but not following IM. The majority of these genes were downregulated and related to aerobic metabolism.

Conclusions

Recent development of technologies such as microarray analysis not only allowed us to measure the differential gene expression of thousands of genes within each dataset, but also high through-put tools such as DAVID and IPA provided us with the ability to interpret these expression patterns within the context of known biological functions. Although the molecular signatures for immobilization, spinal cord injury, and unloading are unique, there are clearly common molecular changes among all three models, particularly those associated with oxidative stress response such as metallothioneins and protein chaperones, as well as the expected function of protein degradation. In addition to the shared enriched function of protein degradation, stress response is an attractive area for further study in the search for potential gene targets as oxidative stress has already been posited as an early upstream regulator of skeletal muscle atrophy.

References

1. Expression profiling--best practices for data generation and interpretation in clinical trials. *Nat Rev Genet* 5: 229-237, 2004.
2. **Adams GR, Caiozzo VJ, and Baldwin KM.** Skeletal muscle unweighting: spaceflight and ground-based models. *J Appl Physiol* 95: 2185-2201, 2003.
3. **Adams GR, Hather BM, and Dudley GA.** Effect of short-term unweighting on human skeletal muscle strength and size. *Aviat Space Environ Med* 65: 1116-1121, 1994.
4. **Alam J, and Cook JL.** How many transcription factors does it take to turn on the heme oxygenase-1 gene? *Am J Respir Cell Mol Biol* 36: 166-174, 2007.
5. **Berg HE, Dudley GA, Haggmark T, Ohlsen H, and Tesch PA.** Effects of lower limb unloading on skeletal muscle mass and function in humans. *J Appl Physiol* 70: 1882-1885, 1991.
6. **Berg HE, Dudley GA, Hather B, and Tesch PA.** Work capacity and metabolic and morphologic characteristics of the human quadriceps muscle in response to unloading. *Clin Physiol* 13: 337-347, 1993.
7. **Berg HE, Eiken O, Miklavcic L, and Mekjavic IB.** Hip, thigh and calf muscle atrophy and bone loss after 5-week bedrest inactivity. *Eur J Appl Physiol* 99: 283-289, 2007.
8. **Berg HE, Larsson L, and Tesch PA.** Lower limb skeletal muscle function after 6 wk of bed rest. *J Appl Physiol* 82: 182-188, 1997.
9. **Berg HE, and Tesch PA.** Changes in muscle function in response to 10 days of lower limb unloading in humans. *Acta Physiol Scand* 157: 63-70, 1996.
10. **Bey L, Akunuri N, Zhao P, Hoffman EP, Hamilton DG, and Hamilton MT.** Patterns of global gene expression in rat skeletal muscle during unloading and low-intensity ambulatory activity. *Physiol Genomics* 13: 157-167, 2003.
11. **Bodine SC, Latres E, Baumhueter S, Lai VK, Nunez L, Clarke BA, Poueymirou WT, Panaro FJ, Na E, Dharmarajan K, Pan ZQ, Valenzuela DM, DeChiara TM, Stitt TN, Yancopoulos GD, and Glass DJ.** Identification of ubiquitin ligases required for skeletal muscle atrophy. *Science* 294: 1704-1708, 2001.
12. **Calura E, Cagnin S, Raffaello A, Laveder P, Lanfranchi G, and Romualdi C.** Meta-analysis of expression signatures of muscle atrophy: gene interaction networks in early and late stages. *BMC Genomics* 9: 630, 2008.

13. **Castro MJ, Apple DF, Jr., Staron RS, Campos GE, and Dudley GA.** Influence of complete spinal cord injury on skeletal muscle within 6 mo of injury. *J Appl Physiol* 86: 350-358, 1999.
14. **Chen Y-W, Gregory CM, Scarborough MT, Shi R, Walter GA, and Vandeborn K.** Transcriptional pathways associated with skeletal muscle disuse atrophy in humans. *Physiol Genomics* 31: 510-520, 2007.
15. **Chen YW, Zhao P, Borup R, and Hoffman EP.** Expression profiling in the muscular dystrophies: identification of novel aspects of molecular pathophysiology. *J Cell Biol* 151: 1321-1336, 2000.
16. **Clark BC, Manini TM, Bolanowski SJ, and Ploutz-Snyder LL.** Adaptations in human neuromuscular function following prolonged unweighting: II. Neurological properties and motor imagery efficacy. *J Appl Physiol* 101: 264-272, 2006.
17. **Colangelo D, Mahboobi H, Viarengo A, and Osella D.** Protective effect of metallothioneins against oxidative stress evaluated on wild type and MT-null cell lines by means of flow cytometry. *Biometals* 17: 365-370, 2004.
18. **Cramer RM, Cooper P, Sinclair PJ, Bryant G, and Weston A.** Effect of load during electrical stimulation training in spinal cord injury. *Muscle Nerve* 29: 104-111, 2004.
19. **Cramer RM, Weston A, Climstein M, Davis GM, and Sutton JR.** Effects of electrical stimulation-induced leg training on skeletal muscle adaptability in spinal cord injury. *Scand J Med Sci Sports* 12: 316-322, 2002.
20. **Cramer RM, Weston AR, Rutkowski S, Middleton JW, Davis GM, and Sutton JR.** Effects of electrical stimulation leg training during the acute phase of spinal cord injury: a pilot study. *Eur J Appl Physiol* 83: 409-415, 2000.
21. **Cross DA, Watt PW, Shaw M, van der Kaay J, Downes CP, Holder JC, and Cohen P.** Insulin activates protein kinase B, inhibits glycogen synthase kinase-3 and activates glycogen synthase by rapamycin-insensitive pathways in skeletal muscle and adipose tissue. *FEBS Lett* 406: 211-215, 1997.
22. **Deboer MD, and Marks DL.** Cachexia: lessons from melanocortin antagonism. *Trends Endocrinol Metab* 17: 199-204, 2006.
23. **Dennis G, Jr., Sherman BT, Hosack DA, Yang J, Gao W, Lane HC, and Lempicki RA.** DAVID: database for annotation, visualization, and integrated discovery. *Genome Biol* 4: P3, 2003.
24. **Dodd S, Hain B, and Judge A.** Hsp70 prevents disuse muscle atrophy in senescent rats. *Biogerontology* 2008.

25. **Drubin DA, Way JC, and Silver PA.** Designing biological systems. *Genes Dev* 21: 242-254, 2007.
26. **Dudley GA, Castro MJ, Rogers S, and Apple DF, Jr.** A simple means of increasing muscle size after spinal cord injury: a pilot study. *Eur J Appl Physiol Occup Physiol* 80: 394-396, 1999.
27. **Favier FB, Benoit H, and Freyssenet D.** Cellular and molecular events controlling skeletal muscle mass in response to altered use. *Pflugers Arch* 456: 587-600, 2008.
28. **Fluck M, Chiquet M, Schmutz S, Mayet-Sornay MH, and Desplanches D.** Reloading of atrophied rat soleus muscle induces tenascin-C expression around damaged muscle fibers. *Am J Physiol Regul Integr Comp Physiol* 284: R792-801, 2003.
29. **Gething MJ, and Sambrook J.** Protein folding in the cell. *Nature* 355: 33-45, 1992.
30. **Goll DE, Thompson VF, Li H, Wei W, and Cong J.** The calpain system. *Physiol Rev* 83: 731-801, 2003.
31. **Gregory CM, Vandenborne K, Castro MJ, and Dudley GA.** Human and rat skeletal muscle adaptations to spinal cord injury. *Can J Appl Physiol* 28: 491-500, 2003.
32. **Haddad F, Adams GR, Bodell PW, and Baldwin KM.** Isometric resistance exercise fails to counteract skeletal muscle atrophy processes during the initial stages of unloading. *J Appl Physiol* 100: 433-441, 2006.
33. **Hather BM, Adams GR, Tesch PA, and Dudley GA.** Skeletal muscle responses to lower limb suspension in humans. *J Appl Physiol* 72: 1493-1498, 1992.
34. **Hosack DA, Dennis G, Jr., Sherman BT, Lane HC, and Lempicki RA.** Identifying biological themes within lists of genes with EASE. *Genome Biol* 4: R70, 2003.
35. **Huang DW, Sherman BT, and Lempicki RA.** Systematic and integrative analysis of large gene lists using DAVID bioinformatics resources. *Nat Protocols* 4: 44-57, 2008.
36. **Jayaraman A, Gregory CM, Bowden M, Stevens JE, Shah P, Behrman AL, and Vandenborne K.** Lower extremity skeletal muscle function in persons with incomplete spinal cord injury. *Spinal Cord* 44: 680-687, 2006.
37. **Jones SW, Hill RJ, Krasney PA, O'Conner B, Peirce N, and Greenhaff PL.** Disuse atrophy and exercise rehabilitation in humans profoundly affects the expression of

- genes associated with the regulation of skeletal muscle mass. *Faseb J* 18: 1025-1027, 2004.
38. **Kauhanen S, Leivo I, and Michelsson JE.** Early muscle changes after immobilization. An experimental study on muscle damage. *Clin Orthop Relat Res* 44-50, 1993.
39. **Kim MV, Seit-Nebi AS, and Gusev NB.** The problem of protein kinase activity of small heat shock protein Hsp22 (H11 or HspB8). *Biochem Biophys Res Commun* 325: 649-652, 2004.
40. **Kondo H, Miura M, and Itokawa Y.** Antioxidant enzyme systems in skeletal muscle atrophied by immobilization. *Pflugers Arch* 422: 404-406, 1993.
41. **Kondo H, Nakagaki I, Sasaki S, Hori S, and Itokawa Y.** Mechanism of oxidative stress in skeletal muscle atrophied by immobilization. *Am J Physiol* 265: E839-844, 1993.
42. **Ku Z, Yang J, Menon V, and Thomason DB.** Decreased polysomal HSP-70 may slow polypeptide elongation during skeletal muscle atrophy. *Am J Physiol* 268: C1369-1374, 1995.
43. **Lawler JM, Song W, and Kwak HB.** Differential response of heat shock proteins to hindlimb unloading and reloading in the soleus. *Muscle Nerve* 33: 200-207, 2006.
44. **Lecker SH, Jagoe RT, Gilbert A, Gomes M, Baracos V, Bailey J, Price SR, Mitch WE, and Goldberg AL.** Multiple types of skeletal muscle atrophy involve a common program of changes in gene expression. *Faseb J* 18: 39-51, 2004.
45. **Leger B, Vergani L, Soraru G, Hespel P, Derave W, Gobelet C, D'Ascenzio C, Angelini C, and Russell AP.** Human skeletal muscle atrophy in amyotrophic lateral sclerosis reveals a reduction in Akt and an increase in atrogin-1. *Faseb J* 20: 583-585, 2006.
46. **Li C, and Hung Wong W.** Model-based analysis of oligonucleotide arrays: model validation, design issues and standard error application. *Genome Biol* 2: RESEARCH0032, 2001.
47. **Li YP, Chen Y, John J, Moylan J, Jin B, Mann DL, and Reid MB.** TNF-alpha acts via p38 MAPK to stimulate expression of the ubiquitin ligase atrogin1/MAFbx in skeletal muscle. *Faseb J* 19: 362-370, 2005.
48. **Liu MJ, Li JX, Lee KM, Qin L, and Chan KM.** Oxidative stress after muscle damage from immobilization and remobilization occurs locally and systemically. *Clin Orthop Relat Res* 246-250, 2005.

49. **Liu WM, Mei R, Di X, Ryder TB, Hubbell E, Dee S, Webster TA, Harrington CA, Ho MH, Baid J, and Smeekens SP.** Analysis of high density expression microarrays with signed-rank call algorithms. *Bioinformatics* 18: 1593-1599, 2002.
50. **McClung JM, Whidden MA, Kavazis AN, Falk DJ, Deruisseau KC, and Powers SK.** Redox regulation of diaphragm proteolysis during mechanical ventilation. *Am J Physiol Regul Integr Comp Physiol* 294: R1608-1617, 2008.
51. **Miles MP, Clarkson PM, Bean M, Ambach K, Mulroy J, and Vincent K.** Muscle function at the wrist following 9 d of immobilization and suspension. *Med Sci Sports Exerc* 26: 615-623, 1994.
52. **Niwa J, Ishigaki S, Hishikawa N, Yamamoto M, Doyu M, Murata S, Tanaka K, Taniguchi N, and Sobue G.** Dorfin ubiquitylates mutant SOD1 and prevents mutant SOD1-mediated neurotoxicity. *J Biol Chem* 277: 36793-36798, 2002.
53. **Ogawa T, Furochi H, Mameoka M, Hirasaka K, Onishi Y, Suzue N, Oarada M, Akamatsu M, Akima H, Fukunaga T, Kishi K, Yasui N, Ishidoh K, Fukuoka H, and Nikawa T.** Ubiquitin ligase gene expression in healthy volunteers with 20-day bedrest. *Muscle Nerve* 34: 463-469, 2006.
54. **Powers SK, Kavazis AN, and McClung JM.** Oxidative stress and disuse muscle atrophy. *J Appl Physiol* 2007.
55. **Sacheck JM, Ohtsuka A, McLary SC, and Goldberg AL.** IGF-I stimulates muscle growth by suppressing protein breakdown and expression of atrophy-related ubiquitin ligases, atrogin-1 and MuRF1. *Am J Physiol Endocrinol Metab* 287: E591-601, 2004.
56. **Senf SM, Dodd SL, McClung JM, and Judge AR.** Hsp70 overexpression inhibits NF-kappaB and Foxo3a transcriptional activities and prevents skeletal muscle atrophy. *Faseb J* 22: 3836-3845, 2008.
57. **Shah PK, Stevens JE, Gregory CM, Pathare NC, Jayaraman A, Bickel SC, Bowden M, Behrman AL, Walter GA, Dudley GA, and Vandenborne K.** Lower-extremity muscle cross-sectional area after incomplete spinal cord injury. *Arch Phys Med Rehabil* 87: 772-778, 2006.
58. **Srikakulam R, and Winkelmann DA.** Chaperone-mediated folding and assembly of myosin in striated muscle. *J Cell Sci* 117: 641-652, 2004.
59. **Stevenson EJ, Giresi PG, Koncarevic A, and Kandarian SC.** Global analysis of gene expression patterns during disuse atrophy in rat skeletal muscle. *J Physiol* 551: 33-48, 2003.

60. **Tesch PA, and Berg HE.** Effects of spaceflight on muscle. *J Gravit Physiol* 5: P19-22, 1998.
61. **Trappe SW, Trappe TA, Lee GA, Widrick JJ, Costill DL, and Fitts RH.** Comparison of a space shuttle flight (STS-78) and bed rest on human muscle function. *J Appl Physiol* 91: 57-64, 2001.
62. **Urso ML, Chen YW, Scrimgeour AG, Lee PC, Lee KF, and Clarkson PM.** Alterations in mRNA expression and protein products following spinal cord injury in humans. *J Physiol* 579: 877-892, 2007.
63. **Urso ML, Scrimgeour AG, Chen YW, Thompson PD, and Clarkson PM.** Analysis of human skeletal muscle after 48 h immobilization reveals alterations in mRNA and protein for extracellular matrix components. *J Appl Physiol* 101: 1136-1148, 2006.
64. **Van Gammeren D, Falk DJ, DeRuisseau KC, Sellman JE, Decramer M, and Powers SK.** Reloading the diaphragm following mechanical ventilation does not promote injury. *Chest* 127: 2204-2210, 2005.
65. **Wing SS.** Control of ubiquitination in skeletal muscle wasting. *Int J Biochem Cell Biol* 37: 2075-2087, 2005.

Table 4.1. Shared changes in gene expression among all three conditions. IM=immobilization, SCI=spinal cord injury, UL=unloading, FC=fold-change relative to control (baseline for IM and UL, control subjects for SCI).

			IM		SCI		UL	
			FC	p-value	FC	p-value	FC	p-value
Chaperone/Protein Folding								
209406_at	BAG2	BCL2-associated athanogene 2	-1.24	3.63E-02	-1.14	4.61E-02	-1.16	1.35E-02
225061_at	DNAJA4	DnaJ (Hsp40) homolog, subfamily A, member 4	-2.50	2.96E-03	-3.20	1.29E-02	-1.76	4.65E-03
200799_at, 200800_s_at	HSPA1A	heat shock 70kda protein 1a	-1.76	4.91E-02	-1.81	3.54E-02	-1.35	4.93E-02
Protein Degradation/Ubiquitin Proteasome Pathway								
200655_s_at, 211985_s_at	CALM1	calmodulin 1 (phosphorylase kinase, delta)	1.36	1.23E-02	1.66	5.39E-03	1.35	1.77E-02
225328_at, 241763_s_at	FBXO32	F-box protein 32 (Atrogin1)	1.79	1.70E-02	4.72	4.15E-03	1.55	2.64E-02
Metallothioneins								
212859_x_at	MT1E	metallothionein 1E	1.91	3.62E-02	5.21	3.26E-03	2.14	2.83E-02
217165_x_at	MT1F	metallothionein 1F	2.31	2.18E-02	10.51	2.30E-03	2.26	2.00E-03
211456_x_at	MT1P2	metallothionein 1 pseudogene 2	1.87	3.78E-02	10.04	2.30E-03	2.00	3.70E-02
204326_x_at	MT1X	metallothionein 1X	1.68	4.51E-02	4.51	2.50E-03	1.54	1.03E-02
208581_x_at	MT1X	metallothionein 1X	1.80	4.50E-02	5.65	2.37E-03	1.71	1.51E-02
212185_x_at	MT2A	metallothionein 2A	1.98	1.90E-02	7.56	5.61E-04	1.88	1.58E-02
mRNA Transcription/Processing								
204113_at, 209489_at	CUGBP1	CUG triplet repeat, RNA binding protein 1	-1.31	4.00E-02	1.87	5.39E-03	1.22	1.20E-02
225310_at	RBMX	RNA binding motif protein, X-linked	1.43	4.30E-02	1.68	8.27E-03	1.38	4.46E-02
226682_at	RORA	RAR-related orphan receptor A	1.45	2.48E-02	2.61	2.69E-03	1.48	2.33E-02
201586_s_at, 214016_s_at	SFPQ	splicing factor proline/glutamine-rich	1.43	1.39E-02	1.56	1.07E-03	1.41	7.09E-03
38918_at	SOX13	SRY (sex determining region Y)-box 13	1.38	2.51E-02	1.52	1.04E-02	1.32	2.27E-03
Metabolism								
203746_s_at, 203745_at	HCCS	holocytochrome c synthase	-1.36	1.25E-02	-1.75	1.13E-03	-1.17	3.38E-02
202464_s_at	PFKFB3	fructose-2,6-biphosphatase 3	3.30	2.37E-02	10.65	3.62E-04	2.70	2.20E-02

Continued

Table 4.1 Continued

			IM		SCI		UL	
			FC	p-value	FC	p-value	FC	p-value
Extracellular Matrix								
222693_at, 225032_at, 242029_at	FNDC3B	fibronectin type III domain containing 3B	1.79	1.30E-03	1.64	4.20E-02	-1.69	1.50E-02
205498_at	GHR	growth hormone receptor	1.33	2.81E-02	1.55	1.43E-02	1.26	4.52E-02
Protein Transport/Binding								
226633_at	RAB8B	RAB8B, member RAS oncogene family	1.45	2.24E-02	2.71	4.03E-02	1.36	4.14E-02
1553177_at	SH2D1B	SH2 domain containing 1B	2.11	7.69E-03	4.45	4.64E-02	1.26	4.90E-02
Striated Muscle Contraction								
208430_s_at, 205741_s_at	DTNA	dystrobrevin, alpha	-1.68	2.28E-02	-2.00	1.48E-02	-1.15	4.02E-03
Cell Cycle								
202769_at	CCNG2	cyclin G2	2.08	8.03E-03	2.80	1.90E-02	1.72	2.08E-02
Immune Response								
222484_s_at	CXCL14	chemokine (C-X-C motif) ligand 14	2.53	1.78E-03	2.43	8.89E-03	1.62	3.52E-04

Table 4.2. Over-represented functional groups associated with each disuse condition. Count =# of genes in each category; Fold enrichment=magnitude of over-representation in dataset. Adjusted p-value=Benjamani and Hockberg multiple testing correction. Functional annotations are listed in order of fold enrichment.

Functional Groups	Count	p-value	Fold Enrichment	Adjusted p-value
heat shock	5	4.88E-04	11.61	3.20E-02
chaperone	25	2.06E-07	3.44	2.75E-05
acetylation	70	1.65E-09	2.17	3.51E-07
mrna processing	25	8.95E-04	2.09	4.66E-02
ubl conjugation	38	6.15E-04	1.81	3.58E-02

SCI Functional Groups	Count	p-value	Enrichment Score	Adjusted p-value
chelation	6	7.47E-05	11.24	4.96E-03
tricarboxylic acid cycle	8	1.40E-04	6.42	8.27E-03
oxidative phosphorylation	11	5.27E-05	4.88	4.01E-03
proteasome	18	9.14E-08	4.82	1.08E-05
mitochondrion	128	7.90E-30	3.01	8.42E-27
acetylation	102	3.29E-22	2.87	1.17E-19
oxidoreductase	77	1.67E-11	2.29	3.56E-09
repressor	36	2.96E-04	1.91	1.42E-02
ubl conjugation	40	0.00103	1.72	3.58E-02

UL Functional Groups	Count	p-value	Enrichment Score	Adjusted p-value
rna-binding	25	6.84E-04	2.15	5.00E-02
acetylation	33	3.89E-05	2.22	0.00E+00
ubl conjugation	28	1.67E-06	2.89	0.00E+00
mrna processing	16	4.33E-04	2.91	3.00E-02
stress response	9	3.23E-04	5.19	3.00E-02
chelation	6	1.05E-06	26.91	0.00E+00

Table 4.3. Gene expression in NRF2-mediated Oxidative Stress Response Pathway. The only canonical pathway that was significantly altered in all three groups was NRF2-mediated Oxidative Stress Response. The genes below are from this canonical pathway. Superscripts denote genes associated with the following molecular complexes/families: ^aActin, ^bERK1/2, ^cGST, ^dHSP22/40/90, ^eMkk3/6, ^fPI3K, ^gPkc, ^hRas

	IM		SCI		UL	
	Gene	FC	Gene	FC	Gene	FC
Up	DNAJC9 ^d	1.3	ABCC1	1.7	ACTG1 ^a	1.2
	FKBP5	1.6	AOX1	7.8	BACH1	1.2
	MAPK6	2.2	DNAJC9 ^d	1.6	GCLM	1.3
	MAPK7	1.6	FKBP5	3.5	GSTM1 ^c	1.3
	PIK3C3 ^f	1.5	FTL	1.9	HMOX1	15.4
	TXNRD1	1.3	GSR	2.2	HSPB8 ^d	1.2
	USP14	1.4	MAFF	6.0	MAFF	1.9
			MAPK1 ^b	2.1		
			MGST1 ^c	10.6		
			PIK3R1 ^f	5.6		
			PIK3R3 ^f	2.0		
			PRKCI ^g	1.2		
			SOD2	9.2		
Down	ACTB ^a	-1.3	AKR7A2	-1.2	DNAJA1 ^d	-1.3
	ATF4	-1.5	DNAJA4 ^d	-2.6	ACTB ^a	-1.8
	CCT7,	-1.3	DNAJB1 ^d	-2.4	ACTG1 ^a	-1.8
	DNAJA4 ^d	-3.0	DNAJB4 ^d	-1.8		
	DNAJB5 ^d	-1.4	DNAJB5 ^d	-2.0		
	DNAJB6 ^d	-1.3	DNAJC19 ^d	-1.4		
	DNAJC5 ^d	-1.5	GSTA4 ^c	-1.6		
	GSTM4 ^c	-1.4	GSTK1 ^c	-1.9		
	JUND	-1.6	GSTM1 ^c	-2.4		
	MAP2K3 ^e	-1.3	GSTM2 ^c	-2.4		
	MAP2K7 ^c	-3.2	GSTM4 ^c	-1.6		
	NFE2L2	-1.4	GSTO1 ^c	-1.2		
	RRAS ^h	-1.5	HERPUD1	-1.6		
	RRAS2 ^h	-1.7	MAF	-2.0		
	STIP1	-1.5	MAP2K3 ^e	-2.7		
			MGST2 ^c	-1.6		
		MGST3 ^c	-1.6			
		PIK3C2B ^f	-3.2			

Table 4.4. Chaperone genes differentially expressed among three models of disuse. IM = immobilizations; SCI =spinal cord injury; UL = unloading. ↓ = downregulated up to -2-fold; ↓↓= downregulated up to -5-fold; ↑ = upregulated up to 2-fold; All are significant p<0.05 except for those denoted *trend, p<0.07.

Gene	Gene Title	IM	SCI	UL
<i>Heat Shock Proteins</i>				
HSP90AA1	heat shock protein 90kDa alpha (cytosolic), class A member 1	↓		↓
HSP90AB1	heat shock protein 90kDa alpha (cytosolic), class B member 1	↓↓		
HSP90B1	heat shock protein 90kDa beta (Grp94), member 1	↓↓		
HSPA1A	heat shock 70kDa protein 1A	↓	↓	↓
HSPA8	heat shock 70kDa protein 8	↓		
HSPB8	heat shock 22kDa protein 8			↑
HSPD1	heat shock 60kDa protein 1 (chaperonin)	↓		
HSPE1	heat shock 10kDa protein 1 (chaperonin 10)	↓		↓
<i>DNAJ co-chaperones</i>				
BAG1	BCL2-associated athanogene	↓		
BAG2	BCL2-associated athanogene 2	↓		
DNAJA1	DnaJ (Hsp40) homolog, subfamily A, member 1		↓	↓
DNAJA4	DnaJ (Hsp40) homolog, subfamily A, member 4	↓↓	↓↓	↓
DNAJB1	DnaJ (Hsp40) homolog, subfamily B, member 1			
DNAJB1	DnaJ (Hsp40) homolog, subfamily B, member 1	↓	↓↓	
DNAJB4	DnaJ (Hsp40) homolog, subfamily B, member 4		↓	↓
DNAJB5	DnaJ (Hsp40) homolog, subfamily B, member 5	↓	↓	↓
DNAJB6	DnaJ (Hsp40) homolog, subfamily B, member 6	↓		
DNAJC19	DnaJ (Hsp40) homolog, subfamily C, member 19		↓	
DNAJC5	DnaJ (Hsp40) homolog, subfamily C, member 5	↓		
DNAJC9	DnaJ (Hsp40) homolog, subfamily C, member 9	↓		
FKBP5	FK506 binding protein 5	↓	↑	
<i>Chaperonin-Containing TCP1</i>				
CCT2	chaperonin containing TCP1, subunit 2 (beta)	↓	↑	
CCT3	chaperonin containing TCP1, subunit 3 (gamma)			↓
CCT4	chaperonin containing TCP1, subunit 4 (delta)	↓		↓
CCT5	chaperonin containing TCP1, subunit 5 (epsilon)	↓	↑	
CCT6A	chaperonin containing TCP1, subunit 6A (zeta 1)	↓		
CCT7	chaperonin containing TCP1, subunit 7 (eta)	↓		
CLPX	ClpX caseinolytic peptidase X homolog (E. coli)	↓		
<i>Miscellaneous</i>				
ABCE1	ATP-binding cassette, sub-family E (OABP), member 1		↑	
AHSA1	AHA1, activator of heat shock 90kDa protein ATPase homolog 1 (yeast)	↓	↓	↓*
ASF1A	ASF1 anti-silencing function 1 homolog A (S. cerevisiae)			
CALR	calreticulin	↓		↓*
MKKS	McKusick-Kaufman syndrome		↓	
PFDN5	prefoldin subunit 5	↓		
PIP5K3	phosphatidylinositol-3-phosphate/phosphatidylinositol 5-kinase, type III	↓		
SEC63	SEC63 homolog (S. cerevisiae)		↑	
TIMM8A	translocase of inner mitochondrial membrane 8 homolog A (yeast)		↓	↓
TIMM8B	translocase of inner mitochondrial membrane 8 homolog B (yeast)			
TXNDC4	thioredoxin domain containing 4 (endoplasmic reticulum)	↓	↑	

Figure 4.1. Distribution of differentially expressed genes among disuse models. It is important to note that in each dataset, there are cases in which multiple probe-sets represent the same gene. The totals in this diagram represent unique genes rather than unique probe-sets. IM = immobilization, SCI = spinal cord injury, UL = unloading.

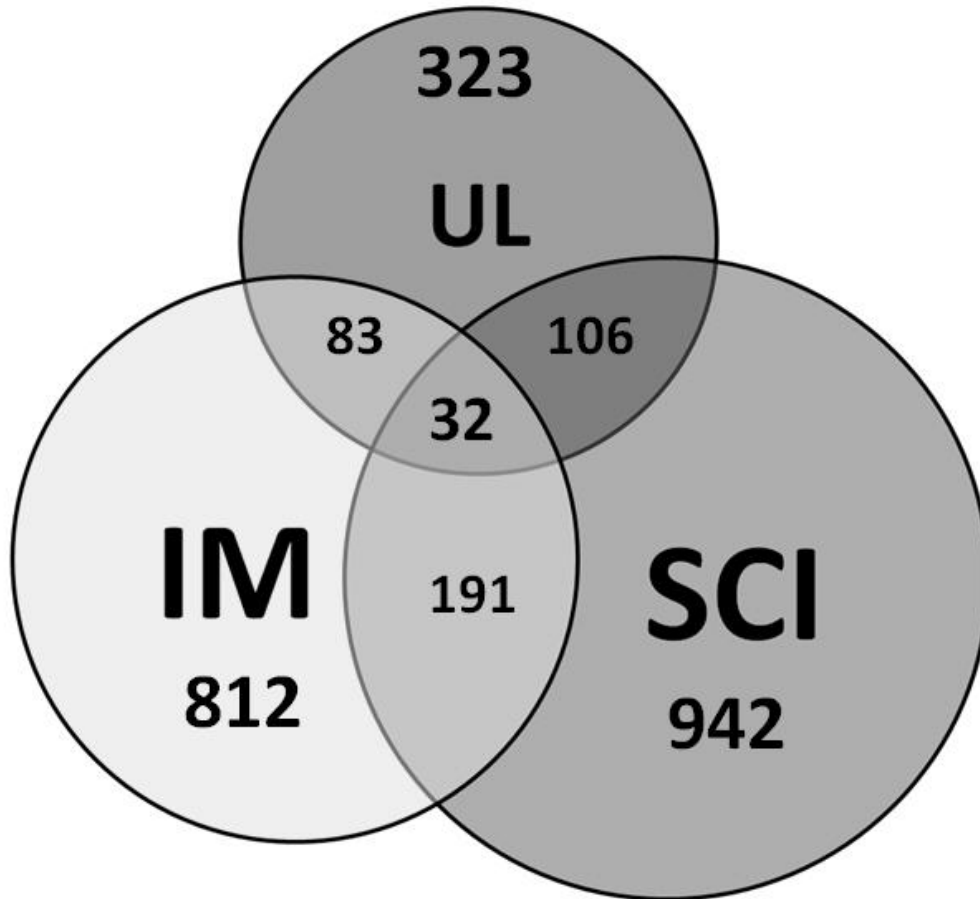


Figure 4.2a. Chaperone-related network associated with immobilization. Network score=31 (log of p-value). Green represents downregulated genes. Red represents upregulated genes.

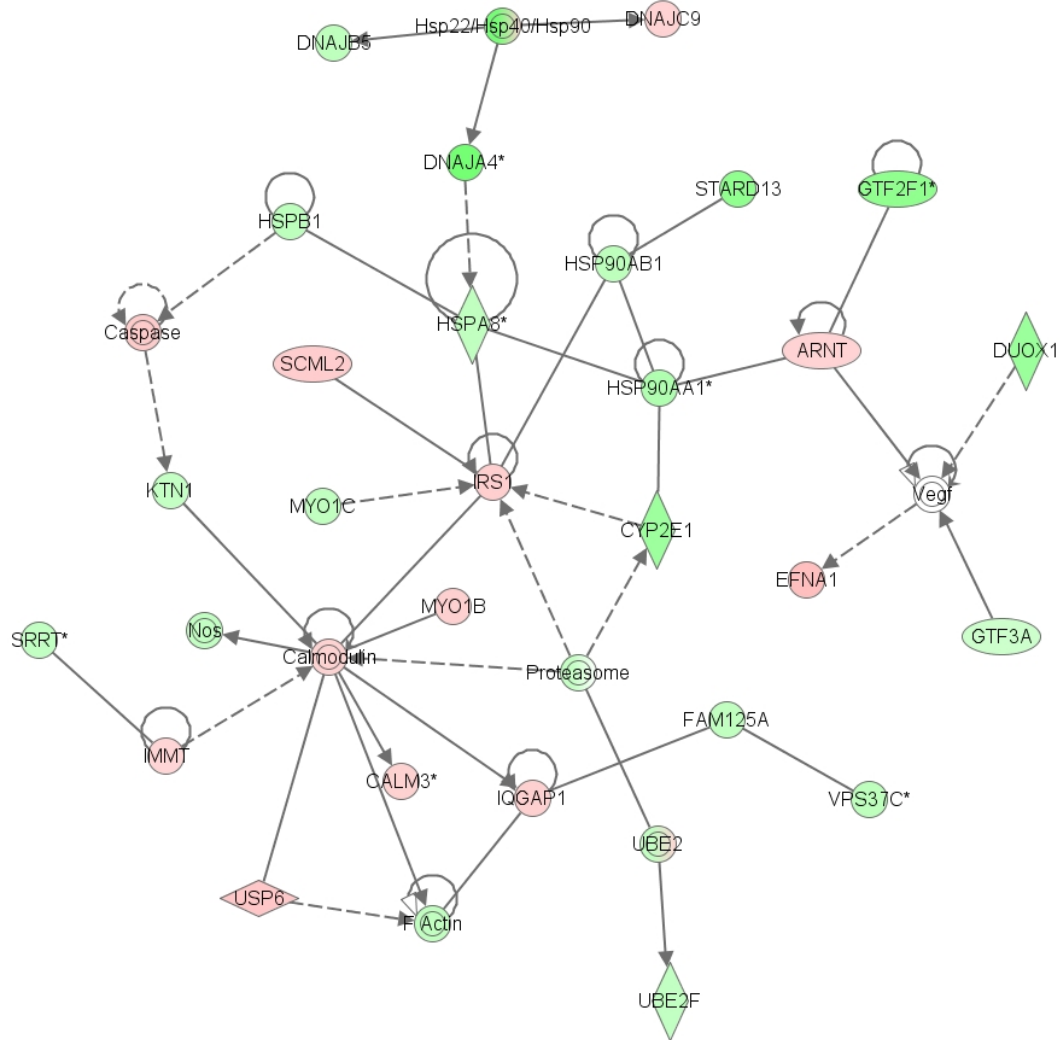
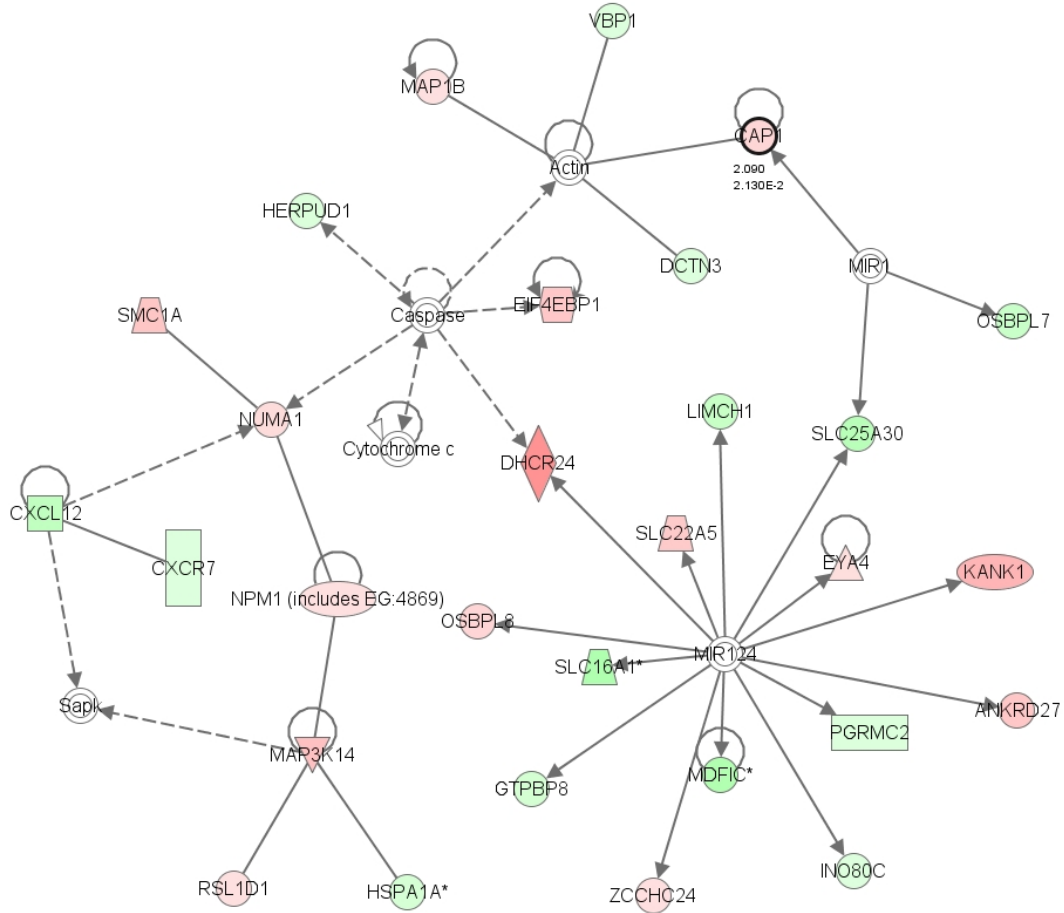


Figure 4.2b. Chaperone-related network associated with spinal cord injury. Network score= 34 (log of p-value). Green represents downregulated genes. Red represents upregulated genes.



© 2000-2009 Ingenuity Systems, Inc. All rights reserved.

CHAPTER V

THE EFFECT OF HEMIN TREATMENT ON E3 LIGASE GENE EXPRESION AND MITOCHONDRIAL DEHYDROGENASE ACTIVITY FOLLOWING AN OXIDATIVE STRESS STIMULUS IN C₂C₁₂ MYOTUBES

Abstract

PURPOSE: Our laboratory and others have shown that gene expression of heme oxygenase-1 (HMOX1) is upregulated with limb unloading in humans and rodents. It has been suggested that this increase is a protective mechanism against atrophy-related oxidative stress at the onset of muscle disuse. The purpose of this study was to measure the effects of hemin-induced changes in HMOX1 transcription on the expression of atrophy-related genes (atrogin1 and MuRF1) and mitochondrial dehydrogenase activity in C₂C₁₂ mouse muscle cells following an oxidative stress stimulus. **METHODS:** C₂C₁₂ myoblasts were incubated in growth medium (Dulbecco's modified Eagle's medium (DMEM) supplemented with 10% Fetal Bovine Serum), and at ~80% confluency, were transferred to differentiation medium (DMEM supplemented with 2% horse serum). At 5d post-differentiation, cultures were treated with hemin (20uM, 50uM, and 100uM doses) to induce HMOX1 expression. At 5.5d post-differentiation, cultures were treated with 100uM hydrogen peroxide (H₂O₂) to induce oxidative stress. RNA was isolated 3h and 6h post-H₂O₂ treatment, after which mRNA levels of HMOX1, atrogin1, and MuRF1 were measured via qRT-PCR. Mitochondrial dehydrogenase (DHO) activity was measured via XTT assay. **RESULTS:** mRNA levels of atrogin1 and MuRF1 decreased with hemin treatment (p<0.05). There was a trend towards a negative correlation between HMOX1 gene expression and atrogin1 gene expression (r=-0.38, p=0.06); furthermore,

atrogin1 and MuRF1 gene expression was strongly correlated ($r=0.92$, $p<0.05$). XTT assays revealed that 50uM and 100uM dose concentrations of hemin resulted in greater mitochondrial DHO activity following the H_2O_2 treatment than 20uM dose concentrations or control cells. CONCLUSIONS: Hemin pretreatment of C_2C_{12} cells resulted in decreases in E3 ligase gene expression, as well as increased mitochondrial DHO following an oxidative stress stimulus, suggesting that HMOX1 may be a promising gene target to protect against oxidative stress associated muscle loss such as that observed following disuse.

Introduction

Extended periods of skeletal muscle disuse lead to atrophy, as seen with limb unloading (1, 6-7), immobilization (26, 62), bed rest (6, 8, 46), spaceflight (1, 59-60), spinal cord injury (12, 23, 51, 61), and mechanical ventilation (17-18, 34). This disuse results in increases in protein degradation characterized by upregulation of genes associated with the ubiquitin proteasome pathway (UPP), such as E3 ligases atrogin1 and MuRF1 (10-11, 14), as well as decrease in protein synthesis (14). It has been posited that oxidative stress exerted by reactive oxygen species (ROS), and other reactive molecules such as reactive nitrogen species (RNS) and reactive iron, may play an important role in the regulation of the atrophy process (4, 18, 21, 28-30, 32, 38, 41, 44, 63). Increases in intracellular oxidant production have been found both *in vitro* (56) and in animal models (18, 27, 30, 47, 55) of atrophy. Furthermore, increases in stress proteins have been observed in muscle after disuse including heme oxygenase-1 (HMOX1) (21, 24, 55). A recent microarray study in our laboratory (50) found that both atrogin1 and HMOX1 gene expression was upregulated during unloading and spinal cord injury.

In the atrophy process, increases in reactive molecules may contribute to the induction of UPP activity. In C₂C₁₂ myotubes, atrogin1, MuRF1, and components of the 26S proteasome (the molecular machinery that degrades ubiquitinated proteins) have been found to be increased with H₂O₂-mediated oxidative stress (36). Since changes in the UPP occur as early as 2d following an atrophy stimulus in humans (50, 61-62), it may be possible to attenuate the rapid muscle wasting that follows by blunting the upregulation of E3 ligases even before measurable atrophy has begun. Antioxidant proteins upregulate in response to disuse stimuli (43-44, 62), but, clearly, not to levels that can restore redox balance and prevent proteolysis. Treatment with exogenous antioxidants such as trolox (9), cysteine (25), and vitamin E (3) have shown promise in that they have been demonstrated to attenuate atrophy when introduced in super-physiological levels.

HMOX1 is an inducible enzyme that participates in heme catabolism (48). Although studies have found pro-oxidant properties for the HMOX1 protein in some tissues (13, 31), it is primarily considered to have antioxidant effects; it leads to the production of bilirubin, a potent antioxidant (48, 66) that is associated with the induction of ferritin, a reactive iron scavenger. While HMOX1 has been shown to be increased at the onset of skeletal muscle disuse, its role during the atrophy process is not well understood. In a recent study, super-physiological HMOX1 induction via exogenous hemin treatment restored redox balance in mouse diaphragm during mechanical ventilation (22). It is not known whether induction of HMOX1 can attenuate the expression of E3 ligases atrogin1 or MuRF1. However, if HMOX1 were to prove to participate in the regulation of one or both of these “atrogenes,” it could be a promising

gene target for future therapies. Hemin, a substrate of HMOX1 (and an inducer of the HMOX1 gene) has been shown to reduce proteolysis in a variety of cell types including rat reticulocytes (19). Hemin is already available as a drug (Panhematin) used to treat the blood disorder, porphyra, under a physicians care in a hospital setting.

As proof of concept to pave the way for further studies in animals and humans, I initiated a series of *in vitro* experiments to investigate the effects of hemin-induced super-physiological levels of HMOX1 gene expression on E3 ligase gene expression and cell viability following an oxidative stress stimulus. The C₂C₁₂ mouse muscle immortal cell line is often used as an *in vitro* model for skeletal muscle because these cells differentiate into multinucleated myotubes that exhibit similar phenotypes and gene expression patterns as mammalian skeletal muscle cells *in vivo*. Hydrogen peroxide (H₂O₂) treatment of C₂C₁₂ cells has been used as a model of skeletal muscle oxidative stress (54), and H₂O₂ treatment has been shown to increase HMOX1(42), atrogin1, and MuRF1 (36) in C₂C₁₂ myotubes. The purpose of the present study was to investigate the effects of pre-treatment of C₂C₁₂ myotubes with hemin on cell viability and expression of HMOX1, atrogin1, and MuRF1 following H₂O₂ treatment.

Methods

Cell Culture

C₂C₁₂ myoblasts were maintained in growth media (Dulbecco's modified Eagles's medium (DMEM) supplemented with 10% fetal bovine serum (FBS) (GIBCO Invitrogen, Carlsbad, CA)) and penicillin/streptomycin in 10% CO₂ at 37°C. They were seeded in either 6-well plates (for gene expression experiments) or 96-well plates (for cell viability assays) at ~50% density. At ~80% confluency, they were switched to differentiation

media (DMEM supplemented with 2% horse serum (GIBCO Invitrogen, Carlsbad, CA).

At 2d post-differentiation and 4d post-differentiation, cells were re-fed with differentiation media supplemented with 20uM cytosine arabinoside to enrich the cultures for myotubes. Cells seeded in 96-well plates were washed with PBS prior to the addition of phenol-red free DMEM supplemented with 2% horse serum and sodium pyruvate. Phenol-red free media was used so as to enhance sensitivity of the cell viability assay.

Hemin pre-treatment

At 5d post-differentiation, cells were treated with cell culture grade hemin. A stock solution was first prepared by dissolving hemin in 0.1N NaOH solution: 20, 50, and 100uM hemin solutions were prepared by serial dilution in sterile-filtered double-distilled H₂O, with final dilutions in differentiation media. pH was then adjusted to 7.2 (consistent with the pH of the non-hemin supplemented differentiation media) and sterile filtered. Cells treated with this hemin-supplemented media in 10% CO₂ for 18h. This treatment duration was chosen based on results of published *in vitro* hemin experiments, which showed that HMOX1 was expressed 14 – 18h post-hemin treatment. Selected wells were treated with NaOH-supplemented, but hemin-free, differentiation media (hemin vehicle solution) to serve as controls. Preliminary experiments were performed to confirm that there were no significant differences between the hemin-vehicle solution and regular differentiation media.

H₂O₂ treatment

Following 18h hemin pre-treatment, cells were treated with cell culture grade H₂O₂ (Sigma-Aldrich, St. Louis, MO). A stock solution of 30% w/w H₂O₂ was used for all experiments. H₂O₂ solutions were prepared by serial dilution in sterile-filtered double-

distilled H₂O₂, with final dilutions in differentiation media. For cells destined for gene expression experiments, final concentrations of H₂O₂ were 100uM, consistent with previous literature (36), and not intended to induce cell death. For cells destined for cell viability assays, final concentrations of H₂O₂ were 100uM, 500uM, 1000uM, and 2mM, with intended cell viability ranging from 100 – 40%, as demonstrated in previous literature (42). Hemin-supplemented media was removed, cells were washed with PBS (so as to remove any residual hemin), and immediately replaced with H₂O₂-supplemented media. Cells were then cultured in 10% CO₂ for a period of 3h or 6h. Selected wells were treated with H₂O₂-free differentiation media to serve as controls. Each experiment was run multiple times to ensure validity.

RNA isolation and cDNA synthesis

Following H₂O₂ treatment, media was removed from experimental and control cells, washed with PBS, treated with trypsin, and lysed directly in the culture dishes. One ml of TRIZOL reagent (Invitrogen, Carlsbad, CA) was added per well, and cell lysate was passed several times through a pipette, collected, and stored at -80°C until analysis. Total mRNA was isolated using TRIZOL reagent (following manufacturer's instructions) and quantified via spectrophotometry (Nanodrop, Wilmington, DE). Equal amounts of total RNA was synthesized into cDNA using a First-Strand cDNA Synthesis kit (Fermentas, Hanover, MD). ABgene Absolute qPCR SYBR Green Master Mix (ABgene, Surrey, UK) with ROX dye was used for all PCR protocols. Forward and reverse primers (Integrated DNA Technologies, Coralville, IA) were designed using NCBI gene sequences with IDT DNA SciTools for all genes of interest (Table 5.1).

Gene Expression Analysis via qRT-PCR

Reactions were run in 96-well plates with all cDNA samples from each treatment condition run in triplicate for each gene of interest. Thus, each plate could accommodate the analysis of two genes of interest and one reference standard (Glyceraldehyde-3-phosphate dehydrogenase (GAPDH)). For each experiment, HMOX1 expression was measured on one plate and atrogin1 and MuRF1 were analyzed on another. When possible, the qRT-PCR experiments were performed on the same day. The average comparative threshold (Ct) value for triplicate samples was used for data analysis. The Ct values directly related to fluorescence of the respective SYBR-green probe after 40 cycles of amplification on a MX3000p Real-Time PCR System (Stratagene, La Jolla, CA) available in the central Bioinformatics and Genomics Facility at the University of Massachusetts. At the end of each reaction, a melting curve analysis was run to identify possible primer dimers. The results of the melting curve were confirmed, and appropriate product size was determined via 1.5% agarose gel electrophoresis with ethidium bromide staining.

XTT Assays

Following H₂O₂ treatment, cell viability was analyzed via the XXT assay (Roche USA, Nutley, NJ). The XTT reagent was prepared per manufacturer's instructions, 50ul of reagent was added to each well for a final concentration of 0.3 mg/ml, and then plates were incubated at room temperature in 5% CO₂ for 4h. During the incubation period, metabolically active cells cleaved yellow tetrazolium salt (XTT) to form an orange formazan dye, which was measured colorimetrically on a fluorostar plate reader (BMG

Laboratories, Chapel Hill, NC) at a wavelength of 480nm. Data were normalized to a blank well and then expressed as percentage of non-treatment controls.

Statistical Analysis

Gene expression data (ΔC_T values) and cell viability data (optical density values normalized to control) were analyzed by factorial ANOVA or ANCOVA when there were significant differences between hemin-pre-treated and hemin-non-pretreated cells prior to H_2O_2 treatment. Tukey post-hoc tests were performed when significance was indicated. Differential gene expression was calculated using the $^{-2}\Delta\Delta C_T$ method as described in (39) and presented as fold-change relative to control. In addition, Pearson correlations were performed to analyze the relationship between HMOX1, atrogin1, and MuRF1 gene expression. Significance was set at $p < 0.05$. Statistics were performed using Systat statistical software, version 12.

Results

Gene Expression

HMOX1 mRNA levels were significantly greater with H_2O_2 treatment, such that there was a mean fold-change of 3.7 in H_2O_2 -treated cells compared to non- H_2O_2 -treated cells (Figure 5.1). This confirmed that HMOX1 gene expression increased following the oxidative stress stimulus. Pre-treatment with 50uM and 100uM hemin resulted in significant increases in HMOX1 mRNA levels compared to hemin-control cells (Figure 5.2), verifying that exogenous hemin treatment successfully induced HMOX1 gene expression. HMOX1 mRNA levels were higher in cells collected 3h after 18h hemin pre-treatment compared to those collected 6h after 18h hemin pre-treatment. Finally,

regardless of timepoint or dose of H₂O₂ treatment, the patterns of HMOX1 expression across increasing doses of hemin were similar.

Atrogin1 and MuRF1 mRNA levels decreased with hemin pre-treatment (Figure 5.3). Expression levels of these two transcripts decreased in a dose-dependent manner and reached significance at the 100uM dose level (mean fold-change = -2.2 for both atrogin1 and MuRF1). There was no significant effect of H₂O₂ treatment on expression levels of either atrogin1 or MuRF1. Furthermore, there was no significant effect of time on mRNA levels of atrogin1.

Correlations: As expected, atrogin1 and MuRF1 gene expression values (ΔC_T) were strongly correlated with one another ($r=0.92$, $p<0.05$). Furthermore, there was a trend towards a negative correlation between HMOX1 expression and atrogin1 expression ($r=-0.38$, $p=0.06$). However, there was no significant correlation between HMOX1 and MuRF1 expression ($r=-0.18$, $p=0.43$).

XTT Assays

Serial dilutions of H₂O₂ (100uM, 500uM, 1mM, 2mM) induced a dose-dependent decrease in XTT cleavage at the 1mM and 2mM doses (Figure 5.4); therefore, 1mM and 2mM doses were the H₂O₂ doses that were included in the XTT assay analysis.

The ANOVA found that there were significant differences in XTT cleavage in hemin pre-treated cells compared with hemin-control cells (independent of H₂O₂ treatment), such that XTT cleavage increased with larger doses of hemin. Therefore, an ANCOVA was then performed that co-varied for H₂O₂-control XTT cleavage (Figure 5.5). There was no significant effect of time, so the following results show pooled data from both the 3h and 6h time points.

Significant main effects of hemin dose and H₂O₂ dose were observed as well as interactions between the two variables (Figure 5.6). As expected, XTT cleavage decreased in H₂O₂-treated cells compared to H₂O₂-control cells in a dose-dependent manner. Following H₂O₂ treatment, XTT cleavage in hemin pre-treated cells was greater compared to hemin-control cells, and these differences were dose-dependent with greater doses of hemin resulting in greater XTT cleavage. Furthermore, the 50uM and 100uM dose concentrations of hemin pre-treatment resulted in greater XTT cleavage than non-pre-treated cells. Because levels of XTT cleavage reflect relative differences in metabolic activity, the results may be interpreted in a number of ways including increased cell viability (survival) or increased mitosis as a result of hemin treatment.

Discussion

Taken together, the results of the XTT and the gene expression experiments found that hemin treatment was associated with increased HMOX1 expression, decreased atrogen1 and MuRF1 expression, and increased XTT cleavage.

Gene Expression

Effects of Hemin Treatment on HMOX1, Atrogen1, and MuRF1 Expression

In the current study, HMOX1 expression was greater in cells treated with H₂O₂ than those that were not (Figure 5.1). This is consistent with results data-mined from the National Biotechnology Information (NCBI) Gene Expression Omnibus (GEO) database, a public domain microarray data repository hosted by the National Institutes of Health (NIH). In a dataset contributed to GEO (Kandarian *et al.*, <http://www.ncbi.nlm.nih.gov>), C₂C₁₂ myotubes were treated with serial dilutions of H₂O₂ (10uM, 100uM, 1mM) for 2h, and microarray experiments were performed. The results showed increased HMOX1 at

the 100uM and 1mM dose levels compared to control cells. The results from the current study and the GEO-submitted study both lend support for the characterization of HMOX1 as a stress protein that responds to oxidative stress in skeletal muscle (2, 47)

HMOX1 has both pro-oxidant and anti-oxidant functions across various tissues in the body. For example, in vascular cells, HMOX1 has been found to cause endothelial injury (13), and in brain cells, to exacerbate early injury after intracerebral hemorrhage (65). The majority of the examples in the literature however provide evidence for the cytoprotective role of HMOX1. Overexpression of HMOX1 has been found to protect neuronal cells against the deleterious effects of ischemic stroke (15), to decrease inflammation during lung injury (57), and to protect liver cells from ischemic/reperfusion injury (40). Furthermore, inhibition of HMOX1 has been found to lead to increased oxidative stress during sepsis in diaphragm muscle (5). Therefore, it is likely that the increased expression of HMOX1 following H₂O₂ treatment in the current study was cytoprotective.

Hemin treatment successfully increased HMOX1 gene expression in C₂C₁₂ myotubes (Figure 5.2), L6G8 rat myoblasts (64), and other cell lines from tissues such as kidney (49) and heart (20). Our findings also showed that 100uM hemin was associated with decreased expression of atrogen1 and MuRF1, E3 ligases that attach ubiquitin to contractile proteins actin and myosin, tagging them for degradation by the proteasome (10-11). Increased gene expression of these ligases is associated with disuse atrophy *in vivo* (26, 33), and experiments in atrogen1 and MuRF1 knockout mice have shown attenuations in atrophy following disuse (11). Because hemin treatment was associated with decreased expression of the genes encoding these molecules, the findings in the

current study suggest that over-expression of HMOX1 could contribute to molecular events that reduce the proteolysis of contractile proteins. Furthermore, the trend towards a negative correlation between HMOX1 and atrogin1 expression ($r=-.38$, $p<0.05$) suggests that this may be achieved in a dose-dependent manner.

The mechanism by which HMOX1 contributed to the negative regulation of atrogin1 or MuRF1 expression was beyond the scope of this study. However, it can be speculated that HMOX1 functions to help maintain redox balance under conditions of increased oxidative stress. This is particularly compelling because oxidative stress has been shown to be a component of molecular events associated with the early stages of skeletal muscle disuse (29-30, 32-33, 38, 41, 43, 45, 47, 52) and has been identified as a likely trigger for proteolysis (reviewed in (47)). It has been hypothesized that increased reactive molecules (*e.g.*, ROS, RNS, and reactive iron) mediates Ca^{2+} disturbances leading to activation of calpains, which in turn release contractile proteins from actomyosin complexes so that they may be degraded by the proteasome (45). It is probable that physiological levels of HMOX1 are no match for the magnitude of oxidative stress that accompanies disuse. However, in a recent study, treatment with hemin restored redox balance in murine diaphragm muscle during mechanical unloading (43). Therefore, it is possible that super-physiological levels of the enzyme could intervene to help maintain redox homeostasis during a disuse stimulus, thereby blunting molecular events upstream of proteolysis.

Effects of H₂O₂ Treatment on HMOX1, Atrogin1, and MuRF1 Gene Expression

100uM concentrations of H₂O₂ were chosen for the gene expression experiments in this study because this level of oxidative stress does not induce cell death (42), yet, has

been shown to lead to increased mRNA levels of atrogin1 (at 4h posts-H₂O₂ treatment) and MuRF1 (at 6h post- H₂O₂ treatment) in C₂C₁₂ cells (36). The gene expression results of the current study were inconsistent with these previous findings in that there was no effect of 100uM H₂O₂ on atrogin1 or MuRF1 expression. I had expected that there would be an interaction between hemin pre-treatment and H₂O₂ treatment such that H₂O₂-induced oxidative stress would lead to increases in E3 ligases, whereas hemin pre-treatment would attenuate these effects. However, the response of these genes to H₂O₂ in C₂C₁₂ cells is limited to the findings of one group of investigators (36-37)

XTT Assays

Hemin pre-treatment resulted in up to a 20% increase in XTT cleavage above control, with 100uM hemin pre-treatment resulting in the greatest increases (Figure 5.6). As XTT cleavage is a marker of mitochondrial dehydrogenase activity (and therefore an indirect marker of cell number/area), there are a number of interpretations of these results. One interpretation of these findings is that hemin pre-treatment led to HMOX1-induced cell proliferation. Although the cultures were enriched for non-dividing myotubes, there were still (potentially mitotic) myoblasts in the cultures. However, studies in smooth muscle (16, 58) have demonstrated that HMOX1 inhibits cell proliferation. An alternative interpretation of these findings in the current study is that increases in HMOX1 protected against apoptosis associated with normal cell turnover (5 and 6d post-differentiation). In murine fibroblasts, it has been shown that HMOX1 can inhibit apoptosis induced by tumor necrosis factor- α (35).

Serial dilutions of H₂O₂ treatment showed that decreases in XTT cleavage were induced at 1mM (~80% of control) and 2mM doses (~40% of control) (Figure 5.4),

consistent with previous literature (42). 100uM hemin pre-treatment attenuated the decreases in mitochondrial DHO induced by 1mM hemin (Figure 5.6). This was the same level of hemin pre-treatment that showed significant decreases in atrogen1 and MuRF1 expression in the related gene expression experiments. Perhaps hemin treatment led to decreases in UPP activity via downregulation of E3 ligase mRNA transcription, which in turn could have prevented decreases in myotube size (53).

The XXT assay measures mitochondrial enzyme activity which is correlated with the number of mitochondria, by extension in the case of mononucleated cells, the number of living cells. Because myotubes can decrease in size (and organelle content) without undergoing apoptosis, it may be more appropriate to interpret XTT results in this study as a possible measurement of not only cell survival, but of cell size. And indeed, although cell size was not measured in this study, it has been observed in our laboratory that myotubes do decrease in size with H₂O₂ treatment (O'fallon, K., unpublished observation). Although Ara-C was used in this study to enrich the culture for terminal myotubes, there were still myoblasts in the culture capable of proliferation. Therefore, future studies could explore this question further by employing bromodeoxyuridine (BrdU), which involves the incorporation of a tag into the DNA of dividing cells and detection of this tag through immunocytochemistry. In this way, proliferation could be quantitatively measured so as to assess whether hemin-associated increases in XTT cleavage is proliferation-dependent or possibly cell size-dependent (as hypothesized in the current study).

Conclusions

Overall, the results of this study suggest that there may be an inverse relationship between HMOX1 expression and proteolytic gene expression, though these findings are preliminary. If therapeutic interventions could be found to blunt the expression or activity of these E3s during the early stages of atrophy, it is possible that atrophy could also be attenuated. The association between HMOX1 overexpression and E3 ligase mRNA levels provides evidence to support HMOX1 as a promising gene target to attenuate atrophy.

References

1. **Adams GR, Caiozzo VJ, and Baldwin KM.** Skeletal muscle unweighting: spaceflight and ground-based models. *J Appl Physiol* 95: 2185-2201, 2003.
2. **Alam J, and Cook JL.** How many transcription factors does it take to turn on the heme oxygenase-1 gene? *Am J Respir Cell Mol Biol* 36: 166-174, 2007.
3. **Appell HJ, Duarte JA, and Soares JM.** Supplementation of vitamin E may attenuate skeletal muscle immobilization atrophy. *Int J Sports Med* 18: 157-160, 1997.
4. **Bar-Shai M, Carmeli E, Ljubuncic P, and Reznick AZ.** Exercise and immobilization in aging animals: the involvement of oxidative stress and NF-kappaB activation. *Free Radic Biol Med* 44: 202-214, 2008.
5. **Barreiro E, Comtois AS, Mohammed S, Lands LC, and Hussain SNA.** Role of heme oxygenases in sepsis-induced diaphragmatic contractile dysfunction and oxidative stress. *Am J Physiol Lung Cell Mol Physiol* 283: L476-484, 2002.
6. **Berg HE, Dudley GA, Haggmark T, Ohlsen H, and Tesch PA.** Effects of lower limb unloading on skeletal muscle mass and function in humans. *J Appl Physiol* 70: 1882-1885, 1991.
7. **Berg HE, Dudley GA, Hather B, and Tesch PA.** Work capacity and metabolic and morphologic characteristics of the human quadriceps muscle in response to unloading. *Clin Physiol* 13: 337-347, 1993.
8. **Berg HE, Eiken O, Miklavcic L, and Mekjavic IB.** Hip, thigh and calf muscle atrophy and bone loss after 5-week bedrest inactivity. *Eur J Appl Physiol* 99: 283-289, 2007.
9. **Bettors JL, Criswell DS, Shanely RA, Van Gammeren D, Falk D, Deruisseau KC, Deering M, Yimlamai T, and Powers SK.** Trolox attenuates mechanical ventilation-induced diaphragmatic dysfunction and proteolysis. *Am J Respir Crit Care Med* 170: 1179-1184, 2004.
10. **Bodine SC, Latres E, Baumhueter S, Lai VK, Nunez L, Clarke BA, Poueymirou WT, Panaro FJ, Na E, Dharmarajan K, Pan ZQ, Valenzuela DM, DeChiara TM, Stitt TN, Yancopoulos GD, and Glass DJ.** Identification of ubiquitin ligases required for skeletal muscle atrophy. *Science* 294: 1704-1708, 2001.
11. **Bodine SC, Stitt TN, Gonzalez M, Kline WO, Stover GL, Bauerlein R, Zlotchenko E, Scrimgeour A, Lawrence JC, Glass DJ, and Yancopoulos GD.** Akt/mTOR pathway is a crucial regulator of skeletal muscle hypertrophy and can prevent muscle atrophy in vivo. *Nat Cell Biol* 3: 1014-1019, 2001.

12. **Castro MJ, Apple DF, Jr., Staron RS, Campos GE, and Dudley GA.** Influence of complete spinal cord injury on skeletal muscle within 6 mo of injury. *J Appl Physiol* 86: 350-358, 1999.
13. **Chen S, Khan ZA, Barbin Y, and Chakrabarti S.** Pro-oxidant role of heme oxygenase in mediating glucose-induced endothelial cell damage. *Free Radic Res* 38: 1301-1310, 2004.
14. **Csibi A, Leibovitch MP, Cornille K, Tintignac LA, and Leibovitch SA.** MAFbx/Atrogin-1 controls the activity of the initiation factor eIF3-f in skeletal muscle atrophy by targeting multiple C-terminal lysines. *J Biol Chem* 2008.
15. **Demougeot C, Van Hoecke M, Bertrand N, Prigent-Tessier A, Mossiat C, Beley A, and Marie C.** Cytoprotective efficacy and mechanisms of the liposoluble iron chelator 2,2'-dipyridyl in the rat photothrombotic ischemic stroke model. *J Pharmacol Exp Ther* 311: 1080-1087, 2004.
16. **Deng Y-M, Wu BJ, Witting PK, and Stocker R.** Probucol protects against smooth muscle cell proliferation by upregulating heme oxygenase-1. *Circulation* 110: 1855-1860, 2004.
17. **DeRuisseau KC, Kavazis AN, Deering MA, Falk DJ, Van Gammeren D, Yimlamai T, Ordway GA, and Powers SK.** Mechanical ventilation induces alterations of the ubiquitin-proteasome pathway in the diaphragm. *J Appl Physiol* 98: 1314-1321, 2005.
18. **DeRuisseau KC, Shanely RA, Akunuri N, Hamilton MT, Van Gammeren D, Zergeroglu AM, McKenzie M, and Powers SK.** Diaphragm unloading via controlled mechanical ventilation alters the gene expression profile. *Am J Respir Crit Care Med* 172: 1267-1275, 2005.
19. **Etlinger JD, and Goldberg AL.** Control of protein degradation in reticulocytes and reticulocyte extracts by hemin. *J Biol Chem* 255: 4563-4568, 1980.
20. **Eyssen-Hernandez R, Ladoux A, and Frelin C.** Differential regulation of cardiac heme oxygenase-1 and vascular endothelial growth factor mRNA expressions by hemin, heavy metals, heat shock and anoxia. *FEBS Lett* 382: 229-233, 1996.
21. **Falk DJ, Deruisseau KC, Van Gammeren DL, Deering MA, Kavazis AN, and Powers SK.** Mechanical ventilation promotes redox status alterations in the diaphragm. *J Appl Physiol* 101: 1017-1024, 2006.
22. **Falk DJ, Whidden MA, Kavazis AN, Smuder AJ, McClung JM, and Powers SK.** Hemin administration during mechanical ventilation attenuates redox disturbances in the diaphragm. *Faseb J* 21: LB117-b-, 2007.

23. **Gregory CM, Vandenborne K, Castro MJ, and Dudley GA.** Human and rat skeletal muscle adaptations to spinal cord injury. *Can J Appl Physiol* 28: 491-500, 2003.
24. **Hunter RB, Mitchell-Felton H, Essig DA, and Kandarian SC.** Expression of endoplasmic reticulum stress proteins during skeletal muscle disuse atrophy. *Am J Physiol Cell Physiol* 281: C1285-1290, 2001.
25. **Ikemoto M, Nikawa T, Takeda S, Watanabe C, Kitano T, Baldwin KM, Izumi R, Nonaka I, Towatari T, Teshima S, Rokutan K, and Kishi K.** Space shuttle flight (STS-90) enhances degradation of rat myosin heavy chain in association with activation of ubiquitin-proteasome pathway. *Faseb J* 15: 1279-1281, 2001.
26. **Jones SW, Hill RJ, Krasney PA, O'Conner B, Peirce N, and Greenhaff PL.** Disuse atrophy and exercise rehabilitation in humans profoundly affects the expression of genes associated with the regulation of skeletal muscle mass. *Faseb J* 18: 1025-1027, 2004.
27. **Kandarian SC, and Stevenson EJ.** Molecular events in skeletal muscle during disuse atrophy. *Exerc Sport Sci Rev* 30: 111-116, 2002.
28. **Kondo H, Miura M, and Itokawa Y.** Antioxidant enzyme systems in skeletal muscle atrophied by immobilization. *Pflugers Arch* 422: 404-406, 1993.
29. **Kondo H, Miura M, and Itokawa Y.** Oxidative stress in skeletal muscle atrophied by immobilization. *Acta Physiol Scand* 142: 527-528, 1991.
30. **Kondo H, Nakagaki I, Sasaki S, Hori S, and Itokawa Y.** Mechanism of oxidative stress in skeletal muscle atrophied by immobilization. *Am J Physiol* 265: E839-844, 1993.
31. **Lamb NJ, Quinlan GJ, Mumby S, Evans TW, and Gutteridge JM.** Haem oxygenase shows pro-oxidant activity in microsomal and cellular systems: implications for the release of low-molecular-mass iron. *Biochem J* 344 Pt 1: 153-158, 1999.
32. **Lawler JM, Song W, and Demaree SR.** Hindlimb unloading increases oxidative stress and disrupts antioxidant capacity in skeletal muscle. *Free Radic Biol Med* 35: 9-16, 2003.
33. **Lecker SH, Jagoe RT, Gilbert A, Gomes M, Baracos V, Bailey J, Price SR, Mitch WE, and Goldberg AL.** Multiple types of skeletal muscle atrophy involve a common program of changes in gene expression. *Faseb J* 18: 39-51, 2004.
34. **Levine S, Nguyen T, Taylor N, Friscia ME, Budak MT, Rothenberg P, Zhu J, Sachdeva R, Sonnad S, Kaiser LR, Rubinstein NA, Powers SK, and Shrager JB.** Rapid disuse atrophy of diaphragm fibers in mechanically ventilated humans. *N Engl J Med* 358: 1327-1335, 2008.

35. **Li YP, Chen Y, John J, Moylan J, Jin B, Mann DL, and Reid MB.** TNF-alpha acts via p38 MAPK to stimulate expression of the ubiquitin ligase atrogin1/MAFbx in skeletal muscle. *Faseb J* 19: 362-370, 2005.
36. **Li YP, Chen Y, Li AS, and Reid MB.** Hydrogen peroxide stimulates ubiquitin-conjugating activity and expression of genes for specific E2 and E3 proteins in skeletal muscle myotubes. *Am J Physiol Cell Physiol* 285: C806-812, 2003.
37. **Li YP, and Reid MB.** NF-kappaB mediates the protein loss induced by TNF-alpha in differentiated skeletal muscle myotubes. *Am J Physiol Regul Integr Comp Physiol* 279: R1165-1170, 2000.
38. **Liu MJ, Li JX, Lee KM, Qin L, and Chan KM.** Oxidative stress after muscle damage from immobilization and remobilization occurs locally and systemically. *Clin Orthop Relat Res* 246-250, 2005.
39. **Livak KJ, and Schmittgen TD.** Analysis of relative gene expression data using real-time quantitative PCR and the 2(-Delta Delta C(T)) Method. *Methods* 25: 402-408, 2001.
40. **Massip-Salcedo M, Casillas-Ramirez A, Franco-Gou R, Bartrons R, Ben Mosbah I, Serafin A, Rosello-Catafau J, and Peralta C.** Heat Shock Proteins and Mitogen-activated Protein Kinases in Steatotic Livers Undergoing Ischemia-Reperfusion: Some Answers. *Am J Pathol* 168: 1474-1485, 2006.
41. **Matsushima Y, Nanri H, Nara S, Okufuji T, Ohta M, Hachisuka K, and Ikeda M.** Hindlimb unloading decreases thioredoxin-related antioxidant proteins and increases thioredoxin-binding protein-2 in rat skeletal muscle. *Free Radic Res* 40: 715-722, 2006.
42. **McArdle F, Spiers S, Aldemir H, Vasilaki A, Beaver A, Iwanejko L, McArdle A, and Jackson MJ.** Preconditioning of skeletal muscle against contraction-induced damage: the role of adaptations to oxidants in mice. *J Physiol* 561: 233-244, 2004.
43. **McClung JM, Kavazis AN, DeRuisseau KC, Falk DJ, Whidden MA, and Powers SK.** Effects of oxidative stress on PI3K/Akt regulation of FOXO transcription factors during diaphragm muscle disuse. *Faseb J* 21: A1306-c-, 2007.
44. **McClung JM, Kavazis AN, Whidden MA, DeRuisseau KC, Falk DJ, Criswell DS, and Powers SK.** Antioxidant administration attenuates mechanical ventilation-induced rat diaphragm muscle atrophy independent of protein kinase B (PKB Akt) signalling. *J Physiol* 585: 203-215, 2007.

45. **McClung JM, Whidden MA, Kavazis AN, Falk DJ, Deruisseau KC, and Powers SK.** Redox regulation of diaphragm proteolysis during mechanical ventilation. *Am J Physiol Regul Integr Comp Physiol* 294: R1608-1617, 2008.
46. **Ogawa T, Furochi H, Mameoka M, Hirasaka K, Onishi Y, Suzue N, Oarada M, Akamatsu M, Akima H, Fukunaga T, Kishi K, Yasui N, Ishidoh K, Fukuoka H, and Nikawa T.** Ubiquitin ligase gene expression in healthy volunteers with 20-day bedrest. *Muscle Nerve* 34: 463-469, 2006.
47. **Powers SK, Kavazis AN, and McClung JM.** Oxidative stress and disuse muscle atrophy. *J Appl Physiol* 2007.
48. **Ryter SW, Alam J, and Choi AM.** Heme oxygenase-1/carbon monoxide: from basic science to therapeutic applications. *Physiol Rev* 86: 583-650, 2006.
49. **Salahudeen AA, Jenkins JK, Huang H, Ndebele K, and Salahudeen AK.** Overexpression of heme oxygenase protects renal tubular cells against cold storage injury: studies using hemin induction and HO-1 gene transfer. *Transplantation* 72: 1498-1504, 2001.
50. **Sewright KA, Urso ML, Thompson PD, Bilbe C, Chen YW, Hoffman EP, and Clarkson PM.** Oxidative stress response genes upregulated during unloading, immobilization, and spinal cord injury. *Med Sci Sports Exerc* 40: S476, 2008.
51. **Shah PK, Stevens JE, Gregory CM, Pathare NC, Jayaraman A, Bickel SC, Bowden M, Behrman AL, Walter GA, Dudley GA, and Vandenborne K.** Lower-extremity muscle cross-sectional area after incomplete spinal cord injury. *Arch Phys Med Rehabil* 87: 772-778, 2006.
52. **Shanely RA, Zergeroglu MA, Lennon SL, Sugiura T, Yimlamai T, Enns D, Belcastro A, and Powers SK.** Mechanical ventilation-induced diaphragmatic atrophy is associated with oxidative injury and increased proteolytic activity. *Am J Respir Crit Care Med* 166: 1369-1374, 2002.
53. **Siu PM, and Alway SE.** Id2 and p53 participate in apoptosis during unloading-induced muscle atrophy. *Am J Physiol Cell Physiol* 288: C1058-1073, 2005.
54. **Stangel M, Zettl UK, Mix E, Zielasek J, Toyka KV, Hartung HP, and Gold R.** H₂O₂ and nitric oxide-mediated oxidative stress induce apoptosis in rat skeletal muscle myoblasts. *J Neuropathol Exp Neurol* 55: 36-43, 1996.
55. **Stevenson EJ, Giresi PG, Koncarevic A, and Kandarian SC.** Global analysis of gene expression patterns during disuse atrophy in rat skeletal muscle. *J Physiol* 551: 33-48, 2003.

56. **Stevenson EJ, Koncarevic A, Giresi PG, Jackman RW, and Kandarian SC.** Transcriptional profile of a myotube starvation model of atrophy. *J Appl Physiol* 98: 1396-1406, 2005.
57. **Suttner DM, Sridhar K, Lee CS, Tomura T, Hansen TN, and Dennery PA.** Protective effects of transient HO-1 overexpression on susceptibility to oxygen toxicity in lung cells. *Am J Physiol* 276: L443-451, 1999.
58. **Taille C, Almolki A, Benhamed M, Zedda C, Megret J, Berger P, Leseche G, Fadel E, Yamaguchi T, Marthan R, Aubier M, and Boczkowski J.** Heme oxygenase inhibits human airway smooth muscle proliferation via a bilirubin-dependent modulation of ERK1/2 phosphorylation. *J Biol Chem* 278: 27160-27168, 2003.
59. **Tesch PA, and Berg HE.** Effects of spaceflight on muscle. *J Gravit Physiol* 5: P19-22, 1998.
60. **Trappe SW, Trappe TA, Lee GA, Widrick JJ, Costill DL, and Fitts RH.** Comparison of a space shuttle flight (STS-78) and bed rest on human muscle function. *J Appl Physiol* 91: 57-64, 2001.
61. **Urso ML, Chen YW, Scrimgeour AG, Lee PC, Lee KF, and Clarkson PM.** Alterations in mRNA expression and protein products following spinal cord injury in humans. *J Physiol* 579: 877-892, 2007.
62. **Urso ML, Scrimgeour AG, Chen YW, Thompson PD, and Clarkson PM.** Analysis of human skeletal muscle after 48 h immobilization reveals alterations in mRNA and protein for extracellular matrix components. *J Appl Physiol* 101: 1136-1148, 2006.
63. **Vassilakopoulos T.** Ventilator-induced diaphragm dysfunction: the clinical relevance of animal models. *Intensive Care Med* 34: 7-16, 2008.
64. **Vesely MJ, Exon DJ, Clark JE, Foresti R, Green CJ, and Motterlini R.** Heme oxygenase-1 induction in skeletal muscle cells: hemin and sodium nitroprusside are regulators in vitro. *Am J Physiol* 275: C1087-1094, 1998.
65. **Wang J, and Dore S.** Heme oxygenase-1 exacerbates early brain injury after intracerebral haemorrhage. *Brain* 130: 1643-1652, 2007.
66. **Zhang M, Zhang BH, Chen L, and An W.** Overexpression of heme oxygenase-1 protects smooth muscle cells against oxidative injury and inhibits cell proliferation. *Cell Res* 12: 123-132, 2002.

Table 5.1. qRT-PCR primers.

Gene Symbol	Forward Primer	Reverse Primer
Atrogin1	5'-AGG CTT CTA ATT GGA TGG CTG GGA-3'	5'-CCC GCA GTT TCA AGC CAA TGC TTA -3'
HMOX1	5'-TAG CCC ACT CCC TGT GTT TCC TTT-3'	5'-TGC TGG TTT CAA AGT TCA GGC CAC-3'
MuRF1	5'-TCC GAG TGG GTT TGG AGA CAA AGA -3'	5'-AGG CTT GGT AAA CAT CTC CAG GCA -3'
GAPDH	5'-AAC TTT GGC ATT GTG GAA GG -3'	5'-ACA CAT TGG GGG TAG GAA CA -3'

Figure 5.1. HMOX1 gene expression (Mean±SEM) increased following 100uM H₂O₂ treatment. *significantly different from control, p<0.05.

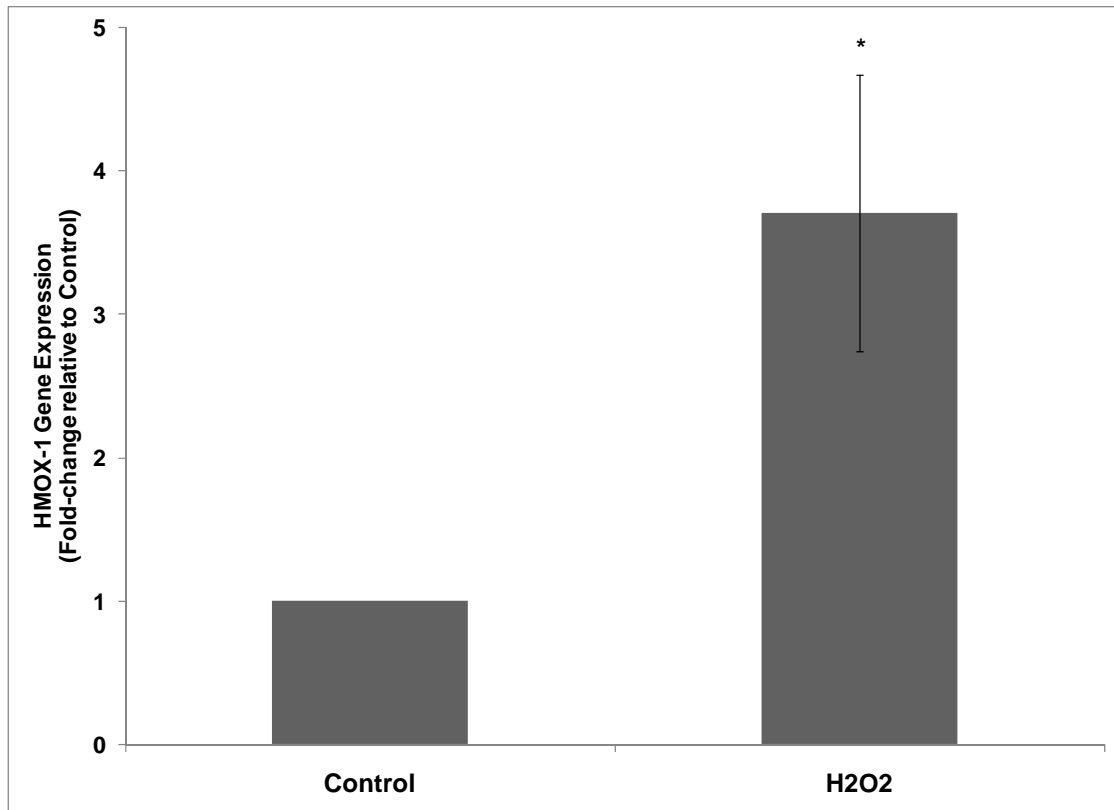


Figure 5.2. HMOX1 gene expression (Mean±SEM) increases with hemin treatment in a dose dependent manner. *significantly different from control and from 20uM hemin treatment.

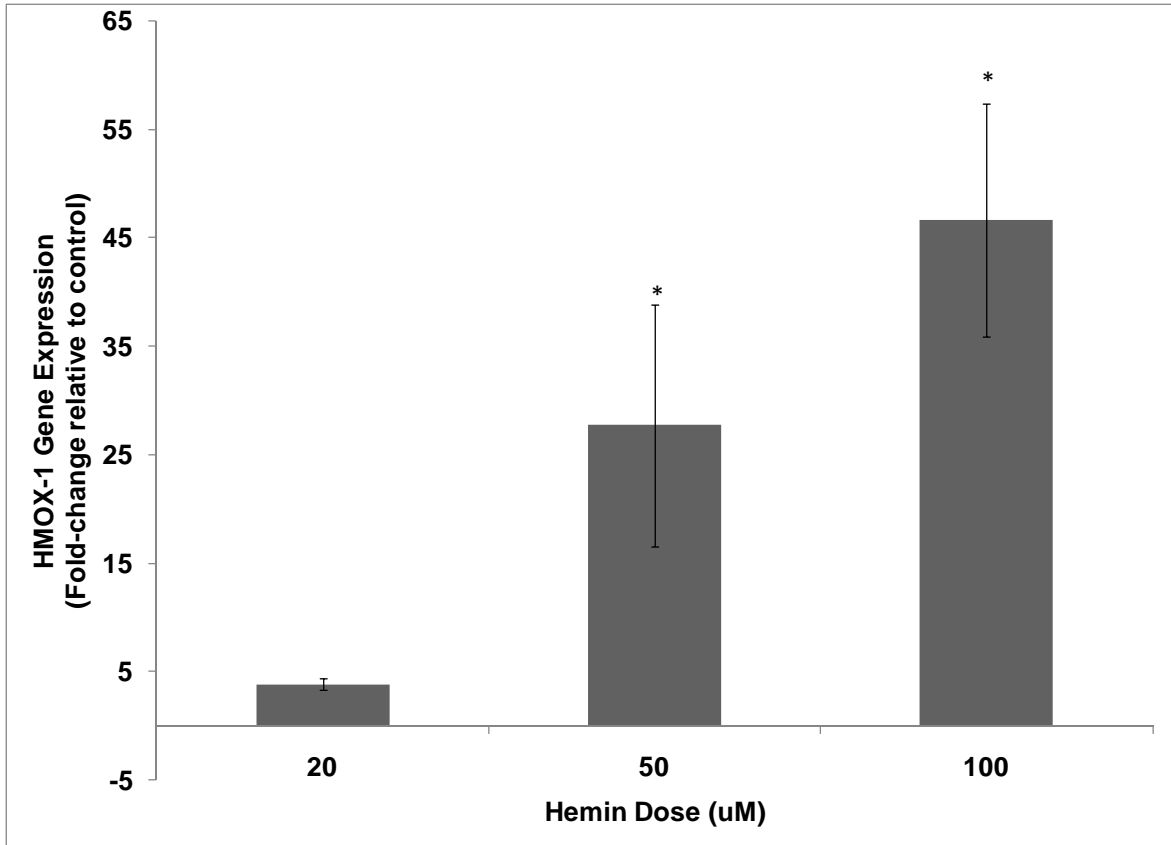


Figure 5.3. Atrogin1 and MuRF1 gene expression decreased with 100uM hemin treatment. *Significantly different from 20uM and from control, $p < 0.05$.

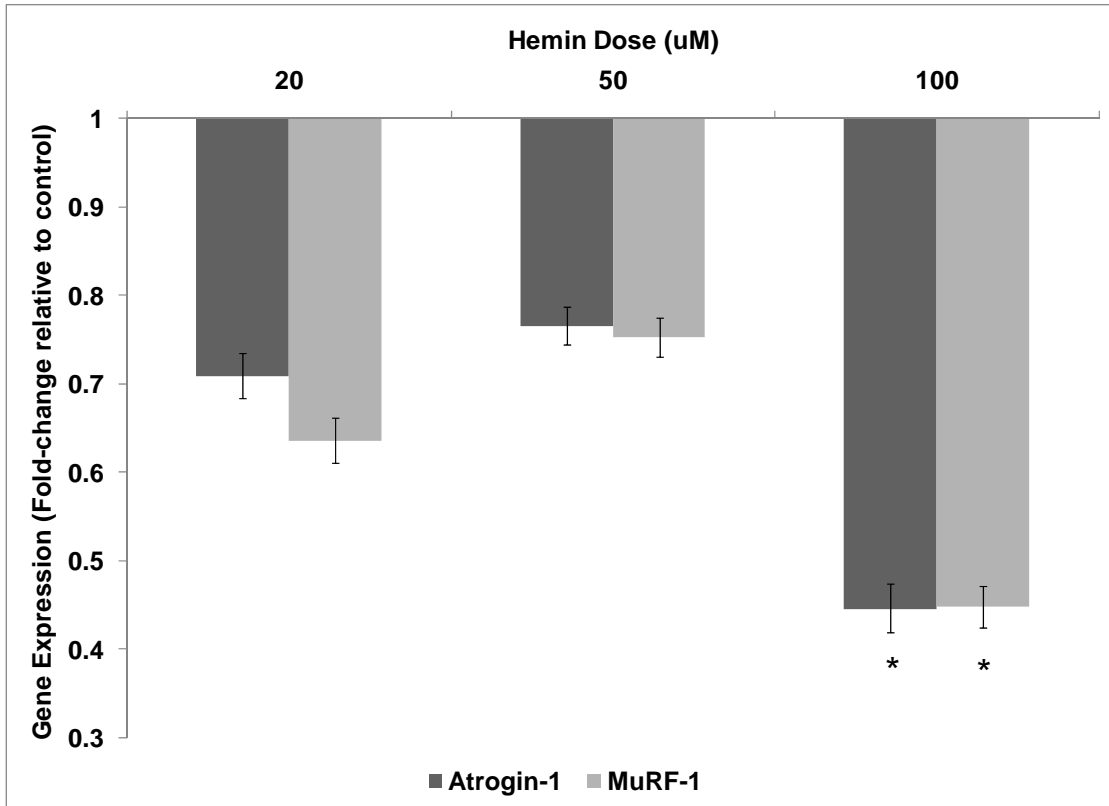


Figure 5.4. XTT Cleavage decreased with H₂O₂ treatment. *significantly different from control, p<0.05. #significantly different from all other H₂O₂ treatment levels.

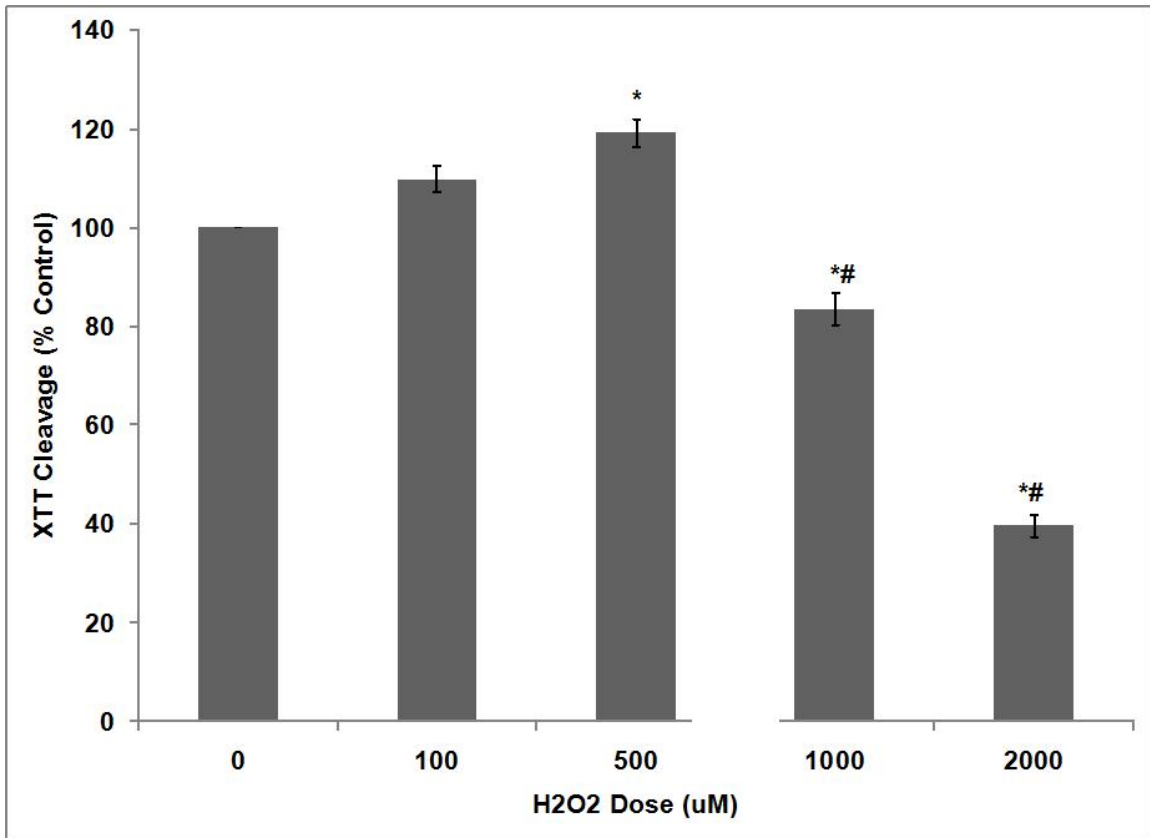


Figure 5.5 Hemin treatment increased cell XTT cleavage. *significantly different compared to control and to 20uM hemin treatment, $p > 0.05$.

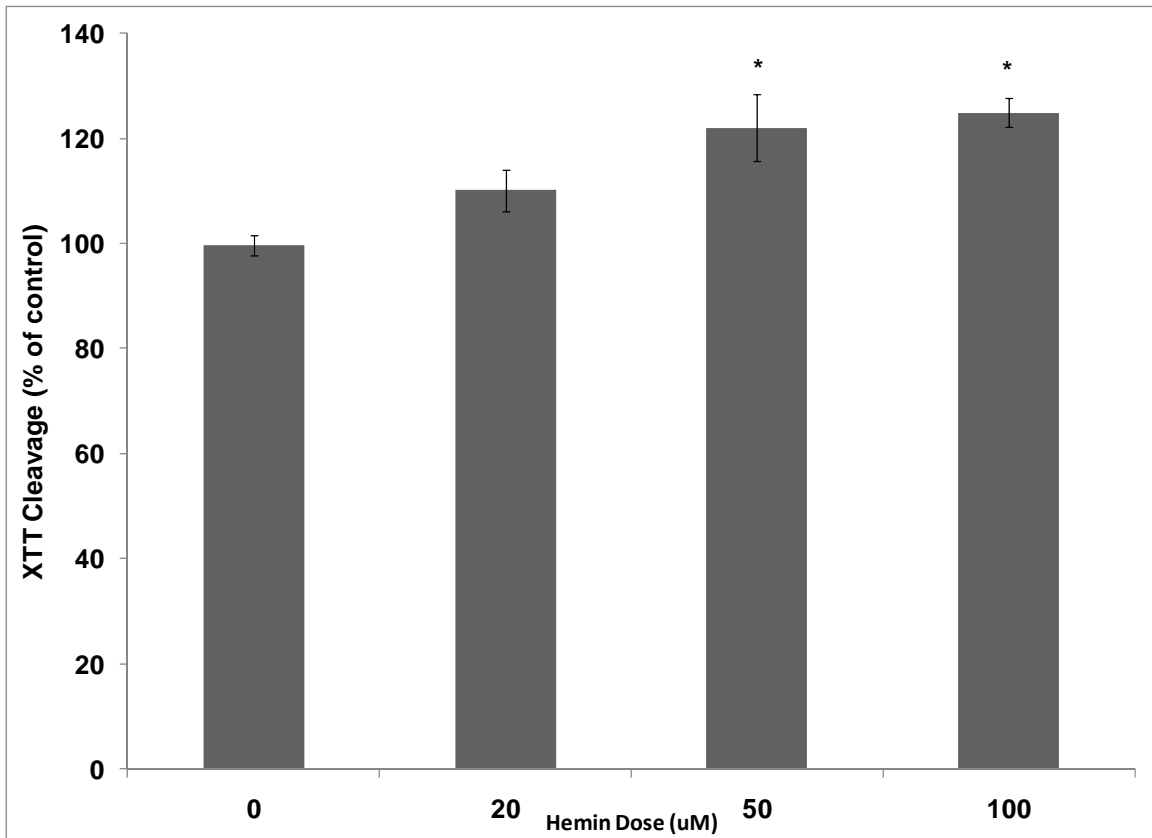
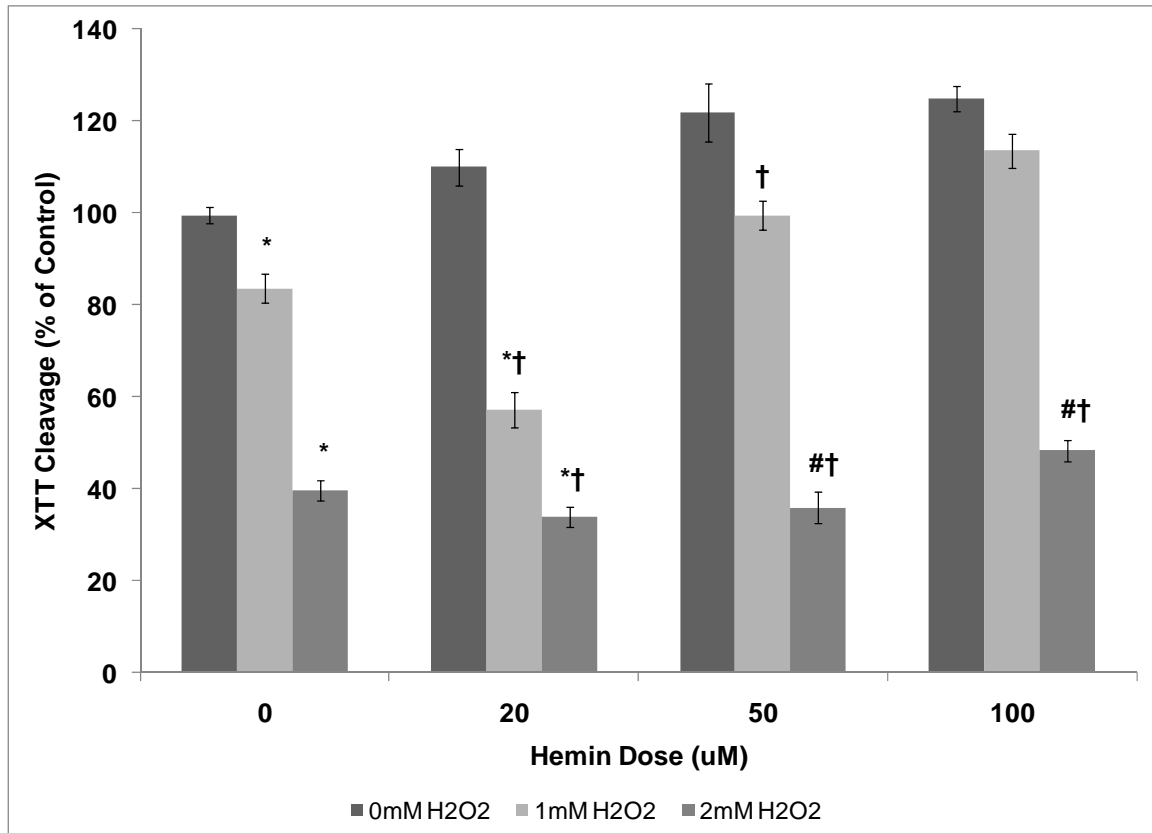


Figure 5.6. 100uM Hemin prevented/reversed effects of 1mM H₂O₂ treatment.
 *significantly different from control, $p < 0.05$; # trend towards a difference from hemin-control (0uM Hemin), $p < 0.07$; † significantly different from H₂O₂ control (0uM H₂O₂), $p < 0.05$.



CHAPTER VI

SUMMARY

Introduction

The molecular mechanisms leading to disuse muscle atrophy are likely complex and involve alterations in molecular signaling of multiple pathways. While it is well known that prolonged disuse, regardless of stimulus (*e.g.*, immobilization, spinal cord injury, limb unloading, bed rest, etc.) results in muscle atrophy and loss of muscle strength, the alterations in gene expression leading to these phenotypic changes are not well understood. It has been hypothesized (1) that genes most sensitive to disuse and reuse may be key regulators in the initiation of the cascade of events leading to the phenotypic changes that occur with prolonged disuse; therefore studying the molecular events in the early stages of disuse (before measurable atrophy occurs) may provide valuable insight into the molecular triggers that begin the process eventually leading these deleterious effects. The experiments and analyses described in this dissertation allowed me explore the following questions: 1) What are the effects of short-term loading and unloading on global gene expression in humans?; 2) Are these patterns similar to those observed in the early stages of other disuse models such as immobilization and spinal cord injury?; And 3) Can the information gained from these experiments allow me to form hypotheses to reverse or attenuate expression of candidate genes *in vitro*? In this Chapter I will summarize the results from these experiments.

Study I

Few studies have examined gene expression in humans following a disuse stimulus. Microarray data has been collected in our laboratory following 48h

immobilization and spinal cord injury, and results from these studies have been published elsewhere (4-5); however, to date, global gene expression has not been investigated in skeletal muscle unloading in humans at this early time point, nor have studies been undertaken to measure changes in gene expression following short-term disuse and reuse in order to identify genes most sensitive to changes in skeletal muscle activity. Therefore, the specific aim of Study I was to investigate global gene expression changes following short-term unloading and reloading in human skeletal muscle.

Hypothesis 1: 48h of unloading via unilateral lower limb suspension (ULLS) will produce patterns of gene expression that include changes in molecular contributors to protein degradation and cellular stress response as well previously unidentified factors in skeletal muscle unloading.

Hypothesis 2: 24h of reloading subsequent to a 48h unloading will result in reversal of molecular changes observed following the unloading period.

In agreement with hypothesis 1, global gene expression patterns showed enriched functions of protein ubiquitination as well the NRF2-mediated Oxidative Stress Response Pathway. Decreases in cellular functions related to mitochondrial metabolism were enriched, as well. qRT-PCR analysis confirmed increases in mRNA for UPP-related E3 ligase Atrogin1 (but not accompanying increases in protein products) and stress response gene HMOX1 (which showed a trend towards increases in protein products at 48h unloading). In contrast to previous work in our laboratory (5) which found decreases in collagen gene expression with 48h immobilization, this study revealed that COL4A3 (a component of COL4) was decreased with unloading. In disagreement with hypothesis 2, gene expression patterns following unloading generally persisted following reloading.

Overall, the results of Study I suggest that alterations in gene expression associated with atrophy-related functions such as protein degradation and oxidative stress may occur very soon after the introduction of a disuse stimulus such as unloading, though increased magnitude or duration of that stimulus may be necessary in order for translation of protein products to occur. While increases in proteolytic gene expression found in this study suggest that there are similarities between expression patterns following unloading and immobilization, differences likely exist between the two disuse models as evidenced by decreases in collagen found with unloading. Furthermore, the gene expression patterns with unloading were not readily reversed upon reloading suggesting that molecular responses to short-term periods of skeletal muscle inactivity may persist even after activity resumes.

Author Contribution to the Study

This study was conceived by me with guidance from Dr. Clarkson. I was responsible for attaining human subjects approval, recruiting subjects, and managing the ULLS protocol. Dr. Paul Thompson (Hartford Hospital, Hartford, CT) and his laboratory group assisted with biopsy collections. Dr. Yi-wen Chen (Children's National Medical Center, Washington, DC) performed the microarray analyses and initial statistical analysis of the microarray data to identify differential gene expression. I performed all subsequent analysis of the microarray data including identification of functional groups via DAVID and canonical pathways via IPA. I then performed all tasks associated with gene expression confirmation including RNA extraction, cDNA synthesis, and qRT-PCR, and statistical analysis. I also performed confirmational DNA gel analysis to confirm proper size of qRT-PCR products with the aid of Jimmy Webb. I conducted all tasks

associated with Western blotting including protein extraction, quantitation, quantification, blotting, and film development, as well as blot analysis and related statistics. I will be primarily responsible for writing the resulting manuscript with expected significant editing contributions from all co-authors.

Study II

Evidence from Study I and previous work in our laboratory (4-5) has provided strong evidence to suggest molecular alterations leading to skeletal muscle atrophy may occur as early as within 48h of the onset of disuse (*i.e.*, immobilization, spinal cord injury, disuse), prior to the observation of measurable atrophy or strength-loss. Further elucidation of global gene expression at this early time point across disuse stimuli may be valuable in identifying gene targets for further research to develop therapies or pharmaceutical interventions to prevent or attenuate atrophy. Of particular value may be the discovery of an intersection between these three models of disuse in key early molecular regulators of atrophy. With the completion of Study I, I had access to the complete microarray datasets reflecting differential gene expression following 48h immobilization, spinal cord injury, and unloading. Therefore, the specific aim of Study II was to investigate global gene expression patterns related to disuse in biopsies collected following 48h immobilization, spinal cord injury, and unloading.

Hypothesis 1: 48h following immobilization, spinal cord injury, and unloading global gene expression patterns will reveal a subset of functions and pathways common to all three models of disuse.

Hypothesis 2: 48h following immobilization, spinal cord injury, and unloading global gene expression patterns will reveal a subset of functions and pathways unique to each model of disuse.

In agreement with hypothesis 1, common molecular changes among all three models of disuse were observed, particularly those associated with oxidative stress response such as metallotheionins and protein chaperones, as well as the expected function of protein degradation. Also, in agreement with hypothesis 2, differences between the disuse models were in evidence. For example, while cellular stress response the only common canonical pathway to all three models, the expression patterns within the pathway differed. Furthermore, changes related to the oxidative phosphorylation may differ between disuse stimuli. Overall, the results of Study II suggest that common functions are, indeed, at play following 48h immobilization, spinal cord injury, and unloading; in addition to the shared enriched function of protein degradation, stress response is an attractive area for further study in the search for potential gene targets as oxidative stress has already been posited as an early upstream regulator of skeletal muscle atrophy.

Author Contribution to the Study

This study was conceived by me with guidance from Dr. Clarkson. The “raw” microarray data for the UL model of disuse were acquired from Study I of this dissertation while the “raw” microarray data for the IM and SCI models of disuse were acquired from previous work in the muscle biology and imaging laboratory by Maria Urso, under the guidance of Dr. Clarkson and in collaboration with Dr. Thompson (Hartford Hospital, Hartford, CT), Dr. Patrick Lee (Baystate Medical Center, Springfield,

MA), and Dr. Eric Hoffman (Children's National Medical Center, Washington, DC). Dr. Yi-Wen Chen (Children's National Medical Center, Washington, DC.) performed initial microarray and statistical analysis to identify differential gene expression and gene clustering. I performed all subsequent analysis of the microarray data including identification of functional groups via DAVID and canonical pathways and gene networks via IPA. I will be primarily responsible for writing the resulting manuscript with expected significant editing contributions from all co-authors.

Study III

Studies I and II provided valuable information regarding the early molecular changes that may portend skeletal muscle atrophy if a disuse stimulus persists. Of particular note were oxidative stress response genes including HMOX1, which has been shown to restore redox balance *in vivo* (2). Since oxidative stress is likely an upstream mediator of skeletal muscle atrophy (3), preventing its effects may be a promising tool in fighting skeletal muscle atrophy. Therefore, HMOX1 may be an attractive gene target for future therapies to attenuate atrophy, though its association with proteolysis was unknown. Therefore, the exploratory aim of Study III was to develop hypotheses based on the findings of the two previous dissertation studies and to devise a proof of concept experiment to test these hypotheses *in vitro*.

Hypothesis 1: H₂O₂ treatment will lead to an increase in HMOX1, Atrogin1, and MuRF1 gene expression compared to control.

Hypothesis 2: Hemin treatment will lead to increases in HMOX1 and decreases in Atrogin1 and MuRF1 gene expression compared to control.

Hypothesis 3: Hemin treatment will increase mitochondrial dehydrogenase activity in the face of oxidative stress.

In agreement with hypothesis 1, H₂O₂ led to an increase in HMOX1. However, there were no accompanying increases in Atrogin1 or MuRF1 expression, possibly because the oxidative stress stimulus (100uM) for the gene expression experiments was mild. In agreement with hypothesis 2, hemin treatment did lead to increases in HMOX1 and decreases in Atrogin1 and MuRF1. Finally, in agreement with hypothesis 3, hemin treatment increased mitochondrial dehydrogenase that was decreased at higher levels (1mM) of H₂O₂ treatment. Overall, the results of Study III suggest that there may be an inverse relationship between HMOX1 expression and proteolytic gene expression, though these findings are preliminary. If therapeutic interventions could be found to blunt the expression or activity of these E3s during the early stages of atrophy, it is possible that atrophy could also be attenuated. The association between HMOX1 overexpression and E3 ligase mRNA levels provides evidence to support HMOX1 as a promising gene target to attenuate atrophy.

Author Contribution to the Study

This study was conceived by me with guidance from Drs Clarkson and Schwartz. I conducted all experiments with the exception of three qRT-PCR plates which were run by Rob Hyldahl. Confirmational DNA gel analysis to confirm proper size of qRT-PCR products were performed by Jimmy Webb. I will be primarily responsible for writing the resulting manuscript with expected significant editing contributions from all co-authors.

References

1. **Bey L, Akunuri N, Zhao P, Hoffman EP, Hamilton DG, and Hamilton MT.** Patterns of global gene expression in rat skeletal muscle during unloading and low-intensity ambulatory activity. *Physiol Genomics* 13: 157-167, 2003.
2. **McClung JM, Whidden MA, Kavazis AN, Falk DJ, Deruisseau KC, and Powers SK.** Redox regulation of diaphragm proteolysis during mechanical ventilation. *Am J Physiol Regul Integr Comp Physiol* 294: R1608-1617, 2008.
3. **Powers SK, Kavazis AN, and McClung JM.** Oxidative stress and disuse muscle atrophy. *J Appl Physiol* 2007.
4. **Urso ML, Chen YW, Scrimgeour AG, Lee PC, Lee KF, and Clarkson PM.** Alterations in mRNA expression and protein products following spinal cord injury in humans. *J Physiol* 579: 877-892, 2007.
5. **Urso ML, Scrimgeour AG, Chen YW, Thompson PD, and Clarkson PM.** Analysis of human skeletal muscle after 48 h immobilization reveals alterations in mRNA and protein for extracellular matrix components. *J Appl Physiol* 101: 1136-1148, 2006.

APPENDIX A

INFORMED CONSENT FORM

INFORMED CONSENT DOCUMENT FOR PARTICIPATION IN RESEARCH

Department of Exercise Science
University of Massachusetts
Amherst, Massachusetts

Preventive Cardiology Department
Hartford Hospital
Hartford, Connecticut

Title: Molecular Changes in Human Muscle with Unloading/Reloading

Principal Investigators:

UMASS: Kimberly Sewright Office: (413) 577-4702, Cell Phone: (413) 687-3246
Priscilla M. Clarkson, PhD (413) 545-6069
Hartford Hospital: Paul D. Thompson, M.D. (860) 545-2899

I. A. Purpose: The purpose of the research is to examine how muscles respond to lack of using them (unloading) and then to resuming activity (reloading) by activating or deactivating certain genes in the muscle.

Please Note: Your participation in this study requires that you undergo 3 muscle biopsies in your leg and a 48-hour period of leg unloading. There is a small risk of bleeding or infection following a muscle biopsy, but this is a safe procedure and will be performed in a hospital by a trained medical doctor. For the unloading condition you will wear a shoe that has about a 5 inch sole on your right foot so that, while standing, the other foot (wearing a normal shoe) will not touch the ground. By not touching the ground, there will be no weight put on this leg. You will use crutches to walk during 48 hours of unloading. During this period of unloading, you will not be allowed to put any weight on your left leg, and the leg unloading may prevent you from taking part in certain activities such as driving your car. We will provide assistance and care during and after the biopsies and unloading procedures. Before you agree to participate, you should be aware of these procedures and confident that you are both willing and able to take part in this study.

B. Procedures: Prior to the start of the study, you will report to the Muscle Biology and Imaging Laboratory at the University of Massachusetts to read and sign an Informed Consent Document, and complete a screening form composed of inclusion/exclusion criteria (see Research Plan below), as well as a physical activity questionnaire. If we feel that you have health concerns (i.e. chronic knee, ankle, wrist or shoulder pain/instability) that prohibit you from performing the unloading condition and using crutches or undergoing a muscle biopsy (like an allergy to lidocaine (which is like novocaine), we will then exclude you from the study. You will also be excluded if at any time you have experienced an injury to your knee, ankle, hip, wrist, or shoulder or have undergone surgery on those joints. Your right foot will be measured and your shoe size will be recorded.

On visit 2, you will return to the Muscle Biology and Imaging Laboratory and will eat a meal that will be provided for you. You will also try on the shoe you will wear on your right foot during the unloading phase of the study to ensure a proper fit. Then you will be transported to Hartford Hospital in Hartford, Connecticut. This visit will last approximately 4 hours including

(Rev 4/17/06) University of Massachusetts Amherst-IRB Page 1 of 8

(413) 545-3428
Approval Date 1-9-07
Valid Through 2-8-08
IRB Signature Nancy Street

Subject Initials _____
Date _____

the travel between UMASS and Hartford Hospital. However, sometimes the physician is delayed or there are more subjects than expected, in which case the visit could be longer.

You will be instructed not to consume any anti-inflammatory drugs (i.e. NSAIDS like Ibuprofen or aspirin) within 4 days of the muscle biopsy to reduce risk of bleeding. Dr. Paul Thompson will perform the biopsy on your left leg (the thigh muscle). The biopsy is done after giving local anesthesia to the skin and muscle with lidocaine. A small incision will be made in the skin of the upper thigh. A needle, the size of a lead pencil, will be inserted into the muscle and a small "plug" of tissue (about the size of three grains of rice) will be removed. The biopsy needle is usually inserted into the muscle 2 times, but sometimes this has to be repeated 3 to 5 times to get enough muscle tissue. Your muscle samples will be frozen and analyzed for gene activity. This type of gene analysis does not reveal anything significant about your genetic profile or that of your family. The biopsy does not permanently injure the muscle because the muscle rapidly heals the biopsy site.

The incision will be closed using a steri-strip (a special band-aid) and wrapped with an elastic bandage. You will be given an instructions sheet detailing how to care for the incision. The study coordinator will give you emergency contact numbers if you have any questions or concerns.

Visit 3 will occur approximately 10 days after visit 2. You will come to the Muscle Biology and Imaging Laboratory to practice the leg unloading and use of the crutches. During this visit, the crutches will be adjusted for your height and comfort. The investigator will demonstrate the use of the shoe to be worn on the right foot and the crutches. Then, under the supervision of the investigator, you will wear the shoe and practice moving (with the aid of the crutches) without putting weight on your right foot. This visit will last approximately 1 hour.

Visit 4 will occur 2 days after visit 3. You will practice the leg unloading and use of the crutches again. At the end of the visit, you will be fitted with a small (about 2.5 inches square) monitor on each of your ankles that you will wear for the next 2 days (during unloading) and a compression sock that you will wear on the unloaded leg. You will be responsible for documenting any time that you remove the monitor or the sock to shower, sleep etc. This visit will last approximately 1 hour.

You will then begin the unloading condition for 2 days. You will not be allowed to put any weight on your left leg, and the leg unloading may prevent you from taking part in certain activities such as driving your car (if you drive a standard shift) or operating equipment. You will have a staff person available to you 24 hours a day to assist you with any problems or needs you encounter due to the unloading condition. You will also be given a 24-hour cell phone number so that you can contact us at ANY time.

Visit 5 will occur after 2 days of unloading. We will again transport you to Hartford Hospital to repeat the biopsy procedure. This visit will last approximately 4 hours including the travel between UMASS and Hartford Hospital. However, sometimes the physician is delayed or there are more subjects than expected, in which case the visit could be longer.

Visit 6 will occur after 1 day of reloading. We will transport you to Hartford Hospital to repeat the biopsy procedure. Again this biopsy will be of the left leg that was unloaded. This visit will last approximately 4 hours including the travel between UMASS and Hartford Hospital. However, sometimes the physician is delayed or there are more subjects than expected, in which case the visit could be longer.

University of Massachusetts Amherst-IRB

(413) 545-3428

Approval Date 1-9-07
Valid Through 2-8-08
IRB Signature Nancy Smith

(Rev 4/17/06)

Page 2 of 8

Subject Initials _____

Date _____

The timetable of measurement collection is shown in the chart below:

Table. General Testing Schedule	
Visit 1	Screening at Muscle Biology & Imaging Laboratory at UMASS
Visit 2	Travel to Hartford Hospital for muscle biopsy of left quadriceps (thigh muscle)
Visit 3	Practice at Muscle Biology & Imaging Laboratory at UMASS (10 days after Visit 2)
Visit 4	Practice at Muscle Biology & Imaging Laboratory at UMASS (2 days after Visit 3)
BEGIN Unloading with activity monitors 2 days	
Visit 5	Travel to Hartford Hospital for muscle biopsy of left quadriceps (2 days after Visit 4)
Visit 6	Travel to Hartford Hospital for muscle biopsy of left quadriceps (1 day after Visit 5)

C. Measurements:

Activity monitors: You will wear a small (about 2.5 inches square) monitor on each of your ankles during the unloading period (2 days). This monitor will allow us to measure your compliance with the unloading protocol. You will be responsible for documenting any time that you remove the monitor from your ankles to shower, sleep, etc. You will be given a diary to record this information.

Muscle needle biopsy: A muscle biopsy will be obtained under local anesthesia (lidocaine (like novocaine)). A small incision will be made in the skin of the upper thigh. A needle will be inserted into the muscle and a small "plug" of tissue remains in the needle when it is removed from the muscle. This tissue will then be frozen until analyzed.

Molecular measures: Muscle samples will be frozen and stored in the Muscle Biology and Imaging Laboratory. Each sample will be analyzed to measure gene expression (which genes are turned on and off) and protein levels (how much of the proteins related to these genes is present).

All the above procedures are considered to be **experimental**.

D. Duration of Participation: Your participation will last approximately 3 weeks.

E. Financial Compensation: You will receive \$300 for completion of this study. This will be reported to the Internal Revenue Service. If you discontinue your participation for a reason deemed medically important by the study physician, your time will be compensated in full. You will not receive the full \$300 if you do not complete the protocol. You will receive \$100 if you only undergo procedures up to and including the first biopsy, \$200 if you complete procedures up to and including the second biopsy, and \$300 if you complete procedures up to and including the third biopsy.

University of Massachusetts Amherst-IRB
 (Rev 4/17/06) (413) 545-3428 Page 3 of 8
 Approval Date 1-9-07
 Valid Through 2-8-08
 IRB Signature Nancy Swett

Subject Initials _____
 Date _____

II. **Risks:** The possible risks, discomforts and side effects of the procedures are described below, including safeguards to be used for your protection.

There are minimal risks associated with muscle biopsy including the slight risk of infection because the skin is cut, bleeding from the puncture site or into the muscle, bruising of the area, and damage to the muscle. These risks are very low because there are no big blood vessels near the biopsy site and because the muscle tissue usually stops any bleeding by pressing against itself. Also, studies have shown that the muscle rapidly repairs itself after the biopsy.

You will be instructed not to consume any anti-inflammatory drugs (i.e. NSAIDS like Ibuprofen or aspirin) or any aspirin-containing drugs such as Alka-Seltzer, Pepto-Bismol, or certain decongestants (i.e. Dristan) within 4 days of the muscle biopsy to reduce risk of bleeding. You will be given a telephone number that may be used to reach the study coordinator 24 hours/day. If you are unsure as to whether a medication you intend to take contains aspirin, it is strongly advised that you call the study coordinator before taking the medication. A trained physician will perform the needle biopsy procedure, which involves the removal and examination of a piece of muscle tissue. This procedure usually produces minimal discomfort, but there can be pain. More often there is a feeling of "pressure" and there can be a brief muscle cramp when the muscle biopsy is taken. The anesthetic (lidocaine (like novocaine)) may burn or sting when injected (before the area becomes numb). After the anesthetic wears off, the area may be sore for about a week. The risks are small and may include the following: Infection (a slight risk any time the skin is broken), bleeding of the site, bleeding inside the muscle, bruising of the area, and damage to the muscle tissue or other tissues in the area (very rare). At the biopsy site, a small scar about 1 centimeter long or less could result, but usually this will fade in time. Risks are minimized by utilizing an experienced medical physician.

There are minimal risks with the unloading condition. The unloading will make it difficult for you to get around easily. You will not be able to put ANY weight on the unloaded leg. This is a small risk of tripping or falling (because you lose your balance) or twisting your ankle because of the 10 cm sole on the shoe you will wear on your right foot. For this reason, you will have the opportunity to practice the use of the crutches and shoes. Also, our study staff will assist you, should you need help during the 2 day unloading phase of the study. The risk of a blood clot is very rare and has only occurred when this unloading condition used a harness on the unloaded leg. We will not use the harness. You will also wear a compression sock on your unloaded leg to further protect against blood clotting.

All possible attempts will be made to minimize the possibility of injury by observation during the testing sessions. Also, a clear explanation of all procedures and equipment will be given to you.

Benefits: There are no direct benefits to you from your participation in this research study.

At the University of Massachusetts, if you have **questions** about the research in general or if you have confidential issues to discuss, such as problems or complaints and want to talk to someone who is not connected with this study, you may contact the university human subjects compliance officer by phone at 413-545-3428 or email at humansubjects@ora.umass.edu. At Hartford Hospital you may call Dr. Laurine Bow, Vice President for Research at Hartford Hospital, at (860) 545-2893 for questions about research in general or if you have any confidential issues to discuss, such as problems or complaints, you may call Patients Relations at Hartford Hospital at (860) 545-1400 and talk to someone who is not connected with the research.

University of Massachusetts Amherst-IRB Page 4 of 8
(Rev 4/17/06) (413) 545-3428
Approval Date 1-9-07
Valid Through 2-8-08
IRB Signature Nancy Austin

Subject Initials _____
Date _____

If you have questions about the research project or a research-related injury, you are free to call Priscilla Clarkson, PhD. at (413) 545-6069 or Paul D. Thompson, M.D. at (860) 545-2899.

III. **Alternative Treatments:** This study does not involve a treatment. You may choose to not participate in this study.

IV. **Confidentiality:** Your confidentiality will be guarded to the extent possible. The University of Massachusetts and Hartford Hospital will protect all the information about you and your part in this study just as is done for all patients at Hartford Hospital. Your records will be maintained in accordance with applicable state and federal laws. However, private identifiable information about you may be used or disclosed for purposes of this research project. You may request that your records be released to your personal physician.

The information that may be used or disclosed includes the following:

1. your study records

This information may be used or disclosed by:

1. Dr. Clarkson, Dr. Thompson, and researchers working under his/her direct supervision.

The information may be disclosed to:

1. The University Human Subjects Review Committee of the University of Massachusetts
2. The Hartford Hospital Department of Research Administration
3. The Hartford Hospital Institutional Review Board

The purpose(s) of the use or disclosure of this information is (are):

1. to answer the research question
2. to ensure the study is being conducted properly and that your rights as a participant are protected.

The use or disclosure of the information is permitted until:

1. completion of the research study

By signing this consent you are agreeing to the use or disclosure of your protected health information as described above. If you do not agree to the use or disclosure of the information as described and therefore do not sign this consent, you may not be in the study.

If, after signing the consent, you change your mind, you have the right to revoke your consent, in writing. However, you may be withdrawn from the study.

Once private information is disclosed, it is subject to redisclosure by the recipient, and no longer can be considered protected. You may obtain a copy of the Hartford Hospital Privacy

University of Massachusetts Amherst-IRB
(413) 545-3428
(Rev 4/17/06) Approval Date 1-9-07 Page 5 of 8
Valid Through 2-8-08
IRB Signature Nancy Swett

Subject Initials _____
Date _____

Notice for a complete description of the Hospital's privacy practices for protected health information. You have the right to review the Notice before signing this consent.

Your right to privacy will be maintained in any ensuing analysis and presentation of the data.

V. Freedom of Consent: You may withdraw consent at any time in writing or by telephone (577-4702, Muscle Biology Laboratory) and discontinue participation in the study without prejudice. Your **participation is voluntary** and you may refuse to participate and/or withdraw your consent and discontinue participation in the project at any time without penalty or loss of benefits to which you are otherwise entitled. Your decision whether or not to participate will not affect your future medical care at Hartford Hospital. If you do not take part, you will have no penalty and lose no care or services. Also, if you do agree to take part, you may stop at any point without any penalty except that you will not be fully compensated for your time and effort as discussed above.

VII. If your participation at the University of Massachusetts results in physical injury to you, medical treatment will be available at the University Health Service. Investigators will aid you in every way to see that you get proper medical attention. The University of Massachusetts will not compensate you for injury.

If your participation at Hartford Hospital results in physical injury, you will receive help in the following way: If you have medical insurance, Hartford Hospital will collect fees for medical treatment from your insurance company. If you are not fully covered or uninsured, Hartford Hospital will cover these expenses. The hospital will not pay medical expenses at other hospitals or pay for pain and suffering, travel, lost wages, or other indirect costs of taking part in this project.

You are encouraged to express any questions, concerns or doubts regarding the study at any time. The investigator will attempt to answer all questions to the best of their ability. The investigators fully intend to conduct the study with your best interest, safety, and comfort in mind. If you have questions about the treatment during the research project, you should call Dr. Priscilla Clarkson, PhD at 413-545-1337 or Dr. Paul Thompson, MD at (860) 545-2899.

The investigators have read and understood the Assurance of Compliance with OHRP Regulations for Protection of Human Research Subjects A copy of this document is available from the principal investigator and can also be found at <http://www.umass.edu/research/humsub.html>.

University of Massachusetts Amherst-IRB
(413) 545-3428
Approval Date 1-9-07
Valid Through 2-8-08
IRB Signature Nancy Sweet

(Rev 4/17/06)

Page 6 of 8

Subject Initials _____
Date _____

VIII. **Signatures:** I have read and understood this document. My questions and concerns have been answered by the researchers, and I have a copy of this consent form. Therefore, I agree to participate in the study: **Molecular Changes in Human Muscle with Unloading/Reloading**, and consent to the performance of the above procedures upon me.

Participant's Signature // Date

Legally authorized healthcare representative // Date

Investigator's Signature or Person Obtaining Consent // Date

Witness (person observing the explanation of the above information to the participant) - optional unless consent is presented orally.

University of Massachusetts Amherst-IRB
(413) 545-3428

Approval Date 1-9-07
Valid Through 2-8-08
IRB Signature Nancy Sweet

(Rev 4/17/06)

Page 7 of 8

Subject Initials _____
Date _____

Subject Information

Name:
School Address:

School Phone:
Home Address:

Home Phone:

Age:
Height:
Weight:

University of Massachusetts Amherst-IRB
(413) 545-3428

Approval Date 1-9-07
Valid Through 2-2-08
IRB Signature Nancy Sweet

(Rev 4/17/06)

Page 8 of 8

Subject Initials _____
Date _____

APPENDIX B

MEDICAL HISTORY QUESTIONNAIRE

Medical History Questionnaire

Department of Exercise Science
University of Massachusetts
Amherst, Massachusetts

Title: Molecular Changes in Human Muscle with Unloading/Loading

Principal Investigators: Priscilla M. Clarkson (545-6069), Kimberly Sewright (545-6072)

1. Have you at any time experienced an injury to your **knee** that required hospitalization or a visit to a physician?
YES _____ **NO** _____
2. Have you at any time experienced an injury to your **hip** that required hospitalization or a visit to a physician?
YES _____ **NO** _____
3. Have you at any time experienced an injury to your **ankle** that required hospitalization or a visit to a physician?
YES _____ **NO** _____
4. Have you ever had surgery on your hip, knee or ankle?
YES _____ **NO** _____
5. Have you ever been diagnosed with tendonitis, arthritis, or ligament damage in your hip, knee or ankle?
YES _____ **NO** _____
6. Do you have any chronic pain in your hip, knee or ankle joint?
YES _____ **NO** _____
7. Have you ever had chronic pain in your hip, knee or ankle joint
YES _____ **NO** _____
8. Do you wear shoe inserts/orthotics or has a physician recommended that you wear inserts/orthotics?
YES _____ **NO** _____
9. In the past 6 months, have you participated in any lower body resistance training exercise?
YES _____ **NO** _____
10. Are you willing to refrain from using any aspirin or NSAIDS during the course of the study?
YES _____ **NO** _____

Signature of Subject

Date

Signature of Investigator

Date

APPENDIX C

RAW DATA STUDY I

Table C1. qRT-PCR Atrogin1

Sample	Ct	GOI-GAPDH	Δ CT Cont	Δ CT UL	Δ CT RL	$\Delta\Delta$ CT UL-Cont	$\Delta\Delta$ CT RL-Cont		Fold Δ UL-Cont (AVG)	Fold Δ RL-Cont (AVG)
1 Control ATR	19.50	5.12	5.12	4.46	4.26	-0.66	-0.86	Fold Δ	1.43	1.29
1 48h UL ATR	19.14	4.46						SD	0.31	0.44
1 24h RL ATR	18.42	4.26						SE	0.12	0.18
2 Control ATR	19.27	5.46	5.46	5.66	5.34	0.19	-0.12	p-value	0.01	0.30
2 48h UL ATR	19.59	5.66								
2 24h RL ATR	19.90	5.34								
3 Control ATR	22.76	6.41	6.41	5.85	7.20	-0.56	0.79			
3 48h UL ATR	24.95	5.85								
3 24h RL ATR	22.07	7.20								
4 Control ATR	19.43	4.68	4.68	4.04	4.03	-0.64	-0.65			
4 48h UL ATR	18.55	4.04								
4 24h RL ATR	18.24	4.03								
5 Control ATR	18.72	4.75	4.75	4.57		-0.17				
5 48h UL ATR	18.53	4.57								
5 24h RL ATR	no ct									
6 Control ATR	19.25	4.83	4.83	4.07	4.63	-0.75	-0.20			
6 48h UL ATR	18.85	4.07								
6 24h RL ATR	19.29	4.63								
7 Control ATR	19.55	5.66	5.66	4.88	5.05	-0.78	-0.62			
7 48h UL ATR	19.59	4.88								
7 24h RL ATR	18.79	5.05								
1 Control GAP	14.38									
1 48h UL GAP	14.68									
1 24h RL GAP	14.16									
2 Control GAP	13.81									
2 48h UL GAP	13.93									
2 24h RL GAP	14.56									
3 Control GAP	16.34									
3 48h UL GAP	19.10									
3 24h RL GAP	14.87									
4 Control GAP	14.74									
4 48h UL GAP	14.51									
4 24h RL GAP	14.20									
5 Control GAP	13.97									
5 48h UL GAP	13.95									
5 24h RL GAP	no ct									
6 Control GAP	14.42									
6 48h UL GAP	14.78									
6 24h RL GAP	14.66									
7 Control GAP	13.88									
7 48h UL GAP	14.71									
7 24h RL GAP	13.74									

Table C2. qRT-PCR COL4A3

Sample	Ct	G0I-GAPDH	Δ CT Cont	Δ CT UL	Δ CT RL	$\Delta\Delta$ CT UL-Cont	$\Delta\Delta$ CT RL-Cont		Fold Δ UL-Cont (AVG)	Fold Δ RL-Cont (AVG)
1 Control COL	21.75	7.62	7.62	6.05	6.96	-1.57	-0.66	Fold Δ	1.78	2.34
1 48h UL COL	20.48	6.05						SD	0.54	2.65
1 24h RL COL	20.86	6.96						SE	0.20	1.08
2 Control COL	21.24	7.96	7.96	7.39	8.04	-0.57	0.08	p-value	0.001	0.34
48h UL COL	20.96	7.39								
2 24h RL COL	22.22	8.04								
3 Control COL	22.62	6.44	7.15	6.44	4.23	-0.71	-2.92			
3 48h UL COL	23.12	4.23								
3 24h RL COL	21.36	6.47								
4 Control COL	21.09	6.24	6.24	5.5	6.31	-0.74	0.07			
4 48h UL COL	19.61	5.5								
4 24h RL COL	20.42	6.31								
5 Control COL	20.66	6.99	6.99	6.19		-0.8				
5 48h UL COL	19.66	6.19								
5 24h RL COL	No Ct									
6 Control COL	20.9	6.66	6.66	6.25	7.52	-0.41	0.86			
6 48h UL COL	20.56	6.25								
6 24h RL COL	21.86	7.52								
7 Control COL	21.97	8.43	8.43	7.7	7.15	-0.73	-1.28			
7 48h UL COL	21.98	7.7								
7 24h RL COL	20.86	7.15								
1 Control GAP	14.13									
1 48h UL GAP	14.43									
1 24h RL GAP	13.9									
2 Control GAP	13.28									
2 48h UL GAP	13.57									
2 24h RL GAP	14.18									
3 Control GAP	16.18									
3 48h UL GAP	18.89									
3 24h RL GAP	14.89									
4 Control GAP	14.85									
4 48h UL GAP	14.11									
4 24h RL GAP	14.11									
5 Control GAP	13.67									
5 48h UL GAP	13.47									
5 24h RL GAP	No Ct									
6 Control GAP	14.24									
6 48h UL GAP	14.31									
6 24h RL GAP	14.34									
7 Control GAP	13.54									
7 48h UL GAP	14.28									
7 24h RL GAP	13.71									

Table C3. qRT-PCR HMOX1

Sample	Ct	GOI- GAPDH	Δ CT Cont	Δ CT UL	Δ CT RL	$\Delta\Delta$ CT UL-Cont	$\Delta\Delta$ CT RL-Cont		Fold Δ UL-Cont (AVG)	Fold Δ RL-Cont (AVG)
1 Control HMX	25.58	10.34	10.34	7.68	10.47	-2.66	0.13	Fold Δ	12.69	1.10
1 48h UL HMX	22.95	7.68						SD	14.86	0.53
1 24h RL HMX	25.71	10.47						SE	5.25	0.20
2 Control HMX	24.70	9.38	9.38	7.77	8.70	-1.61	-0.68	p-value	0.01	0.09
2 48h UL HMX	23.20	7.77								
2 24h RL HMX	24.30	8.70								
3 Control HMX	25.60	10.39	10.39	9.98	9.90	-0.41	-0.49			
3 48h UL HMX	24.90	9.98								
3 24h RL HMX	25.00	9.90								
4 Control HMX	25.70	10.40	10.40	7.97	9.70	-2.43	-0.70			
4 48h UL HMX	23.10	7.97								
4 24h RL HMX	25.10	9.70								
5 Control HMX	26.20	10.58	10.58	5.69		-4.89				
5 48h UL HMX	21.00	5.69								
5 24h RL HMX	no ct									
6 Control HMX	25.77	10.90	10.90	10.10	7.15	-0.79	-3.75			
6 48h UL HMX	25.28	10.10								
6 24h RL HMX	22.90	7.15								
7 Control HMX	26.08	11.52	11.52	6.15	9.90	-5.37	3.75			
7 48h UL HMX	21.82	6.15								
7 24h RL HMX	24.70	9.90								
1 Control GAP	15.24									
1 48h UL GAP	15.27									
1 24h RL GAP	15.24									
2 Control GAP	15.32									
2 48h UL GAP	15.43									
2 24h RL GAP	15.60									
3 Control GAP	15.21									
3 48h UL GAP	14.92									
3 24h RL GAP	15.10									
4 Control GAP	15.3									
4 48h UL GAP	15.13									
4 24h RL GAP	15.4									
5 Control GAP	15.62									
5 48h UL GAP	15.31									
5 24h RL GAP	no ct									
6 Control GAP	14.87									
6 48h UL GAP	15.18									
6 24h RL GAP	15.75									
7 Control GAP	14.55									
7 48h UL GAP	15.67									
7 24h RL GAP	14.80									

Table C4. qRT-PCR MuRF1

Sample	Ct	GOI- GAPDH	Δ CT Cont	Δ CT UL	Δ CT RL	$\Delta\Delta$ CT UL-Cont	$\Delta\Delta$ CT RL-Cont		Fold Δ UL-Cont (AVG)	Fold Δ RL-Cont (AVG)
1 Control MUR	27.68	7.49	7.49	5.62	5.92	-1.87	-1.57	Fold Δ	1.53	1.90
1 48h UL MUR	20.19	5.62						SD	0.97	0.86
1 24h RL MUR	19.95	5.92						SE	0.40	0.39
2 Control MUR	19.70	6.66	6.66	6.91	6.14	0.25	-0.53	p-value	0.44	0.12
2 48h UL MUR	21.34	6.91								
2 24h RL MUR	20.00	6.14								
3 Control MUR	23.02	6.82	6.82	8.24	7.75	1.42	0.92			
3 48h UL MUR	27.01	8.24								
3 24h RL MUR	22.42	7.75								
4 Control MUR	19.74	5.87	5.87	5.60	4.59	-0.27	-1.28			
4 48h UL MUR	20.16	5.60								
4 24h RL MUR	18.93	4.59								
5 Control MUR	20.68	6.98	6.98	6.13		-0.85				
5 48h UL MUR	20.61	6.13								
5 24h RL MUR	no ct									
6 Control MUR	19.75	6.16	6.16	5.83	4.71	-0.34	-1.45			
6 48h UL MUR	20.07	5.83								
6 24h RL MUR	18.86	4.71								
7 Control MUR	20.20	6.53	6.53	5.85	6.10	-0.68	-0.43			
7 48h UL MUR	20.14	5.85								
7 24h RL MUR	19.75	6.10								
1 Control GAP	20.20									
1 48h UL GAP	14.58									
1 24h RL GAP	14.02									
2 Control GAP	13.04									
2 48h UL GAP	14.43									
2 24h RL GAP	13.86									
3 Control GAP	16.19									
3 48h UL GAP	18.77									
3 24h RL GAP	14.67									
4 Control GAP	13.87									
4 48h UL GAP	14.56									
4 24h RL GAP	14.34									
5 Control GAP	13.70									
5 48h UL GAP	14.47									
5 24h RL GAP	no ct									
6 Control GAP	13.59									
6 48h UL GAP	14.24									
6 24h RL GAP	14.15									
7 Control GAP	13.67									
7 48h UL GAP	14.28									
7 24h RL GAP	13.65									

APPENDIX D

RAW DATA STUDY III

Table D.1. C₂C₁₂ XTT Raw Data

TIME (HR)	HEMIN (uL)	H2O2 (ul)	XTT
3	0	0	1.021
3	0	0	1.148
3	0	0	1.058
3	0	0	1.055
3	0	0	0.981
3	0	0	1.026
3	0	0	0.952
3	0	0	0.747
3	100	0	1.345
3	100	0	1.29
3	100	0	1.259
3	100	0	1.354
3	100	0	1.386
3	100	0	1.235
3	100	0	1.259
3	100	0	1.095
3	0	100	1.151
3	0	100	1.175
3	0	100	1.34
3	0	100	1.091
3	0	100	1.035
3	0	100	1.033
3	0	100	0.904
3	0	100	0.801
3	100	100	1.205
3	100	100	1.498
3	100	100	1.494
3	100	100	1.483
3	100	100	1.347
3	100	100	1.348
3	100	100	1.532
3	100	100	1.017
3	0	500	1.203
3	0	500	1.323
3	0	500	1.233
3	0	500	1.151
3	0	500	1.04

3	0	500	1.03
3	0	500	1.125
3	0	500	0.886
3	100	500	1.493
3	100	500	1.765
3	100	500	1.477
3	100	500	1.338
3	100	500	1.295
3	100	500	1.292
3	100	500	1.264
3	100	500	1.107
3	0	1000	0.912
3	0	1000	1.144
3	0	1000	0.999
3	0	1000	0.913
3	0	1000	0.904
3	0	1000	0.784
3	0	1000	0.908
3	0	1000	0.738
3	100	1000	1.081
3	100	1000	1.189
3	100	1000	1.128
3	100	1000	1.227
3	100	1000	1.07
3	100	1000	0.957
3	100	1000	0.98
3	100	1000	0.854
3	0	2000	0.483
3	0	2000	0.473
3	0	2000	0.593
3	0	2000	0.389
3	0	2000	0.343
3	0	2000	0.313
3	0	2000	0.35
3	0	2000	0.4
3	100	2000	0.512
3	100	2000	0.554
3	100	2000	0.5
3	100	2000	0.405
3	100	2000	0.352
3	100	2000	0.34
3	100	2000	0.379
3	100	2000	0.398

3	0	0	1.358433735
3	0	0	0.96746988
3	0	0	0.877710843
3	0	0	1.019879518
3	0	0	1.068072289
3	0	0	0.898795181
3	0	0	0.993975904
3	0	0	0.804216867
3	20	0	1.342771084
3	20	0	1.31686747
3	20	0	0.942168675
3	20	0	0.909036145
3	20	0	1.028313253
3	20	0	1.010240964
3	20	0	0.931325301
3	20	0	0.836144578
3	0	100	1.334939759
3	0	100	0.925301205
3	0	100	0.989759036
3	0	100	1.139156627
3	0	100	1.204216867
3	0	100	0.935542169
3	0	100	0.925301205
3	0	100	0.724096386
3	20	100	1.389759036
3	20	100	1.31626506
3	20	100	1.31686747
3	20	100	1.294578313
3	20	100	1.263855422
3	20	100	1.187349398
3	20	100	1.18373494
3	20	100	0.936144578
3	0	500	1.439156627
3	0	500	1.055421687
3	0	500	1.101204819
3	0	500	1.301807229
3	0	500	1.209638554
3	0	500	1.040361446
3	0	500	1.03373494
3	0	500	0.837951807
3	20	500	1.460843373
3	20	500	1.362650602
3	20	500	1.280120482

3	20	500	1.509638554
3	20	500	1.310240964
3	20	500	1.191566265
3	20	500	1.187951807
3	20	500	1.03313253
3	0	1000	0.676506024
3	0	1000	0.752409639
3	0	1000	0.707228916
3	0	1000	0.737951807
3	0	1000	0.901807229
3	0	1000	0.578313253
3	0	1000	0.673493976
3	0	1000	0.503012048
3	20	1000	0.753012048
3	20	1000	0.797590361
3	20	1000	0.610843373
3	20	1000	0.769277108
3	20	1000	0.807831325
3	20	1000	0.503614458
3	20	1000	0.528313253
3	20	1000	0.51746988
3	0	2000	0.465060241
3	0	2000	0.385542169
3	0	2000	0.305421687
3	0	2000	0.377710843
3	0	2000	0.242168675
3	0	2000	0.278313253
3	0	2000	0.252409639
3	0	2000	0.193373494
3	20	2000	0.463855422
3	20	2000	0.437951807
3	20	2000	0.348795181
3	20	2000	0.304216867
3	20	2000	0.243975904
3	20	2000	0.262048193
3	20	2000	0.211445783
3	20	2000	0.204819277
3	0	0	1.361538462
3	0	0	1.11958042
3	0	0	1.058041958
3	0	0	0.843356643
3	0	0	0.848951049
3	0	0	0.888811189

3	0	0	1.097202797
3	0	0	0.786713287
3	50	0	1.682517483
3	50	0	1.302097902
3	50	0	1.106993007
3	50	0	1.208391608
3	50	0	0.906993007
3	50	0	1.023776224
3	50	0	1.05034965
3	50	0	1.260839161
3	0	100	1.70979021
3	0	100	1.496503497
3	0	100	1.13986014
3	0	100	1.33986014
3	0	100	1.076923077
3	0	100	1.133566434
3	0	100	1.245454545
3	0	100	1.106993007
3	50	100	1.683916084
3	50	100	1.579020979
3	50	100	1.33986014
3	50	100	1.500699301
3	50	100	1.421678322
3	50	100	1.303496503
3	50	100	1.393706294
3	50	100	1.230769231
3	0	500	1.675524476
3	0	500	1.486013986
3	0	500	1.323776224
3	0	500	1.49020979
3	0	500	1.469230769
3	0	500	1.237762238
3	0	500	1.431468531
3	0	500	1.067832168
3	50	500	1.897202797
3	50	500	1.864335664
3	50	500	1.742657343
3	50	500	1.783916084
3	50	500	1.559440559
3	50	500	1.593006993
3	50	500	1.565734266
3	50	500	1.152447552
3	0	1000	1.179020979

3	0	1000	1.218181818
3	0	1000	1.092307692
3	0	1000	1.011888112
3	0	1000	0.948951049
3	0	1000	1.116083916
3	0	1000	0.906293706
3	0	1000	0.637062937
3	50	1000	1.144055944
3	50	1000	1.144055944
3	50	1000	1.207692308
3	50	1000	1.217482517
3	50	1000	1.088811189
3	50	1000	0.967832168
3	50	1000	0.959440559
3	50	1000	0.862937063
3	0	2000	0.574825175
3	0	2000	0.51958042
3	0	2000	0.474825175
3	0	2000	0.439160839
3	0	2000	0.295804196
3	0	2000	0.315384615
3	0	2000	0.309090909
3	0	2000	0.336363636
3	50	2000	0.637062937
3	50	2000	0.555944056
3	50	2000	0.597202797
3	50	2000	0.434965035
3	50	2000	0.400699301
3	50	2000	0.328671329
3	50	2000	0.379020979
3	50	2000	0.348951049
6	0	0	1.125
6	0	0	0.989
6	0	0	1.003
6	0	0	1.074
6	0	0	0.889
6	0	0	0.878
6	0	0	1.03
6	0	0	1.005
6	100	0	1.293
6	100	0	1.398
6	100	0	1.362
6	100	0	1.264

6	100	0	1.172
6	100	0	1.112
6	100	0	1.091
6	100	0	1.07
6	0	100	1.112
6	0	100	1.15
6	0	100	1.129
6	0	100	1.125
6	0	100	0.997
6	0	100	0.911
6	0	100	0.94
6	0	100	0.871
6	100	100	1.346
6	100	100	1.314
6	100	100	1.289
6	100	100	1.297
6	100	100	1.18
6	100	100	1.208
6	100	100	1.16
6	100	100	1.18
6	0	500	1.236
6	0	500	1.124
6	0	500	1.115
6	0	500	0.958
6	0	500	0.867
6	0	500	1.042
6	0	500	0.844
6	0	500	0.905
6	100	500	1.515
6	100	500	1.437
6	100	500	1.247
6	100	500	1.377
6	100	500	1.367
6	100	500	1.379
6	100	500	1.409
6	100	500	1.219
6	0	1000	1.129
6	0	1000	1.073
6	0	1000	0.998
6	0	1000	1.119
6	0	1000	1.01
6	0	1000	0.948
6	0	1000	1.074

6	0	1000	0.932
6	100	1000	1.446
6	100	1000	1.376
6	100	1000	1.2
6	100	1000	1.266
6	100	1000	1.1
6	100	1000	1.13
6	100	1000	1.151
6	100	1000	1.02
6	0	2000	0.599
6	0	2000	0.662
6	0	2000	0.958
6	0	2000	0.677
6	0	2000	0.507
6	0	2000	0.574
6	0	2000	0.597
6	0	2000	0.458
6	100	2000	0.497
6	100	2000	0.635
6	100	2000	0.45
6	100	2000	0.653
6	100	2000	0.522
6	100	2000	0.531
6	100	2000	0.525
6	100	2000	0.483
6	0	0	0.95
6	0	0	1.27
6	0	0	0.97
6	0	0	0.94
6	0	0	0.98
6	0	0	0.96
6	0	0	0.99
6	0	0	0.93
6	20	0	1.22
6	20	0	1.37
6	20	0	1.17
6	20	0	1.14
6	20	0	1.16
6	20	0	1.09
6	20	0	1.1
6	20	0	1.05
6	0	100	1.14
6	0	100	1.26

6	0	100	1
6	0	100	1.03
6	0	100	1.01
6	0	100	1.07
6	0	100	1.11
6	0	100	1.07
6	20	100	1.19
6	20	100	1.25
6	20	100	1.19
6	20	100	1.14
6	20	100	1.12
6	20	100	1.21
6	20	100	1.23
6	20	100	1.15
6	0	500	1.35
6	0	500	1.45
6	0	500	1.3
6	0	500	1.43
6	0	500	1.25
6	0	500	1.38
6	0	500	1.32
6	0	500	1.21
6	20	500	1.48
6	20	500	1.53
6	20	500	1.36
6	20	500	1.42
6	20	500	1.38
6	20	500	1.37
6	20	500	1.31
6	20	500	1.34
6	0	1000	0.76
6	0	1000	0.36
6	0	1000	0.6
6	0	1000	0.44
6	0	1000	0.57
6	0	1000	0.43
6	0	1000	0.43
6	0	1000	0.41
6	20	1000	0.66
6	20	1000	0.64
6	20	1000	0.41
6	20	1000	0.52
6	20	1000	0.42

6	20	1000	0.48
6	20	1000	0.46
6	20	1000	0.3
6	0	2000	0.48
6	0	2000	0.4
6	0	2000	0.3
6	0	2000	0.43
6	0	2000	0.35
6	0	2000	0.27
6	0	2000	0.29
6	0	2000	0.31
6	20	2000	0.48
6	20	2000	0.43
6	20	2000	0.4
6	20	2000	0.42
6	20	2000	0.29
6	20	2000	0.34
6	20	2000	0.3
6	20	2000	0.29
6	0	0	1.209
6	0	0	1.09
6	0	0	0.966
6	0	0	0.937
6	0	0	0.994
6	0	0	0.882
6	0	0	0.922
6	0	0	1
6	50	0	1.91
6	50	0	1.132
6	50	0	1.189
6	50	0	1.246
6	50	0	1.006
6	50	0	1.094
6	50	0	1.154
6	50	0	1.247
6	0	100	1.724
6	0	100	1.104
6	0	100	1.024
6	0	100	1.024
6	0	100	0.998
6	0	100	1.007
6	0	100	0.898
6	0	100	1.111

6	50	100	1.769
6	50	100	1.251
6	50	100	1.205
6	50	100	1.298
6	50	100	1.18
6	50	100	1.197
6	50	100	1.116
6	50	100	1.288
6	0	500	1.396
6	0	500	1.138
6	0	500	1.154
6	0	500	1.171
6	0	500	1.016
6	0	500	1.177
6	0	500	1.055
6	0	500	1.158
6	50	500	1.6
6	50	500	1.426
6	50	500	1.283
6	50	500	1.229
6	50	500	1.243
6	50	500	1.202
6	50	500	1.18
6	50	500	1.309
6	0	1000	0.941
6	0	1000	0.884
6	0	1000	0.77
6	0	1000	0.877
6	0	1000	0.879
6	0	1000	0.88
6	0	1000	0.814
6	0	1000	0.863
6	50	1000	0.905
6	50	1000	0.954
6	50	1000	0.874
6	50	1000	0.888
6	50	1000	1.026
6	50	1000	0.889
6	50	1000	0.869
6	50	1000	0.915
6	0	2000	0.339
6	0	2000	0.284
6	0	2000	0.249

6	0	2000	0.245
6	0	2000	0.259
6	0	2000	0.232
6	0	2000	0.213
6	0	2000	0.26
6	50	2000	0.311
6	50	2000	0.34
6	50	2000	0.254
6	50	2000	0.25
6	50	2000	0.167
6	50	2000	0.233
6	50	2000	0.253
6	50	2000	0.258

Table D2. C2C2 Gene Expression Raw Data

Experiment	Time (h)	Hemin (uM)	H2O2 (uM)	HMOX dCT	ATR dCT	MURF dCT	HMOX-ddCT-hemin-control	ATR-ddCT-Hemin Control	MuRF-ddCT-Hemin Control	HMOX-dCT-H2O2 Control	ATR-ddCT-H2O2 Control	MURF-ddCT-Hemin Control	HMOX-hemin Control FC	Atrogin-Hemin Control FC	MuRF Hemin Control FC
1	3	Control	Control	3.03	3.58	3.46	0.00	0.00	0.00	0.00	0.00	0.00	1.00	1.00	1.00
1	3	20	Control	0.45	4.40	3.65	-2.58	0.82	0.19	0.00	0.00	0.00	5.99	0.57	0.87
1	3	50	Control	-1.43	4.04	3.66	-4.46	0.46	0.20	0.00	0.00	0.00	22.01	0.73	0.87
1	3	100	Control	-3.72	5.06	4.60	-6.75	1.48	1.15	0.00	0.00	0.00	107.26	0.36	0.45
1	3	Control	100	1.14	2.67	2.90	0.00	0.00	0.00	-1.89	-0.91	-0.55	1.00	1.00	1.00
1	3	20	100	-0.21	3.59	3.85	-1.35	0.93	0.94	-0.65	-0.80	0.20	2.54	0.53	0.52
1	3	50	100	-4.64		3.29	-5.78		0.39	-3.21		-0.37	54.95		0.77
1	3	100	100	-4.04	3.86	4.43	-5.18	1.19	1.53	-0.33	-1.20	-0.17	36.25	0.44	0.35
2	3	Control	Control	5.01	4.14	3.37	0.00	0.00	0.00	0.00	0.00	0.00	1.00	1.00	1.00
2	3	20	Control	2.25	4.45	3.98	-2.76	0.31	0.62	0.00	0.00	0.00	6.77	0.81	0.65
2	3	50	Control	0.00	4.71	3.47	-5.01	0.57	0.10	0.00	0.00	0.00	32.15	0.68	0.93
2	3	100	Control	-1.57	5.34	4.38	-6.58	1.20	1.02	0.00	0.00	0.00	95.67	0.43	0.49
2	3	Control	100	2.99	3.15	2.92	0.00	0.00	0.00	-2.02	-0.99	-0.45	1.00	1.00	1.00
2	3	20	100	1.26	4.06	4.27	-1.73	0.90	1.35	-0.99	-0.39	0.28	3.32	0.54	0.39
2	3	50	100	-3.89		2.79	-6.88		-0.13	-3.89		-0.69	117.78		1.10
2	3	100	100	-2.24	4.82	3.99	-5.23	1.67	1.08	-0.67	-0.53	-0.39	37.44	0.32	0.47
3	3	Control	Control	2.74	5.22	5.08	0.00	0.00	0.00	0.00	0.00	0.00	1.00	1.00	1.00
3	3	20	Control	0.25	5.25	5.54	-2.50	0.02	0.46	0.00	0.00	0.00	5.64	0.98	0.73
3	3	50	Control	-0.83	5.64	6.19	-3.57	0.42	1.11	0.00	0.00	0.00	11.89	0.75	0.46
3	3	100	Control	-1.62	5.82	5.44	-4.36	0.60	0.36	0.00	0.00	0.00	20.53	0.66	0.78
3	3	Control	100	2.96	5.59	5.13	0.00	0.00	0.00	0.22	0.36	0.05	1.00	1.00	1.00
3	3	20	100	0.78	5.90	5.93	-2.18	0.31	0.80	0.53	0.65	0.39	4.53	0.81	0.57
3	3	50	100	-0.35	5.64	5.78	-3.31	0.05	0.65	0.48	0.00	-0.40	9.94	0.96	0.64

3	3	100	100	-2.07	5.41	5.32	-5.03	-0.18	0.19	-0.45	-0.41	-0.12	32.60	1.13	0.88
4	6	Control	Control	3.92	4.31	4.36	0.00	0.00	0.00	0.00	0.00	0.00	1.00	1.00	1.00
4	6	20	Control	2.56	4.64	4.67	-1.36	0.33	0.31	0.00	0.00	0.00	2.57	0.80	0.81
4	6	50	Control	0.53	4.46	4.47	-3.40	0.15	0.12	0.00	0.00	0.00	10.53	0.90	0.92
4	6	100	Control	-2.37	6.16	5.87	-6.29	1.85	1.51	0.00	0.00	0.00	78.34	0.28	0.35
4	6	Control	100	0.48	3.98	3.89	0.00	0.00	0.00	-3.45	-0.33	-0.47	1.00	1.00	1.00
4	6	20	100	-1.00	4.24	4.23	-1.48	0.25	0.34	-3.56	-0.40	-0.45	2.78	0.84	0.79
4	6	50	100	-1.31	4.59	4.70	-1.79	0.61	0.81	-1.84	0.13	0.22	3.46	0.66	0.57
4	6	100	100	-3.06	5.72	5.89	-3.54	1.73	2.00	-0.69	-0.44	0.02	11.60	0.30	0.25
5	6	Control	Control	.	4.68	4.42		0.00	0.00		0.00	0.00		1.00	1.00
5	6	20	Control	.	4.61	4.54		-0.07	0.12		0.00	0.00		1.05	0.92
5	6	50	Control	.	4.71	4.62		0.03	0.21		0.00	0.00		0.98	0.87
5	6	100	Control	.	6.11	6.02		1.43	1.60		0.00	0.00		0.37	0.33
5	6	Control	100	.	4.24	3.82					-0.44	-0.60		1.00	1.00
5	6	20	100	.	6.70	7.05		2.46	3.24		2.09	2.52		0.18	0.11
5	6	50	100	.	5.31	5.11		1.06	1.29		0.60	0.49		0.48	0.41
5	6	100	100	.	6.75	6.76		2.51	2.94		0.65	0.74		0.18	0.13
6	6	Control	Control	5.09	.	.	0.00			0.00			1.00		
6	6	20	Control	3.99	.	.	-1.10			0.00			2.15		
6	6	50	Control	2.31	.	.	-2.78			0.00			6.88		
6	6	100	Control	0.55	.	.	-4.55			0.00			23.37		
6	6	Control	100	5.07	.	.				-0.02			1.00		
6	6	20	100	3.72	.	.	-1.36			-0.27			2.56		
6	6	50	100	2.18	.	.	-2.89			-0.13			7.43		
6	6	100	100	0.54	.	.	-4.53			-0.01			23.16		

BIBLIOGRAPHY

1. Expression profiling--best practices for data generation and interpretation in clinical trials. *Nat Rev Genet* 5: 229-237, 2004.
2. **Adams GR, Caiozzo VJ, and Baldwin KM.** Skeletal muscle unweighting: spaceflight and ground-based models. *J Appl Physiol* 95: 2185-2201, 2003.
3. **Adams GR, Hather BM, and Dudley GA.** Effect of short-term unweighting on human skeletal muscle strength and size. *Aviat Space Environ Med* 65: 1116-1121, 1994.
4. **Ahtikoski AM, Koskinen SO, Virtanen P, Kovanen V, Risteli J, and Takala TE.** Synthesis and degradation of type IV collagen in rat skeletal muscle during immobilization in shortened and lengthened positions. *Acta Physiol Scand* 177: 473-481, 2003.
5. **Ahtikoski AM, Koskinen SO, Virtanen P, Kovanen V, and Takala TE.** Regulation of synthesis of fibrillar collagens in rat skeletal muscle during immobilization in shortened and lengthened positions. *Acta Physiol Scand* 172: 131-140, 2001.
6. **Alam J, and Cook JL.** How Many Transcription Factors Does It Take to Turn On the Heme Oxygenase-1 Gene? 2007, p. 166-174.
7. **Al-Majid S, and Waters H.** The Biological Mechanisms of Cancer-Related Skeletal Muscle Wasting: The Role of Progressive Resistance Exercise. 2008, p. 7-20.
8. **Appell HJ, Duarte JA, and Soares JM.** Supplementation of vitamin E may attenuate skeletal muscle immobilization atrophy. *Int J Sports Med* 18: 157-160, 1997.
9. **Argiles JM, Alvarez B, Carbo N, Busquets S, Van Royen M, and Lopez-Soriano FJ.** The divergent effects of tumour necrosis factor-alpha on skeletal muscle: implications in wasting. *Eur Cytokine Netw* 11: 552-559, 2000.
10. **Arthur PG, Grounds MD, and Shavlakadze T.** Oxidative stress as a therapeutic target during muscle wasting: considering the complex interactions. *Curr Opin Clin Nutr Metab Care* 11: 408-416, 2008.
11. **Aszodi A, Legate KR, Nakchbandi I, and Fassler R.** What mouse mutants teach us about extracellular matrix function. *Annu Rev Cell Dev Biol* 22: 591-621, 2006.
12. **Attaix D, Aurousseau E, Combaret L, Kee A, Larbaud D, Ralliere C, Souweine B, Taillandier D, and Tilignac T.** Ubiquitin-proteasome-dependent proteolysis in skeletal muscle. *Reprod Nutr Dev* 38: 153-165, 1998.
13. **Barreiro E, Comtois AS, Mohammed S, Lands LC, and Hussain SNA.** Role of heme oxygenases in sepsis-induced diaphragmatic contractile dysfunction and oxidative stress. 2002, p. L476-484.

14. **Bar-Shai M, Carmeli E, Ljubuncic P, and Reznick AZ.** Exercise and immobilization in aging animals: the involvement of oxidative stress and NF-kappaB activation. *Free Radic Biol Med* 44: 202-214, 2008.
15. **Battistuzzi G, Petrucci R, Silvagni L, Urbani FR, and Caiola S.** delta-Aminolevulinate dehydrase: a new genetic polymorphism in man. 1981, p. 223-229.
16. **Bendotti C, Atzori C, Piva R, Tortarolo M, Strong MJ, DeBiasi S, and Migheli A.** Activated p38MAPK is a novel component of the intracellular inclusions found in human amyotrophic lateral sclerosis and mutant SOD1 transgenic mice. *J Neuropathol Exp Neurol* 63: 113-119, 2004.
17. **Berg HE, Dudley GA, Haggmark T, Ohlsen H, and Tesch PA.** Effects of lower limb unloading on skeletal muscle mass and function in humans. *J Appl Physiol* 70: 1882-1885, 1991.
18. **Berg HE, Dudley GA, Hather B, and Tesch PA.** Work capacity and metabolic and morphologic characteristics of the human quadriceps muscle in response to unloading. *Clin Physiol* 13: 337-347, 1993.
19. **Berg HE, Eiken O, Miklavcic L, and Mekjavic IB.** Hip, thigh and calf muscle atrophy and bone loss after 5-week bedrest inactivity. *Eur J Appl Physiol* 99: 283-289, 2007.
20. **Berg HE, Larsson L, and Tesch PA.** Lower limb skeletal muscle function after 6 wk of bed rest. *J Appl Physiol* 82: 182-188, 1997.
21. **Berg HE, and Tesch PA.** Changes in muscle function in response to 10 days of lower limb unloading in humans. *Acta Physiol Scand* 157: 63-70, 1996.
22. **Berry P, Berry I, and Manelfe C.** Magnetic resonance imaging evaluation of lower limb muscles during bed rest--a microgravity simulation model. *Aviat Space Environ Med* 64: 212-218, 1993.
23. **Bettters JL, Criswell DS, Shanely RA, Van Gammeren D, Falk D, Deruisseau KC, Deering M, Yimlamai T, and Powers SK.** Trolox attenuates mechanical ventilation-induced diaphragmatic dysfunction and proteolysis. *Am J Respir Crit Care Med* 170: 1179-1184, 2004.
24. **Bey L, Akunuri N, Zhao P, Hoffman EP, Hamilton DG, and Hamilton MT.** Patterns of global gene expression in rat skeletal muscle during unloading and low-intensity ambulatory activity. *Physiol Genomics* 13: 157-167, 2003.
25. **Bodine SC, Latres E, Baumhueter S, Lai VK, Nunez L, Clarke BA, Poueymirou WT, Panaro FJ, Na E, Dharmarajan K, Pan ZQ, Valenzuela DM,**

DeChiara TM, Stitt TN, Yancopoulos GD, and Glass DJ. Identification of ubiquitin ligases required for skeletal muscle atrophy. *Science* 294: 1704-1708, 2001.

26. **Bodine SC, Stitt TN, Gonzalez M, Kline WO, Stover GL, Bauerlein R, Zlotchenko E, Scrimgeour A, Lawrence JC, Glass DJ, and Yancopoulos GD.** Akt/mTOR pathway is a crucial regulator of skeletal muscle hypertrophy and can prevent muscle atrophy in vivo. *Nat Cell Biol* 3: 1014-1019, 2001.

27. **Booth FW, and Gollnick PD.** Effects of disuse on the structure and function of skeletal muscle. *Med Sci Sports Exerc* 15: 415-420, 1983.

28. **Booth FW, and Kelso JR.** Effect of hind-limb immobilization on contractile and histochemical properties of skeletal muscle. *Pflugers Arch* 342: 231-238, 1973.

29. **Bowker-Kinley MM, Davis WI, Wu P, Harris RA, and Popov KM.** Evidence for existence of tissue-specific regulation of the mammalian pyruvate dehydrogenase complex. *Biochem J* 329 (Pt 1): 191-196, 1998.

30. **Brailsford S, Lunec J, Winyard P, and Blake DR.** A possible role for ferritin during inflammation. *Free Radic Res Commun* 1: 101-109, 1985.

31. **Budde SM, van den Heuvel LP, Janssen AJ, Smeets RJ, Buskens CA, DeMeirleir L, Van Coster R, Baethmann M, Voit T, Trijbels JM, and Smeitink JA.** Combined enzymatic complex I and III deficiency associated with mutations in the nuclear encoded NDUFS4 gene. *Biochem Biophys Res Commun* 275: 63-68, 2000.

32. **Byrne KA, Wang YH, Lehnert SA, Harper GS, McWilliam SM, Bruce HL, and Reverter A.** Gene expression profiling of muscle tissue in Brahman steers during nutritional restriction. 2005, p. 1-12.

33. **Caiozzo VJ, Baker MJ, Herrick RE, Tao M, and Baldwin KM.** Effect of spaceflight on skeletal muscle: mechanical properties and myosin isoform content of a slow muscle. *J Appl Physiol* 76: 1764-1773, 1994.

34. **Calura E, Cagnin S, Raffaello A, Laveder P, Lanfranchi G, and Romualdi C.** Meta-analysis of expression signatures of muscle atrophy: gene interaction networks in early and late stages. *BMC Genomics* 9: 630, 2008.

35. **Cary SPL, and Marletta MA.** The case of CO signaling: why the jury is still out. 2001, p. 1071-1073.

36. **Castro MJ, Apple DF, Jr., Staron RS, Campos GE, and Dudley GA.** Influence of complete spinal cord injury on skeletal muscle within 6 mo of injury. *J Appl Physiol* 86: 350-358, 1999.

37. **Chen S, Khan ZA, Barbin Y, and Chakrabarti S.** Pro-oxidant role of heme oxygenase in mediating glucose-induced endothelial cell damage. 2004, p. 1301-1310.
38. **Chen YW, Zhao P, Borup R, and Hoffman EP.** Expression profiling in the muscular dystrophies: identification of novel aspects of molecular pathophysiology. *J Cell Biol* 151: 1321-1336, 2000.
39. **Chen Y-W, Gregory CM, Scarborough MT, Shi R, Walter GA, and Vandenborne K.** Transcriptional pathways associated with skeletal muscle disuse atrophy in humans. 2007, p. 510-520.
40. **Childs TE, Spangenburg EE, Vyas DR, and Booth FW.** Temporal alterations in protein signaling cascades during recovery from muscle atrophy. 2003, p. C391-398.
41. **Chrysis D, and Underwood LE.** Regulation of Components of the Ubiquitin System by Insulin-Like Growth Factor I and Growth Hormone in Skeletal Muscle of Rats Made Catabolic with Dexamethasone. 1999, p. 5635-5641.
42. **Clark BC, Manini TM, Bolanowski SJ, and Ploutz-Snyder LL.** Adaptations in human neuromuscular function following prolonged unweighting: II. Neurological properties and motor imagery efficacy. *J Appl Physiol* 101: 264-272, 2006.
43. **Colangelo D, Mahboobi H, Viarengo A, and Osella D.** Protective effect of metallothioneins against oxidative stress evaluated on wild type and MT-null cell lines by means of flow cytometry. *Biomaterials* 17: 365-370, 2004.
44. **Combaret L, Adegoke OAJ, Bedard N, Baracos V, Attaix D, and Wing SS.** USP19 is a ubiquitin-specific protease regulated in rat skeletal muscle during catabolic states. 2005, p. E693-700.
45. **Coutinho EL, Gomes AR, Franca CN, and Salvini TF.** A new model for the immobilization of the rat hind limb. *Braz J Med Biol Res* 35: 1329-1332, 2002.
46. **Cramer RM, Cooper P, Sinclair PJ, Bryant G, and Weston A.** Effect of load during electrical stimulation training in spinal cord injury. *Muscle Nerve* 29: 104-111, 2004.
47. **Cramer RM, Weston A, Climstein M, Davis GM, and Sutton JR.** Effects of electrical stimulation-induced leg training on skeletal muscle adaptability in spinal cord injury. *Scand J Med Sci Sports* 12: 316-322, 2002.
48. **Cramer RM, Weston AR, Rutkowski S, Middleton JW, Davis GM, and Sutton JR.** Effects of electrical stimulation leg training during the acute phase of spinal cord injury: a pilot study. 2000, p. 409-415.

49. **Criswell DS, Shanely RA, Betters JJ, McKenzie MJ, Sellman JE, Van Gammeren DL, and Powers SK.** Cumulative effects of aging and mechanical ventilation on in vitro diaphragm function. *Chest* 124: 2302-2308, 2003.
50. **Cross DA, Watt PW, Shaw M, van der Kaay J, Downes CP, Holder JC, and Cohen P.** Insulin activates protein kinase B, inhibits glycogen synthase kinase-3 and activates glycogen synthase by rapamycin-insensitive pathways in skeletal muscle and adipose tissue. *FEBS Lett* 406: 211-215, 1997.
51. **Crossland H, Constantin-Teodosiu D, Gardiner SM, Constantin D, and Greenhaff PL.** A potential role for Akt/FOXO signalling in both protein loss and the impairment of muscle carbohydrate oxidation during sepsis in rodent skeletal muscle. *J Physiol* 586: 5589-5600, 2008.
52. **Csibi A, Leibovitch MP, Cornille K, Tintignac LA, and Leibovitch SA.** MAFbx/Atrogin-1 controls the activity of the initiation factor eIF3-f in skeletal muscle atrophy by targeting multiple C-terminal lysines. *J Biol Chem* 2008.
53. **Dalla Libera L, Ravara B, Gobbo V, Tarricone E, Vitadello M, Biolo G, Vescovo G, and Gorza L.** A transient antioxidant stress response accompanies the onset of disuse atrophy in human skeletal muscle. *J Appl Physiol* 107: 549-557, 2009.
54. **Dalle B, Payen E, and Beuzard Y.** Modulation of transduced erythropoietin expression by iron. *Exp Hematol* 28: 760-764, 2000.
55. **Daniel S, Bradley G, Longshaw VM, Soti C, Csermely P, and Blatch GL.** Nuclear translocation of the phosphoprotein Hop (Hsp70/Hsp90 organizing protein) occurs under heat shock, and its proposed nuclear localization signal is involved in Hsp90 binding. *Biochim Biophys Acta* 1783: 1003-1014, 2008.
56. **Darr KC, and Schultz E.** Hindlimb suspension suppresses muscle growth and satellite cell proliferation. *J Appl Physiol* 67: 1827-1834, 1989.
57. **de Boer MD, Maganaris CN, Seynnes OR, Rennie MJ, and Narici MV.** Time course of muscular, neural and tendinous adaptations to 23 day unilateral lower-limb suspension in young men. 2007, p. 1079-1091.
58. **de Palma L, marinelli M, pavan M, and orazi A.** UBIQUITIN LIGASES MURF1 AND MAFBX IN HUMAN MUSCLE ATROPHY. 2009, p. 6-b-.
59. **Deboer MD, and Marks DL.** Cachexia: lessons from melanocortin antagonism. *Trends Endocrinol Metab* 17: 199-204, 2006.
60. **Dehoux M, Gobier C, Lause P, Bertrand L, Ketelslegers J-M, and Thissen J-P.** IGF-I does not prevent myotube atrophy caused by proinflammatory cytokines despite

activation of Akt/Foxo and GSK-3beta pathways and inhibition of atrogen-1 mRNA. 2007, p. E145-150.

61. **Demougeot C, Van Hoecke M, Bertrand N, Prigent-Tessier A, Mossiat C, Beley A, and Marie C.** Cytoprotective Efficacy and Mechanisms of the Liposoluble Iron Chelator 2,2'-Dipyridyl in the Rat Photothrombotic Ischemic Stroke Model. 2004, p. 1080-1087.
62. **Deng Y-M, Wu BJ, Witting PK, and Stocker R.** Probucol Protects Against Smooth Muscle Cell Proliferation by Upregulating Heme Oxygenase-1. 2004, p. 1855-1860.
63. **Dennis G, Jr., Sherman BT, Hosack DA, Yang J, Gao W, Lane HC, and Lempicki RA.** DAVID: Database for Annotation, Visualization, and Integrated Discovery. *Genome Biol* 4: P3, 2003.
64. **DeRuisseau KC, Kavazis AN, Deering MA, Falk DJ, Van Gammeren D, Yimlamai T, Ordway GA, and Powers SK.** Mechanical ventilation induces alterations of the ubiquitin-proteasome pathway in the diaphragm. *J Appl Physiol* 98: 1314-1321, 2005.
65. **DeRuisseau KC, Shanely RA, Akunuri N, Hamilton MT, Van Gammeren D, Zengeroglu AM, McKenzie M, and Powers SK.** Diaphragm unloading via controlled mechanical ventilation alters the gene expression profile. *Am J Respir Crit Care Med* 172: 1267-1275, 2005.
66. **Deschenes MR, Giles JA, McCoy RW, Volek JS, Gomez AL, and Kraemer WJ.** Neural factors account for strength decrements observed after short-term muscle unloading. *Am J Physiol Regul Integr Comp Physiol* 282: R578-583, 2002.
67. **Di Marco S, Mazroui R, Dallaire P, Chittur S, Tenenbaum SA, Radzioch D, Marette A, and Gallouzi I-E.** NF- κ B-Mediated MyoD Decay during Muscle Wasting Requires Nitric Oxide Synthase mRNA Stabilization, HuR Protein, and Nitric Oxide Release. 2005, p. 6533-6545.
68. **Dodd S, Hain B, and Judge A.** Hsp70 prevents disuse muscle atrophy in senescent rats. *Biogerontology* 2008.
69. **Droge W.** Free Radicals in the Physiological Control of Cell Function. 2002, p. 47-95.
70. **Drubin DA, Way JC, and Silver PA.** Designing biological systems. 2007, p. 242-254.

71. **Drummond MJ, Glynn EL, Lujan HL, Dicarlo SE, and Rasmussen BB.** Gene and protein expression associated with protein synthesis and breakdown in paraplegic skeletal muscle. *Muscle Nerve* 37: 505-513, 2008.
72. **Dudley GA, Castro MJ, Rogers S, and Apple DF, Jr.** A simple means of increasing muscle size after spinal cord injury: a pilot study. *Eur J Appl Physiol Occup Physiol* 80: 394-396, 1999.
73. **Dudley GA, Duvoisin MR, Convertino VA, and Buchanan P.** Alterations of the in vivo torque-velocity relationship of human skeletal muscle following 30 days exposure to simulated microgravity. *Aviat Space Environ Med* 60: 659-663, 1989.
74. **Dudley GA, Hather BM, and Buchanan P.** Skeletal muscle responses to unloading with special reference to man. *J Fla Med Assoc* 79: 525-529, 1992.
75. **Duguez S, Bartoli M, and Richard I.** Calpain 3: a key regulator of the sarcomere? *Febs J* 273: 3427-3436, 2006.
76. **Duvoisin MR, Convertino VA, Buchanan P, Gollnick PD, and Dudley GA.** Characteristics and preliminary observations of the influence of electromyostimulation on the size and function of human skeletal muscle during 30 days of simulated microgravity. *Aviat Space Environ Med* 60: 671-678, 1989.
77. **Etlinger JD, and Goldberg AL.** Control of protein degradation in reticulocytes and reticulocyte extracts by hemin. 1980, p. 4563-4568.
78. **Eyssen-Hernandez R, Ladoux A, and Frelin C.** Differential regulation of cardiac heme oxygenase-1 and vascular endothelial growth factor mRNA expressions by hemin, heavy metals, heat shock and anoxia. 1996, p. 229-233.
79. **Falk DJ, Deruisseau KC, Van Gammeren DL, Deering MA, Kavazis AN, and Powers SK.** Mechanical ventilation promotes redox status alterations in the diaphragm. *J Appl Physiol* 101: 1017-1024, 2006.
80. **Falk DJ, Whidden MA, Kavazis AN, Smuder AJ, McClung JM, and Powers SK.** Hemin administration during mechanical ventilation attenuates redox disturbances in the diaphragm. 2007, p. LB117-b-.
81. **Favier FB, Benoit H, and Freyssenet D.** Cellular and molecular events controlling skeletal muscle mass in response to altered use. *Pflugers Arch* 456: 587-600, 2008.
82. **Ferrando AA, Stuart CA, Brunder DG, and Hillman GR.** Magnetic resonance imaging quantitation of changes in muscle volume during 7 days of strict bed rest. *Aviat Space Environ Med* 66: 976-981, 1995.

83. **Fitts RH, Riley DR, and Widrick JJ.** Physiology of a microgravity environment invited review: microgravity and skeletal muscle. *J Appl Physiol* 89: 823-839, 2000.
84. **Fluck M, Chiquet M, Schmutz S, Mayet-Sornay MH, and Desplanches D.** Reloading of atrophied rat soleus muscle induces tenascin-C expression around damaged muscle fibers. *Am J Physiol Regul Integr Comp Physiol* 284: R792-801, 2003.
85. **Frimel TN, Kapadia F, Gaidosh GS, Li Y, Walter GA, and Vandenborne K.** A model of muscle atrophy using cast immobilization in mice. 2005, p. 672-674.
86. **Funato K, Matsuo A, Yata H, Akima H, Suzuki Y, Gunji A, and Fukunaga T.** Changes in force-velocity and power output of upper and lower extremity musculature in young subjects following 20 days bed rest. *J Gravit Physiol* 4: S22-30, 1997.
87. **Furukawa-Hibi Y, Kobayashi Y, Chen C, and Motoyama N.** FOXO transcription factors in cell-cycle regulation and the response to oxidative stress. *Antioxid Redox Signal* 7: 752-760, 2005.
88. **Furuno K, and Goldberg AL.** The activation of protein degradation in muscle by Ca²⁺ or muscle injury does not involve a lysosomal mechanism. *Biochem J* 237: 859-864, 1986.
89. **Furuyama K, Kaneko K, and Vargas PD.** Heme as a magnificent molecule with multiple missions: heme determines its own fate and governs cellular homeostasis. 2007, p. 1-16.
90. **Gething MJ, and Sambrook J.** Protein folding in the cell. *Nature* 355: 33-45, 1992.
91. **Giannelli G, De Marzo A, Marinosci F, and Antonaci S.** Matrix metalloproteinase imbalance in muscle disuse atrophy. *Histol Histopathol* 20: 99-106, 2005.
92. **Glass DJ.** Signalling pathways that mediate skeletal muscle hypertrophy and atrophy. *Nat Cell Biol* 5: 87-90, 2003.
93. **Glickman MH, and Ciechanover A.** The ubiquitin-proteasome proteolytic pathway: destruction for the sake of construction. *Physiol Rev* 82: 373-428, 2002.
94. **Gogia P, Schneider VS, LeBlanc AD, Krebs J, Kasson C, and Pientok C.** Bed rest effect on extremity muscle torque in healthy men. *Arch Phys Med Rehabil* 69: 1030-1032, 1988.
95. **Goldspink G.** Gene expression in muscle in response to exercise. *J Muscle Res Cell Motil* 24: 121-126, 2003.

96. **Goldspink G, and Yang SY.** Effects of activity on growth factor expression. *Int J Sport Nutr Exerc Metab* 11 Suppl: S21-27, 2001.
97. **Goll DE, Thompson VF, Li H, Wei W, and Cong J.** The calpain system. *Physiol Rev* 83: 731-801, 2003.
98. **Gomes MD, Lecker SH, Jagoe RT, Navon A, and Goldberg AL.** Atrogin-1, a muscle-specific F-box protein highly expressed during muscle atrophy. *Proc Natl Acad Sci U S A* 98: 14440-14445, 2001.
99. **Goto K, Honda M, Kobayashi T, Uehara K, Kojima A, Akema T, Sugiura T, Yamada S, Ohira Y, and Yoshioka T.** Heat stress facilitates the recovery of atrophied soleus muscle in rat. *Jpn J Physiol* 54: 285-293, 2004.
100. **Graber SG, and Woodworth RC.** Myoglobin expression in L6 muscle cells. Role of differentiation and heme. *J Biol Chem* 261: 9150-9154, 1986.
101. **Gregory CM, Vandenborne K, Castro MJ, and Dudley GA.** Human and rat skeletal muscle adaptations to spinal cord injury. *Can J Appl Physiol* 28: 491-500, 2003.
102. **Grune T, Merker K, Sandig G, and Davies KJ.** Selective degradation of oxidatively modified protein substrates by the proteasome. *Biochem Biophys Res Commun* 305: 709-718, 2003.
103. **Gustafsson T, Osterlund T, von Walden F, Trappe T, Linnehan R, and Tesch P.** Three days of unloading induces pre-translational changes in human skeletal muscle. 2008, p. 754.712-.
104. **Guttridge DC, Mayo MW, Madrid LV, Wang CY, and Baldwin AS, Jr.** NF-kappaB-induced loss of MyoD messenger RNA: possible role in muscle decay and cachexia. *Science* 289: 2363-2366, 2000.
105. **Haddad F, Adams GR, Bodell PW, and Baldwin KM.** Isometric resistance exercise fails to counteract skeletal muscle atrophy processes during the initial stages of unloading. *J Appl Physiol* 100: 433-441, 2006.
106. **Haddad F, Adams GR, Bodell PW, and Baldwin KM.** Isometric resistance exercise fails to counteract skeletal muscle atrophy processes during the initial stages of unloading. 2006, p. 433-441.
107. **Haddad F, Baldwin KM, and Tesch PA.** Pretranslational markers of contractile protein expression in human skeletal muscle: effect of limb unloading plus resistance exercise. 2005, p. 46-52.
108. **Halliwell B.** Antioxidant defence mechanisms: from the beginning to the end (of the beginning). *Free Radic Res* 31: 261-272, 1999.

109. **Han XY, Wang W, Myllyla R, Virtanen P, Karpakka J, and Takala TE.** mRNA levels for alpha-subunit of prolyl 4-hydroxylase and fibrillar collagens in immobilized rat skeletal muscle. *J Appl Physiol* 87: 90-96, 1999.
110. **Hather BM, Adams GR, Tesch PA, and Dudley GA.** Skeletal muscle responses to lower limb suspension in humans. *J Appl Physiol* 72: 1493-1498, 1992.
111. **Hawke TJ, Meeson AP, Jiang N, Graham S, Hutcheson K, DiMaio JM, and Garry DJ.** p21 is essential for normal myogenic progenitor cell function in regenerating skeletal muscle. 2003, p. C1019-1027.
112. **Heinemeier KM, Olesen JL, Haddad F, Schjerling P, Baldwin KM, and Kjaer M.** Effect of unloading followed by reloading on expression of collagen and related growth factors in rat tendon and muscle. 2009, p. 178-186.
113. **Herrmann J, Lerman LO, and Lerman A.** Ubiquitin and ubiquitin-like proteins in protein regulation. *Circ Res* 100: 1276-1291, 2007.
114. **Hespeel P, Op't Eijnde B, Van Leemputte M, Urso B, Greenhaff PL, Labarque V, Dymarkowski S, Van Hecke P, and Richter EA.** Oral creatine supplementation facilitates the rehabilitation of disuse atrophy and alters the expression of muscle myogenic factors in humans. *J Physiol* 536: 625-633, 2001.
115. **Hill M, Pereira V, Chauveau C, Zagani R, Remy S, Tesson L, Mazal D, Ubbilos L, Brion R, Ashgar K, Mashreghi MF, Kotsch K, Moffett J, Doebis C, Seifert M, Boczkowski J, Osinaga E, and Anegon I.** Heme oxygenase-1 inhibits rat and human breast cancer cell proliferation: mutual cross inhibition with indoleamine 2,3-dioxygenase. 2005, p. 1957-1968.
116. **Hishikawa N, Niwa J, Doyu M, Ito T, Ishigaki S, Hashizume Y, and Sobue G.** Dofin localizes to the ubiquitylated inclusions in Parkinson's disease, dementia with Lewy bodies, multiple system atrophy, and amyotrophic lateral sclerosis. *Am J Pathol* 163: 609-619, 2003.
117. **Hofer T, Marzetti E, Xu J, Seo AY, Gulec S, Knutson MD, Leeuwenburgh C, and Dupont-Versteegde EE.** Increased iron content and RNA oxidative damage in skeletal muscle with aging and disuse atrophy. 2008, p. 563-570.
118. **Hoffman EP, and Nader GA.** Balancing muscle hypertrophy and atrophy. *Nat Med* 10: 584-585, 2004.
119. **Hornberger TA, and Esser KA.** Mechanotransduction and the regulation of protein synthesis in skeletal muscle. *Proc Nutr Soc* 63: 331-335, 2004.

120. **Hornberger TA, Hunter RB, Kandarian SC, and Esser KA.** Regulation of translation factors during hindlimb unloading and denervation of skeletal muscle in rats. *Am J Physiol Cell Physiol* 281: C179-187, 2001.
121. **Hortobagyi T, Dempsey L, Fraser D, Zheng D, Hamilton G, Lambert J, and Dohm L.** Changes in muscle strength, muscle fibre size and myofibrillar gene expression after immobilization and retraining in humans. 2000, p. 293-304.
122. **Hosack DA, Dennis G, Jr., Sherman BT, Lane HC, and Lempicki RA.** Identifying biological themes within lists of genes with EASE. *Genome Biol* 4: R70, 2003.
123. **Huang DW, Sherman BT, and Lempicki RA.** Systematic and integrative analysis of large gene lists using DAVID bioinformatics resources. *Nat Protocols* 4: 44-57, 2008.
124. **Huang W, Kutner N, and Bliwise DL.** A systematic review of the effects of acupuncture in treating insomnia. *Sleep Med Rev* 13: 73-104, 2009.
125. **Hunter RB, Mitchell-Felton H, Essig DA, and Kandarian SC.** Expression of endoplasmic reticulum stress proteins during skeletal muscle disuse atrophy. *Am J Physiol Cell Physiol* 281: C1285-1290, 2001.
126. **Hunter RB, Stevenson E, Koncarevic A, Mitchell-Felton H, Essig DA, and Kandarian SC.** Activation of an alternative NF-kappaB pathway in skeletal muscle during disuse atrophy. *Faseb J* 16: 529-538, 2002.
127. **Ikemoto M, Nikawa T, Takeda S, Watanabe C, Kitano T, Baldwin KM, Izumi R, Nonaka I, Towatari T, Teshima S, Rokutan K, and Kishi K.** Space shuttle flight (STS-90) enhances degradation of rat myosin heavy chain in association with activation of ubiquitin-proteasome pathway. *Faseb J* 15: 1279-1281, 2001.
128. **Irminger-Finger I, Busquets S, Calabrio F, Lopez-Soriano FJ, and Argiles JM.** BARD1 content correlates with increased DNA fragmentation associated with muscle wasting in tumour-bearing rats. 2006, p. 1425-1428.
129. **Isfort RJ, Wang F, Greis KD, Sun Y, Keough TW, Bodine SC, and Anderson NL.** Proteomic analysis of rat soleus and tibialis anterior muscle following immobilization. *J Chromatogr B Analyt Technol Biomed Life Sci* 769: 323-332, 2002.
130. **Isfort RJ, Wang F, Greis KD, Sun Y, Keough TW, Farrar RP, Bodine SC, and Anderson NL.** Proteomic analysis of rat soleus muscle undergoing hindlimb suspension-induced atrophy and reweighting hypertrophy. *Proteomics* 2: 543-550, 2002.
131. **Ishigaki S, Hishikawa N, Niwa J-i, Iemura S-i, Natsume T, Hori S, Kakizuka A, Tanaka K, and Sobue G.** Physical and Functional Interaction between Dorsin and

Valosin-containing Protein That Are Colocalized in Ubiquitylated Inclusions in Neurodegenerative Disorders. 2004, p. 51376-51385.

132. **Ito K, Adachi S, Iwakami R, Yasuda H, Muto Y, Seki N, and Okano Y.** N-Terminally extended human ubiquitin-conjugating enzymes (E2s) mediate the ubiquitination of RING-finger proteins, ARA54 and RNF8. *Eur J Biochem* 268: 2725-2732, 2001.

133. **Jackman RW, and Kandarian SC.** The molecular basis of skeletal muscle atrophy. 2004, p. C834-843.

134. **Jayaraman A, Gregory CM, Bowden M, Stevens JE, Shah P, Behrman AL, and Vandenborne K.** Lower extremity skeletal muscle function in persons with incomplete spinal cord injury. *Spinal Cord* 44: 680-687, 2006.

135. **Jones SW, Hill RJ, Krasney PA, O'Conner B, Peirce N, and Greenhaff PL.** Disuse atrophy and exercise rehabilitation in humans profoundly affects the expression of genes associated with the regulation of skeletal muscle mass. *Faseb J* 18: 1025-1027, 2004.

136. **Kabe Y, Ando K, Hirao S, Yoshida M, and Handa H.** Redox regulation of NF-kappaB activation: distinct redox regulation between the cytoplasm and the nucleus. *Antioxid Redox Signal* 7: 395-403, 2005.

137. **Kaminski HJ, and Andrade FH.** Nitric oxide: biologic effects on muscle and role in muscle diseases. *Neuromuscul Disord* 11: 517-524, 2001.

138. **Kandarian SC, and Jackman RW.** Intracellular signaling during skeletal muscle atrophy. *Muscle Nerve* 33: 155-165, 2006.

139. **Kandarian SC, and Stevenson EJ.** Molecular events in skeletal muscle during disuse atrophy. *Exerc Sport Sci Rev* 30: 111-116, 2002.

140. **Kaneki H, Guo R, Chen D, Yao Z, Schwarz EM, Zhang YE, Boyce BF, and Xing L.** Tumor necrosis factor promotes Runx2 degradation through up-regulation of Smurf1 and Smurf2 in osteoblasts. *J Biol Chem* 281: 4326-4333, 2006.

141. **Kauhanen S, Leivo I, and Michelsson JE.** Early muscle changes after immobilization. An experimental study on muscle damage. *Clin Orthop Relat Res* 44-50, 1993.

142. **Kerscher O, Felberbaum R, and Hochstrasser M.** Modification of proteins by ubiquitin and ubiquitin-like proteins. *Annu Rev Cell Dev Biol* 22: 159-180, 2006.

143. **Kim JW, Kwon OY, and Kim MH.** Differentially expressed genes and morphological changes during lengthened immobilization in rat soleus muscle. 2007, p. 147-157.
144. **Kim MV, Seit-Nebi AS, and Gusev NB.** The problem of protein kinase activity of small heat shock protein Hsp22 (H11 or HspB8). *Biochem Biophys Res Commun* 325: 649-652, 2004.
145. **Kitahara A, Hamaoka T, Murase N, Homma T, Kurosawa Y, Ueda C, Nagasawa T, Ichimura S, Motobe M, Yashiro K, Nakano S, and Katsumura T.** Deterioration of muscle function after 21-day forearm immobilization. *Med Sci Sports Exerc* 35: 1697-1702, 2003.
146. **Kjaer M.** Role of extracellular matrix in adaptation of tendon and skeletal muscle to mechanical loading. *Physiol Rev* 84: 649-698, 2004.
147. **Kobzik L, Reid MB, Brecht DS, and Stamler JS.** Nitric oxide in skeletal muscle. *Nature* 372: 546-548, 1994.
148. **Koh TJ, and Tidball JG.** Nitric oxide inhibits calpain-mediated proteolysis of talin in skeletal muscle cells. *Am J Physiol Cell Physiol* 279: C806-812, 2000.
149. **Koncarevic A, Jackman RW, and Kandarian SC.** The ubiquitin-protein ligase Nedd4 targets Notch1 in skeletal muscle and distinguishes the subset of atrophies caused by reduced muscle tension. 2007, p. 427-437.
150. **Kondo H, Miura M, and Itokawa Y.** Antioxidant enzyme systems in skeletal muscle atrophied by immobilization. *Pflugers Arch* 422: 404-406, 1993.
151. **Kondo H, Miura M, and Itokawa Y.** Oxidative stress in skeletal muscle atrophied by immobilization. *Acta Physiol Scand* 142: 527-528, 1991.
152. **Kondo H, Nakagaki I, Sasaki S, Hori S, and Itokawa Y.** Mechanism of oxidative stress in skeletal muscle atrophied by immobilization. *Am J Physiol* 265: E839-844, 1993.
153. **Kondo H, Nishino K, and Itokawa Y.** Hydroxyl radical generation in skeletal muscle atrophied by immobilization. *FEBS Lett* 349: 169-172, 1994.
154. **Kotamraju S, Chitambar CR, Kalivendi SV, Joseph J, and Kalyanaraman B.** Transferrin receptor-dependent iron uptake is responsible for doxorubicin-mediated apoptosis in endothelial cells: role of oxidant-induced iron signaling in apoptosis. *J Biol Chem* 277: 17179-17187, 2002.
155. **Kourie JI.** Interaction of reactive oxygen species with ion transport mechanisms. 1998, p. C1-24.

156. **Kramerova I, Kudryashova E, Venkatraman G, and Spencer MJ.** Calpain 3 participates in sarcomere remodeling by acting upstream of the ubiquitin-proteasome pathway. *Hum Mol Genet* 14: 2125-2134, 2005.
157. **Krawiec BJ, Frost RA, Vary TC, Jefferson LS, and Lang CH.** Hindlimb casting decreases muscle mass in part by proteasome-dependent proteolysis but independent of protein synthesis. *Am J Physiol Endocrinol Metab* 289: E969-980, 2005.
158. **Krawiec BJ, Frost RA, Vary TC, Jefferson LS, and Lang CH.** Hindlimb casting decreases muscle mass in part by proteasome-dependent proteolysis but independent of protein synthesis. 2005, p. E969-980.
159. **Ku Z, and Thomason DB.** Soleus muscle nascent polypeptide chain elongation slows protein synthesis rate during non-weight-bearing activity. *Am J Physiol* 267: C115-126, 1994.
160. **Ku Z, Yang J, Menon V, and Thomason DB.** Decreased polysomal HSP-70 may slow polypeptide elongation during skeletal muscle atrophy. *Am J Physiol* 268: C1369-1374, 1995.
161. **Lalani SR, Vladutiu GD, Plunkett K, Lotze TE, Adesina AM, and Scaglia F.** Isolated mitochondrial myopathy associated with muscle coenzyme Q10 deficiency. *Arch Neurol* 62: 317-320, 2005.
162. **Lamb NJ, Quinlan GJ, Mumby S, Evans TW, and Gutteridge JM.** Haem oxygenase shows pro-oxidant activity in microsomal and cellular systems: implications for the release of low-molecular-mass iron. 1999, p. 153-158.
163. **Lang D, Reuter S, Buzescu T, August C, and Heidenreich S.** Heme-induced heme oxygenase-1 (HO-1) in human monocytes inhibits apoptosis despite caspase-3 up-regulation. 2005, p. 155-165.
164. **Laskowska E.** [Small heat shock proteins--role in apoptosis, cancerogenesis and diseases associated with protein aggregation]. *Postepy Biochem* 53: 19-26, 2007.
165. **Latres E, Amini AR, Amini AA, Griffiths J, Martin FJ, Wei Y, Lin HC, Yancopoulos GD, and Glass DJ.** Insulin-like growth factor-1 (IGF-1) inversely regulates atrophy-induced genes via the phosphatidylinositol 3-kinase/Akt/mammalian target of rapamycin (PI3K/Akt/mTOR) pathway. *J Biol Chem* 280: 2737-2744, 2005.
166. **Lawler JM, Song W, and Demaree SR.** Hindlimb unloading increases oxidative stress and disrupts antioxidant capacity in skeletal muscle. *Free Radic Biol Med* 35: 9-16, 2003.

167. **Lawler JM, Song W, and Kwak HB.** Differential response of heat shock proteins to hindlimb unloading and reloading in the soleus. *Muscle Nerve* 33: 200-207, 2006.
168. **LeBlanc A, Gogia P, Schneider V, Krebs J, Schonfeld E, and Evans H.** Calf muscle area and strength changes after five weeks of horizontal bed rest. *Am J Sports Med* 16: 624-629, 1988.
169. **LeBlanc AD, Schneider VS, Evans HJ, Pientok C, Rowe R, and Spector E.** Regional changes in muscle mass following 17 weeks of bed rest. *J Appl Physiol* 73: 2172-2178, 1992.
170. **Lecker SH, Jagoe RT, Gilbert A, Gomes M, Baracos V, Bailey J, Price SR, Mitch WE, and Goldberg AL.** Multiple types of skeletal muscle atrophy involve a common program of changes in gene expression. *Faseb J* 18: 39-51, 2004.
171. **Lecker SH, Solomon V, Mitch WE, and Goldberg AL.** Muscle protein breakdown and the critical role of the ubiquitin-proteasome pathway in normal and disease states. *J Nutr* 129: 227S-237S, 1999.
172. **Leger B, Cartoni R, Praz M, Lamon S, Deriaz O, Crettenand A, Gobelet C, Rohmer P, Konzelmann M, Luthi F, and Russell AP.** Akt signalling through GSK-3beta, mTOR and Foxo1 is involved in human skeletal muscle hypertrophy and atrophy. *J Physiol* 576: 923-933, 2006.
173. **Leger B, Vergani L, Soraru G, Hespel P, Derave W, Gobelet C, D'Ascenzio C, Angelini C, and Russell AP.** Human skeletal muscle atrophy in amyotrophic lateral sclerosis reveals a reduction in Akt and an increase in atrogin-1. *Faseb J* 20: 583-585, 2006.
174. **Leick L, Wojtaszewski JFP, Johansen ST, Kiilerich K, Comes G, Hellsten Y, Hidalgo J, and Pilegaard H.** PGC-1{alpha} is not mandatory for exercise- and training-induced adaptive gene responses in mouse skeletal muscle. 2008, p. E463-474.
175. **Levine S, Nguyen T, Taylor N, Friscia ME, Budak MT, Rothenberg P, Zhu J, Sachdeva R, Sonnad S, Kaiser LR, Rubinstein NA, Powers SK, and Shrager JB.** Rapid disuse atrophy of diaphragm fibers in mechanically ventilated humans. *N Engl J Med* 358: 1327-1335, 2008.
176. **Li C, and Hung Wong W.** Model-based analysis of oligonucleotide arrays: model validation, design issues and standard error application. *Genome Biol* 2: RESEARCH0032, 2001.
177. **Li HH, Kedar V, Zhang C, McDonough H, Arya R, Wang DZ, and Patterson C.** Atrogin-1/muscle atrophy F-box inhibits calcineurin-dependent cardiac hypertrophy by participating in an SCF ubiquitin ligase complex. *J Clin Invest* 114: 1058-1071, 2004.

178. **Li LY, Luo X, and Wang X.** Endonuclease G is an apoptotic DNase when released from mitochondria. *Nature* 412: 95-99, 2001.
179. **Li YP.** TNF-alpha is a mitogen in skeletal muscle. *Am J Physiol Cell Physiol* 285: C370-376, 2003.
180. **Li YP, Chen Y, John J, Moylan J, Jin B, Mann DL, and Reid MB.** TNF-alpha acts via p38 MAPK to stimulate expression of the ubiquitin ligase atrogin1/MAFbx in skeletal muscle. *Faseb J* 19: 362-370, 2005.
181. **Li YP, Chen Y, Li AS, and Reid MB.** Hydrogen peroxide stimulates ubiquitin-conjugating activity and expression of genes for specific E2 and E3 proteins in skeletal muscle myotubes. *Am J Physiol Cell Physiol* 285: C806-812, 2003.
182. **Li YP, and Reid MB.** NF-kappaB mediates the protein loss induced by TNF-alpha in differentiated skeletal muscle myotubes. *Am J Physiol Regul Integr Comp Physiol* 279: R1165-1170, 2000.
183. **Liu MJ, Li JX, Lee KM, Qin L, and Chan KM.** Oxidative stress after muscle damage from immobilization and remobilization occurs locally and systemically. *Clin Orthop Relat Res* 246-250, 2005.
184. **Liu WM, Mei R, Di X, Ryder TB, Hubbell E, Dee S, Webster TA, Harrington CA, Ho MH, Baid J, and Smeekens SP.** Analysis of high density expression microarrays with signed-rank call algorithms. *Bioinformatics* 18: 1593-1599, 2002.
185. **Livak KJ, and Schmittgen TD.** Analysis of relative gene expression data using real-time quantitative PCR and the 2(-Delta Delta C(T)) Method. *Methods* 25: 402-408, 2001.
186. **MacDougall JD, Elder GC, Sale DG, Moroz JR, and Sutton JR.** Effects of strength training and immobilization on human muscle fibres. *Eur J Appl Physiol Occup Physiol* 43: 25-34, 1980.
187. **Mackey AL, Donnelly AE, Turpeenniemi-Hujanen T, and Roper HP.** Skeletal muscle collagen content in humans after high-force eccentric contractions. *J Appl Physiol* 97: 197-203, 2004.
188. **Maes K, Testelmans D, Cadot P, Deruisseau K, Powers SK, Decramer M, and Gayan-Ramirez G.** Effects of acute administration of corticosteroids during mechanical ventilation on rat diaphragm. *Am J Respir Crit Care Med* 178: 1219-1226, 2008.

189. **Maes K, Testelmans D, Powers S, Decramer M, and Gayan-Ramirez G.** Leupeptin inhibits ventilator-induced diaphragm dysfunction in rats. *Am J Respir Crit Care Med* 175: 1134-1138, 2007.
190. **Maeshima Y, Sudhakar A, Lively JC, Ueki K, Kharbanda S, Kahn CR, Sonenberg N, Hynes RO, and Kalluri R.** Tumstatin, an endothelial cell-specific inhibitor of protein synthesis. *Science* 295: 140-143, 2002.
191. **Mammucari C, Milan G, Romanello V, Masiero E, Rudolf R, Del Piccolo P, Burden SJ, Di Lisi R, Sandri C, Zhao J, Goldberg AL, Schiaffino S, and Sandri M.** FoxO3 controls autophagy in skeletal muscle in vivo. *Cell Metab* 6: 458-471, 2007.
192. **Mammucari C, Schiaffino S, and Sandri M.** Downstream of Akt: FoxO3 and mTOR in the regulation of autophagy in skeletal muscle. *Autophagy* 4: 524-526, 2008.
193. **Martin D, Rojo AI, Salinas M, Diaz R, Gallardo G, Alam J, De Galarreta CM, and Cuadrado A.** Regulation of heme oxygenase-1 expression through the phosphatidylinositol 3-kinase/Akt pathway and the Nrf2 transcription factor in response to the antioxidant phytochemical carnosol. *J Biol Chem* 279: 8919-8929, 2004.
194. **Massip-Salcedo M, Casillas-Ramirez A, Franco-Gou R, Bartrons R, Ben Mosbah I, Serafin A, Rosello-Catafau J, and Peralta C.** Heat Shock Proteins and Mitogen-activated Protein Kinases in Steatotic Livers Undergoing Ischemia-Reperfusion: Some Answers. 2006, p. 1474-1485.
195. **Matsushima Y, Nanri H, Nara S, Okufuji T, Ohta M, Hachisuka K, and Ikeda M.** Hindlimb unloading decreases thioredoxin-related antioxidant proteins and increases thioredoxin-binding protein-2 in rat skeletal muscle. *Free Radic Res* 40: 715-722, 2006.
196. **Mazzatti DJ, Smith MA, Oita RC, Lim F-L, White AJ, and Reid MB.** Muscle unloading-induced metabolic remodeling is associated with acute alterations in PPAR{delta} and UCP-3 expression. 2008, p. 149-161.
197. **McArdle F, Spiers S, Aldemir H, Vasilaki A, Beaver A, Iwanejko L, McArdle A, and Jackson MJ.** Preconditioning of skeletal muscle against contraction-induced damage: the role of adaptations to oxidants in mice. *J Physiol* 561: 233-244, 2004.
198. **McClung JM, Kavazis AN, DeRuisseau KC, Falk DJ, Deering MA, Lee Y, Sugiura T, and Powers SK.** Caspase-3 regulation of diaphragm myonuclear domain during mechanical ventilation-induced atrophy. *Am J Respir Crit Care Med* 175: 150-159, 2007.
199. **McClung JM, Kavazis AN, DeRuisseau KC, Falk DJ, Whidden MA, and Powers SK.** Effects of oxidative stress on PI3K/Akt regulation of FOXO transcription factors during diaphragm muscle disuse. 2007, p. A1306-c-.

200. **McClung JM, Kavazis AN, Whidden MA, DeRuisseau KC, Falk DJ, Criswell DS, and Powers SK.** Antioxidant administration attenuates mechanical ventilation-induced rat diaphragm muscle atrophy independent of protein kinase B (PKB Akt) signalling. *J Physiol* 585: 203-215, 2007.
201. **McClung JM, Whidden MA, Kavazis AN, Falk DJ, Deruisseau KC, and Powers SK.** Redox regulation of diaphragm proteolysis during mechanical ventilation. *Am J Physiol Regul Integr Comp Physiol* 294: R1608-1617, 2008.
202. **McElhinny AS, Kakinuma K, Sorimachi H, Labeit S, and Gregorio CC.** Muscle-specific RING finger-1 interacts with titin to regulate sarcomeric M-line and thick filament structure and may have nuclear functions via its interaction with glucocorticoid modulatory element binding protein-1. *J Cell Biol* 157: 125-136, 2002.
203. **Miles MP, Clarkson PM, Bean M, Ambach K, Mulroy J, and Vincent K.** Muscle function at the wrist following 9 d of immobilization and suspension. *Med Sci Sports Exerc* 26: 615-623, 1994.
204. **Morey-Holton ER, and Globus RK.** Hindlimb unloading rodent model: technical aspects. *J Appl Physiol* 92: 1367-1377, 2002.
205. **Mrosek M, Labeit D, Witt S, Heerklotz H, von Castelmur E, Labeit S, and Mayans O.** Molecular determinants for the recruitment of the ubiquitin-ligase MuRF-1 onto M-line titin. 2007, p. 1383-1392.
206. **Mrosek M, Labeit D, Witt S, Heerklotz H, von Castelmur E, Labeit S, and Mayans O.** Molecular determinants for the recruitment of the ubiquitin-ligase MuRF-1 onto M-line titin. *Faseb J* 21: 1383-1392, 2007.
207. **Nader GA.** Molecular determinants of skeletal muscle mass: getting the "AKT" together. *Int J Biochem Cell Biol* 37: 1985-1996, 2005.
208. **Nguyen HX, and Tidball JG.** Expression of a muscle-specific, nitric oxide synthase transgene prevents muscle membrane injury and reduces muscle inflammation during modified muscle use in mice. *J Physiol* 550: 347-356, 2003.
209. **Nikawa T, Ishidoh K, Hirasaka K, Ishihara I, Ikemoto M, Kano M, Kominami E, Nonaka I, Ogawa T, Adams GR, Baldwin KM, Yasui N, Kishi K, and Takeda S.** Skeletal muscle gene expression in space-flown rats. *Faseb J* 18: 522-524, 2004.
210. **Ninichuk V, Gross O, Segerer S, Hoffmann R, Radomska E, Buchstaller A, Huss R, Akis N, Schlondorff D, and Anders HJ.** Multipotent mesenchymal stem cells reduce interstitial fibrosis but do not delay progression of chronic kidney disease in collagen4A3-deficient mice. *Kidney Int* 70: 121-129, 2006.

211. **Niwa J, Ishigaki S, Hishikawa N, Yamamoto M, Doyu M, Murata S, Tanaka K, Taniguchi N, and Sobue G.** Dorfin ubiquitylates mutant SOD1 and prevents mutant SOD1-mediated neurotoxicity. *J Biol Chem* 277: 36793-36798, 2002.
212. **Odunuga OO, Longshaw VM, and Blatch GL.** Hop: more than an Hsp70/Hsp90 adaptor protein. *Bioessays* 26: 1058-1068, 2004.
213. **Ogawa T, Furochi H, Mameoka M, Hirasaka K, Onishi Y, Suzue N, Oarada M, Akamatsu M, Akima H, Fukunaga T, Kishi K, Yasui N, Ishidoh K, Fukuoka H, and Nikawa T.** Ubiquitin ligase gene expression in healthy volunteers with 20-day bedrest. *Muscle Nerve* 34: 463-469, 2006.
214. **Ohashi N, Yamamoto T, Uchida C, Togawa A, Fukasawa H, Fujigaki Y, Suzuki S, Kitagawa K, Hattori T, Oda T, Hayashi H, Hishida A, and Kitagawa M.** Transcriptional induction of Smurf2 ubiquitin ligase by TGF-beta. *FEBS Lett* 579: 2557-2563, 2005.
215. **Ohira Y, Yoshinaga T, Nonaka I, Ohara M, Yoshioka T, Yamashita-Goto K, Izumi R, Yasukawa K, Sekiguchi C, Shenkman BS, and Kozzlovskaya IB.** Histochemical responses of human soleus muscle fibers to long-term bedrest with or without countermeasures. *Jpn J Physiol* 50: 41-47, 2000.
216. **Ohira Y, Yoshinaga T, Ohara M, Nonaka I, Yoshioka T, Yamashita-Goto K, Shenkman BS, Kozlovskaya IB, Roy RR, and Edgerton VR.** Myonuclear domain and myosin phenotype in human soleus after bed rest with or without loading. *J Appl Physiol* 87: 1776-1785, 1999.
217. **Oishi Y, Ishihara A, Talmadge RJ, Ohira Y, Taniguchi K, Matsumoto H, Roy RR, and Edgerton VR.** Expression of heat shock protein 72 in atrophied rat skeletal muscles. *Acta Physiol Scand* 172: 123-130, 2001.
218. **Oishi Y, Taniguchi K, Matsumoto H, Kawano F, Ishihara A, and Ohira Y.** Upregulation of HSP72 in reloading rat soleus muscle after prolonged hindlimb unloading. *Jpn J Physiol* 53: 281-286, 2003.
219. **Otis JS, Brown LA, and Guidot DM.** Oxidant-induced atrogen-1 and transforming growth factor-beta1 precede alcohol-related myopathy in rats. *Muscle Nerve* 36: 842-848, 2007.
220. **Pantano C, Reynaert NL, van der Vliet A, and Janssen-Heininger YM.** Redox-sensitive kinases of the nuclear factor-kappaB signaling pathway. *Antioxid Redox Signal* 8: 1791-1806, 2006.

221. **Park HJ, Costa RH, Lau LF, Tyner AL, and Raychaudhuri P.** Anaphase-Promoting Complex/Cyclosome-Cdh1-Mediated Proteolysis of the Forkhead Box M1 Transcription Factor Is Critical for Regulated Entry into S Phase. 2008, p. 5162-5171.
222. **Park J-J, Berggren JR, Hulver MW, Houmard JA, and Hoffman EP.** GRB14, GPD1, and GDF8 as potential network collaborators in weight loss-induced improvements in insulin action in human skeletal muscle. 2006, p. 114-121.
223. **Pattison JS, Folk LC, Madsen RW, and Booth FW.** Selected Contribution: Identification of differentially expressed genes between young and old rat soleus muscle during recovery from immobilization-induced atrophy. *J Appl Physiol* 95: 2171-2179, 2003.
224. **Pescatori M, Broccolini A, Minetti C, Bertini E, Bruno C, D'Amico A, Bernardini C, Mirabella M, Silvestri G, Giglio V, Modoni A, Pedemonte M, Tasca G, Galluzzi G, Mercuri E, Tonali PA, and Ricci E.** Gene expression profiling in the early phases of DMD: a constant molecular signature characterizes DMD muscle from early postnatal life throughout disease progression. *Faseb J* 21: 1210-1226, 2007.
225. **Pfaffl MW.** A new mathematical model for relative quantification in real-time RT-PCR. *Nucleic Acids Res* 29: e45, 2001.
226. **Phillips SM, Glover EI, and Rennie MJ.** Alterations of protein turnover underlying disuse atrophy in human skeletal muscle. *J Appl Physiol* 2009.
227. **Pichler A, and Melchior F.** Ubiquitin-related modifier SUMO1 and nucleocytoplasmic transport. *Traffic* 3: 381-387, 2002.
228. **Pistilli EE, Siu PM, and Alway SE.** Interleukin-15 responses to aging and unloading-induced skeletal muscle atrophy. 2007, p. C1298-1304.
229. **Ploutz-Snyder LL, Tesch PA, Crittenden DJ, and Dudley GA.** Effect of unweighting on skeletal muscle use during exercise. *J Appl Physiol* 79: 168-175, 1995.
230. **Ploutz-Snyder LL, Tesch PA, Hather BM, and Dudley GA.** Vulnerability to dysfunction and muscle injury after unloading. *Arch Phys Med Rehabil* 77: 773-777, 1996.
231. **Ponka P, Beaumont C, and Richardson DR.** Function and regulation of transferrin and ferritin. *Semin Hematol* 35: 35-54, 1998.
232. **Powell SR.** The Antioxidant Properties of Zinc. 2000, p. 1447S-1454.
233. **Powers SK, Decramer M, Gayan-Ramirez G, and Levine S.** Pressure support ventilation attenuates ventilator-induced protein modifications in the diaphragm. *Crit Care* 12: 191, 2008.

234. **Powers SK, Kavazis AN, and DeRuisseau KC.** Mechanisms of disuse muscle atrophy: role of oxidative stress. *Am J Physiol Regul Integr Comp Physiol* 288: R337-344, 2005.
235. **Powers SK, Kavazis AN, and McClung JM.** Oxidative stress and disuse muscle atrophy. *J Appl Physiol* 2007.
236. **Raffaello A, Laveder P, Romualdi C, Bean C, Toniolo L, Germinario E, Megighian A, Danieli-Betto D, Reggiani C, and Lanfranchi G.** Denervation in murine fast-twitch muscle: short-term physiological changes and temporal expression profiling. *Physiol Genomics* 25: 60-74, 2006.
237. **Rall LC, Rosen CJ, Dolnikowski G, Hartman WJ, Lundgren N, Abad LW, Dinarello CA, and Roubenoff R.** Protein metabolism in rheumatoid arthritis and aging. Effects of muscle strength training and tumor necrosis factor alpha. *Arthritis Rheum* 39: 1115-1124, 1996.
238. **Reid MB.** Response of the ubiquitin-proteasome pathway to changes in muscle activity. *Am J Physiol Regul Integr Comp Physiol* 288: R1423-1431, 2005.
239. **Reznick AZ, Menashe O, Bar-Shai M, Coleman R, and Carmeli E.** Expression of matrix metalloproteinases, inhibitor, and acid phosphatase in muscles of immobilized hindlimbs of rats. *Muscle Nerve* 27: 51-59, 2003.
240. **Richard I, Broux O, Allamand V, Fougereuse F, Chiannikulchai N, Bourg N, Brenguier L, Devaud C, Pasturaud P, Roudaut C, and et al.** Mutations in the proteolytic enzyme calpain 3 cause limb-girdle muscular dystrophy type 2A. *Cell* 81: 27-40, 1995.
241. **Ricort JM.** Insulin-like growth factor binding protein (IGFBP) signalling. *Growth Horm IGF Res* 14: 277-286, 2004.
242. **Rommel C, Bodine SC, Clarke BA, Rossman R, Nunez L, Stitt TN, Yancopoulos GD, and Glass DJ.** Mediation of IGF-1-induced skeletal myotube hypertrophy by PI(3)K/Akt/mTOR and PI(3)K/Akt/GSK3 pathways. *Nat Cell Biol* 3: 1009-1013, 2001.
243. **Rozier CK, Elder JD, and Brown M.** Prevention of atrophy by isometric exercise of a casted leg. *J Sports Med Phys Fitness* 19: 191-194, 1979.
244. **Ryter SW, Alam J, and Choi AM.** Heme oxygenase-1/carbon monoxide: from basic science to therapeutic applications. *Physiol Rev* 86: 583-650, 2006.
245. **Sacheck JM, Hyatt JP, Raffaello A, Jagoe RT, Roy RR, Edgerton VR, Lecker SH, and Goldberg AL.** Rapid disuse and denervation atrophy involve

transcriptional changes similar to those of muscle wasting during systemic diseases. *Faseb J* 21: 140-155, 2007.

246. **Sacheck JM, Ohtsuka A, McLary SC, and Goldberg AL.** IGF-I stimulates muscle growth by suppressing protein breakdown and expression of atrophy-related ubiquitin ligases, atrogin-1 and MuRF1. *Am J Physiol Endocrinol Metab* 287: E591-601, 2004.

247. **Sadhu C, and Gedamu L.** Regulation of human metallothionein (MT) genes. Differential expression of MTI-F, MTI-G, and MTII-A genes in the hepatoblastoma cell line (HepG2). *J Biol Chem* 263: 2679-2684, 1988.

248. **Salahudeen AA, Jenkins JK, Huang H, Ndebele K, and Salahudeen AK.** Overexpression of heme oxygenase protects renal tubular cells against cold storage injury: studies using hemin induction and HO-1 gene transfer. 2001, p. 1498-1504.

249. **Sandri M, Sandri C, Gilbert A, Skurk C, Calabria E, Picard A, Walsh K, Schiaffino S, Lecker SH, and Goldberg AL.** Foxo transcription factors induce the atrophy-related ubiquitin ligase atrogin-1 and cause skeletal muscle atrophy. *Cell* 117: 399-412, 2004.

250. **Saville MK, Sparks A, Xirodimas DP, Wardrop J, Stevenson LF, Bourdon JC, Woods YL, and Lane DP.** Regulation of p53 by the ubiquitin-conjugating enzymes UbcH5B/C in vivo. *J Biol Chem* 279: 42169-42181, 2004.

251. **Saville MK, Sparks A, Xirodimas DP, Wardrop J, Stevenson LF, Bourdon J-C, Woods YL, and Lane DP.** Regulation of p53 by the Ubiquitin-conjugating Enzymes UbcH5B/C in Vivo. 2004, p. 42169-42181.

252. **Senf SM, Dodd SL, McClung JM, and Judge AR.** Hsp70 overexpression inhibits NF-kappaB and Foxo3a transcriptional activities and prevents skeletal muscle atrophy. *Faseb J* 22: 3836-3845, 2008.

253. **Sewright KA, Urso ML, Thompson PD, Bilbe C, Chen YW, Hoffman EP, and Clarkson PM.** Oxidative Stress Response Genes Upregulated During Unloading, Immobilization, and Spinal Cord Injury. *Med Sci Sports Exerc* 40: S476, 2008.

254. **Shah PK, Stevens JE, Gregory CM, Pathare NC, Jayaraman A, Bickel SC, Bowden M, Behrman AL, Walter GA, Dudley GA, and Vandenborne K.** Lower-extremity muscle cross-sectional area after incomplete spinal cord injury. *Arch Phys Med Rehabil* 87: 772-778, 2006.

255. **Shanely RA, Van Gammeren D, Deruisseau KC, Zergeroglu AM, McKenzie MJ, Yarasheski KE, and Powers SK.** Mechanical ventilation depresses protein synthesis in the rat diaphragm. *Am J Respir Crit Care Med* 170: 994-999, 2004.

256. **Shanely RA, Zergeroglu MA, Lennon SL, Sugiura T, Yimlamai T, Enns D, Belcastro A, and Powers SK.** Mechanical ventilation-induced diaphragmatic atrophy is associated with oxidative injury and increased proteolytic activity. *Am J Respir Crit Care Med* 166: 1369-1374, 2002.
257. **Shen C, Ye Y, Robertson SE, Lau AW, Mak DO, and Chou MM.** Calcium/calmodulin regulates ubiquitination of the ubiquitin-specific protease TRE17/USP6. *J Biol Chem* 280: 35967-35973, 2005.
258. **Shenkman B, Belozeroва I, Nemirovskaya T, Cheglova I, Yudaitcheva A, Kiseleva E, and Mazin M.** Time-course of human muscle fibre size reduction during head-down tilt bedrest. *J Gravit Physiol* 5: P71-72, 1998.
259. **Siu PM, and Alway SE.** Id2 and p53 participate in apoptosis during unloading-induced muscle atrophy. *Am J Physiol Cell Physiol* 288: C1058-1073, 2005.
260. **Siu PM, and Alway SE.** Mitochondria-associated apoptotic signalling in denervated rat skeletal muscle. *J Physiol* 565: 309-323, 2005.
261. **Smith IJ, and Dodd SL.** Calpain activation causes a proteasome-dependent increase in protein degradation and inhibits the Akt signalling pathway in rat diaphragm muscle. *Exp Physiol* 92: 561-573, 2007.
262. **Srikakulam R, and Winkelmann DA.** Chaperone-mediated folding and assembly of myosin in striated muscle. *J Cell Sci* 117: 641-652, 2004.
263. **St-Amand J, Okamura K, Matsumoto K, Shimizu S, and Sogawa Y.** Characterization of control and immobilized skeletal muscle: an overview from genetic engineering. *Faseb J* 15: 684-692, 2001.
264. **Stangel M, Zettl UK, Mix E, Zielasek J, Toyka KV, Hartung HP, and Gold R.** H₂O₂ and nitric oxide-mediated oxidative stress induce apoptosis in rat skeletal muscle myoblasts. *J Neuropathol Exp Neurol* 55: 36-43, 1996.
265. **Steffen BT, Lees SJ, and Booth FW.** Anti-TNF treatment reduces rat skeletal muscle wasting in monocrotaline-induced cardiac cachexia. 2008, p. 1950-1958.
266. **Stein TP, and Wade CE.** Metabolic Consequences of Muscle Disuse Atrophy. 2005, p. 1824S-1828.
267. **Stevenson EJ, Giresi PG, Koncarevic A, and Kandarian SC.** Global analysis of gene expression patterns during disuse atrophy in rat skeletal muscle. *J Physiol* 551: 33-48, 2003.

268. **Stevenson EJ, Koncarevic A, Giresi PG, Jackman RW, and Kandarian SC.** Transcriptional profile of a myotube starvation model of atrophy. *J Appl Physiol* 98: 1396-1406, 2005.
269. **Sugiura T, Abe N, Nagano M, Goto K, Sakuma K, Naito H, Yoshioka T, and Powers SK.** Changes in PKB/Akt and calcineurin signaling during recovery in atrophied soleus muscle induced by unloading. 2005, p. R1273-1278.
270. **Suttner DM, Sridhar K, Lee CS, Tomura T, Hansen TN, and Dennery PA.** Protective effects of transient HO-1 overexpression on susceptibility to oxygen toxicity in lung cells. 1999, p. L443-451.
271. **Suzuki N, Motohashi N, Uezumi A, Fukada S, Yoshimura T, Itoyama Y, Aoki M, Miyagoe-Suzuki Y, and Takeda S.** NO production results in suspension-induced muscle atrophy through dislocation of neuronal NOS. *J Clin Invest* 117: 2468-2476, 2007.
272. **Taillandier D, Aurousseau E, Meynial-Denis D, Bechet D, Ferrara M, Cottin P, Ducastaing A, Bigard X, Guezennec CY, Schmid HP, and et al.** Coordinate activation of lysosomal, Ca²⁺-activated and ATP-ubiquitin-dependent proteinases in the unweighted rat soleus muscle. *Biochem J* 316 (Pt 1): 65-72, 1996.
273. **Taille C, Almolki A, Benhamed M, Zedda C, Megret J, Berger P, Leseche G, Fadel E, Yamaguchi T, Marthan R, Aubier M, and Boczkowski J.** Heme Oxygenase Inhibits Human Airway Smooth Muscle Proliferation via a Bilirubin-dependent Modulation of ERK1/2 Phosphorylation. 2003, p. 27160-27168.
274. **Tesch PA, and Berg HE.** Effects of spaceflight on muscle. *J Gravit Physiol* 5: P19-22, 1998.
275. **Tesch PA, von Walden F, Gustafsson T, Linnehan RM, and Trappe TA.** Skeletal muscle proteolysis in response to short-term unloading in humans. 2008, p. 902-906.
276. **Thom JM, Thompson MW, Ruell PA, Bryant GJ, Fonda JS, Harmer AR, De Jonge XA, and Hunter SK.** Effect of 10-day cast immobilization on sarcoplasmic reticulum calcium regulation in humans. *Acta Physiol Scand* 172: 141-147, 2001.
277. **Thompson MG, Thom A, Partridge K, Garden K, Campbell GP, Calder G, and Palmer RM.** Stimulation of myofibrillar protein degradation and expression of mRNA encoding the ubiquitin-proteasome system in C(2)C(12) myotubes by dexamethasone: effect of the proteasome inhibitor MG-132. *J Cell Physiol* 181: 455-461, 1999.

278. **Tidball JG, and Spencer MJ.** Expression of a calpastatin transgene slows muscle wasting and obviates changes in myosin isoform expression during murine muscle disuse. *J Physiol* 545: 819-828, 2002.
279. **Tintignac LA, Lagirand J, Batonnet S, Sirri V, Leibovitch MP, and Leibovitch SA.** Degradation of MyoD mediated by the SCF (MAFbx) ubiquitin ligase. *J Biol Chem* 280: 2847-2856, 2005.
280. **Tisdale MJ.** Is there a common mechanism linking muscle wasting in various disease types? *Curr Opin Support Palliat Care* 1: 287-292, 2007.
281. **Trappe SW, Trappe TA, Lee GA, Widrick JJ, Costill DL, and Fitts RH.** Comparison of a space shuttle flight (STS-78) and bed rest on human muscle function. *J Appl Physiol* 91: 57-64, 2001.
282. **Urso ML, Chen YW, Scrimgeour AG, Lee PC, Lee KF, and Clarkson PM.** Alterations in mRNA expression and protein products following spinal cord injury in humans. *J Physiol* 579: 877-892, 2007.
283. **Urso ML, Scrimgeour AG, Chen YW, Thompson PD, and Clarkson PM.** Analysis of human skeletal muscle after 48 h immobilization reveals alterations in mRNA and protein for extracellular matrix components. *J Appl Physiol* 101: 1136-1148, 2006.
284. **Van Gammeren D, Falk DJ, DeRuisseau KC, Sellman JE, Decramer M, and Powers SK.** Reloading the diaphragm following mechanical ventilation does not promote injury. *Chest* 127: 2204-2210, 2005.
285. **Vandenburgh H, Chromiak J, Shansky J, Del Tatto M, and Lemaire J.** Space travel directly induces skeletal muscle atrophy. *Faseb J* 13: 1031-1038, 1999.
286. **Vandenburgh HH, Karlisch P, Shansky J, and Feldstein R.** Insulin and IGF-I induce pronounced hypertrophy of skeletal myofibers in tissue culture. *Am J Physiol* 260: C475-484, 1991.
287. **Vassilakopoulos T.** Ventilator-induced diaphragm dysfunction: the clinical relevance of animal models. *Intensive Care Med* 34: 7-16, 2008.
288. **Veldhuizen JW, Verstappen FT, Vroemen JP, Kuipers H, and Greep JM.** Functional and morphological adaptations following four weeks of knee immobilization. *Int J Sports Med* 14: 283-287, 1993.
289. **Vesely MJ, Exon DJ, Clark JE, Foresti R, Green CJ, and Motterlini R.** Heme oxygenase-1 induction in skeletal muscle cells: hemin and sodium nitroprusside are regulators in vitro. *Am J Physiol* 275: C1087-1094, 1998.

290. **Vile GF, Basu-Modak S, Waltner C, and Tyrrell RM.** Heme oxygenase 1 mediates an adaptive response to oxidative stress in human skin fibroblasts. *Proc Natl Acad Sci U S A* 91: 2607-2610, 1994.
291. **Voisin L, Breuille D, Combaret L, Pouyet C, Taillandier D, Aurousseau E, Obled C, and Attaix D.** Muscle wasting in a rat model of long-lasting sepsis results from the activation of lysosomal, Ca²⁺-activated, and ubiquitin-proteasome proteolytic pathways. *J Clin Invest* 97: 1610-1617, 1996.
292. **Vyas DR, Spangenburg EE, Abraha TW, Childs TE, and Booth FW.** GSK-3 β negatively regulates skeletal myotube hypertrophy. *Am J Physiol Cell Physiol* 283: C545-551, 2002.
293. **Wang J, and Dore S.** Heme oxygenase-1 exacerbates early brain injury after intracerebral haemorrhage. 2007, p. 1643-1652.
294. **Ward GR, MacDougall JD, Sutton JR, Toews CJ, and Jones NL.** Activation of human muscle pyruvate dehydrogenase with activity and immobilization. *Clin Sci (Lond)* 70: 207-210, 1986.
295. **Watanabe TK, Kawai A, Fujiwara T, Maekawa H, Hirai Y, Nakamura Y, and Takahashi E.** Molecular cloning of UBE2G, encoding a human skeletal muscle-specific ubiquitin-conjugating enzyme homologous to UBC7 of *C. elegans*. 1996, p. 146-148.
296. **Weinstein RB, Slentz MJ, Webster K, Takeuchi JA, and Tischler ME.** Lysosomal proteolysis in distally or proximally denervated rat soleus muscle. *Am J Physiol* 273: R1562-1565, 1997.
297. **Wen-Hui Hu ONHM-SYWMWPKYWJRB.** Identification and characterization of a novel Nogo-interacting mitochondrial protein (NIMP). 2002, p. 36-45.
298. **Widmann M, and Christen P.** Differential effects of molecular chaperones on refolding of homologous proteins. *FEBS Lett* 377: 481-484, 1995.
299. **Wilson EM, and Rotwein P.** Selective control of skeletal muscle differentiation by Akt1. *J Biol Chem* 282: 5106-5110, 2007.
300. **Wing SS.** Control of ubiquitination in skeletal muscle wasting. *Int J Biochem Cell Biol* 37: 2075-2087, 2005.
301. **Yajid F, Mercier JG, Mercier BM, Dubouchaud H, and Prefaut C.** Effects of 4 wk of hindlimb suspension on skeletal muscle mitochondrial respiration in rats. *J Appl Physiol* 84: 479-485, 1998.

302. **Young P, Deveraux Q, Beal RE, Pickart CM, and Rechsteiner M.** Characterization of two polyubiquitin binding sites in the 26 S protease subunit 5a. *J Biol Chem* 273: 5461-5467, 1998.
303. **Yu ZB, Gao F, Feng HZ, and Jin J-P.** Differential regulation of myofilament protein isoforms underlying the contractility changes in skeletal muscle unloading. 2007, p. C1192-1203.
304. **Yue GH, Bilodeau M, Hardy PA, and Enoka RM.** Task-dependent effect of limb immobilization on the fatigability of the elbow flexor muscles in humans. *Exp Physiol* 82: 567-592, 1997.
305. **Zhang M, Zhang BH, Chen L, and An W.** Overexpression of heme oxygenase-1 protects smooth muscle cells against oxidative injury and inhibits cell proliferation. *Cell Res* 12: 123-132, 2002.
306. **Zhao J, Brault JJ, Schild A, Cao P, Sandri M, Schiaffino S, Lecker SH, and Goldberg AL.** FoxO3 coordinately activates protein degradation by the autophagic/lysosomal and proteasomal pathways in atrophying muscle cells. *Cell Metab* 6: 472-483, 2007.